THE ROLE OF THE $P2X_7$ RECEPTOR IN CIGARETTE SMOKE DRIVEN-INFLAMMATION ASSOCIATED WITH COPD

Suffwan Eltom

2011

A Thesis Submitted for the Degree of Doctor of Philosophy in the Faculty of Medicine of Imperial College London

Respiratory Pharmacology Group
National Heart and Lung Institute
Faculty of Medicine
Imperial College London
Sir Alexander Fleming Building
Exhibition Road
London
SW7 2AZ

Abstract

Chronic Obstructive Pulmonary Disease (COPD) is a cigarette smoke (CS)-driven inflammatory airway disease with an increasing global prevalence. Currently, there are no effective therapies to stop the relentless progression of this disease. In the inflammatory milieu present in the lungs of animal models of, and human patients with COPD are increased levels of cytokines (IL-1β/IL-18) linked to activation of the NLRP3-Inflammasome. It has been postulated that exposure to CS leads to the release of endogenous danger signals (e.g. ATP) activating the NLRP3-Inflammasome via the $P2X_7$ receptors driving the maturation and release of IL-1β and IL-18. The literature suggests that these cytokines are central to the chronic inflammation in the airway which drives the pathological changes seen in COPD. My hypothesis is that blockade of the $P2X_7$ - NLRP3-Inflammasome pathway will attenuate the inflammation present in CS-induced airway inflammation.

I developed an acute (3-day) model of COPD-like inflammation to investigate the role of the $P2X_7$ receptor in this *pathway*. I demonstrated that CS-induced neutrophilia in a pre-clinical model is temporally associated with markers of Inflammasome activation (increased caspase 1 activity and release of IL-1β/IL-18) in the lungs. I used genetically modified mice lacking functional $P2X_7$ receptors to show attenuation in caspase-1 activity, IL-1β release and airway neutrophilia in response to acute CS exposure but not LPS-induced airway inflammation. These findings were validated using a specific $P2X_7$ receptor antagonist. Furthermore, I confirmed that the role of this pathway was not restricted to early stages of disease development by showing increased caspase-1 activity in lungs from a more chronic exposure to CS (28-day) and patients with COPD. This translational data suggests the $P2X_7$-Inflammasome pathway plays an on-going role in disease pathogenesis.

These results advocate the crucial role of the $P2X_7$ – caspase-1 axis in CS-induced inflammation, highlighting this as a possible therapeutic target in combating COPD.

Acknowledgements

First and foremost, I would like to thank my supervisors, Professor Maria Belvisi and Dr Mark Birrell for allowing me to complete my PhD under their expert guidance and for their continual generosity with their time, advice and support. I would like to thank them for making the experience not only rewarding, but also enjoyable. I am truly in your debt.

I would like to extend my gratitude to Dr Christopher Stevenson (Roche), for his teaching and endless and invaluable support that continued even after he moved back across the pond. A big thank you goes to the Respiratory Pharmacology Group, for their friendship and support, and for creating a positive atmosphere in which I could prosper. I thank Dr Sissie Wong for her kind instruction of *in vitro* techniques. Dr Deborah Clarke, Dr Kristof Raemdonck and Dr Sarah Maher's assistance throughout my PhD was invaluable. Special mentions go to Abd El-ilah Dekkak, Bilel Dekkak, Megan Grace, Joseph Rastrick, Nicole Dale and Liang Yew-Booth for all their help and backing in the 'Dream Team'.

I would also like to thank Dr Matthew Catley (UCB Celltech) and Dr Anthony Coyle (Pfizer) for their advice and support throughout the project and Dr Jean Kanellopoulos (Université Paris Sud) for providing the $P2X_7$ knockout mice. Furthermore, I extend my thanks to AstraZeneca for providing the $P2X_7$ receptor antagonist and the Transplant Coordinators at the Royal Brompton and Harefield NHS Trust for providing human tissue to support my research.

Of course, many thanks are due to my friends Adeel, Richard, Halim, Amir, Asim and Farhad for their undying support. I would like to thank my siblings Ali, Ala'a, Eissra and my special little sister Memo (Maryam) for being there for me every step of the way and for each providing their own form of motivation. Thank you to my fiancée Sally for her infinite love, encouragement and support. You are everything and more.

Finally, my biggest 'thank you' is for my parents. Dad, I thank you for everything you have done for me, I could not have possibly asked for a better role model; not only did you leave footsteps in the sand for me to follow, but you also taught me how to believe in myself and find my own way. Dear Mama, because I have you, I know there is nowhere in this world I can go where a prayer has not already been, thank you for everything. No gift from me to you could ever equal your gift to me; I pray that my actions provide you with joy and happiness.

Statement

The development and characterisation of the Cigarette Smoke exposure model described in Chapter 3 was completed with the assistance of Joseph Rastrick. The measurement of inflammatory cytokines using the MSD technology presented in Chapter 3 was carried out with technical assistance from Joseph Rastrick. The quantification of mRNA expression described in Chapter 3 was performed with expert guidance from Dr Sissie Wong.

Table of Contents

List of Figures

List of Abbreviations

AECOPD	Acute exacerbations of COPD
ANOVA	Analysis of Variance
AP-1	Activating Protein-1
ASC	Apoptosis-Associated Speck-like Protein Containing A CARD
ATP	Adenosine Triphosphate
ATPγS	Adenosine 5′-[γ-thio]triphosphate tetralithium salt
AZ11645373	3-(1-(3′-nitrobiphenyl-4-yloxy)-4-(pyridine-4-yl)butan-2-yl)thiazolidine-2,4-dione
BAL	Bronchoalveolar Lavage
BALF	Bronchoalveolar Lavage Fluid
Bcl	B-cell Lymphoma
CAPS	Cryopyrin-Associated Periodic Syndrome
CARD	Caspase Activation and Recruitment Domain
CCL	Chemokine C-C Motif Ligand
CD	Cluster of Differentiation
cDNA	Complimentary Deoxyribonucleic Acid
CLR	Calcitonin Receptor-Like Receptor
COPD	Chronic Obstructive Pulmonary Disease
CS	Cigarette Smoke
CSM	Cigarette Smoke Conditioned Media
Ct	Critical Threshold Cycle
CXCL	Chemokine C-X-C Motif Ligand
DAMP	Danger Associated Molecular Pattern

DMSO	Dimethyl Sulphoxide
DNA	Deoxyribonucleic Acid
dNTP	Deoxynucleoside Triphosphate
ELISA	Enzyme-Linked Immunosorbent Assay
ER	Endoplasmic Reticulum
ExNO	Exhaled Nitric Oxide
FBS	Foetal Bovine Serum
FCS	Foetal Calf Serum
FEV_1	Forced Expiratory Volume in One Second
FTC	Federal Trade Commission
FVC	Forced Vital Capacity
G-CSF	Granulocyte-Colony Stimulating Factor
GM-CSF	Granulocyte Macrophage-Colony Stimulating Factor
GOLD	Global Initiative for Chronic Obstructive Lung Disease
H_2SO_4	Hydrosulphuric Acid
HDAC -2	Histone Deacetylase 2
HRQL	Health Related Quality of Life
i.p.	intraperitoneal
I-κB	Inhibitor of κB
ICAM	Inter-cellular Adhesion Molecule-1
IFN-γ	Interferon-γ
IKK	Inhibitor of κB Kinase
IL	Interleukin
IP-10	Interferon-Inducible Protein-10
IRAK	Interleukin-1 Receptor-Associated Kinase

KC	Keratinocyte-derived Chemokine
kDA	Kilo Daltons
KO	Knockout
kPa	Kilopascal
LABA	Long-Acting β_2-Agonists
LMN	Lymphomononuclear Cells
LPS	Lipopolysaccharide (Endotoxin)
LRR	Leucine Rich Repeat
LT	Lethal Toxin
LTOT	Long-Term Oxygen Therapy
LVRS	Lung Volume Reduction Surgery
MAM	Mitochondria-Associated ER Membrane
MCP-1	Monocyte Chemotactic Protein 1
MDP	Muramyl Dipeptide
MIP-1α	Macrophage Inflammatory Protein 1α
MMP	Matrix Metalloproteinase
mRNA	Messenger RNA
MSD	Mesoscale Discovery
MSU	Monosodium Urate
MTT	3-[4,5-dimethylthiazol-2-yl]-2,5-diphenyltetrazolium bromide
MyD88	Myeloid Differentiation Primary Response Gene 88
NAD+/H	Nicotinamide Adenine Dinucleotide
NaN_3	Sodium Azide
NE	Neutrophil Elastase
NF-κB	Nuclear Factor-κB

NK	Natural Killer
NLR	NOD-Like Receptor
NLRP	NACHT, LRR and PYD domains-containing protein
p.o.	*per os* (by mouth)
P2X	P2X Purinoceptor
P2Y	P2Y Purinoceptor
PAF	Platelet Activating Factor
PAMP	Pathogen Associated Molecular Pattern
PBS	Phosphate Buffered Saline
pO2	Partial Pressure of Oxygen in the Blood
PRR	Pattern Recognition Receptor
PYD	Pyrin Domain
RLH	RIG-Like Helicase
RNA	Ribonucleic Acid
ROS	Reactive Oxygen Species
RPMI	Roswell Park Memorial Institute
RT-PCR	Real-Time Polymerase Chain Reaction
S.E.M.	Standard Error of the Mean
Syk	Spleen Tyrosine Kinase
TIMP	Tissue Inhibitor of Metalloproteinases
TLR	Toll-Like Receptor
TNF-α	Tumour Necrosis Factor-α
TSP	Total Smoke Particulate
WBC	White Blood Cell

Chapter 1

Introduction

1.1 COPD

1.1.1 Background

Chronic Obstructive Pulmonary Disease (COPD) is an inflammatory disease of the airways, characterised by a progressive and irreversible decline in lung function caused by airflow obstruction (Rabe et al., 2007; MacNee, 2005) with cigarette smoking being identified as the largest single causative agent associated with COPD (Pauwels *et al.*, 2001). In 2005 COPD alone caused 3 million deaths worldwide (WHO 2007). Furthermore, the disease is currently reported to be the fourth leading cause of death worldwide and is predicted to be the third ranked disease in the year 2020 (Lopez & Murray, 1998). Significantly, COPD is the only leading global cause of death that is on the increase, in part due to the fact there are currently no treatments that can slow or prevent the progression of the disease or alternatively provide patients with relief from the symptoms. The current gold standard treatment for COPD is a combination of long-acting bronchodilators and/or inhaled glucocorticoids. Unfortunately, bronchodilators provide limited symptomatic relief (Cazzola & Donner, 2000), whilst steroids are ineffective in reducing the inflammation seen in COPD patients (Culpitt *et al*. 1999; Keatings *et al*., 1997). COPD healthcare costs globally have become a massive burden, in 2007 alone the disease cost the US economy $47 billion (American Lung Association, 2007). The majority of these vast costs are due to acute exacerbations of COPD that require hospitalisation and extensive medical attention. Therefore finding therapies to aid patients suffering from these airway diseases is a matter of urgency.

1.1.2 Definition & Symptoms

1.1.2.1 Definition

The Global Initiative for Chronic Obstructive Lung Disease (GOLD) defines COPD as "*a disease state characterized by airflow limitation that is not fully reversible. The airflow limitation is usually progressive and associated with abnormal inflammatory response of the lungs to noxious particles or gases*".

1.1.2.2 Disease Progression

COPD is directly related to three underlying disorders characterised by three distinct pathologies; emphysema, chronic bronchitis and small-airway disease. The GOLD classification divides COPD into 4 phases. The mild phase has few signs or symptoms, although there may be occasional shortness of breath following exercise, recurrent respiratory infections and morning cough. In the moderate phase these symptoms are seen more frequently with an increase in severity. In the severe form severe cough, constant wheezing, and shortness of breath following minimal exertion can be witnessed. These symptoms of COPD appear in patients due to airway obstruction, loss of lung elasticity and destruction of lung parenchyma (Barnes, 2000).

1.1.2.3 Chronic Bronchitis

Chronic bronchitis results from an immune response to toxic particles and gases that are inhaled during cigarette smoking. The pathology of the disease includes inflammation in the epithelium of central airways and in the mucus secreting glands. Hypertrophy (enlargement)

and hyperplasia (increased numbers) of the globlet cells leads to increased secretion and mucus production (sputum). Chronic hyper secretion may contribute to the later stages of the disease (Hogg, 2004). Coughing is a symptom of COPD although the mechanism remains unknown.

1.1.2.4 Emphysema

Emphysema is a term used to describe the enlargement of distal airspaces beyond the terminal bronchioles (alveoli), caused by destruction of the airway walls. The alveolar walls collapse during exhalation, leading to effort-independent airflow limitation (meaning no matter how hard the patient breathes, airflow does not increase). This has the detrimental effect of reducing the maximal expiratory flow by decreasing the elastic recoil force driving air out of the lungs making it difficult for the patient to breath. The surface of the lung is reduced causing a reduction in the area available for gaseous exchange causing hypoxemia (Barnes *et al.*, 2003).

1.1.2.5 Small airways disease

Small airways disease involves the smaller conducting airways, which are less than 2mm in diameter. This pathology is difficult to diagnose in patients. Recent studies have highlighted that there are structural abnormalities in the small airways of smokers (Figure 1.1) (Hogg *et al*., 2004). The severity of the COPD also determines the level of occlusion of airway lumen by inflammatory mucous. Airway obstruction in the small airways may also result from peribronchial fibrosis and inflammation, whilst progression in the inflammation will lead to destruction of the alveolar attachments on the outer walls of the small airways (restricting the amount the airways can open or close) (MacNee, 2005).

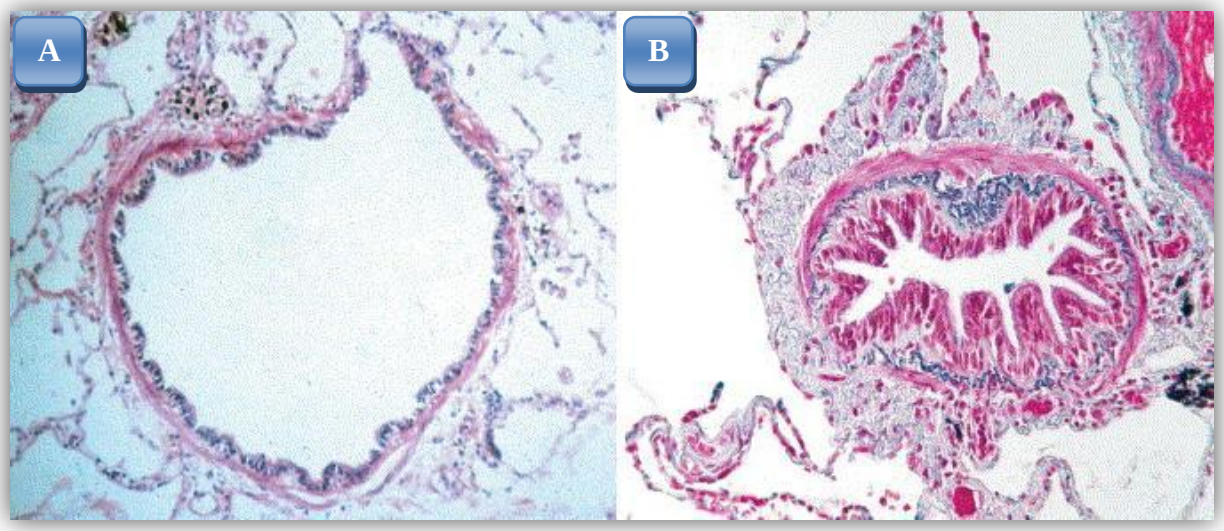

Figure 1.1 – Small Airway Obstruction: *(A) - Normal small airway. (B) - Occluded small airway in COPD patient (Adapted from Hogg, 2004).*

1.1.3 Aetiology

Recent studies have documented that 25% of smokers develop COPD therefore there must be a strong link to environmental and genetic factors. Cigarette smoking leads to loss of lung function, however, increasing age has also been shown to play a significant role. It is interesting to note that whilst all smokers develop lung inflammation, not all smokers develop COPD. This suggests there is a genetic predisposition to developing COPD as a result of smoking. Though these genetic factors remain unidentified, several hypotheses have been suggested. Due to a complex mixture of over 4,700 chemical compounds including high concentrations of free radicals (10^{17} radicals per puff) and other oxidants it is difficult to determine the main causative agents (Pryor & Stone, 1993). Recently identified candidate genes that are potentially responsible for COPD are α-1-anti-trypsin, α-1-quimitrypsine and α-2-macroglobuline genes. A definite association has only been found in the α-1-anti-trypsin gene (Sandford *et al.*, 1999). Though studies remain inconclusive, there is an indication of an increased risk of COPD in females. Studies of two cohort populations (13,897) in Denmark

showed that the risk of hospital admission due to COPD was higher in females than in males (Prescott *et al.,* 1997).

Air pollution has also been linked to COPD for many years with studies conducted in panels of patients suffering from chronic bronchitis in the UK and USA confirming an association between pollution and increase in chronic bronchitis cases (Lawther *et al.,* 1970). The increased levels of oxidants and protease to anti-protease levels detected in the lungs have been associated with COPD. Proteases function by breaking down of connective tissue components in the lung parenchyma, particularly elastin, affecting a critical mechanism in the pathogenesis of emphysema particularly in smokers. This may occur as a result of an imbalance of proteases and endogenous anti-proteases (Barnes *et al.,* 2003). The roles of matrix-degrading proteases have been investigated in COPD and linked to loss of lung function. Application of gene-targeted macrophage elastase (MMP-12) and neutrophil elastase (both proteases) in mouse models of emphysema have uncovered the roles of these proteases in airspace enlargement (Shapiro *et al*., 2003).

Pollution also contributes to COPD with a large range of oxidants known to cause oxidative stress in the lungs e.g. sulphur dioxide and ozone. Oxidants such as ozone are free radicals that play a role in redox reactions within the lung to produce harmful secondary and tertiary products (Barnes, 2000). An association between inhalation of smoke from fires and wood smoke (used in third world countries) has also been established. Other pollution factors include occupational chemicals e.g. cadmium (MacNee & Donaldson, 2000).

Further studies have demonstrated that apoptosis in human emphysematous lungs may be a cause of alveolar wall destruction in emphysema patients (Aoshiba *et al*., 2003). It must be

recognized that no single mechanism can be responsible for the complex pathology witnessed in COPD. It is more likely to be due to interactions between complex mechanisms.

1.1.4 Exacerbations of COPD

Patients suffering from COPD are known to endure periods of disease exacerbation. In the clinic acute exacerbations of COPD (AECOPD) are considered a worsening of a patient's symptoms from their stable COPD state that is maintained and requires a change in medication (Rodriguez-Roisin, 2000). Episodes of AECOPD lead to declined lung function and an acute deterioration of respiratory health. Studies have shown that respiratory infections were associated with a more rapid decline in FEV1 (Kanner *et al*., 2001). Furthermore, a wide variation in the frequency of exacerbations exists among patients, with the average figure reported to be one to two episodes annually (Hurst *et al*., 2010), thus AECOPD are considered a significant cause of death (Soler-Cataluna *et al*., 2005). Interestingly, various inflammatory expression profiles have been reported in AECOPD that are dependent on the cause of the exacerbation (Dal Negro *et al*., 2005).

The two main causes of AECOPD are reported to be viral and bacterial infections (Wedzicha, 2001), whilst environmental factors such as air pollution are believed to play a less significant role (Papi *et al*., 2006). It is reported that 40 – 60% of AECOPD incidents are caused by respiratory viral infections (Mallia & Johnston, 2005). As COPD patients are always under threat of viral and bacterial infections and that airway inflammation in COPD patients is further amplified in AECOPD, a better understanding of how CS contributes to the inflammatory response may provide valuable insight into COPD pathogenesis.

1.2 LUNG ANATOMY AND FUNCTION

The lungs are located inside the thoracic cavity surrounded by a double walled sac (pleura) whilst being protected by the rib cage. The outer layer of the sac (parietal pleura) is attached to the chest cavity whilst the inner layer (visceral pleura) is tightly bound to the lungs. The layers are separated by a space called the pleural cavity that is filled with pleural fluid allowing the layers to slide over each other without friction and to prevent them being separated. The lungs are attached to the trachea and heart via the bronchi and pulmonary vessels. The left and right lungs can be easily distinguished as the right lung has three lobes and the left lung has two.

The lungs are connected to the trachea by the bronchi. The trachea is located at the front of the neck and runs down to the sternal angle. Here it divides into the left and right bronchi. The right bronchus, considered the main one, is shorter and runs more vertical. The bronchi enter the lung and branch out forming a bronchial tree that divides further into smaller bronchioles (8 – 24 divisions) that end at the alveoli. This is where gaseous exchange takes place in the lungs. The inhalation (inflow) and expiration (outflow) of air into the lungs is controlled by muscular action. The diaphragm as well as the intercostal muscles (to some extent) force ventilation by changing the intra-thoracic properties such as volume and pressure. Inspiration is achieved by increasing volume and decreasing pressure within the lungs. Expiration however is caused by reducing volume and increasing pressure.

The lungs have several functions, predominantly serving as a respiratory organ with the primary function being gaseous exchange. Many other functions include acid-base balance, phonation, pulmonary defence and metabolism.

The blood supply to the lungs is from two sources: the pulmonary vessels and the bronchial vessels. The bronchial vessels support the non-respiratory tissue whilst the pulmonary vessels provide support to the respiratory tissue. The function of the pulmonary arteries is to carry deoxygenated blood that has returned to the heart from the venous system to the lungs to be oxygenated. The pulmonary veins carry oxygenated blood back to the heart to go to the arterial system. The right and left pulmonary arteries arise from the pulmonary trunk and carry blood to the lungs. The pulmonary veins, two on each side, carry blood to the left atrium of the heart. The bronchial arteries supply the non-respiratory tissue of the lung. The left bronchial arteries branch away from the thoracic aorta; however, the right bronchial artery has a variable source.

Air is brought into the lungs by the airways, oxygen (O_2, O=O) that is required for respiration diffuses into the bloodstream in the alveoli across the thin alveolar membranes, and carbon dioxide (CO_2, O=C=O) a by-product of respiration moves from the blood into the alveoli by diffusion. The removal of CO_2 from the blood causes a change in blood pH levels; this is related to the lung's acid-base balance function. The increase levels of CO_2 causes an increase in levels of H^+ ions due to the following reaction.

$$\mathbf{CO_2 + H_20 \leftrightarrow H_2CO_3 \leftrightarrow H^+ + HCO_3^-}$$

The cerebrospinal fluid and arterial blood contain sensors for CO_2 and pH levels that constantly monitor these levels and send signals to the areas that control breathing in the brain in a feedback system.

To aid with clinical diagnosis of pulmonary disorders, lung function measurements can be assessed. The volume of gas exhaled in one second by a forced expiration is identified as the forced expiratory volume in one second or FEV_1. The amount of gas that can be exhaled after a full inspiration is identified as the forced vital capacity or FVC. These measurements are analysed clinically by calculating the ratio of FEV_1/ FVC. In a healthy individual this ratio is expected to be around 80%, but as the FEV_1 drops so does the ratio. COPD patients usually portray a drop in FEV_1 and FEV_1/ FVC ratio, with declining FEV1 values with the progression of the disease (Levitsky, 1999).

1.3 CELLULAR AND INFLAMMATORY COMPONENTS OF COPD

1.3.1 The immune response in the lung

The immune system can be divided into two types, the innate response and the adaptive response. The innate response is comprised of germ-line encoded components that provide an immediate "first-line" defence to continuously remove noxious influences (pathogens) or microorganisms faced on a daily basis. The “first-line” of defence involves physical barriers to infection that prevent any interaction between the pathogen and the host. The “second-line” of defence involves the action of phagocytic cells. This response can destroy any of these microorganisms within a matter minutes or hours following their entry into the body. It involves certain mediators that take part in this type of response that include histamine, prostaglandins, leukotrienes, platelet-activating-factor (PAF) and particularly interleukins. This response often leads to inflammation (witnessed by oedema) and the accumulation of white blood cells at the site of entry. (Janeway *et al.,* 2001).

Alternatively the adaptive immune response is the provision of long lasting and specific protection against formerly encountered pathogens, which takes days to develop, achieving specificity through somatic recombination and selection of pathogen (antigen) receptors. If any pathogens are not removed by the innate response then the adaptive response will be activated. This response ensures immunity to further illness following an initial infection caused by that same pathogen. This response is specific to the particular pathogen and involves several cell types, the most prominent being lymphocytes.

Lymphocytes can be divided into three different cell types; B cells, T cells and natural killer (NK) cells. The adaptive response consists an induction phase and an effector phase. During the induction phase both B and T cells recognise the pathogen through surface receptors. Division of these cells occurs to produce a large colony of cloned cells that can recognise the pathogen. These cloned cells then form the effector response and have the ability to differentiate into plasma cells (B cells) that produce antibodies or take part in the cell-mediated response (T cells). Some cells become antigen-sensitive memory cells, such that if the same antigen enters the body there will be a greater immune response (Rang *et al*., 1999).

The immune response also includes the significant role performed by chemokines and cytokines. Their particular role is to attract specific inflammatory cells when activated, thus mediating the inflammatory response (Rang *et al.*, 1999). Typically an inflammatory response is a positive response targeted at protecting the host's normal biological functions; however, chronic inflammation that is associated with disease can have a negative impact on the host.

1.3.2 Lung repair and fibrosis

The lung, with its massive surface area and unique gas exchange function remains the frontline of defence against harmful environmental pathogens/factors. Therefore, injury to large conducting airways through to terminal air exchange alveoli is a recurrent process over time for every living individual and related repair and remodelling processes are crucial in maintaining normal lung function (Strieter, 2008). There are a wide variety of epithelial cells lining the airway and alveolar surfaces to serve as the first line of defence against harmful foreign agents/pathogens. As described previously, this defensive approach includes mucus secretion, ciliary movement, electrolyte and fluid transportation across respiratory surface membranes and surfactant production. During lung injury, damaged epithelial cells are released from the lining surface, which leaves a bared epithelial surface with disrupted barrier function. In order to restore normal functions a regeneration process is initiated. In distal lung, resident progenitor cells inherited from developing lung cell lineages and/or recruited circulating stem cells migrate, proliferate, and differentiate to re-epithelialize the surface, and replace the original cell types and functions if the structural scaffold is not extensively damaged. The state of the underlying extracellular matrix may be crucial in guiding repair of injury, which may provide niches for appropriate cell expansion and differentiation.

Studies in lung injury-repair have identified changes in cell behaviour and gene expression that are indicative of specific developmental processes in the lung. However, lung repair has its own unique features in addition to these growth factors. For example, the involvement of pulmonary inflammation and the secretion of cytokines/chemokines related to the process. The process of lung fibrosis may be regarded as an abnormal healing process related to failure of resolution of lung damage and restoration of normal structure (Strieter, 2008).

1.3.3 The cellular and inflammatory responses in COPD

Within the complex vapour and particulate matter that makes up cigarette smoke are more than 4700 various compounds (Ingebrethsen, 1986). Following cigarette smoke inhalation, this wide range of carcinogens and oxidants are believed to exert biological effects by stimulating the epithelial cells and resident immune cells leading to the recruitment and activation of a host of various inflammatory cell types (Figure 1.2). In similar fashion to an infection, the recruitment of cells into the lung in response to cigarette smoke is due to pro-inflammatory mediators that are produced locally (Janeway *et al*., 2001). The process is further facilitated by the increased permeability of the endothelium, allowing the leakage of plasma proteins, complement and clotting factors into the tissue and consequently leads to increased adhesion molecule expression on the endothelial cells. This facilitates the recruitment of leukocytes to the site of injury or infection.

1.3.4 The cellular components of COPD

Studies suggest that the inflammation in the lungs of COPD patients appears to be a magnification of the normal inflammatory response following exposure to insults such as cigarette smoke (Pauwels *et al*., 2001). The first line of defence in the face of the inhaled insults is the epithelium, which produces inflammatory mediators initiating the chemotaxis and accumulation of a selection of inflammatory cells including neutrophils, macrophages and lymphocytes. Furthermore, oxidative stress and proteases further amplify this inflammatory response and drive the classic pathological changes seen in COPD patients. However, COPD is a complex disease; therefore the types of inflammatory cells involved and their patterns or sequences of appearance are relatively poorly understood. Studies examining

the lungs of COPD patients show infiltration by immune cells including CD8+ T-cells and a large number of neutrophils and macrophages (Grumelli *et al*., 2004). Macrophages are considered a key cell in the pathogenesis of COPD since they are located in areas of active tissue destruction (Barnes, 2004).

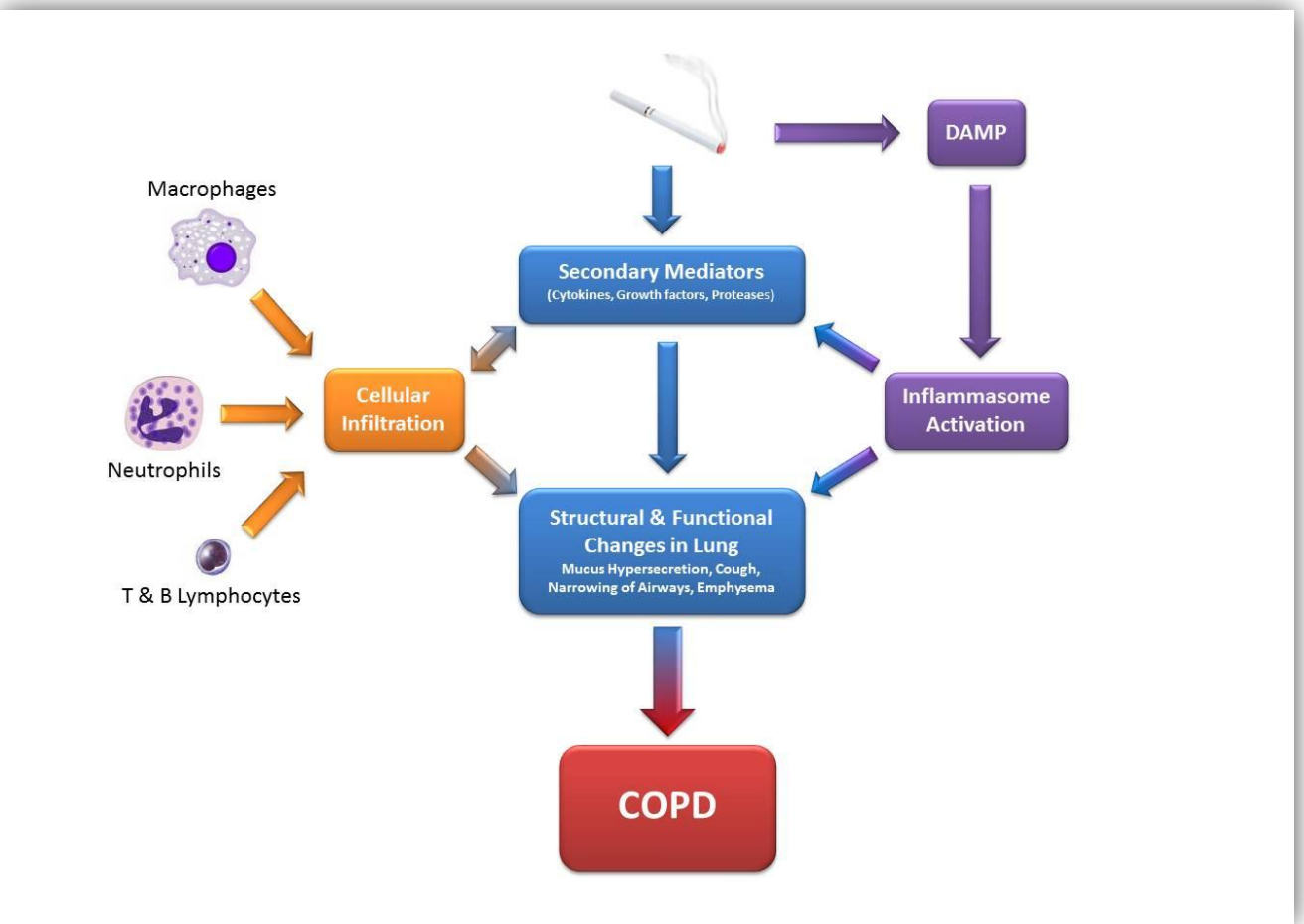

Figure 1.2 – Cigarette smoke and inflammatory processes in the lung.

1.3.4.1 The epithelium

As the first line of defence against invading pathogens is the barrier between host and the environment, the epithelium plays a major role in responses to inhaled insults such as cigarette smoke. An important role in the defence of the airways is the production of mucus

from goblet cells to trap bacteria and inhaled particulates (Adler & Li, 2001). Various hypotheses have been suggested for a role of the epithelium in initiating and maintaining the inflammatory responses following cigarette smoke inhalation. Epithelial cells are activated by cigarette smoke to produce inflammatory mediators, including TNF-α, IL-1β, GM-CSF, and IL-8 (Mio *et al*., 1997; Hellermann *et al*., 2002; Floreani *et al*., 2003). Primary human bronchial epithelial cells have been shown to release increased levels of inflammatory chemokine IL-8 in response to treatment with cigarette smoke condensate (Fields *et al*., 2005). In addition, human bronchial epithelial cells have also been demonstrated to be responsive to very low levels of IL-1β, when examining IL-8 release in culture (Coulter et al., 1999). Furthermore, primary epithelial cells from patients with COPD have been demonstrated to release more IL-8 than those from smokers without airflow limitation (Schulz *et al*., 2004). These findings suggest that the epithelium plays an important role as the first line of defence by producing inflammatory mediators required for the chemotaxis of immune cells into the lung.

1.3.4.2 Neutrophils

Neutrophils are one of the dominant cell types recruited into the lung in COPD, however, their role in this disease is not yet fully understood. The percentage of neutrophils in samples taken from COPD patients are increased with GOLD stage (Singh *et al*., 2010). Studies have shown increased numbers of activated neutrophils are found in sputum and BAL fluid of patients with COPD (Lacoste *et al*., 1993; Keatings *et al*., 1996), however, this increase is not mirrored in the airways or lung parenchyma (Finkelstein *et al*., 1995). Smoking may also increase neutrophil retention in the lung (MacNee *et al*., 1989). Furthermore, the literature suggests that neutrophils recruited to the airways of COPD patients are activated, based on

the increased concentrations of granule proteins, such as myeloperoxidase and human neutrophil lipocalin, in the sputum supernatant (Keatings & Barnes, 1997; Yamamoto *et al*., 1997; Peleman *et al*., 1999).

Although neutrophils are believed to be predominantly involved in the control of bacterial and viral infections of the lung (Laws *et al*., 2010; Tate *et al*., 2009), they have also been shown to provide a source of serine proteases such as neutrophil elastase (NE), matrix metalloproteinases (MMPs) and cathepsins, which may contribute to alveolar destruction. These serine proteases also potentiate mucus hypersecretion (Geraghty *et al*., 2007).

1.3.4.3 Macrophages

Macrophages are derived from blood borne monocytes and mature into macrophages when they enter tissue. In the lung they function as long-lived effector cells. They play a crucial role in the pathogenesis of COPD defending against endogenous and exogenous stimuli. Furthermore, they produce mediators to initiate or alternate the actions of other local cells as well as being responsible for the clearance of apoptotic neutrophils (Tetley, 2002). The numbers of alveolar macrophages are increased between 5 – 10 fold in the airways, parenchyma, bronchoalveolar lavage (BALF) and sputum of smokers and patients with COPD (Finkelstein *et al*., 1995). This is further supported by the correlation between macrophage numbers in the airways and COPD disease severity (Di Stefano *et al*., 1998). Examination of macrophages taken from smokers identified that there are morphological and functional changes in this cell type (Harris *et al*., 1970).

Macrophages are activated upon exposure to cigarette smoke to release inflammatory mediators, thus providing a cellular mechanism that links smoking with inflammation in COPD. Alveolar macrophages also secrete elastolytic enzymes, including MMP-2, MMP-9, MMP-12, cathepsins K, L, and S, and neutrophil elastase taken up from neutrophils (Punturieri *et al*., 2000; Russell *et al*., 2002). Another function of macrophages is to ingest apoptotic cells; therefore, the reported decreased phagocytic activity of alveolar macrophages in COPD patients may explain the increased numbers of neutrophils in the airways (Hodge *et al*., 2003).

1.3.4.4 T Lymphocytes

The role of T lymphocytes in COPD is a relatively unknown area. Recent studies have demonstrated an increase in the total numbers of T lymphocytes; particularly the sub-type cluster of differentiation (CD) 8^+ T cells, in lung parenchyma and airways of patients with COPD (Finkelstein *et al*., 1995; Saetta *et al*., 1999; Retamales *et al*., 2001). Furthermore, a correlation between the numbers of T cells, the degree of airflow obstruction and the amount of alveolar destruction exists. An increase in the absolute number of $CD4^+$ T cells has been shown in COPD patients, but the ratio of $CD4^+/CD8^+$ cells is reversed in COPD. This finding has been demonstrated in smokers with COPD but not smokers that do not show signs of airflow limitation (Majo *et al*., 2001).

Dendritic cells may migrate from the airways to regional lymph nodes and stimulate proliferation of $CD8^+$ and $CD4^+$ T cells. $CD8^+$ T cells are typically increased in airway infections, and it is possible that bacterial and viral pathogens, occupying the lower respiratory tract of COPD patients, are responsible for this inflammatory response (Hill *et al*.,

1999). Current dogma suggests that the epithelium plays a role in the recruitment of cells into the airways in response to oxidative DNA damage to lung epithelial barrier cells. One possible hypothesis is that upon damage of the lung epithelial barrier cells, dendritic cells mistake these as foreign, leading to the clonal expansion of $CD8^+$ T cells upon entering the lymph nodes. This in turn leads to proliferation of cytotoxic $CD8^+$ T cells and the subsequent release of perforin and granzyme, which can attack altered epithelial cells thus propagating the immune response (Tzortzaki & Siafakis, 2009).

1.3.5 Inflammatory mediators in COPD

Although much effort has been placed on identifying the variety of cell types involved in the pathogenesis of COPD, there has also been extensive research focused on identifying the presence and role of various pro-inflammatory mediators (cytokines and chemokines) in samples taken from COPD patients. Several cytokines have been implicated in COPD (Churg, 2001); the most well characterised mediators will be discussed in the following section.

1.3.5.1 TNF-α

The primary function of TNF-α is in the regulation of immune cells. It also functions as a pro-apoptotic cytokine that is secreted from macrophages and epithelial cells (Carswell *et al*., 1975). Sputum from COPD patients contains high concentration of TNF-α (Keatings *et al*., 1996), that is potentiated in exacerbations of the disease (Aaron *et al*., 2001). However, although it is highly abundant in samples from COPD patients blocking TNF-α using *infliximab* (a monoclonal antibody against human TNF-α) failed to improve the symptoms or

respiratory function of COPD patients (van der Vaart *et al*., 2005; Rennard *et al*., 2007). This finding taken into account, one could determine that other cytokines are possibly more fundamental in driving the inflammation seen in COPD patients.

1.3.5.2 IL-1β

A member of the IL-1 family of cytokines, the functions of IL-1β are similar to those of TNF-α as a potent activator of alveolar macrophages in COPD patients. IL-1β is an important cytokine that plays a significant role in the initiation and persistence of the inflammatory response. The effectiveness of IL-1β as an inflammatory cytokine means that unregulated release could cause considerable tissue damage and situations of chaotic inflammation witnessed in many diseases including COPD. For this reason the release of IL-1β needs to be tightly regulated. IL-1β expression in macrophages via LPS-stimulation may be controlled at a number of levels (Meylan *et al*., 2006). LPS binds to toll-like receptor 4 (TLR4) causing the up-regulation of IL-1β mRNA and protein. The IL-1β produced however, is a 31 kDa pro-protein and must be enzymatically cleaved to produce a 17 kDa active form of the cytokine (Giri *et al*., 1985; Bayne *et al*., 1986). The cleavage process of IL-1β is mediated by caspase 1, which itself is produced as a catalytically inactive pro-enzyme requiring enzymatic cleavage (Thornberry *et al*., 1992). Caspase 1 activation requires the assembly of the inflammasome of which there are a number of different types, the best characterised being the NLRP3 inflammasome a protein complex present within the cytosol (Martinon *et al*., 2004).

Elevated IL-1β levels are found in induced sputum and BAL fluid from COPD patients (Ekberg-Janssen *et al*., 2001; Zeidel *et al*., 2002). More recently Singh et al. demonstrated

that IL-1β levels were significantly raised in COPD patients, with IL-1β showing a negative correlation with FEV1 suggesting that in COPD, IL-1β serum levels correlate with clinical aspects of disease severity (Singh *et al*., 2010). Furthermore mice over-expressing IL-1β in lung epithelium display a COPD-like phenotype consisting of lung inflammation, emphysema and airway fibrosis (Lappalainen *et al*., 2005). In contrast, mice lacking IL-1 Receptor type 1 (IL-1R) exhibited a significant decrease in airway neutrophilia in response to cigarette smoke (CS) (Doz *et al*., 2008; Churg *et al*., 2009). Based on this evidence, IL-1β is believed to play an important role in the pathogenesis of COPD.

1.3.5.3 IL-6

Although it is known to have anti-inflammatory properties, its role in COPD it believed to be pro-inflammatory in nature. Released mainly by T cells and macrophages to stimulate immune responses, IL-6 is important in initiating the immune response to specific microbial molecules, known as pathogen associated molecular patterns (PAMPs). IL-6 concentrations have been demonstrated to be increased in induced sputum, BALF, and exhaled breath condensate of COPD patients, particularly during exacerbations (Bhowmik *et al*., 2000; Song *et al*., 2001; Bucchioni *et al*., 2003). Furthermore, blood serum from COPD patients contains increased levels of IL-6 (Debigare *et al*., 2003; Godoy *et al*., 2003). Aldonyte et al., demonstrated that monocytes from COPD patients release more IL-6 following LPS stimulation when compared to healthy subjects (Aldonyte *et al*., 2003).

1.3.5.4 IL-8

As a potent chemoattractant for neutrophils, it is no surprise that IL-8 plays a significant role in COPD. It is produced by a wide range of cell types, mainly epithelial cells, macrophages, and neutrophils, in response to stimulation of these cells by various inflammatory agents (Mukaida, 2003). IL-8 levels are significantly increased in induced sputum of COPD patients and this correlates with increased neutrophilia (Keatings *et al*., 1996; Yamamoto *et al*., 1997). Emphysema patients with a α1-antitrypisn deficiency exhibit even more elevated levels of IL-8 (Woolhouse *et al*., 2002). Furthermore, during acute exacerbations of COPD the concentrations of IL-8 in induced sputum are increased further which may contribute to the increased neutrophilia in these patients (Crooks *et al*., 2000; Gompertz *et al*., 2001). BALF samples taken from COPD patients also exhibit elevated levels of IL-8 (Nocker *et al*., 1996).

In the clinic, anti-IL-8 antibodies have been demonstrated to have a partial effect in reducing the neutrophil chemotactic activity of COPD sputum (Crooks *et al*., 2000; Beeh *et al*., 2003). Furthermore, Yang *et al*, developed a monoclonal antibody to IL-8 that showed little efficacy in COPD patients (Yang *et al*., 1999). Although IL-8 is a potent neutrophil chemoattractant, limited success in treating COPD symptoms has be achieved by targeting this chemokine. Another complexity is that mice do not express a homologue to IL-8; therefore, utilising KO animals to examine its role in animal models is not possible.

1.3.5.5 IL-18

Although it is a member of the IL-1 family of cytokines, the role and significance of IL-18 in inflammatory disease is not as well characterised as IL-1β. IL-18 is produced by a whole host of cells including macrophages, monocytes, neutrophils and T and B cells under varying conditions (Reddy, 2004). IL-18 receptor which is identical in sequence to a member of the

IL-1 receptor family previously designated IL-1 receptor-related protein (Torigoe *et al*., 1997) have been identified on T, B, NK, epithelial and a whole host of immune cells (including macrophages and neutrophils). It is thought to activate p38 MAPK (mitogen activated protein kinases), the transcription factor AP-1 (activation protein 1) and stimulate the production of GM-CSF, TNFα, CXCL8, IL-1β and IFNγ, highlighting the important role that IL-18 may play in the recruitment and activation of neutrophils (Tschoeke *et al*., 2006). The production of mature IL-18 from its precursor is also controlled by NLRP3 dependent caspase 1 function (Muneta *et al*., 2001).

Recent studies have discovered elevated levels of IL-18 in plasma, skeletal muscle and circulation in COPD patients in comparison to healthy subjects (Petersen *et al*., 2007; Imaoka *et al*., 2007). It has been demonstrated that CS activates the release of IL-18 in humans and mice, furthermore, IL-18 knockout mice show significantly decreased inflammation and emphysema compared to wild-type mice following CS exposure (Kang *et al*., 2007). Additionally, it has also been demonstrated that over expression of IL-18 in the mouse lung leads to a COPD like phenotype (Hoshino *et al*., 2007).

1.3.5.6 GM-CSF

The granulocyte-macrophage colony-stimulating factor (GM-CSF) has been implicated in airway disease. Released by alveolar macrophages, GM-CSF is believed to be important for neutrophil and macrophage survival and priming (Culpitt *et al*., 2003), and it may play an enhancing role in neutrophilic inflammation (Vlahos *et al*., 2006). GM-CSF has been shown to be increased in BALF samples from COPD patients and those with exacerbations. These increases have been linked to increased neutrophilia (Balbi *et al*., 1997). Furthermore, GM-

CSF has been implicated to play an important role in CS-induced inflammation. Animals treated with anti-GM-CSF and exposed to smoke show markedly less neutrophilia and macrophages in the BALF (Vlahos *et al*., 2010).

1.3.5.7 Other pro-inflammatory mediators

As a complex inflammatory disease, a vast range of inflammatory mediators are proposed to play a role in the recruitment of inflammatory cells into the lungs. Bronchial biopsies from COPD patients have highlighted an increased expression of IL-12 (Di Stefano *et al*., 2004). Monocyte chemoattractant protein 1 (MCP-1) is expressed by epithelial cells, macrophages and T cells and has been shown to be increased in BALF, sputum and lung tissue from COPD patients (de Boer *et al*., 2000; Traves *et al*., 2002). The monocyte chemoattractant, CCL2 and growth related oncogene alpha (GRO-α) have both been demonstrated to be markedly increased in induced sputum from COPD patients.

Interestingly, overexpression of IL-13 and interferon-γ in murine lungs has been shown to unexpectedly cause emphysema believed to be mediated by increased expression of MMPs and cathepsins (Wang *et al*., 2000; Zheng *et al*., 2000). Furthermore, the expression of IL-13 is increased in bronchial biopsies of smokers with mucus hypersecretion compared with normal smokers (Miotto *et al*., 2003).

1.3.6 Protease/Antiprotease imbalance

Increases in the production (or activity) of proteases or inactivation (or reduced production) of antiproteases causes an imbalance. It is hypothesised that exposure to CS and

inflammation in general leads to conditions of oxidative stress, which initiates the release of a combination of proteases and inactivates several antiproteases by oxidation. The major proteases and anti-proteases believed to be involved in COPD pathogenesis are listed below (Figure 1.3).

Proteinases	Antiproteinases
Serine proteinases	α-1-antitrypsin
Neutrophil elastase	Secretory leukoprotease inhibitor
Cathepsin G	Elafin
Proteinase 3	Cystatins
Cysteine proteinases	Tissue inhibitors of MMP (TIMP1-4)
Cathepsins B, K, L, S	
Matrix metalloproteinases (MMP-8, MMP-9, MMP-12)	

Figure 1.3 - List of Proteinases and antiproteinases involved in COPD

The leading mechanism of alveolar destruction in the lung is believed to be via the breakdown of the lung elastin. This process is facilitated by the release of neutrophil elastase and metalloproteinasese from neutrophils and macrophages infiltrating the lung in response to an inflammatory insult being inhaled (Turino, 2002). The natural antiprotease defences in the lung are overpowered by excessive proteolytic activity which the final outcome being destruction of the lung tissues. In the clinic, a study examining COPD patients with emphysema showed that they had increased levels of neutrophil elastase that correlated with reduced lung function (Betsuyaku *et al*., 2000). Animal models have been using neutrophil elastase to obtain emphysematous changes and neutrophilia in the lung for many years

(Senior *et al*., 1977). Recently, CS exposed mice deficient in neutrophil elastase were shown to be resistant to emphysematous changes and demonstrated less inflammation in the lung (Shapiro *et al*., 2003). These finding all support the hypothesis that an imbalance in proteases-antiproteases may contribute to the emphysematous changes seen in COPD.

1.3.7 Oxidative Stress

Oxidative stress is a major factor in the pathogenesis of COPD. The lung is a unique organ in that it has large epithelial surfaces that are constantly exposed to external sources of oxidative stress. Considering a typical adult inhales an average of 10,000 litres of air per day containing a wide variety of oxidants, particulates and infectious agents, this leaves individuals highly susceptible to the effects of oxidants entering the body through the lungs. However, both the airways and alveolar septa are designed to manage normal levels of oxidative stress that result from daily environmental exposures. There are two main sources of oxidative stress causing agents, atmospheric pollutants and endogenous oxidants. The lung does however contain defences in the form of enzymatic and non-enzymatic anti-oxidants that can protect it from the damaging effects of oxidative stress.

Cigarette smoke is a potent mix of highly concentrated soluble and gaseous electrophiles that place the lungs at high risk of protein and lipid oxidation, endoplasmic reticulum (ER) stress and cell death (Babior, 2000). Cigarette smoke is believed to contain up to 10^{15} free radicals per puff, thus greatly increasing the oxidative burden of the lung (Pryor & Stone, 1993). Many markers of oxidative stress are increased in stable COPD and further in exacerbations of the disease. Various studies have shown increased markers of oxidative stress in the lungs of patients with COPD when compared with healthy patients and with smoking patients

without COPD (Ceylan *et al*., 2006; Kanazawa *et al*., 2005). Oxidative stress can lead to inactivation of antiproteinases and stimulation of mucus production. Inflammation can also be further increased under conditions of oxidative stress by the activation of various inflammatory pathways including leading to increased gene expression of pro-inflammatory mediators.

1.4 RESPIRATORY HOST DEFENSE

The lung features a complex set of systems in order to protect the host from potentially harmful foreign agents that threaten normal biological functions. The combination of physical barriers and the innate and adaptive immune systems provide this protection. Upon entering the lung, foreign agents attach to the mucociliary surface, which provides the first line of fence and propels objects upwards in order to clear them from the lungs. However, CS has been demonstrated to have a negative effect on the ability of cilia to beat and therefore reduce mucociliary clearance (Foster, 2002). As a result other defence systems must be employed in order to maintain the protection of the lung from inhaled foreign objects.

The next level of protection is provided by the innate immune system (Section 1.3.1). The adaptive system, whilst playing an equally important role is dependent on the innate immune response in the lung (Martin & Frevert, 2005). Therefore, the innate immune response is primarily responsible for protecting the lung from the vast range of potentially harmful microbes that we are exposed to on a daily basis.

1.4.1 PAMPs and DAMPs

Recent studies have suggested that apart from differentiating between self and non-self the immune system must identify if a molecule represents a potential threat (Matzinger *et al*., 1994). The innate immune system functions as the primary defence against invading infections, a crucial function for survival. Initially the innate immune response is non-specific; however, it activates the adaptive immune functions leading to specific pathogen directed humoral and cellular responses. A crucial property of the innate immune system is the ability to distinguish invading microbes from 'self' via germline-encoded pattern recognition receptors (PRRs), capable of recognising conserved markers specific to microbes referred to as pathogen associated molecular patterns (PAMPs) such as lipopolysaccharide (LPS), flagellin, peptidoglycan and microbial nucleic acids (Medzhitov & Janeway, 1997; Ishii *et al*., 2008). These receptors include Toll-like receptors (TLRs), Nod-like receptors (NLRs), RIG-I-like RNA helicases (RLHs), C-type lectin receptors (CLRs) (Trinchieri & Sher, 2007) and the recently identified HIN-200 family members (Palsson-McDermott & O'Neill, 2007; Hornung & Latz, 2010). TLRs are known to recognize PAMPs on the cell surface, whereas NLRs sense microbial molecules in the cytosol of the host (Franchi *et al*., 2006).

The functions of the innate immune response extend beyond patrolling for the presence of microbes or invading pathogens. There are also PRRs that function to sense danger signals produced by cells in response to pathogenic conditions or invasion. These are referred to as danger signals or danger associated molecular patterns (DAMPs) and are released in response to cellular damage, conditions of stress or are produced by modification of host proteins by pathogens and can be recognized by the PRRs of the innate immune system. This provides

the innate immune system with an ability to identify pathology occurring independent of infection. In response to recognition of microbial or danger stimuli, these receptors activate downstream signalling events that trigger the necessary immune response (Creagh & O'Neill, 2006). Some examples of molecules believed to function as DAMPs include adenosine triphosphate (ATP), monosodium urate crystals, silica and asbestos (Dostert *et al*., 2008; Cassel *et al*., 2008; Hornung *et al*., 2008). The role played by DAMPs has been identified as vital in sterile inflammatory responses, where the innate immune system responds to tissue injury independent of microbial infection (eg. trauma or ischemia) (Kono & Rock, 2008). It has been postulated that the presence of an endogenous "danger signal" to indicate when tissue is undergoing damage would provide the immune system with a mechanism to distinguish between harmless bacteria and harmful pathogenic bacteria. Many endogenous proteins are proposed to play the role of danger signals, however, it is yet to be determined the range of specific receptors that mediate the activation of inflammatory responses (Skoberne *et al*., 2004).

1.4.2 The inflammasomes

The NLR family of cytoplasmic proteins is composed of 22 family members in humans, whereas the mouse genome contains at least 34 NLR-encoding genes (Ting *et al*., 2008; Dostert *et al*., 2008; Mariathasan & Monack, 2007). This family has a unique structure composed of a central nucleotide-binding domain called NACHT, which is located between an N-terminal protein-binding domain (CARD (Caspase-Recruitment Domain) or PYD (Pyrin Domain)), and a C-terminal LRR (Leucine-Rich Repeat) domain. These molecules are a given the NLR prefix, with a suffix of P or C dependent on the N-terminal moiety, PYD or CARD and an ensuing number. A selection of NLRs have been demonstrated to form a

complex with two pro-inflammatory molecules, caspase 1 and ASC (apoptosis associated speck-like protein containing a CARD), to form a complex known as the inflammasome. Each particular inflammasome is given a prefix name dependent on the NLR molecule within the complex (e.g. NLRP1 inflammasome). The fundamental molecule bringing about the effects of an inflammasome is the cysteine protease caspase 1.

Present within the cell, caspases are a family of cysteine proteases that function to cleave a select number of substrates. Their function has been well examined in apoptosis, where they are believed to play a vital role in the processes involved in apoptotic cell death (Nicholson, 1999). A selection of caspases including human caspase 1, caspase 4 and caspase 5 as well as mouse caspase 1, caspase 11 and caspase 12, are involved in the maturation, processing and release of pro-inflammatory molecules and thus referred to as 'pro-inflammatory caspases' (Martinon & Tschopp, 2007). Caspase 1 was the first member of this family to be identified, and upon stimulation by microbial and endogenous signals the inactive pro-caspase 1 is activated by proteolytic cleavage into an active heterodimer (composed of two 10- and 20-kilodalton subunits) referred to as active caspase 1 (Martinon & Tschopp, 2004). The active form caspase 1 plays a crucial role in the cleavage of two potent pro-inflammatory cytokines pro–interleukin 1β (pro-IL-1β) and pro-IL-18 into their mature, biologically active forms. These two cytokines are members of the IL-1 family and play an significant role in modulating the adaptive immune response (Dunne & O'Neill, 2003).

IL-1β is an important cytokine that plays a significant role in the initiation and persistence of the inflammatory response. The effectiveness of IL-1β as an inflammatory cytokine means that unregulated release could cause considerable tissue damage and situations of chaotic inflammation witnessed in many diseases. The role and significance of IL-18 in inflammatory

disease is not as well characterised as IL-1β. IL-18 is produced by a whole host of cells including macrophages, monocytes, neutrophils and T and B cells under varying conditions (Reddy, 2004). IL-18 receptor which is identical in sequence to a member of the IL-1 receptor family previously designated IL-1 receptor-related protein have been identified on T, B, NK, epithelial and a whole host of immune cells (including macrophages and neutrophils). It is thought to activate p38 and AP-1 as well as stimulating the production of GM-CSF, TNFα, CXCL8, IL-1B and IFNγ, highlighting the important role that IL-18 may play in the recruitment and activation of neutrophils (Tschoeke *et al*., 2006). The role of caspase 1 in the processing of IL-1β and IL-18 is seen as a fundamental finding. Three key NLR molecules have been shown to modulate caspase 1 activity including NLRP1, NLRP3, and NLRC4. Furthermore, a selection of other NLR molecules including, NLRP2, NLRP6, NLRP7, NLRP10, and NLRP12 have been shown to modulate caspase 1 activity *in vitro*. However, current literature focuses on NLRP1, NLRP3, and NLRC4 (Mariathasan & Monack, 2007).

A link between mutation in both NLRP1 and NLRP3 genes and human diseases has been established. Variances in sequences of the NLRP1 gene have been linked to automimmune and autoinflammatory diseases including vitiligo (Jin *et al*., 2007). Furthermore, there is evidence to suggest that NLRP3 mutations are responsible for a host of autoinflammatory syndromes including Muckle-Wells syndrome, familial cold autoinflammatory syndrome and neonatal-onset multisystem inflammatory disease referred to as cryopyrin associated periodic syndrome (CAPS) (Hoffman *et al*., 2001; Dodé *et al*., 2002). Interestingly, mutations identified within the NLRP3 gene have been linked with CAPS, resulting in a predominant active form of NLRP3 leading to potentiated activation of the inflammasome and increased secretion of IL-1β (Ting *et al*., 2006). The use of recombinant human IL-1 receptor

antagonist (IL-1Ra) Anakinra has been shown to be successful in inhibiting IL-1β production and therefore reducing disease severity (Hoffman *et al*., 2004).

1.4.2.1 NLRC4 inflammasome

Upon activation the NLRC4 (IPAF) inflammasome leads to rapid cell death. The components of NLRC4 are an N-terminal CARD, a central NACHT domain and C-terminal LRRs. This complex may also regulate caspase 1 activation and the release of mature IL-1β. Many recent studies have established possible routes for activation of the NLRC4 inflammasome through Gram-negative bacteria (type III or type IV), *Salmonella*, *Shigella*, *Legionella*, and *Pseudomonas*. This is supported by the reduced caspase 1 activation and subsequent IL-1β secretion following the infection of ASC-deficient macrophages with *Salmonella*, *Shigella*, and *Pseudomonas* (Mariathasan *et al*., 2004; Zamboni *et al*., 2006; Suzuki *et al*., 2007; Sutterwala *et al*., 2007; Franchi *et al*., 2007). Although it remains a vital component of the NLRC4 inflammasome, ASC is required for the processing and release of IL-1β, but in its absence the NLRC4 may recruit another caspase in order to mediate cell death. Further investigation of the system is required in order to decipher these NLRC4-dependent but caspase 1-independent cell death programs.

1.4.2.2 NLRP1 inflammasome

The NLRP1 (NALP1) inflammasome is a complex composed of caspase 1, caspase 5, and the adaptor molecule ASC (Martinon *et al*., 2002). It has recently been suggested that NLRP1 activation is dependent on a two-step process, firstly the bacterial cell wall component muramyl dipeptide (MDP) leads to a conformational change in NLRP1, allowing the protein

to bind ribonucleotide triphosphates and oligomerize (Faustin *et al*., 2007). The physiologic role of MDP activation of the NLRP1 inflammasome has yet to be addressed. Surprisingly, ASC was not required for NLRP1 inflammasome activation although caspase 1 activation was potentiated in its presence. Caspase 1 activation and IL-1β production can be suppressed by the interactions of anti-apoptotic proteins Bcl-2 and Bcl-XL with NLRP1. It has been demonstrated that macrophages that lack Bcl-2, exposed to MDP, show increased caspase 1 activity and IL-1β release, however, overexpression of Bcl-2 led to an inhibition of caspase 1 activity and IL-1β production (Bruey *et al*., 2006). A lethal toxin (LT) *Bacillus anthracis* has been shown to cause caspase 1 dependent cell death of macrophages. Furthermore, a murine paralogue of the NLRP1, *Nlrp1b* gene is accountable for this susceptibility of macrophages to LT (Boyden & Dietrich, 2006).

1.4.2.3 NLRP3 inflammasome

Often referred to simply as "the inflammasome", the NLRP3 (NALP3 or cryopyrin) inflammasome is the most well understood of the three main inflammasome complexes. It is well documented that NLRP3 can form a multimeric protein complex with ASC, caspase 1 and Cardinal, which is referred to as the "NLRP3 inflammasome" (Martinon *et al*., 2002). There are still discrepancies between the human and murine NLRP3 inflammasomes based around the role and function of Cardinal, that is present in the human complex but not in the murine version with no homolog having been identified. Several reports have indicated the fundamental role of the NLRP3 inflammasome in activating caspase 1 in response to both microbial and non-microbial stimuli (Franchi *et al*., 2010). A combination of LPS and extracellular ATP activates caspase 1 in a NLRP3-dependent fashion leading to the subsequent processing and release of pro-inflammatory cytokines IL-1β and IL-18

(Mariathasan *et al*., 2006). This is achieved by the activity of the ATP on the $P2X_7$ purinergic receptor, which in turn leads to a potassium efflux and the recruitment of the pannexin-1 channel forming a membrane pore, required for caspase 1 activation (Pelegrin & Surprenant, 2006; Brough *et al*., 2009). Recent studies have demonstrated that the NLRP3 inflammasome can also be activated by many crystalline molecules. This has been shown with monosodium urate crystals and calcium pyrophosphate dihydrate, both involved in the development of gout (Martinon *et al*., 2006). Furthermore, silica and asbestos have been demonstrated to cause fibrotic lung disorders silicosis and asbestosis through a similar pathway (Dostert *et al*., 2008; Cassel *et al*., 2008). Interestingly, the actions of a known adjuvant aluminium hydroxide have also been demonstrated to be dependent upon its activity on the NLRP3 inflammasome (Eisenbarth *et al*., 2008; Kool *et al*., 2008).

Activation of the NLRP3 inflammasome can also be triggered by the actions of various toxins. The actions of nigericin (bacterial potassium ionophore), maitotoxin (marine toxin), and various bacterial pore forming toxins such as listeriolysin O from *Listeria monocytogenes*, aerolysin from *Aeromonas hydrophila* and *Staphylococcus aureus* hemolysins (Mariathasan *et al*., 2006; Gurcel *et al*., 2006). Activation of the NLRP3 inflammasome can also be achieved by the actions of *Mycobacterium tuberculosis*, whilst others have demonstrated the *M. tuberculosis* gene, *zmp1*, can reduce inflammasome activation (Koo *et al*., 2008; Master *et al*., 2007). Furthermore, DNA, bacterial RNA and two antiviral imidazoquinoline compounds (R837 and R848) also induce the NLRP3 inflammasome activation independent of TLR and RIG-I (Kanneganti *et al*., 2006; Muruve *et al*., 2008).

1.4.3 Mechanisms of inflammasome activation

Although it remains unclear if a direct ligand activates the NLRP3 inflammasome, a few mechanisms of activation have been postulated (Figure 1.4). The majority of these mechanisms are based around pore formation on the cell membrane, an action which can be performed by a host of stimuli that include ATP (in combination with pannexin-1) and many bacterial pore-forming toxins. There are two predominant theories as to how pore-formation activated the NLRP3 inflammasome. Firstly disruption of the membrane may release an endogenous molecule that can stimulate the NLRP3 inflammasome (Mariathasan & Monack, 2007; Ogura *et al*., 2006). Secondly, microbial molecules access the intracellular cytosol through these pores and thus can interact directly with the NLRP3 inflammasome (Petrilli *et al*., 2007). It has been demonstrated that silica, alum and amyloid-β lead to lysosomal damage and the subsequent release of cathepsin B that activated the NLRP3 inflammasome (Hornung *et al*., 2008; Halle *et al*., 2008). Although this finding promotes the theory that membrane damage is the major event in the activation of the inflammasome, it provides no insight into the action of molecules such at ATP in NLRP3 inflammasome activation.

Uric acid is a product of purine catabolism that has been identified in dying cells. It is believed that the active form of Uric acid is monosodium urate (MSU), which functions by promoting immune responses, through stimulation of dendritic cells (Shi et al., 2003). Uric acid can form crystals in high localised concentrations, as seen in clinical gout. These crystals can activate the NLRP3 inflammasome leading to the maturation of caspase 1 and subsequent production of active IL-1b (Martinon et al., 2006). It could be hypothesised that cell/tissue injury and necrosis can lead to the production of Uric acid and the production of MSU crystals. These MSU crystals at the site of the injury may subsequently present a danger

signal thus activating the inflammasome and leading to the ensuing inflammation. But this effect may not be universal as Kool et al., show that UA-mediated Th2 responses in the airway are not mediated through the inflammasome (Kool *et al*., 2001).

The activation of the NLRP3 inflammasome via toxins and crystals appears to be dependent on two factors, an intracellular potassium efflux and the production of reactive oxygen species (ROS). It has been suggested formation of the NLRP3 inflammasome may be dependent on decreased potassium levels within the cell (Petrilli *et al*., 2007). Additionally, the capacity of ATP, silica and asbestos to activate the NLRP3 inflammasome are diminished by blocking ROS production using chemical inhibitors (Dostert *et al*., 2008; Cassel *et al*., 2008; Cruz *et al*., 2007). However, NLRP3 inflammasome activation by ROS may be dependent on mitochondrial sources. A recent paper published by Zhou *et al*., NLRP3 inflammasome activation can be achieved through the generation of mitochondrial reactive oxygen species. Furthermore, macrophages treated with NLRP3 activators resulted in the recruitment of NLRP3 proteins to the mitochondria-associated ER membrane (MAMs). This is the site on which the adaptor protein ASC is recruited in order to form a functional NLRP3 inflammasome complex (Zhou *et al*., 2010). Studies have demonstrated mice deficient in NOX2 (gp91phox), a component of the NADPH oxidase system, still undergo inflammasome activation (Hornung *et al*., 2008; Meissner *et al*., 2008). More recently it has been shown that monosodium urate crystals activate spleen tyrosine kinase (Syk) kinase-dependent signalling pathways through actions with rich cellular membranes (Ng *et al*., 2008). This area requires further investigation to determine if it plays a significant role in NLRP3 inflammasome activation.

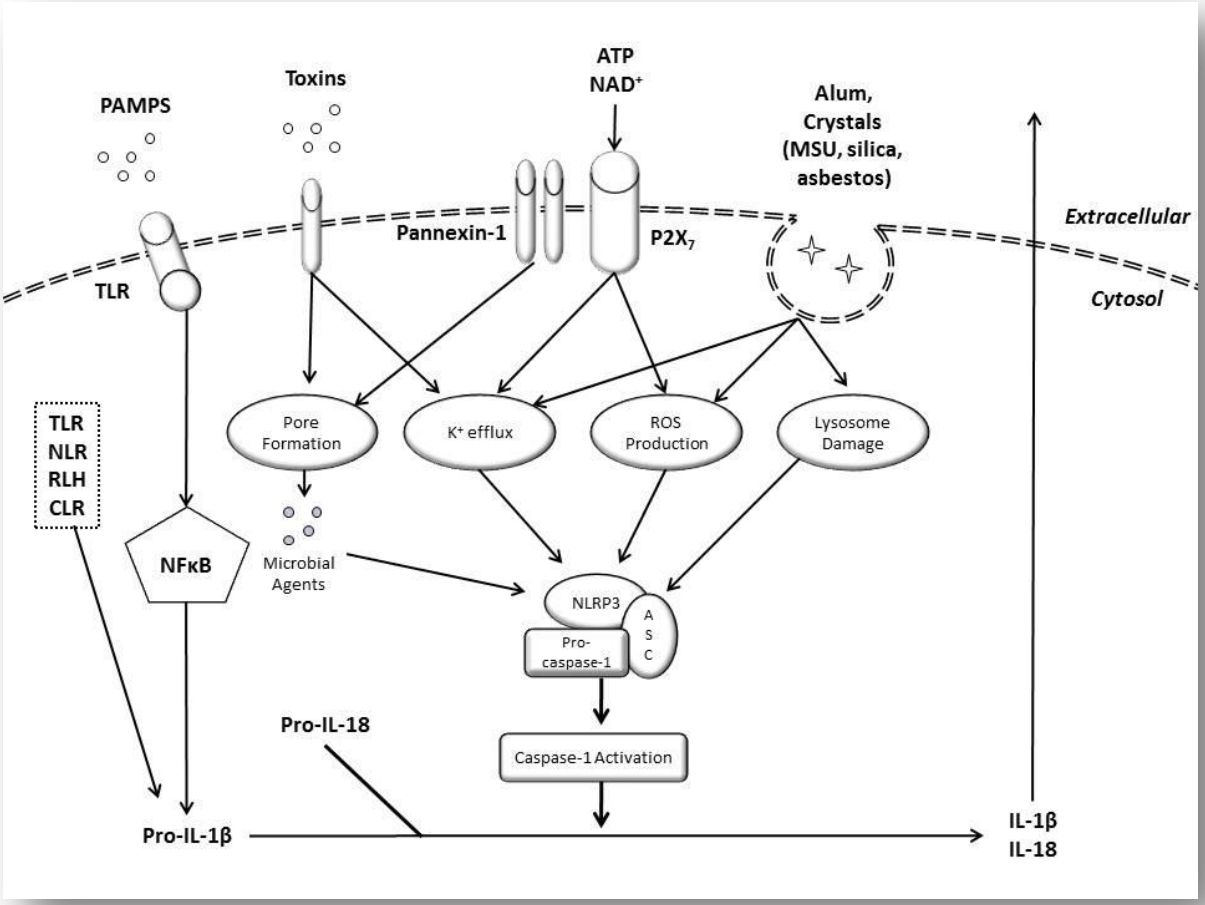

Figure 1.4 – Activation of the NLRP3 inflammasome. *An overview of the signalling cascade associated with the NLRP3 Inflammasome illustrating the array of ways it can be activated (Adapted from Franchi et al., 2009). The processing and subsequent release of pro-inflammatory cytokines IL-1β and IL-18 via caspase 1 can be dependent on the activation of the NLRP3 Inflammasome.*

1.4.4 The inflammasome in COPD

A growing number of recent publications have suggested a role for the NLRP3 inflammasome and its products in the inflammation seen in COPD patients. The NLRP3 inflammasome can be activated through ATP acting on the $P2X_7$ receptor (Mariathasan *et al*., 2006; Sutterwala *et al*., 2007). Extracellular concentrations of ATP are maintained at low physiological concentrations by ectonucleotidases, but these concentrations increase under

conditions such as infection or inflammation. This increase can be due to either greater release of non-neuronal ATP from cells such as epithelial or leukocytes, and/or down-regulation of ectonucleotidases (Lazarowski *et al*., 2003; Robson *et al*., 1997). Recently, increases in ATP levels have been reported in *in vitro/in vivo* models of COPD and pre-clinical smoke-exposure models (Mohsenin & Blackburn, 2006; Polosa & Blackburn, 2009; Mortaz *et al*., 2010; Lucatelli *et al*., 2010). Additionally, increased ATP levels in the lungs of patients with COPD have been shown to be associated with a decline in lung function and an increase in inflammatory cellular burden (Lommatzsch *et al*., 2010; Cicko *et al*., 2010). This increase in ATP levels has been suggested to play a role in the chemotaxis and activation of inflammatory cells, such as neutrophils, through P2Y receptors (Cicko *et al*., 2010; Mortaz *et al*., 2010). Further evidence for a role of the ATP- $P2X_7$ axis comes from the fact that the expression of the $P2X_7$ receptor is increased in disease tissues/cells (Cicko *et al*., 2010; Lucatelli *et al*., 2010). Interestingly, $P2X_7$ Inhibitors have reached phase II clinical trials specifically for rheumatoid arthiritis and COPD. One trial in moderate to severe COPD patients, carried out across 5 countries (28 centres) was unsuccessful. The trial showed no clinically significant findings in any patients for any of the clinical parameters examined during the course of the trial (Arulkumaran et al., 2011).

Although Couillin *et al.*, (2009) have shown a role for the ASC and the IL-1R in an elastase driven model of airway inflammation and associated emphysema, the role of the inflammasome components (NLRP3 and ASC) in smoke driven models of COPD has not been investigated but there is some indirect downstream evidence. A study has shown that CS induced inflammation was blocked with the caspase 1 inhibitor Z-WEHD-FMK (Churg *et al*., 2009).

In the inflammatory *milieu* present in the lungs of human patients with COPD and animals exposed to CS are increased levels of cytokines linked to the activation of the NLRP3 inflammasome i.e. IL-1β and IL-18. Furthermore, there is some evidence to suggest that these cytokines are central to the inflammation seen in models of COPD (Kang *et al*., 2007; Lucey *et al*., 2002; Churg *et al* 2009). Elevated IL-1β levels are found in induced sputum and BAL fluid from COPD patients (Ekberg-Janssen *et al*., 2001; Zeidel *et al*., 2002). More recently Singh *et al*. demonstrated that IL-1β levels were significantly raised in COPD patients, with IL-1β showing a negative correlation with FEV1 suggesting that in COPD, IL-1β serum levels correlate with clinical aspects of disease severity (Singh *et al*., 2010). Furthermore mice over-expressing IL-1β in lung epithelium display a COPD-like phenotype consisting of lung inflammation, emphysema and airway fibrosis (Lappalainen *et al*., 2005). In contrast, mice lacking IL-1 Receptor type 1 (IL-1R) exhibited a significant decrease in airway neutrophilia in response to CS (Doz *et al*., 2008; Churg *et al* 2009). A recently published paper by Pauwels et al., suggests that the inflammation seen in response to cigarette smoke exposure is dependent on IL-1β, however, the release of IL-1β in this model is independent of NLRP3/caspase 1 signalling (Pauwels et al., 2011).

Elevated IL-18 levels have also been found in COPD patients (Petersen *et al*., 2007). These findings are further corroborated by recent publications demonstrating significantly increased levels of IL-18 in sputum supernatants of COPD patients compared to healthy smokers and non-smokers, suggesting that IL-18 may be implicated in the pathogenesis of COPD (Imaoka *et al*., 2008; Rovina *et al*., 2009). Furthermore, IL-18 knockout mice show significantly decreased inflammation and emphysema compared to wild-type mice following CS exposure (Kang *et al*., 2007), whilst mice over-expressing IL-18 in the lung display a COPD-like

phenotype (Hoshino *et al*., 2007). In view of these findings, a strong argument can be made for a role of the inflammasome in the inflammation observed after exposure to CS.

1.5 EXPERIMENTAL MODELS OF COPD

Experimental models provide crucial tools that allow us to investigate and better comprehend the development of disease. Furthermore, they are important for the development and pre-clinical testing of drug discovery efforts that aim to target specific pathways involved in disease progression and exacerbation. In a disease such as COPD, where very few effective therapies exist, models provide an essential tool to obtain vital insight into the underlying mechanisms that drive the disease progression. The complexity of COPD as a disease makes replicating the pathophysiological changes seen in the disease very challenging, particularly the diverse features such as emphysema and small airway disease that are yet to be convincingly reproduced in an animal model. A further degree of complication is introduced by the fact that COPD is exacerbated by viral and bacterial agents.

Currently, there are no standard models (using standardised exposure protocols, chambers or smoking machinery) used to study COPD making the comparison or interpretation of data from various studies very difficult. The limitation of these various modelling systems must be carefully examined and considered before drawing conclusions about disease pathology or linking finding to human health.

1.5.1 *In vitro* models

As cigarette smoke is the primary etiological factor driving the pathogenesis of COPD, various *in vitro* models have incorporated cigarette smoke (CS) to determine its effects on particular pathways of interest. Cigarette smoke contains more than 4700 identified compounds in its vapour and particulate phases (Ingebrethsen, 1986; Green *et al*., 1996). Examination of the literature indicates a wide variety in the methods used to expose cell lines or cultures to CS by different research groups, including exposure to constituents of CS (either purified or extracted from cigarette smoke vapour), whole cigarette smoke or cigarette smoke condensate. In more recent times, various groups have examined the effect of CS on *in vitro* cultures using cigarette smoke conditioned media (CSM) that has been disputed to deliver a more physiologically relevant method of exposure (Bernhard *et al*., 2004).

A wide range of different cell types within the lung are exposed to CS following inhalation, therefore a plethora of cells in the literature have been exposed to CS in culture including cell lines and primary cells. A study demonstrated differences in CS exposure of cell lines and primary cells, where cell lines did not secrete any inflammatory cytokines in response to CS, however, primary epithelial cells secreted two cytokines implicated with COPD, IL-6 and IL-8 (Kode *et al*., 2006). Conversely, alveolar type II cells isolated from normal lung tissue from carcinoma resection surgeries no longer basally expressed IL-8, TNF-α and monocyte chemotactic protein (MCP)-1 following cigarette smoke extract treatment (Witherden *et al*., 2004). Furthermore, Birrell *et al*., demonstrated that exposure of cell lines and primary cells to CSM inhibits LPS-induced inflammatory cytokine release (Birrell *et al*., 2006). These differences in responses to CS in various cell types and cell preparations can be attributed to difference in the preparations of CS, type of cigarettes used and the duration (protocol) of

exposure. Studies in the past have typically focused on single cell type cultures for simplicity purposes, however, more recently the effects of CS on certain disease phenotypes are being examined in more complex cell cultures.

Complex cell cultures incorporating two or more cell types allow a wider range of cell types to be examined to mimic the exposure of various cell types to CS following inhalation. As different cell types may have varying inflammatory profiles depending on the expression of biological components required for inflammatory processes, combining two or more cell types in cultures may paint a more accurate picture of the conditions that are seen *in vivo*. *In vitro* cell systems offer a simple and cost-effective way to test particular tools and targets prior to moving research into a complex *in vivo* setting. However, the valuable insight provided by *in vitro* cell cultures in dissecting the mechanisms and pathways involved in COPD pathogenesis does not mimic the complexity of an *in vivo* system. Therefore the data obtained from these studies must also be carefully considered.

1.5.2 *In vivo* models

The data provided by a clinical sample demonstrating a specific result or particular association with a disease or its progression is considered crucial for validating a particular target for drug discovery purposes. However, in order to obtain powerful evidence that highlights a specific cause-effect relationship between a target and disease-like phenotype animal models have historically proven to be the best tool. For decades animal have played an instrumental role in broadening our understanding of disease mechanisms and pathogenesis. Various approaches have been attempted in order to replicate the phenotype of COPD in animal models, including exposure of animals to CS, inflammatory stimuli (e.g.

LPS) or instilling proteolytic enzymes into the airways and studying the effects of specific KO animals (Mahadeva & Shapiro, 2002; Groneburg & Chung, 2004; Stevenson & Birrell, 2010). However, as the studies in this thesis will be utilising CS, the primary etiological factor for COPD, background will be focused around animal models of CS exposure. Furthermore, the inflammation seen in this model has also been shown to be insensitive to glucocorticoid inhibition both rats and mice (Marwick et al., 2004; Wan *et al*., 2010), providing the most accurate model of disease phenotype in animals. The second model used in this thesis is driven by lipopolysaccharide (LPS), a model previously shown to be sensitive to glucocorticoid inhibition (Birrell et al., 2005), that will facilitate paralleling experiments using a stimulus of the normal innate defence system that induces airway neutrophilia.

1.5.2.1 Models of cigarette smoke exposure

A wide range of CS exposure models are commercially available, whilst some groups also create or adapt their own. Although models vary predominantly around the way animals are exposed to CS, either nose-only or whole body, other variations include the concentration of smoke, duration and frequency of the exposures. The length of the CS exposure protocol is typically believed to replicate different aspects of the disease; acute (3 day) exposures typically produce a neutrophilic inflammatory response (Stevenson *et al*., 2005), whereas chronic (>6 month) exposure are required to bring about emphysematous changes in the lung (Churg *et al*., 2004).

The concentration of CS used to induce inflammation in the lungs of laboratory animals varies from model to model in the literature. Although most report a value using the TSP (total suspended particulate) standard, these figures vary significantly based on the type of

cigarette used and the amount of CS being drawn/pumped into the chamber at any given time. The duration and frequency of exposures is also variable, however, typically a 1 hour exposure twice daily seems to be the standard used by most research groups.

1.5.2.2 Choice of animal species

Various species have been used to investigate CS-induced inflammation, including guinea pigs, rats and mice (Churg *et al*., 2008). It has been demonstrated that chronic CS exposure in guinea pigs led to progressive emphysematous changes that were associated with changes in lung function consistent to those observed in human emphysema patients (Wright & Churg, 1990). Whilst there are many advantages to working with guinea pigs, the disadvantages working with this species outweigh using others. Guinea pigs are expensive, and there is a serious lack of tools and antibodies commercially available that cross react with guinea pig proteins. Therefore most laboratories use rodents in order to develop CS-driven models of inflammation.

Most of the complex features of COPD have been replicated in mice, rats and guinea pigs including chronic inflammation, emphysema and small airway remodelling (Churg *et al*., 2004; Wright *et al*., 2007). However, other aspects of the disease such as mucus hypersecretion have been difficult to reproduce, although they have been reported in rats (Zheng *et al*., 2009). The literature affirms that most models of CS exposure have preferentially selected mice over rats as mouse models offer many advantages. These include, cost effectiveness, extensive gene and protein sequences and a wide range of biological tools/antibodies available. More importantly, the ability to produce mice with specific gene

modifications provides major insight into the underlying mechanisms driving the pathogenesis of COPD (Wright *et al*., 2008).

1.5.2.3 Limitations of CS models

One of the limitations of the CS exposure as an *in vivo* model is that there is currently no standardised method or protocol by which animals are exposed. There are many variations in how different groups expose animals, these include differences in strains or species used, different cigarettes used to generate smoke (commercial vs. research cigarettes), differences in the component of the smoke animals are exposed to (mainstream vs. sidestream), different delivery systems (whole body vs. nose-only) and most significantly the dose of smoke that is delivered to the animals. Variations in the dose of smoke delivered to the animals can be attributed to many design or mechanical factors in the various cigarette smoke exposure apparatus, however, the puff profile of each system may also vary. Many groups however, attempt to replicate the FTC (Federal Trade Commission) puff profile which suggests that smokers draw smoke for 2 seconds. Variations in the length of time air is drawn through a cigarette can affect the composition of the smoke generated as the temperature of the tip may vary. These differences make comparisons between findings of different research groups extremely difficult, although many groups have used different systems and reported similar findings (Vlahos *et al*., 2006; Morris *et al*., 2008). The protocol and dosing regimen developed here is similar to that of Morris *et al*., and produced similar results with 3 days of acute cigarette smoke exposure in C57BL/6 mice causing an increase in neutrophils peaking at 24 hours after challenge, followed later by macrophages (Morris *et al*, 2008).

Another limitation observed with CS models of inflammation is that the disease phenotype produced is typically mild, corresponding to GOLD I or II of human COPD (Hogg *et al*., 2004). Furthermore, most *in vivo* studies have examined a single aspect of COPD, such as inflammation, emphysema or mucus hypersecretion, but not the entire disease with all its features. This has the effect of making it difficult to model AECOPD as there is a lack of a comprehensive model of COPD. To address this problem, studies have begun to focus on factors that are associated with both COPD and AECOPD, and incorporate them in combination into experimental models (Gaschler *et al*., 2009; Kang *et al*., 2009)

Approximately 25% of smokers develop COPD, whilst 80% of COPD patients are smokers. Therefore there is a portion of COPD patients who get COPD independently of smoking. This model of COPD does not take into account patients who have a genetic predisposition to COPD development, or suffer from the disease as a result of alternative causative agents such as pollution. As models of CS exposure aim to replicate a complex disease that manifests itself over a long period of time, it is imperative to carefully interpret the data in order to provide insight into the mechanisms behind a very complex disease.

1.6 TREATMENTS FOR COPD

1.6.1 Smoking Cessation/Alternatives

Smoking cessation has been shown to slow the progress of COPD; however this will not terminate the progression of the disease (Barnes, 2000). Quitting smoking addiction is a difficult process and most smokers will require additional aid, as very few manage to quit through will power alone. There are currently two commonly available therapies to battle

nicotine addiction; nicotine-replacement therapy (available as gum, inhaler or a transdermal patch) and *Bupropion* (Zyban®), a noradrenergic anti-depressant. Nicotine-replacement therapy is often the first option, however if this is unsuccessful, treatment of bupropion chewing can be administered. Studies have shown that following a nine week course of bupropion 30% of subjects had successfully quit smoking compared to 15% taking the placebo (12 months following course) (Jorenby *et al.,* 1999). Recently, *Varenicline* (Champix®) an α4β2 nicotinic cholinergic receptor partial agonist has been marketed to have a 44% success rate at smoking cessation (Jorenby *et al*., 2006), however, many argue that this figure is closer to 1 in 5 (Mahvan *et al*., 2011). Furthermore, many side-effects have been linked to *Varenicline* administration, including nausea, headaches, difficulty sleeping and abnormal dreams. The psychiatric side-effects of this drug associated with suicidal behaviour have raised question marks about its ethical use as a smoking cessation drug (Gunnell *et al*., 2009; Moore & Furberg, 2009).

The Hookah (water pipe) is growing in popularity worldwide as a fashionable social smoking activity, with the general population erroneously assuming that the water in the pipe is able to filter the harmful agents in the smoke. Two recent studies reported an association between WPS and lung cancer, decreased respiratory function and respiratory illness (Raad *et al*., 2011; Hakim *et al*., 2011; Chan & Murin, 2011).

An alternative approach to combat nicotine addiction is the use of nicotine delivery systems, such as electronic cigarettes. Electronic cigarettes (e-cigarettes) use a battery-powered atomiser to produce vapour that is passed through cartridges containing nicotine, flavouring agents and humectants (e.g. glycerol) (Flouris & Oikonomou, 2009; Hadwiger *et al*., 2010). They are often marketed as the "safe way" to smoke as they don't contain the harmful

substances found in cigarette smoke, however, recent studies have demonstrated that the humectants in e-cigarettes often contain diethylene glycol a harmful agent found in antifreeze. At this current time the long-term effects of e-cigarette use remain unclear and further investigation into its components and effects must be examined (Etter & Bullen, 2010). Other smoking cessation options include unproven treatments such as hypnosis and Chinese herbal remedies which may be successful for some individuals.

1.6.2 Long-term oxygen treatment

Long-term oxygen treatment (LTOT) has been documented to reduce COPD mortality; however, this has only been successful in patients suffering from advanced COPD, particularly severe hypoxemia but with little co-morbidity. A large proportion of the costs of treating COPD patients is due to home oxygen therapy. It is estimated that there are approximately 800,000 patients in the United States alone receiving LTOT, at a cost of $1.8 billion annually (O'Donohue & Plummer, 1995). The mortality of stable COPD patients with a resting pO_2 of less than 7.3 kPa (Kilopascals) can be reduced by oxygen therapy for 15 hours or more a day (Calverley, 2001). However, this is seen as a major disadvantage as patients must remain on oxygen for the majority of the day. LTOT reduces mortality from secondary vascular complications; however it has no effect on the progression of the disease and limited impact on the survival of these patients (Crockett *et al*., 2001).

1.6.3 Pulmonary Rehabilitation

In patients with severe COPD, introduction of a weekly routine made up of education, exercise and physiotherapy has been shown to produce some improvements in exercise

capacity (longer walking distances and reduced fatigue) and health-related quality-of-life (HRQL) (Lacasse *et al.,* 1996; Boueri *et al*., 2001).

1.6.4 Lung-volume reduction surgery

Lung-volume reduction surgery (LVRS) necessitates removal of the emphysematous parts of the lung. Patient selection is an important part of this procedure and patients with localised upper-lobe emphysema and low lung resistance during inspiration are preferred and have been shown to respond best to this treatment (Ingenito *et al.,* 1998). The overall effect is a reduction in the volume required to fill by each inspiration, aiming to achieve full inflation of the lungs. This reduction in hyperinflation has the effect of improving the mechanical efficacy of the inspiratory muscles. Functional improvements in FEV1, ventilatory function, function of respiratory muscles, exercise capacity and overall quality of life have all been documented (Gaissert *et al.,* 1996). However there are several drawbacks to LVRS that include the risk associated with surgery in patients that are already compromised and the expenses associated with the procedure, with lifetime costs following surgery estimated to reach approximately $100,000 in the United States (Patel *et al*., 2008).

1.6.5 Lung transplant

Lung transplantation is now an established end-point for various respiratory diseases. Refinements in surgical techniques and medical management have been effective in increasing the success rate of most lung transplants (Gomez & Reynaud-Gaubert, 2010). Patients also report a significant improvement in quality of life following a successful lung transplant operation (Ramsey *et al*., 2005). However, the lifetime costs of surgery and post-

operative care are significant; with the average costs in the United States reported to be approximately $450,000 (Ramsey *et al*., 1995; Anyanwu *et al*., 2002). Post-transplantation survival rates for COPD patients undergoing lung transplantation are approximately 80% at year 1, 65% at 3 years and 49% at 5 years (Trulock *et al*., 2007). The availability of lungs for transplantation does not meet the numbers required by patients suffering from COPD or other diseases of the lung. Furthermore, there are many difficulties and risks involved with lung transplant surgery including variable waiting-list times and post-transplantation complications such as opportunistic infections, organ rejection and side-effects to post-transplantation medication (Trulock *et al*., 2007; Patel *et al*., 2006)**.**

1.6.6 Bronchodilators

Bronchodilators have not been shown to have an effect on the progression of COPD; but they are proven to be useful symptom controllers. There are two types of bronchodilators used to treat COPD, β_2-adrenoceptor agonists (β_2-agonists) and anti-cholinergics.

β_2-agonists activate the β_2-adrenoceptors on smooth muscle, causing relaxation of the bronchi. β_2-agonists themselves are further sub-categorised into short and long-acting groups. Shorter-acting β_2-agonists agonists, e.g. *salbutamol*, are not as effective in treating COPD with less than 15% improvement as the disease encompasses irreversible airflow obstruction (Hay, 2000). Long-lasting β_2-agonists agonists (LABA) such as *salmeterol* are now used and shown to provide modest improvements in lung function and symptom control clinically associated with an improvement in well-being (Jones & Bosh, 1997; Leckie *et al*., 2000).

Anti-cholinergic drugs act upon muscarinic receptors. They are used as bronchodilators in treating COPD and are also thought to inhibiting mucus secretions in the airways (Kerstjens & Postma, 2003). In COPD patients, Tiotropium Bromide achieves a significant and prolonged bronchodilation, lasting up to 32 hours (Maesen *et al*., 1995). However, similar to β_2-agonists, there is no evidence that anticholinergic bronchodilators impact the rate of decline in lung function (FEV1) in COPD patients; therefore, they do not alter disease progression (Anthonisen *et al*., 1994). Anti-cholinergics however, are often used in conjunction with β_2-agonists as a combination therapy, proving to be more effective than anti-cholinergic treatment alone (Rennard *et al*., 2001).

1.6.7 Corticosteroids

COPD, like asthma, has an inflammatory component; therefore inhaled corticosteroids are commonly administered as part of treatment. There is little evidence that suggests corticosteroids are effective in treatment of COPD. Four large trials (ISOLDE – Burge *et al*., 2000; EUROSCORE – Pauwels *et al*., 1999; COPENHAGEN – Vestbo *et al*., 1999; Lung Health Study Research Group, 2000) conducted over three-year periods administering inhaled corticoid steroids showed little effect in improving lung function in COPD patients. A reduction in the number of exacerbations has been demonstrated (Alsaeedi *et al.,* 2002), however, recent meta-analysis suggests that inhaled corticosteroids have little effect on the decrease in lung function that is characteristic of the disease in patients with no evidence of concomitant asthma (Highland *et al*., 2003)**.**

Corticosteroids do slow the progression of COPD. The current GOLD standard treatment for COPD in the clinic is a combination of corticosteroids and long-acting β_2-agonists (Adcock *et*

al., 2010). Furthermore, studies have demonstrated that combination therapy of corticosteroids and the methylxanthine drug theophylline may attenuate airway inflammation in patients with COPD (Ford *et al*., 2010). Much recent work into its in-effectiveness has been related to the action of histone deacetylases, such as histone deacetylase 2 (HDAC-2) which has been shown to have decreased levels in COPD patients (Barnes *et al*., 2004). The current dogma suggests that corticosteroids can inhibit the activation of inflammatory genes through the recruitment of HDAC-2 which in turn can deacetylate histones to allow the chromatin structure to remain tightly bound thus decreasing the binding of transcription factors (Barnes, 2006; Adcock *et al*., 2005). Furthermore, the actions of ROS and CS can inhibit HDAC-2 activity, leading to reduced responses to corticosteroids in COPD patients (Barnes, 2009).

1.7 THESIS AIMS

Although giant leaps have been made over the last decade in understanding the immune responses and identifying the underlying mechanisms driving the pathophysiological changes seen in COPD, there is still a large area of uncertainty with regards to the causative factors or agents. Furthermore, there are currently no effective therapies to combat the relentless progression of this disease therefore novel pharmacotherapies are a crucial requirement. However, the proposal of the inflammasome as a possible pathway involved in the inflammation associated with chronic inflammation of the airways is a logical one given the convincing evidence to suggest its involvement in COPD.

The aim of this thesis was to investigate the role of the $P2X_7$ – inflammasome pathway in CS-induced inflammation associated with COPD. The broad hypothesis within this thesis was

that exposure of the lung to an insult such as cigarette smoke leads to the release of endogenous danger signals such at ATP, which activate the $P2X_7$ receptor leading to inflammasome activation. Upon activation of the inflammasome, caspase 1 matures into its active form facilitating the processing and release of the two potent inflammatory cytokines IL-1β and IL-18. These cytokines in turn drive the ensuing inflammation within the lung and bring about the acute changes seen in COPD. Upon repeated exposure to the insult, this process becomes chronic leading to the long term changes seen in COPD patients such as emphysema and small airways disease.

The studies in this thesis were completed in a sequential manner with each study building on the findings of the previous. In chapter 3, in order to determine the role of the *pathway* in CS driven models of airway inflammation my first step was to optimise and characterise the airway responses to CS exposure. I chose to do this in the C57BL/6 strain as this is the background strain the genetically modified mice our group has access to. I began with a dose response to CS and from this data I selected a sub-maximal exposure protocol to adopt for my future work. I then performed a detailed characterisation (i.e. cellular burden, mediator production at the mRNA and protein level) of the temporal inflammatory changes in the lung after acute (3 days) CS exposures. In parallel to the CS driven model I wanted to compare the role of the *pathway* in the inflammation evoked by a different stimulus. For this I chose an endotoxin challenge (lipopolysaccharide, LPS) as the inflammatory profile has similarities to the CS model i.e. reported increase in IL-1β and neutrophilia in the lung. I observed temporal increases in airway neutrophilia and inflammasome linked cytokines (IL-1β and IL-18) in both the LPS and CS models. When I measured caspase 1 activity, as a marker of *pathway* activation, in the lung samples, I could only detect increases in the CS models and not the LPS model. In chapter 4, I found that the increased caspase 1 activation, IL-1β production

and neutrophils seen following acute CS exposure were attenuated in the $P2X_7$ KO mice; however these mice did not have decreased levels of IL-1β or neutrophils after LPS challenge.

In chapter 5, I wanted to confirm the effect observed in the genetically modified mice using pharmacological inhibitors of the $P2X_7$ receptors. Before performing the *in vivo* studies I first wanted to demonstrate that the inhibitors I acquired would block murine receptors. Therefore I developed human and mouse cell based assay systems, using disease relevant cells, in which the *pathway* played a central role. I showed that the combination of LPS and ATP exhibited an enhancement in the release in IL-1β and IL-18 when compared to the sum of the two individual treatments alone. In these assay systems I showed that one of the inhibitors (A-438079) was effective at blocking murine $P2X_7$ receptors. What is more the data demonstrated that the inhibitor had no impact on other non-*pathway* linked mediators like TNFα and IL-6. Using this inhibitor in the smoke driven murine model I was able to parallel the findings with the genetically modified mice. Together these data are strong evidence for a role of the $P2X_7$ receptor in this murine model of CS induced inflammation.

COPD is a chronic disease that manifests itself over a prolonged period of time, therefore it was essential to investigate the involvement of the *pathway* in a more chronic model. In chapter 6, I performed a detailed characterisation of the temporal inflammatory changes in the lung after sub-chronic (28 days) CS exposures. I demonstrated an increase in caspase 1 activity, inflammasome-linked cytokines and neutrophilia throughout the 28 day exposure protocol. Furthermore, macrophages were also seen 14 days into the exposure protocol. In an attempt to translate these findings in the human disease, the same assay utilised in the *in vivo* models was used to measure caspase 1 activity in donors or recipients lung tissue samples

collected from lung transplant surgery performed on end stage emphysema/COPD patients. Whilst there are some issues as to whether a direct comparison is appropriate, i.e. the groups are not age matched, there appears to be an increased level of caspase 1 activity in the diseased lung.

Chapter 2

Methodology

2.1 Animals

All studies were conducted using C57BL/6 mice (18 – 20 g) as this is the background strain of the knockout mice used in this thesis. The animals were obtained from Harlan-Olac (Bicester, UK) and housed for at least 5 days prior to any experimental procedures being carried out. Food and water was supplied *ad libitum* throughout housing and experimental periods. All experimental protocols were approved by a local ethical review process and conformed to the strict Animals (Scientific Procedures) Act 1986 (UK Home Office guidelines).

2.2 In vivo models

The various challenging and exposure protocols for the *in vivo* experiments performed for the purpose of this thesis are described in more detail in their specific chapters. This chapter provides an overview of the general methodologies used in all the models.

2.2.1 LPS-induced airway inflammation

A lipopolysaccharide (LPS) challenging system (Figure 2.1) was set up using a Perspex chamber (600 x 240 x 350 mm) and a System 22 nebuliser (Medic-Aid Ltd., Pagham, Sussex) driven by a high-flow-rate compressor (Medic-Aid Ltd., Pagham, Sussex). Animals were exposed to either aerosolised LPS (Escherichia coli, serotype 0111:B4, Sigma-Aldrich Ltd. Poole, UK) or endotoxin free saline (Fresenius Kabi, Warrington, UK) blown into the Perspex chamber for a 30 minute challenge period.

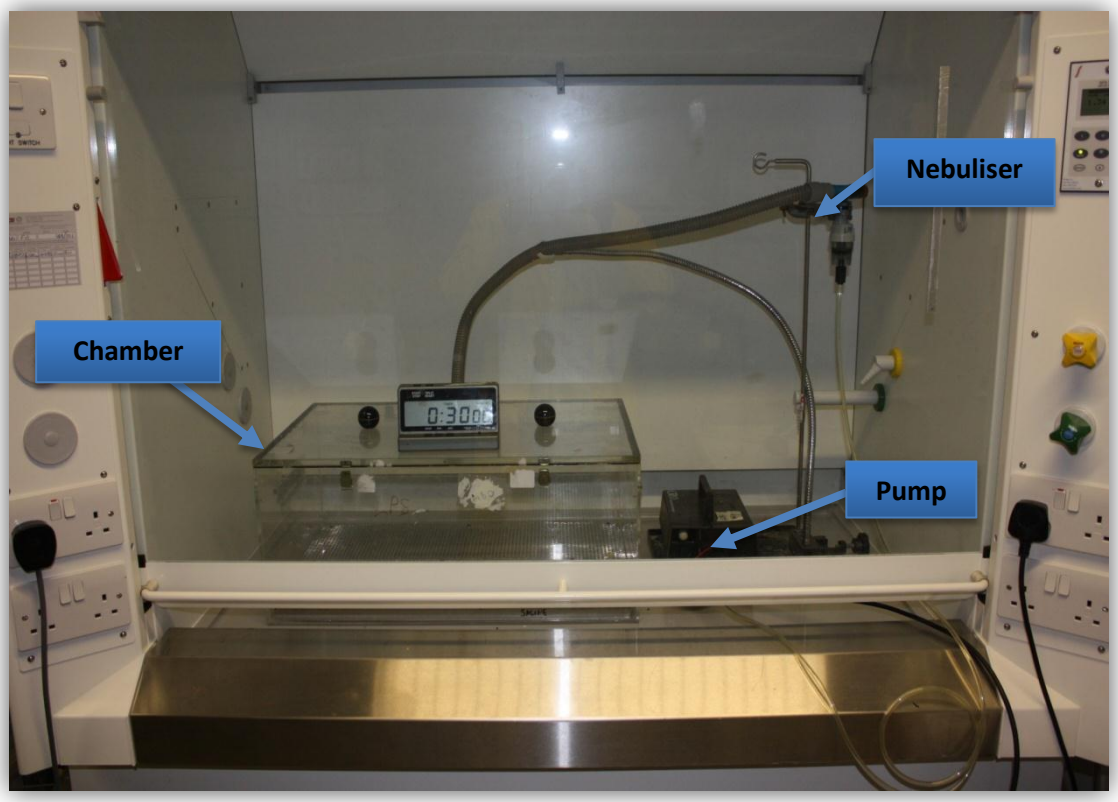

Figure 2.1: LPS challenging system

2.2.2 Cigarette smoke-induced airway inflammation

A whole body cigarette smoke exposure system (Figure 2.2) was developed consisting of a Time-Set Pinch Valve (C Lee Machining, Horsham, UK), Exposure Chambers (Teague Enterprises, CA, USA), Extraction Unit (Grainger Industrial Supply, USA) and TSP Sampling Unit (Teague Enterprises, CA, USA).

Animals were exposed to either room air or cigarette smoke using 3R4F cigarettes (Tobacco Health Research Institute, University of Kentucky, Lexington, KY). Cigarette smoke is generated using a negative pressure system (flow-rate set at 1500 ml/min through the system) and timer pinch-valve to pump in smoke for pre-determined times based on the concentration

of smoke required within the chambers. Room air is continuously pumped into the chamber for the remaining period between puffs. The duration of exposure periods was 50 minutes followed by a 10 minute venting period at the end where the flow is increased to maximum. Exposures for each group will take place in one of the Teague chambers (136 L) chambers. A fan is placed at the bottom of the chamber on the left side where the smoke enters the chamber to ensure that the smoke is well dispersed throughout the chamber. Total suspended particulate (TSP) levels are assessed for each chamber at 15 minute intervals (15, 30, 45 minutes - 1 min sampling period) in order to validate the consistency of the smoke concentration within the chambers.

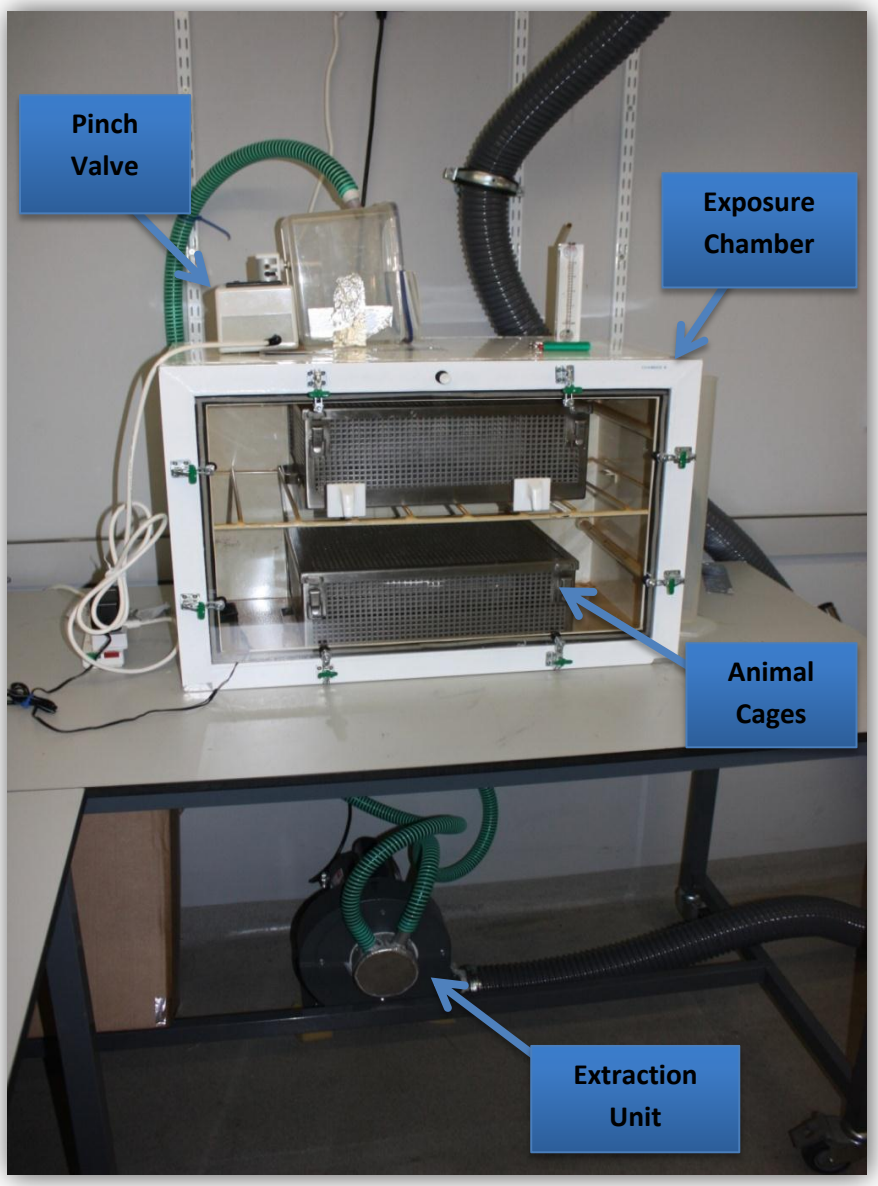

Figure 2.2: Cigarette smoke exposure system

2.3 General Experimental Protocols

2.3.1 Bronchoalveolar lavage and lung tissue processing

Mice were euthanized at specified time-points with an overdose of intraperitoneal (i.p.) sodium pentobarbitone (200 mg/kg). To facilitate the recovery of cells from the airway lumen, the trachea was isolated by blunt dissection and cannulated. Brochoalveolar lavage

was performed by instilling the lungs with 0.3 ml of Roswell Park Memorial Institute 1640 medium + GlutaMAX-I (RPMI, Invitrogen, Paisley, UK,) and then removing the media 30 seconds later. This process was repeated three times and the samples pooled for each animal. For each individual sample, aliquots were taken for total cell counts and differential cell counts (described in section *2.3.2*). The remaining BALF samples were spun at 1900 rpm (Mistrall 3000i, MSE) for 10 minutes at 4°C. The supernatant was then removed and stored at -20°C for future analysis.

After BAL was performed, the thorax of the animal was opened and the lungs were surgically removed. Lungs were either flash frozen in liquid nitrogen (stored at -80°C) or weighed and finely chopped using a McIlwain tissue chopper (Campden Instruments Ltd, Loughborough, UK), and transferred to 1 ml RPMI 1640 / 10% Foetal Bovine Serum (FBS) (Gibco, Invitrogen Ltd., Paisley, UK) for enzymatic digestion (Underwood *et al*. 1997).

Enzymatic digestion was performed by incubating the samples in a water bath (37°C for 1 hour) with gentle agitation with a further 4 ml of RPMI / 10% FBS containing collagenase (1 mg/ml, Roche Diagnostics, Mannheim, Germany) and DNAse (0.025 mg/ml, Roche Diagnostics, Mannheim, Germany). The samples were then filtered using a cell sieve (70 μm mesh size) and washed twice by centrifuging for 10 minutes at 1900 rpm, discarding the supernatant each time and re-suspending the pellet in 10 ml RPMI / 10% FBS. After the second wash, the sample was centrifuged again for 10 minutes at 1900 rpm, the supernatant was discarded and the cells re-suspended in 1 ml RPMI / 10% FBS with penicillin/streptomycin (Roche Diagnostics, Mannheim, Germany). This was then used for the total tissue cell count and differential cell counts (described in section *2.3.3*) the samples underwent a further 1:5 dilution in RPMI / 10% FBS.

2.3.2 Blood sampling

Cardiac puncture was performed using heparinised syringes in order to extract one millilitre of blood. The samples were centrifuged at 2500 rpm (Mistrall 3000i, MSE) for 10 minutes at 4°C. Plasma was collected and stored at -20°C for future analysis.

2.3.3 Cell counts

Total cell counts were performed on the cells recovered in the BALF from the airway lumen and lung tissue using an automated Sysmex cell counter (Sysmex UK Ltd, Milton Keynes, UK). The automated cell counter was calibrated with a reference blood sample containing a known number of white and red blood cells prior to every experiment.

Furthermore, differential cell counts were performed on the cells recovered in the BALF from the airway lumen and lung tissue by light microscopy (x40 magnification) utilising cytospin preparations. These were prepared by centrifuging 100 µl aliquots in a cytospin (Shandon, Runcorn, UK) at 700 rpm with low acceleration for 5 minutes at room temperature. The slides were then fixed and stained on a Hema-tek 2000 (Ames Co., Elkhart, USA) using modified Wright-Giemsa stain. Differential cell counts on 200 cells per slide were carried out using standard morphological criteria and the percentage of neutrophils, eosinophils, lymphocytes and macrophages/monocytes were determined. The staining allows each cell type to be identified based on unique characteristics (Figure 2.3). Neutrophils are medium sized cells that can be identified by their polymorph multi-lobed nucleus, whilst their cytoplasm is faintly stained. Eosinophils are unique due to their "figure eight" or bilobed nucleus that stains dark blue, whilst their cytoplasm stains a unique shade of pink due to the

presence of granules. Lymphocytes cells are the smallest of all cell types and can be characteristically identified due to their dark staining nucleus and almost no presence of cytoplasm. Macrophages/monocytes are larger cells that have a dark staining nucleus and rather large cytoplasm that is slightly darker staining in monocytes when compared to macrophages.

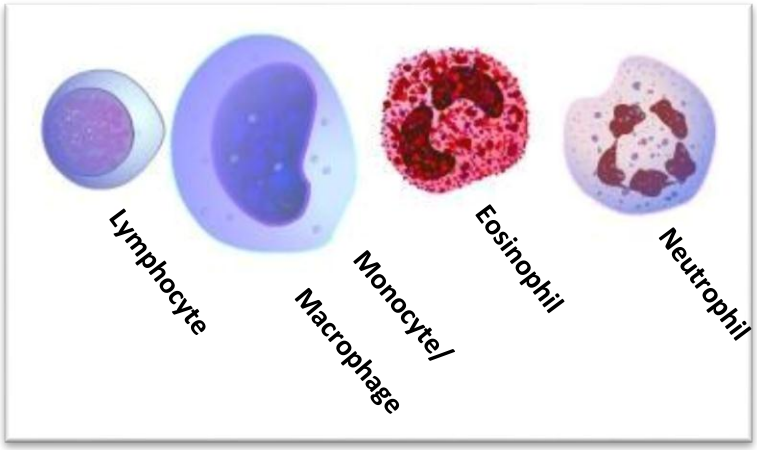

Figure 2.3: Differential inflammatory cell staining

Throughout this thesis cell counts from LPS exposure studies will be performed using a 3-way cell count (neutrophils, eosinophils and lymphomononuclear cells) where lymphocytes and monocyte/macrophages were grouped in one category. However, cell counts from CS exposure studies will be performed using the above detailed 4-way cell count.

2.3.4 Measurement of cytokine release

In order to accurately determine the levels of cytokine/chemokine release in samples, two assays were used based around the enzyme-linked immunosorbant assay (ELISA) techinique. The simple ELISA facilitates the accurate determination of cytokine/chemokine levels in samples. However, in experiments where a wider range of cytokines was to be investigated,

the more complex MSD platform was used as it requires a much smaller amount of sample to examine a wider range of targets.

2.3.4.1 ELISA – Enzyme-linked immunosorbant assay

The presence of various cytokines of interest in BALF supernatants were determined by ELISA. The mouse DuoSet® kits were purchased from R&D Systems Europe (Oxfordshire, UK) and performed according to manufacturer's instructions. These assays employ the quantitative sandwich enzyme immunoassay technique. This involves a monoclonal antibody, specific for the cytokine of interest, being coated onto a microplate. Standards and samples which contain the cytokine present are bound to the immobilised antibody. After a wash step of removing any unbound substance, an enzyme-linked polyclonal antibody specific for the cytokine of interest is then added to the wells. Following another wash step to remove any unbound antibody-enzyme reagent, the assay is visualised using a streptavidin-enzyme, an ensuing chromagenic substrate reaction and stopped using an acid solution (H_2SO_4). The plate is read at 405 nM using a spectrophotometer (Biotek PowerWave XS Plate Reader, Potton, UK). The amount of cytokine detected in each sample is compared to a standard curve of the cytokine of interest, which demonstrates a direct relationship between the absorbance measured and cytokine concentration. The higher the cytokine concentration, the darker the colour intensity, hence the higher the absorbance value. The accuracy of the ELISA is restricted by the detection limit of the assay, these being the concentrations of the lowest and highest standards.

2.3.4.2 MSD multiplexed cytokine assay

The advantage of using the MSD system to measure BALF cytokines is that a small volume of sample (10 µl/well) can be used to measure multiple targets in a single well. Each target binds to the plate via a specific capture antibody and is detected using a SULFO-TAG-labelled secondary antibody. SULFO-TAG labels emit an electrochemiluminescent signal following electrochemical stimulation at electrodes integrated into each well.

Cytokine measurements were made using a Mouse TH1/TH2 96-well, 9-plex Ultrasensitive plate (Mesoscale Discovery, Cat. No: N05013B-1, Gaithersburg, ML, USA) and two multispot 96-well high binding 5-plex and single-plex prototype plates (Mesoscale discovery, Cat. No: N75ZB-1, Gaithersburg, ML, USA). The cytokines measured on each plate are summarised in Figure 2.4. Analysis was carried out according to the manufacturer's instructions using a SECTOR® Imager 2400 (Mesoscale Discovery, Cat. No: N05013B-1, Gaithersburg, ML, USA) at UCB-Celltech, Slough, UK.

MSD Plate Name	Cytokines & Chemokines measured
Mouse TH1/TH2 96-well, 9-plex Ultrasensitive plate	KC, IL-1β, TNFα, IFNγ, IL-4, IL-5, IL-2, IL-10 & IL-12
Mouse multispot 96-well high binding 5-plex prototype plate	Eotaxin, G-CSF, IL-13, IP-10 & MIP-1α
Mouse multispot 96-well high binding single-plex prototype plates	IL-18

Figure 2.4: Summary of cytokines measured using MSD technology.

2.3.5 Measurement of Caspase-1 Activation

Caspase 1 is an enzyme that is responsible for the proteolytic cleavage of other proteins, such as the precursor forms of the inflammatory cytokines IL-1β and IL-18, into their mature active forms. This enzyme has been demonstrated to be present in the cytoplasmic fraction of cells. Therefore, in order to determine the activity of this protein in various samples, the cytoplasmic fraction must be isolated first.

2.3.5.1 Isolation of cytosolic and nuclear cell fractions

Nuclear and cytosolic fractions were prepared using an NXTRACT CelLytic NuCLEAR Extraction kit (Sigma-Aldrich Ltd., Poole, UK) according to the manufacturer's instructions. The procedure for the nuclear protein extraction method is to allow cells to swell with hypotonic buffer. The cells are then disrupted, the cytosolic fraction is removed, and the nuclear proteins are released from the nuclei by a high salt buffer. Following the extraction of both the cytosolic and nuclear fraction, the total protein concentration of each fraction was determined by Bradford assay (Biorad, Munich, Germany, 500-0006).

2.3.5.2 Caspase 1 activity assay

The level of caspase 1 activation in samples was determined using a commercially available caspase 1 Colorimetric Assay Kit (Enzo Life Sciences, Exeter, UK) performed according to manufacturer's instructions in a 96 well plate. The assay facilitates examining the activity of caspase 1 via its ability to recognize the YVAD sequence. The assay is based on spectrophotometric detection of the chromophore p-nitroaniline (*p*NA) after cleavage from

the labelled substrate YVAD-*p*NA. The light emission of *p*NA is detected using a spectrophotometer at 405 nm. By comparing the absorbance of *p*NA from control and treated groups, the fold increase in caspase-1 activity can be determined.

2.3.6 Measurement of ATP release

The ATPlite luminescence ATP detection system (Perkin Elmer, Cambridge, UK) was used according to manufacturer's protocol to determine the levels of ATP in various samples. The advantages of this assay being its rapid, simple and highly sensitive. The ATPLite assay system is based light emitted by the reaction of ATP with added luciferase and D-luciferin. This is illustrated in the following reaction scheme:

$$\text{ATP} + \text{D-Luciferin} + O_2 \xrightarrow[Mg^{2+}]{\text{LUCIFERASE}} \text{Oxyluciferin} + \text{AMP} + PP_i + CO_2 + \text{Light}$$

Thus, the amount of light emitted is proportional to the ATP concentration.

2.3.7 Measurement of NAD+/NADH

To determine the levels of NAD+/NADH the Amplite Colorimetric NAD/NADH Assay Kit (Stratech Scientific, Suffolk, UK) was used according to the manufacturer's instructions. Similar to the ATP assay described in previously (section *2.3.6*) the advantages of this assay are its sensitivity, speed and simplicity. The assay functions by utilising specific enzymes that recognize NAD/NADH in an enzyme cycling reaction that significantly increases detection sensitivity (Figure 2.5).

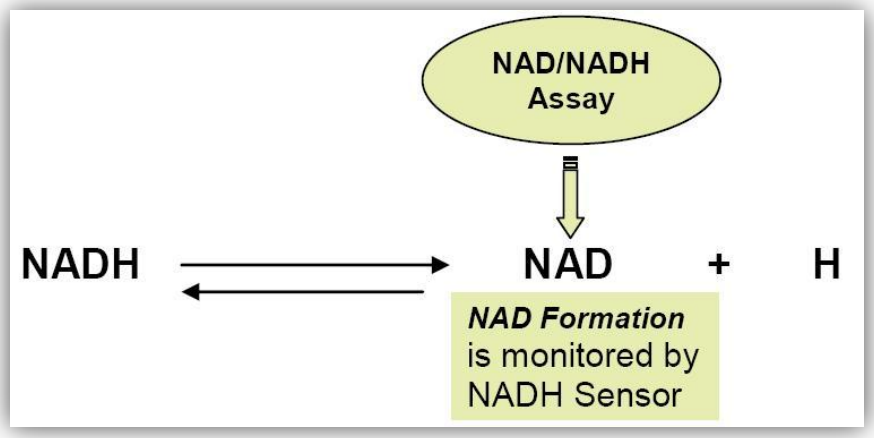

Figure 2.5: Principle of the Amplite NAD+/NADH Colorimetric Assay

2.3.8 Quantification of mRNA expression

2.3.8.1 RNA extraction

Total cellular ribonucleic acid (RNA) was isolated from mouse lung using Tri Reagent, a mixture of guanidine thiocyanate and phenol in a non-phase solution. Tri Reagent dissolves RNA, DNA and protein facilitating the simultaneous isolation of these different components, and subsequent addition of chloroform will separate the RNA, DNA and proteins in 3 different phases. As only RNA was required for gene expression analysis, 50-100 mg of mouse lung tissue was ground using a pestle and mortar to create a powder. The powder was then transferred to an eppendorf tube and 1 ml of Tri Reagent was added to the tube followed by centrifugation at 15000 x g for 15 minutes at 4ºC in a benchtop microcentrifuge (Sigma 2K15, Sigma-Aldrich Co., Poole, UK). The clear supernatant was collected and 200 µl of chloroform was added. This was followed by another centrifugation step, and the aqueous fraction was collected and isopropanol was added (one tenth of the aqueous fraction). Samples were then centrifuged at 12000 g for 10 minutes at 4^{o}C. In the next step, the

supernatants were transferred to a new eppendorf prior to the addition of isopropanol (500 µl) that will cause precipitation of RNA. The samples were centrifuged at 12000 g for 10 minutes at 4ºC and the supernatant discarded, consequently leaving the RNA pellet. This RNA pellet was washed by adding 70% (v/v) ethanol followed by centrifugation at 12000 g for 5 minutes at 4ºC. Taking care not to disturb the pellet, the ethanol was removed and the samples were left to dry in room air. The RNA pellet was resuspended in 50 µl of nuclease-free water. To assess the purity and integrity of the RNA samples, A_{260}/A_{280} spectrophotometric measurements on a GeneQuant RNA/DNA quantifier (Amersham Pharmacia Biotech, U.K.) were performed.

2.3.8.2 Reverse transcription and gene expression analysis

Reverse transcription of the RNA (1 µg/ml) to cDNA was performed using 50 µl of master mix (Taqman reverse transcription reagents) containing 1 x Taqman reverse transcription buffer, 5.5 mM $MgCl_2$, deoxyNTP mixture (500 µM per NTP), 2.5 µM Random hexamers, 0.4 U/µl RNAse inhibitor and 1.25 U/µl multiscribe reverse transcriptase. Tubes were incubated for 10 minutes at 25^{o}C followed by 30 minutes incubation at 48^{o}C in a Perkin Elmer 480 thermal cycler (Perkin Elmer, Boston MA, USA). Reverse transcriptase was inactivated by incubation of sample for 5 minutes at 95^{o}C. This product (10 ng/µl) of the reverse transcription process was diluted one in four for the purpose of analysis by real time polymerase chain reaction (PCR).

Transcriptional expression of target messenger (m)RNA transcripts in the cRNA samples created previously were detected by PCR amplification and quantified by 5'-nuclease assay utilising fluorescent labelled Taqman probes and analysed using real time quantitative PCR

with the ABI PRISM 7000 Sequence Detection System (Applied Biosystems, Warrington, UK). TaqMan probes have a fluorescent reporter dye (i.e. FAM or VIC) covalently linked to its 5'-end and a downstream quencher dye (TAMRA) that is linked to its 3'-end. The quenching of the fluorescence is dependent on the spatial proximity of the reporter and quencher dyes. The advantage of Real Time PCR is that since two different dyes can be used, i.e. FAM and VIC, the reactions can be internally controlled by an endogenously expressed gene, such as 18S. For the experiments performed in this thesis, reactions were internally controlled using the 18S RNA assay. The 18S uses VIC as the reporter dye whereas all of the target genes have a FAM reporter dye.

PCR reactions were performed in a total reaction volume of 25 µl. This volume contained 3 µl of sample cDNA (2.5 ng/µl), with the designed reverse primer, forward primers and the probe or alternatively the purchased Assay on Demand of the target gene, 2x TaqMan universal master mix and 18S internal control. The specific products were amplified and detected using the ABI PRISM 7000 Sequence Detection System (Applied Biosystems, Warrington, Cheshire, U.K.) and an amplification protocol consisting of 1 cycle for 2 minutes at 50°C, 1 cycle for 10 minutes at 95°C, 40 cycles for 15 seconds at 95°C, and 1 minute at 60°C. The results were analysed using a Sequence Detection Software (Applied Biosystems, Warrington, Cheshire, U.K.), and the relative amount of target gene transcript was normalised to the amount of 18S internal control transcript in the same cDNA sample. The critical threshold cycle (Ct), simply defined as the cycle at which the fluorescence from the TaqMan probe becomes detectable above background, is inversely proportional to the logarithm of the initial number of template molecules. Therefore, the higher the concentration of the target, the lower the number of amplification cycles required to detect the rise above baseline. The ct, which following guidelines from Applied Biosystems is manually determined by the operator, will

always be set during the exponential phase of amplification and will thus be unaffected by reaction components becoming limited in the plateau phase and consequently leading to false results.

The PCR reaction is exponential, therefore, the data has been expressed as arbitrary values with the exponential reaction taken into account, using the following equation: $2^{-\text{delta ct}}$ i.e. $2^{-(\text{target ct} - \text{18s ct})}$, written as $2^{-\Delta ct}$.

Assays on demand were obtained from Applied Biosystems for mouse IL-1β, IL-18 and KC.

2.3.8.3 Validation of Multiplexed Reactions

To ensure that the assay worked efficiently, the assays on demand were validated in a reaction carried out in the presence of an 18S internal control (multiplex reaction). Using a panel of tissues from mouse, target gene rich samples were identified for the purposes of validation. The tissue containing the highest level of gene was selected and a cDNA standard curve was created using the concentrations 25, 8.333, 2.778, 0.926, 0.309, 0.103, 0.034 and 0.011 ng/25 µl. Once the Ct values for both the target gene and the 18S internal control were plotted, the efficiency was examined. Typically, an efficient reaction will have a slope of about -3.3 and an R^2 value close to 1, but no lower than 0.98. For an efficient multiplex reaction the slope of the graph when the delta Ct values (change in Ct values between 18S and target) are plotted against RNA concentration will be less than 0.1.

Using guidelines from the manufacturer (Applied Biosystems), the Ct value can be obtained for each reaction from the corresponding amplification plot. The baseline is set to incorporate

the range of cycles in which the PCR product is not amplified. To avoid the results being affected by the reaction components becoming limited in the plateau phase, the threshold line is set in the centre of the exponential phase of amplification. For each reaction, the Ct value is the cycle number at the point where the threshold line crosses the amplification plot. Throughout this thesis the data was expressed as arbitrary values using an equation ($2^{-\text{delta Ct}}$, i.e. $2^{-(\text{Target Ct} - \text{18S Ct})}$) that allows for the exponential nature of the PCR reaction.

2.4 In vitro models

2.4.1 Culture of cell lines

The THP-1 human monocytic cell line was originally derived from the peripheral blood of a 1 year old human male with acute monocytic leukemia. Whilst this cell line is monocytic, they can be differentiated into alveolar macrophages-like cells. Furthermore, they have TLR4 and $P2X_7$ receptors and have been shown to produce IL-1β and IL-18, both cytokines of interest associated with inflammasome activation (Grahames *et al*., 1999).

To provide a link between the human cell based assays and the *in vivo* mouse modelling systems I also used a mouse monocyte cell line to investigate the pathway using *in vitro* cell based assays. The J774.2 mouse macrophage cell line was originally recloned from the original ascites and solid tumour J774.1. Similar to the THP-1 human monocytic cell line, these cells express both TLR4 and $P2X_7$ receptors and have been demonstrated to produce IL-1β and IL-18. However, whilst the THP-1 cell line is non-adherent, the J774.2 mouse macrophages are semi-adherent.

Both cell lines were purchased from the European Collection of Cell Cultures (ECACC, Salisbury, Wiltshire, UK) and the frozen ampoule was left at room temperature for approximately 1 minute and then transferred to a 37°C water bath for 1-2 minutes until fully thawed. The cells were then cultured in RPMI 1640 with glutamax I (Invitrogen Ltd, UK) supplemented with 10% FCS and 1% antibiotic and antimycotic solution (Penicillin/Streptomycin – Sigma-Aldrich Co., Poole, UK) at 37°C in a humidified atmosphere (95% air, 5% (v/v) CO_2). They were cultured into 75 cm^3 flasks, and the media was replaced after 3 days and thereafter every 48 hours. The J774.2 cell line must be scraped from the bottom of the flask before replacing the media. The media was changed by centrifuging the cell suspension at 800 x g for 5 minutes at room temperature, in a centrifuge (Mistrall 3000i, MSE). The supernatant was discarded, and the pellet of cells was resuspended in 1 ml of RPMI 1640 with glutamax I, supplemented with 10% FCS and 1% antibiotic and antimycotic solution. Trypan Blue exclusion was performed to determine cell viability and cells were passaged into 2 x 75 cm^3 flasks when cell numbers reached 10 x 10^6 cells/ml. Both cell lines have a doubling time of approximately 48 hours.

2.4.2 Cell viability assays

For the purpose of determining cell viability in these studies, two different techniques were used. Conventionally, cell growth determination is undertaken by counting viable cells after staining with a vital dye.

2.4.2.1 Trypan blue exclusion

The cell viability of non-adherent cell (e.g. THP-1 human monocytic cell line) was determined using the Trypan Blue (Sigma-Aldrich Co., Poole, UK) exclusion method. 10 µl of cell suspension was added to 90 µl of Trypan Blue solution, mixed and left at room temperature for 5 minutes. 10 µl was then added to an Improved Neubaur haemocytometer and observed under a light microscope at x40 magnification. Viable cells will exclude the dye and appear unstained, whilst dead cells are stained blue. Cell viability was calculated as a percentage by dividing the number of viable cells by the number of dead and viable cells.

2.4.2.2 MTT Assay

An alternative method to determine cell viability is by measuring mitochondrial dehydrogenase activity in living cells. A technique used when assessing the cell viability of adherent cells (e.g. J774.2 mouse macrophage cell line). At the end of each experiment cell viability of these adherent macrophages were examined by measuring the mitochondria-dependent reduction of 3-[4,5-dimethylthiazol-2-yl]-2,5-diphenyltetrazolium bromide (MTT) to formazan. Mitochondrial dehydrogenases of viable cells cleave the tetrazolium ring, yielding purple MTT formazan crystals which are insoluble in aqueous solutions. The crystals can be dissolved in acidified MTT solvent, such as dimethylsulphoxide (DMSO). The resulting purple solution is then measured spectrophotometrically. The supernatant from adherent macrophages were removed and retained for ELISA and 500 µl of RPMI containing 1 mg/ml MTT (Sigma-Aldrich Co., Poole, UK) was added to each well. Cells were then incubated for 15 minutes at 37°C. The MTT-containing RPMI was removed by inverting the plate and 500 µl of DMSO was added to each well. The plate was shaken to allow formazan

to dissolve in the DMSO, and the absorbance was read in a plate reader at a 540 nM. An increase in cell viability results in an increase in the amount of MTT formazan formed and therefore, results in an increase in absorbance measured.

2.5 Human Tissue

Human lung tissue samples were obtained from a transplant programme. Ethical approval for the study was obtained from the Royal Brompton and Harefield ethics committee. Patient details will be reported where necessary in the appropriate section of this thesis.

2.6 Statistical Analysis

All values are expressed as mean ± S.E.M. of n observations. The data was assessed for statistical significance by applying an unpaired t-test for parametric data or alternatively Mann-Whitney U-test for non-parametric data with independent groups compared with their specific time-matched controls. For multiple comparisons tests, statistical analysis was performed by applying a one-way ANOVA (analysis of variance) with a Dunnett's or Bonferroni's multiple comparisons post-test for parametric data or alternatively a Kruskal-Wallis incorporating Dunn's multiple comparison post-test for non-parametric data. In all tests, statistical analysis was performed by comparing treatment groups with relevant vehicle controls. A p-value of less than 0.05 was considered statistically significant. All statistical analysis was performed in 'GraphPad Instat' as part of the GraphPad software.

2.7 Materials

Amersham Pharmacia Biotech, U.K - GeneQuant RNA/DNA quantifier

Applied Biosystems, Warrington, UK - 18S endogenous control, universal mastermix, reverse transcription kit, assays on demand for target genes, optical reaction plates and optical adhesive covers.

AstraZeneca – AZ11645373

Biorad, Munich, Germany – Bradford assay

CP Pharmaceuticals Ltd, Wrexham, UK - Heparin

ECACC, Salisbury, Wiltshire, UK - human THP-1 monocytic cell-line, mouse J774.2 macrophage cell-line

Enzo Life Sciences, Exeter, UK - Caspase 1 colorimetric assay

Fisher Scientific, Loughborough UK - Nunc 96 well maxisorb ELISA plates

Fresenius Kabi, Warrington, UK - Endotoxin free saline

Harlan-Olac, Bicester, UK - C57BL/6 mice

Invitrogen Ltd, Paisley, UK - Foetal calf serum, Foetal bovine serum, RPMI-1640,

Mesoscale Discovery, Gaithersburg, ML, USA - MSD ultrasensitive plates, reagents

National Veterinary Services Ltd, Stoke-on-Trent, UK - Sodium pentobarbitone (Euthatal)

Peakdale Molecular – A-438079

Perkin Elmer, Cambridge, UK - ATPlite luminescence ATP detection system

R&D Systems, Abingdon, UK - ELISA kit Duoset for human (IL-1β, TNF-α, IL-6, IL-8 and IL-18) and mouse (IL-1β, TNF-α, IL-6, KC and IL-18), streptavidin horse radish peroxidase.

Roche Diagnostics, East Sussex, UK - Collagenase, DNAse, penicillin/streptomycin

Sigma-Aldrich Co Ltd, Poole, UK - 3-[4,5-dimethylthiazol-2-yl]-2,5-diphenyltetrazolium bromide (MTT), bovine serum albumin (BSA), chloroform, dimethylsulphoxide (DMSO),

isopropanol, lipopolysaccharide, modified Wright-Giemsa stain, methyl cellulose, NXTRACT CelLytic NuCLEAR Extraction kit, Penicillin/Streptomycin, phosphate buffered saline (PBS), T-75 cell culture flask, Tri-reagent, Trypan Blue solution, tween80

Stratech Scientific, Suffolk, UK - Amplite Colorimetric NAD/NADH Assay Kit

Tobacco Health Research Institute, University of Kentucky, Lexington, KY - 3R4F cigarettes

VWR International LTD, Lutterworth, UK – 24-well cell culture plate, ethanol, glucose, magnesium chloride ($MgCl_2$), magnesium sulphate, potassium chloride (KCl), sodium chloride (NaCl), sulphuric acid.

Chapter 3

Inflammasome Activation in Acute Models of Airway Inflammation

3.1 Rationale

It has been demonstrated that the inflammation seen in the lungs of COPD patients is initially driven by neutrophils in the acute phase, with the phenotype of the disease changing to incorporate the actions of macrophages and lymphocytes in more chronic conditions (Di Stefano *et al*. 1996; Saetta *et al.*, 1997), in particular $CD8^+$ T cells and B cells (Hogg *et al*., 2004; Van der Strate *et al*., 2006). Recent publications have also shown that airway neutrophilia is involved in animal models of the disease (Shapiro, 2000; Churg & Wright, 2007). In order to determine the role of the $P2X_7$ – inflammasome signalling axis in COPD, I wanted to characterise *in vivo* modelling systems in animals that could replicate the disease phenotype.

Two acute models of COPD-like inflammation that elicit neutrophilia were characterised in C57BL/6 mice, as this is the background strain on which the $P2X_7$ receptor knockout mice are bred. Male mice were used as they would eliminate a range of physiological variables. The first model selected is driven by exposure to cigarette smoke, the primary etiological factor driving the pathogenesis of the disease. This model will provide the most accurate model of disease phenotype in animals. The second model is driven by lipopolysaccharide (LPS), which will facilitate paralleling experiments using a stimulus of the normal innate defence system that induces airway neutrophilia. Preliminary dose-response experiments would aim to establish a sub-maximal challenge to cigarette smoke and LPS that would induce inflammation in the lungs of mice in order to detect any modulation of the inflammatory response. This would then be followed with temporal characterisation of these models to identify an optimal time point at which to assess inflammatory end-points of interest. By comparing the differences in the inflammatory profiles of both insults, it will be

possible to identify if particular differences are specific to the disease or as a result of a more general immunological phenomenon. Markers of NLRP3 inflammasome activation, such as caspase 1 activity and the processing and release of IL-1β/IL-18, will then be examined to determine if these are linked to the inflammation seen in response to these stimuli.

3.2 Methods

3.2.1 Determination of a sub-maximal dose of cigarette smoke to induce airway inflammation in C57BL/6 mice.

The aim of this preliminary experiment was to establish a sub-maximal exposure challenge to cigarette smoke that would induce an inflammatory response in the lungs of mice. This sub-maximal challenge would allow us to determine the role of the inflammasome, by using specific $P2X_7$ receptor antagonists and knockout animals and examining any modulation of the inflammatory response.

Male C57BL/6 mice (18-20 g) to either room air or 250, 500 or 750 ml (maximum smoke challenge possible in this system) mainstream cigarette smoke per minute using 3R4F cigarettes (Tobacco Health Research Institute, University of Kentucky, Lexington, KY) for a total exposure period of 50 minutes (excluding 10 minute venting period), either once or twice daily, for three consecutive days (as detailed in section 2.*2.2*). Each group consisted of n=8 animals. The total suspended particulate (TSP) levels within the chamber were assessed at 15, 30 and 40 minutes (sampled over a 1 minute period) in order to confirm the consistency of the exposures.

Mice were culled 24 hours after the last challenge with an overdose of intraperitoneal (i.p.) sodium pentobarbitone (200 mg/kg) and the lungs were lavaged (as described in section 2.*3.1*) for total cell counts and 4-part differential cell counts (neutrophils, eosinophils, monocytes/macrophages and lymphocytes, see section *2.3.3*).

3.2.2. Determination of a sub-maximal dose of aerosolised LPS to induce airway inflammation in C57BL/6 mice.

An appropriate sub-maximal challenge of LPS was determined by challenging animals (male C57BL/6 mice, 18-20 g) with either 0.1, 1 or 10 mg/ml aerosolised LPS (Escherichia coli, serotype 0111:B4, Sigma-Aldrich Ltd. Poole, UK) or endotoxin free saline (Fresenius Kabi, Warrington, UK) in a Perspex treatment box (600 x 240 x 350 mm) for 30 minutes using a System 22 nebuliser (Medic-Aid Ltd., Pagham, Sussex) driven by a high-flow-rate compressor (Medic-Aid Ltd., Pagham, Sussex) (as detailed in section *2.2.1*). Each group consisted of n=6 animals.

Mice were culled 4 hours after the LPS challenge with an overdose of intraperitoneal (i.p.) sodium pentobarbitone (200 mg/kg) and BALF was collected (as described in section 2.*3.1*) for total cell counts and 3-part differential cell counts (neutrophils, eosinophils and lymphomononuclear cells, see section 2.*3.3*).

3.2.3. Temporal characterisation of cigarette smoke-induced airway inflammation in C57BL/6 mice.

Having previously identified a robust sub-maximal exposure level of cigarette smoke, further temporal characterisation of this model would facilitate the process of identifying an optimal time point at which to assess inflammatory end-points of interest including cellular infiltration, pro-inflammatory mediator release and caspase 1 activity. These markers of "inflammasome activation" will provide essential end-points to evaluate the role of the

inflammasome in the inflammation associated with COPD by using specific $P2X_7$ receptor antagonists and knockout animals.

To track the inflammatory response to cigarette smoke exposure, mice were exposed to either room air or a sub-maximal (500 ml/min) dose of cigarette smoke (as detailed in section *2.2.2*) for a total exposure period of 50 minutes (excluding 10 minute venting period), twice daily, for 3 consecutive days. Each group consisted of n=18 animals at each time point. Mice were euthanised with an overdose (200 mg/kg) of i.p sodium pentobarbitone at various time points after challenge (2, 6, 24, 48, 72, 96 and 168 hours). BALF and lung tissue samples were collected for analysis as follows;

- BALF (processed as described in section *2.3.1*):
  - Total cell counts and 4-part differential cell counts (neutrophils, eosinophils, monocytes/macrophages and lymphocytes, as described in section 2.*3.3*), n=8.
  - Cytokine analysis in BALF determined by MSD technology, n=5 (as described in section *2.3.4.2*).
  - ATP levels were analysed in the BALF by using a commercially available assay, n=6 (as described in section *2.3.6*)

- Lung tissue (processed as described in section *2.3.1*):
  - Collagenase digest (as described in section *2.3.1*) for total cell counts and 4-part differential cell counts (neutrophils, eosinophils, monocytes/macrophages and lymphocytes, as described in section 2.*3.3*), n=6.
  - Flash frozen in liquid nitrogen for cytosolic and nuclear cell fraction extraction (as described in section *2.3.5.1*), determination of caspase 1 activity (as described in

section *2.3.5.2*) and quantification of mRNA expression (as described in section *2.3.7*), n=6.

3.2.4. Temporal characterisation of LPS-induced airway inflammation in C57BL/6 mice.

By tracking the inflammatory response following acute LPS exposure an optimal time point at which to measure key inflammatory end points can be determined. This will facilitate the process of identifying if the inflammasome pathway is involved in the innate immune response activated in response to an endotoxin challenge by utilising pharmacological tools to target the $P2X_7$ receptors and knockout animals.

To track the inflammatory response, male C57BL/6 mice (18-20 g) were challenged with endotoxin free saline (Fresenius Kabi, Warrington, UK) or a sub-maximal dose of 1 mg/ml LPS (*Escherichia coli*, serotype 0111:B4, Sigma-Aldrich Ltd. Poole, UK) for 30 minutes (as detailed in section *2.2.1*). Animals were euthanised with an overdose of i.p sodium pentobarbitone (200 mg/kg) at various time points after challenge (2, 6, 24, 48, 72, 96 and 168 hours). BALF and lung tissue samples were collected for analysis as detailed in section *3.2.3*.

3.2.5. Statistical analysis

Data is expressed as mean ± S.E.M of n observations. For data where each independent group is compared to its time matched control, statistical significance was determined using a Student's t-test for parametric or a Mann-Whitney U-test (or Wilcoxon rank test) for non-

parametric data. For multiple comparisons tests, statistical analysis was performed by applying a one-way ANOVA (analysis of variance) with a Dunnett's (comparing with a single control group) or Bonferroni's (multiple comparisons) post-test for parametric data or alternatively a Kruskal-Wallis incorporating Dunn's multiple comparison post-test for non-parametric data. A P value < 0.05 was taken as significant and all treatments were compared with the appropriate control group.

3.3. Results

3.3.1 Determination of a sub-maximal dose of cigarette smoke to induce airway inflammation in C57BL/6 mice.

To establish a sub-maximal exposure of cigarette smoke that would elicit an inflammatory response, mice were exposed to increasing doses of cigarette smoke (250, 500, 750 ml/min) once or twice daily, for three consecutive days. Mice were culled 24 hours after challenge with an overdose of intraperitoneal (i.p.) sodium pentobarbitone. This time point was chosen based on findings in the literature that demonstrate that neutrophilia is increased at this time point (Morris *et al,* 2008).

No increases in BALF neutrophilia were seen in mice exposed to CS once daily at any dose. In contrast, a significant dose-dependent increase in BALF neutrophilia was shown in mice exposed twice daily at the higher doses of 500 and 750 ml/min of cigarette smoke (Figure 3.1) when compared to the air exposed animals. Interestingly, monocytes/macrophages (Figure 3.2) numbers recovered in the BALF exhibited significant decreases at all three cigarette smoke doses, in both once and twice daily exposure groups when compared to their air exposed controls groups. A similar decrease was also observed for BALF lymphocyte numbers in both once and twice daily exposure groups; however this did not reach significance when compared to the air exposed groups (Figure 3.2).

Based on these findings, 500 ml/min cigarette smoke, administered twice daily was selected as the sub-maximal exposure dose to use in the temporal characterisation of this model as it provided a significant increase in BALF neutrophilia.

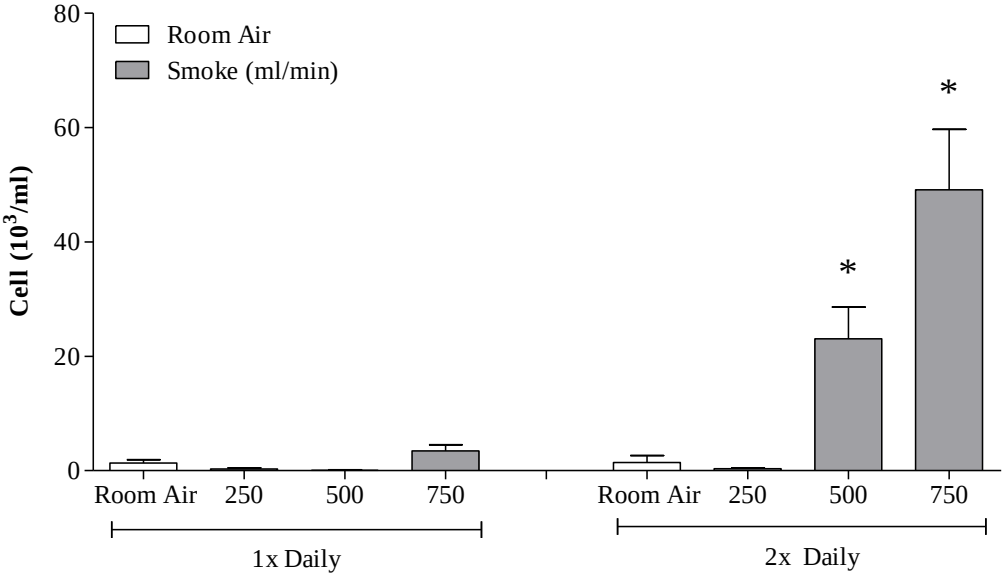

Figure 3.1 – Effect of cigarette smoke exposure on airway neutrophilia in the BALF. *C57BL/6 mice were challenged with room air or cigarette smoke at 250, 500 or 750 ml/min, once or twice daily for 3 consecutive days and BALF neutrophilia was determined by differential counting under light microscopy. Data represented as Mean ± SEM for n=8 observations. Statistical significance determined with a Kruskal-Wallis incorporating Dunn's post-test for non-parametric data. * = P<0.05 and denotes a significant difference to the air exposed control group.*

	1x Daily				2x Daily			
Cells (10^3/ml)	**Room Air**	**250**	**500**	**750**	**Room Air**	**250**	**500**	**750**
Eosinophils	0.0±0.0	0.0±0.0	0.0±0.0	0.0±0.0	0.0±0.0	0.0±0.0	0.06±0.06	0.0±0.0
Monocyte/ Macrophage	159.80±11.6	102.20±12.3	70.81±5.0*	79.93±5.1*	181.70±23.9	82.68±10.8*	68.62±12.3*	58.62±9.3*
Lymphocytes	8.48±3.0	3.96±1.0	3.47±0.9	4.99±1.0	13.35±6.7	3.76±1.1	4.67±1.0	6.14±0.8

Figure 3.2 – Effect of cigarette smoke exposure on inflammatory cell recruitment in the BALF. *C57BL/6 mice were challenged with room air or cigarette smoke at 250, 500 or 750 ml/min once or twice daily for 3 consecutive days and numbers of neutrophils, eosinophils, monocytes/macrophages and lymphocytes recovered from the BALF was determined by differential counting under light microscopy. Data represented as Mean ± SEM for n=8 observations. Statistical significance determined with a Kruskal-Wallis incorporating Dunn's post-test for non-parametric data. * = P<0.05 and denotes a significant difference to the air exposed control group.*

3.3.2 Determination of a sub-maximal dose of LPS to induce airway inflammation in C57BL/6 mice.

Having identified an appropriate sub-maximal exposure limit to elicit an inflammatory response to cigarette smoke, the same was determined for the endotoxin challenge utilising LPS. Mice were challenged with either saline or increasing doses of aerosolised LPS (0.1, 1, or 10 mg/ml) for 30 minutes. Mice were culled 4 hours after challenge with an overdose of intraperitoneal (i.p.) sodium pentobarbitone.

Animals exposed to LPS showed a significant dose-related increase in BALF neutrophilia (Figure 3.3) when compared to the saline challenged control group at the four top doses. This increase was also mirrored with increased numbers of BALF eosinophils (Figure 3.4) compared to saline challenged controls. In contrast however, a significant decrease in lymphomononuclear cell number was also seen in response to the LPS challenge (Figure 3.4). These findings suggest that the 1 mg/ml dose of LPS will provide the most appropriate submaximal exposure limit in order to examine the temporal changes seen in the inflammatory response following endotoxin challenge.

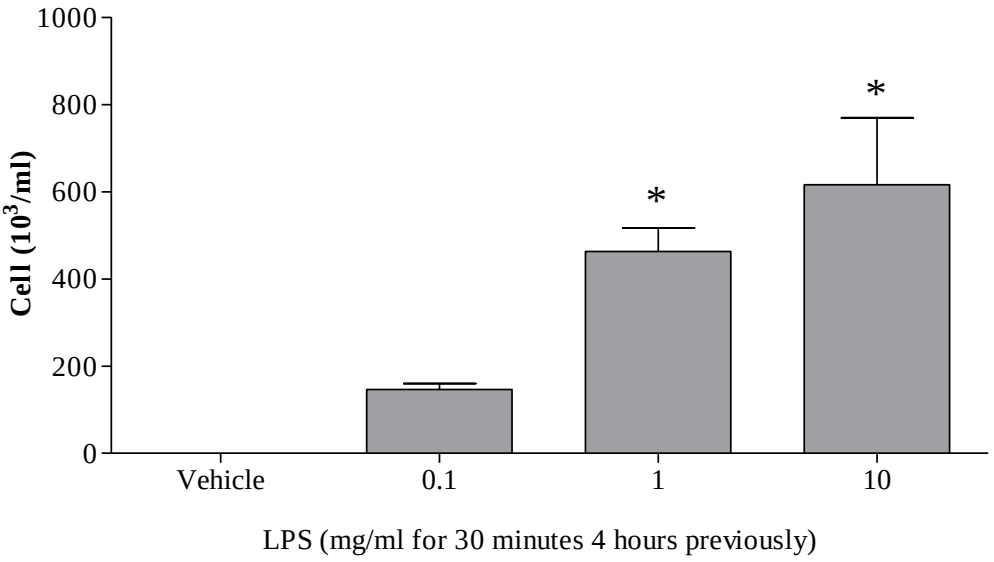

Figure 3.3 – Effect of LPS exposure on airway neutrophilia in the BALF. *C57BL/6 mice were challenged with saline or LPS (0.03, 0.1, 0.3, 1, 3 or 10 mg/ml) and BALF neutrophilia was determined by differential counting under light microscopy. Data represented as Mean ± SEM for n=6 observations. Statistical significance determined with a Kruskal-Wallis incorporating Dunn's post-test for non-parametric data. * = P<0.05 and denotes a significant difference to the saline exposed control group.*

Cells (10^3/ml)	Saline	0.1	1	10
Eosinophils	0.0±0.0	33.0±5.0	92.0±15.0*	61.0±18.0*
Lymphomononuclear	63.0±6.0	11.0±3.0*	18.0±4.0*	31.0±6.0

Figure 3.4 – Effect of LPS exposure on inflammatory cell recruitment in the BALF. *C57BL/6 mice were challenged with with saline or LPS (0.03, 0.1, 0.3, 1, 3 or 10 mg/ml) and numbers of neutrophils, eosinophils and lymphomononuclear cells recovered from the BALF was determined by differential counting under light microscopy. Data represented as Mean ± SEM for n=6 observations. Statistical significance determined with a Kruskal-Wallis incorporating Dunn's post-test for non-parametric data. * = P<0.05 and denotes a significant difference to the saline exposed control group.*

3.3.3. Temporal characterisation of cigarette smoke-induced airway inflammation in C57BL/6 mice.

To track the inflammatory response to elicited by sub-maximal exposure to cigarette smoke, mice were exposed to either room air or a sub-maximal (500ml/min) dose of cigarette smoke for 50 minutes, twice daily, for 3 consecutive days. Mice were euthanised with an overdose (200 mg/kg) of i.p. sodium pentobarbitone at various time points after challenge (2, 6, 24, 48, 72, 96 and 168 hours).

A significant increase in BALF neutrophils was exhibited at 24, 48 and 72 hours following the final smoke exposure when compared to their time matched controls (Figure 3.5) that peaked 48 hours following the final smoke exposure. There were no significant changes in eosinophil numbers at any time point following cigarette smoke exposure in the BALF (Figure 3.6). The monocyte/macrophages were significantly elevated at the 2, 24 and 72 hours time points when compared to their time-matched air exposed controls however, this increase was less profound compared to the neutrophilia in response to the smoke exposure (Figure 3.6). The lymphocytes demonstrated increases at similar time points; however, these were smaller in magnitude when compared to that of the neutrophils (Figure 3.6)

Examination of the differential counts in the lung tissue indicated no significant increases in neutrophils (Figure 3.7) eosinophils, monocyte/macrophages and lymphocytes (Figure 3.8).

A significant increase in caspase 1 activity in the lung tissue was shown at 24 and 48 hours following the final smoke exposure when compared to their time matched controls (Figure 3.9). Moreover, increases at these time points were mirrored in the levels of IL-1β and IL-18

detected in the BALF following CS exposure that were shown to be increased at 24 and 48 hours following the exposure when compared to their time matched controls (Figure 3.10B & 3.11B). This suggests that there appears to be a correlation between the increase in airway neutrophilia, caspase 1 activity and IL-1β/IL-18 release. These increases were not reflected at the gene level, as examination of mRNA expression in the lung tissue saw no significant increases (Figure 3.10A & 3.11A).

Interestingly, a significant increase in KC expression was shown at all time points following the final smoke exposure at both the gene (Figure 3.12A) and protein (Figure 3.12B) levels. However, this increase in KC production did not seem to temporally correlate with cellular inflammation. I could not detect an increase in ATP levels in the BAL fluid in response to CS exposure. To check whether the processing techniques or storage conditions could be masking the levels of ATP, I performed a series of tests and examined the level of ATP (Figure 3.13). Increasing concentrations of ATP were dissolved in the following preparations:

1. Water
2. Water – Frozen and thawed
3. RPMI
4. RPMI – with ATP level assessed 2 hours later
5. RPMI - Frozen and thawed

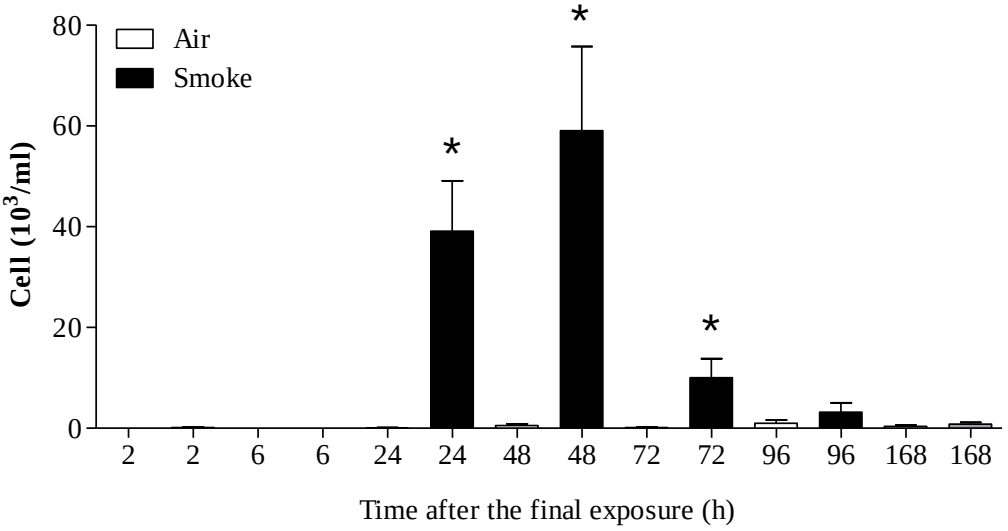

Figure 3.5 – Temporal characterisation of cigarette smoke exposure on airway neutrophilia in the BALF. *C57BL/6 mice were challenged with room air or 500 ml/min cigarette smoke, twice daily for 3 consecutive days. Samples were collected at 2, 6, 24, 48, 72, 96 and 168 hours after challenge and the BALF neutrophilia was determined by differential counting under light microscopy. Data represented as Mean ± SEM for n=8 observations. Statistical significance determined with a Mann-Whitney U-test for non-parametric data. * = P<0.05 and denotes a significant difference to the time-matched air exposed control group.*

	Cells (10^3/ml)	**Eosinophils**	**Monocytes/ Macrophages**	**Lymphocytes**
2 hrs	Air	0.00±0.00	81.56±7.74	3.93±0.83
	Smoke	0.00±0.00	150.10±13.85*	4.26±1.19
6 hrs	Air	0.65±0.48	103.50±12.18	4.98±1.01
	Smoke	0.25±0.17	98.95±6.95	4.96±0.98
24 hrs	Air	0.00±0.00	59.31±11.05	1.79±0.41
	Smoke	0.00±0.00	137.70±17.20*	5.73±1.35*
48 hrs	Air	0.13±0.13	90.35±4.79	6.08±2.43
	Smoke	2.80±2.80	117.90±9.70	4.45±1.05
72 hrs	Air	0.00±0.00	91.70±12.43	4.79±1.13
	Smoke	0.00±0.00	166.10±22.43*	6.34±1.18
96 hrs	Air	0.08±0.08	92.09±18.26	3.00±0.79
	Smoke	0.00±0.00	107.40±14.63	7.78±1.74*
168 hrs	Air	1.88±1.88	69.91±3.99	2.93±0.97
	Smoke	0.00±0.00	108.80±10.50*	5.98±1.42

Figure 3.6 – Temporal characterisation of cigarette smoke exposure on inflammatory cell recruitment in the BALF. *C57BL/6 mice were challenged with room air or 500 ml/min cigarette smoke, twice daily for 3 consecutive days. Samples were collected at 2, 6, 24, 48, 72, 96 and 168 hours after challenge and the numbers of neutrophils, eosinophils, monocytes/macrophages and lymphocytes recovered from the BALF was determined by differential counting under light microscopy. Data represented as Mean ± SEM for n=8 observations. Statistical significance determined with a Mann-Whitney U-test for non-parametric data. * = P<0.05 and denotes a significant difference to the time-matched air exposed control group.*

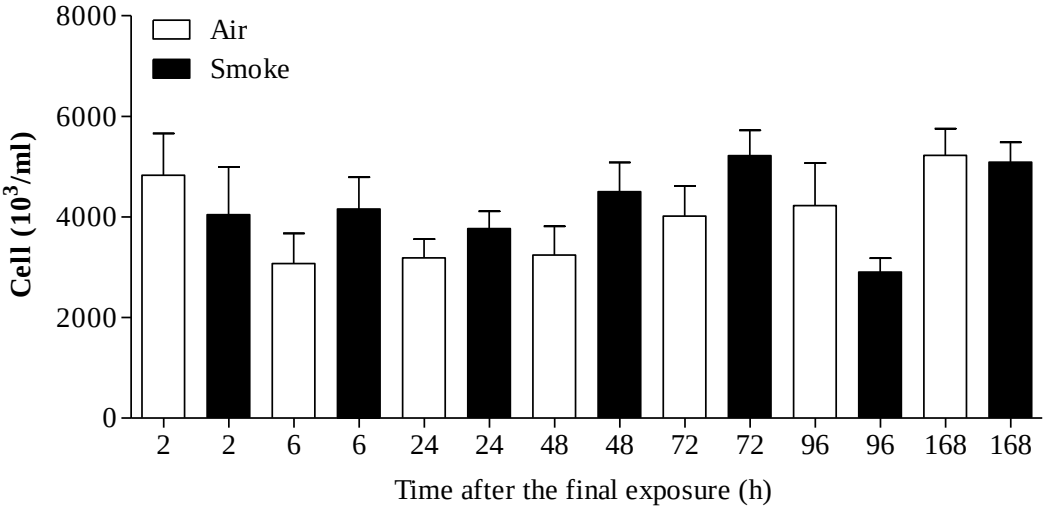

Figure 3.7 – Temporal characterisation of cigarette smoke exposure on neutrophilia in the lung tissue. *C57BL/6 mice were challenged with room air or 500 ml/min cigarette smoke, twice daily for 3 consecutive days. Samples were collected at 2, 6, 24, 48, 72, 96 and 168 hours after challenge and the neutrophilia in the lung tissue was determined by differential counting under light microscopy. Data represented as Mean ± SEM for n=8 observations. Statistical significance determined with a paired student's t-test for parametric data. * = P<0.05 and denotes a significant difference to the time-matched air exposed control group.*

	Cells (10^3/ml)	**Eosinophils**	**Monocytes/ Macrophages**	**Lymphocytes**
2 hrs	Air	636±136.9	3965±561.2	1742±255.1
	Smoke	391±96.55	4075±975.6	1595±383.4
6 hrs	Air	334±190.6	3282±657.4	1205±275.3
	Smoke	205±37.69	1519±356.0	901±227.7
24 hrs	Air	1701±122.6	1484±158.1	755±137.3
	Smoke	1669±252.3	1690±229.4	738±125.5
48 hrs	Air	1268±236.5	1533±234.2	589±89.61
	Smoke	1781±258.2	2166±394.9	858±113.5
72 hrs	Air	1338±67.02	1595±265.7	564±93.62
	Smoke	1744±229.4	1990±177.2	666±115.3
96 hrs	Air	1584±432.7	1833±471.9	1393±231.0
	Smoke	1842±263.3	2100±228.3	1232±252.2
168 hrs	Air	3416±584.3	2791±592.0	2144±456.1
	Smoke	1923±159.9*	2560±85.01	1152±150.3

Figure 3.8 – Temporal characterisation of cigarette smoke exposure on inflammatory cell recruitment in the lung tissue. *C57BL/6 mice were challenged with room air or 500 ml/min cigarette smoke, twice daily for 3 consecutive days. Samples were collected at 2, 6, 24, 48, 72, 96 and 168 hours after challenge and the numbers of neutrophils, eosinophils, monocytes/macrophages and lymphocytes in the lung tissue was determined by differential counting under light microscopy. Data represented as Mean ± SEM for n=8 observations. Statistical significance determined with a Mann-Whitney U-test for non-parametric data. * = P<0.05 and denotes a significant difference to the time-matched air exposed control group.*

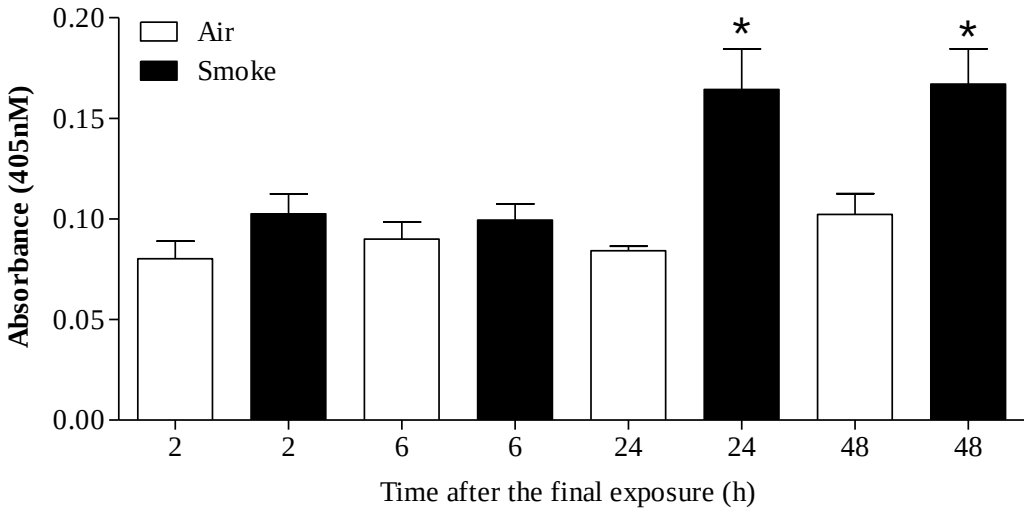

Figure 3.9 – Temporal characterisation of cigarette smoke exposure on Caspase 1 activity in the lung tissue. *C57BL/6 mice were challenged with room air or 500 ml/min cigarette smoke, twice daily for 3 consecutive days. Samples were collected at 2, 6, 24 and 48 hours after challenge and the Caspase 1 activity in the cytosolic fraction of the lung tissue was determined by a commercially available colourimetric assay. Data represented as Mean ± SEM for n=6 observations. Statistical significance determined with a Mann-Whitney U-test for non-parametric data. * = P<0.05 and denotes a significant difference to the time-matched air exposed control group..*

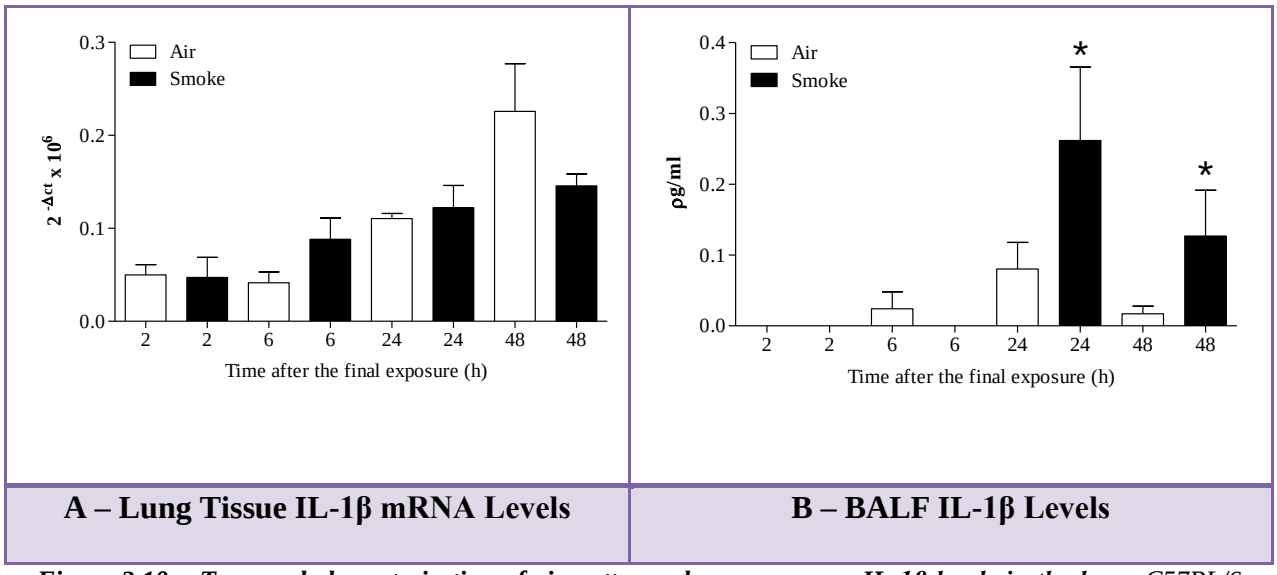

A – Lung Tissue IL-1β mRNA Levels | **B – BALF IL-1β Levels**

Figure 3.10 – Temporal characterisation of cigarette smoke exposure on IL-1β levels in the lung. *C57BL/6 mice were challenged with room air or 500 ml/min cigarette smoke, twice daily for 3 consecutive days. Samples were collected at 2, 6, 24 and 48 hours after challenge and the expression of IL-1β mRNA levels in lung tissue (A) and cytokine release in the BALF (B) were determined. Data represented as Mean ± SEM for n=6 observations. Statistical significance determined with a Mann-Whitney U-test for non-parametric data. * = P<0.05 and denotes a significant difference to the time-matched air exposed control group.*

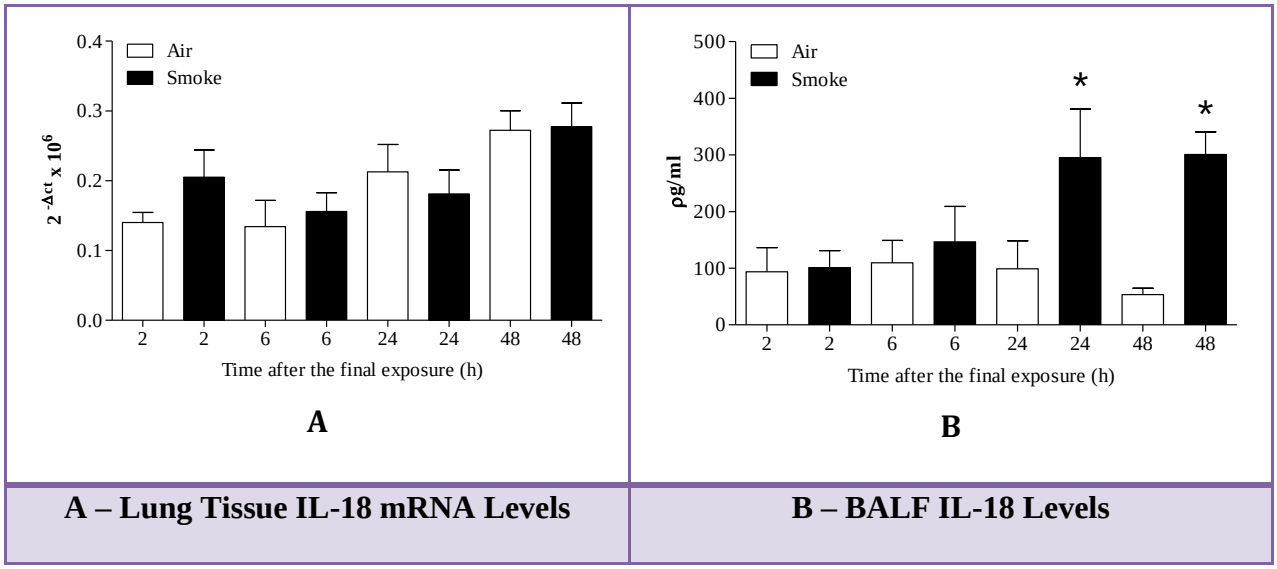

Figure 3.11 – Temporal characterisation of cigarette smoke exposure on IL-18 levels in the lung. *C57BL/6 mice were challenged with room air or 500 ml/min cigarette smoke, twice daily for 3 consecutive days. Samples were collected at 2, 6, 24 and 48 hours after challenge and the expression of IL-18 mRNA levels in lung tissue (A) and cytokine release in the BALF (B) were determined. Data represented as Mean ± SEM for n=6 observations. Statistical significance determined with a Mann-Whitney U-test for non-parametric data. * = P<0.05 and denotes a significant difference to the time-matched air exposed control group.*

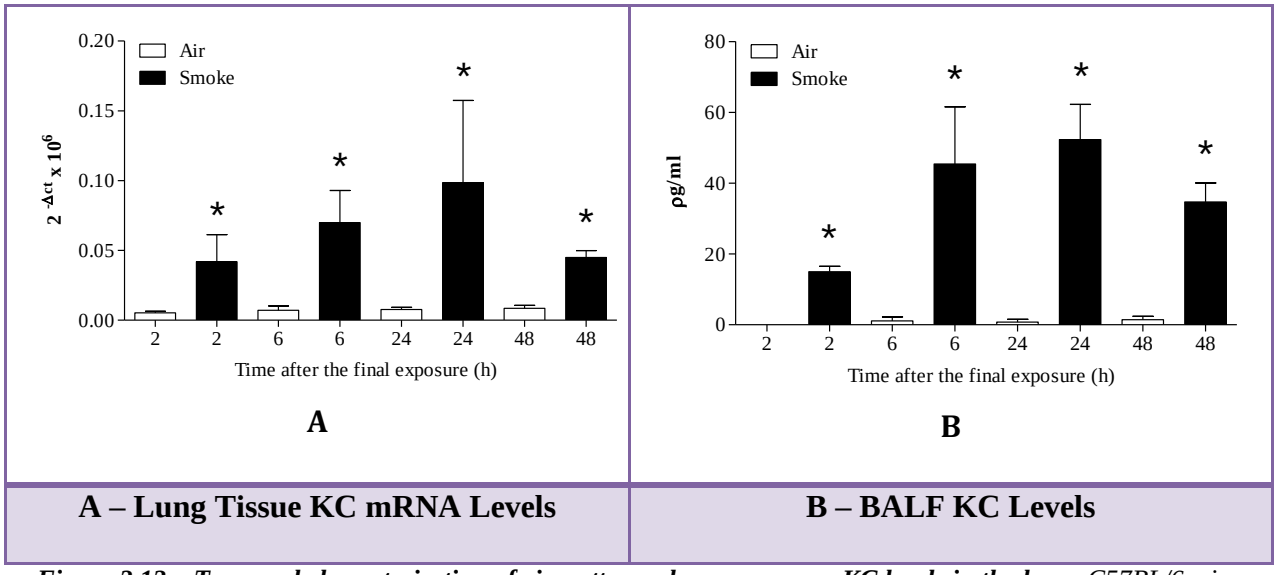

Figure 3.12 – Temporal characterisation of cigarette smoke exposure on KC levels in the lung. *C57BL/6 mice were challenged with room air or 500 ml/min cigarette smoke, twice daily for 3 consecutive days. Samples were collected at 2, 6, 24 and 48 hours after challenge and the expression of KC mRNA levels in lung tissue (A) and cytokine release in the BALF (B) were determined. Data represented as Mean ± SEM for n=6 observations. Statistical significance determined with a Mann-Whitney U-test for non-parametric data. * = P<0.05 and denotes a significant difference to the time-matched air exposed control group.*

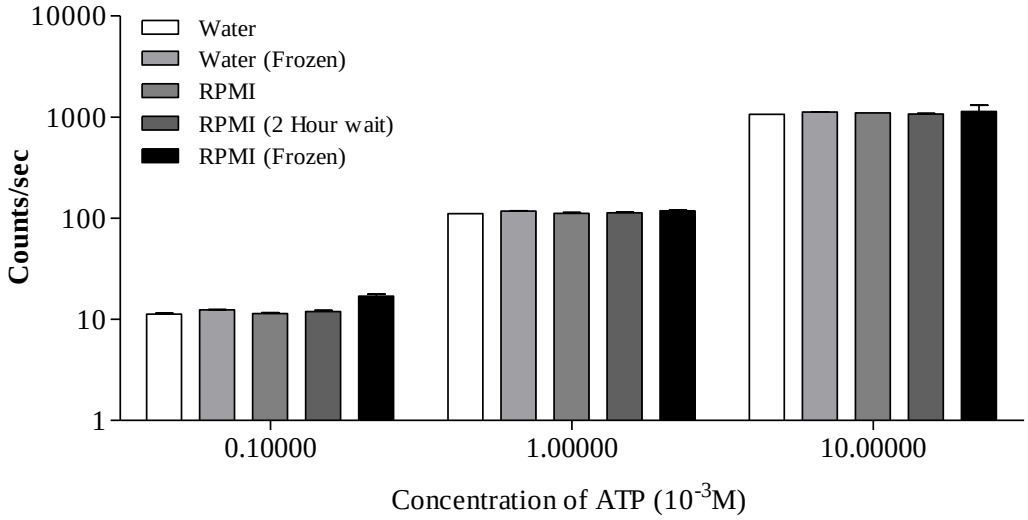

Figure 3.13 – Examination of various processing conditions on the detection of ATP using a commercially available assay. *Various mediums were prepared with increasing concentrations of ATP. The levels of ATP in these solutions were then assessed in response to various processing conditions. Water, Water – Frozen and thawed, RPMI, RPMI – with ATP assessed 2 hours later, RPMI – Frozen and thawed. Data represented as Mean ± SEM for n=2 observations.*

3.3.4 Temporal characterisation of LPS-induced airway inflammation in C57BL/6 mice.

To identify an appropriate time point following LPS challenge to examine the end-points of interest, an inflammatory response was elicited in animals by exposure to either saline or 1 mg/ml LPS for 30 minutes. Mice were euthanised with an overdose (200 mg/kg) of i.p. sodium pentobarbitone at various time points after challenge (2, 6, 24, 48, 72, 96 and 168 hours).

BALF neutrophilia peaked at 24 hours after LPS exposure but was only increased at all time-points up to and including 48 hours when compared to the time matched controls (Figure 3.14). Furthermore, the numbers of eosinophils in the BALF were significantly increased when compared to the time matched controls, peaking at 2 hours and returning to normal levels 48 hours post challenge (Figure 3.15). Initially, lymphomononuclear cells were significantly reduced in response to the LPS exposure at 2 and 6 hours post challenge, however, they become significantly increased between 24 and 96 hours post challenge when compared to the time matched controls (Figure 3.15).

Differential cell counts of the lung tissue samples demonstrated a significant increase in lung tissue neutrophilia when compared to the time matched controls at 2 hours post challenge that is resolved by 72 hours (Figure 3.16). Similar to the neutrophils, the eosinophils peaked early on in response to the LPS challenge and were resolved by 48 hours post exposure (Figure 3.17). The lymphomononuclear cells were also significantly increased in LPS exposed groups, however they peaked at the later 48 hour time point (Figure 3.17).

Determination of caspase 1 activity in the lung tissue highlighted that there was no increase in response to LPS exposure at any time point following LPS exposure when compared to their time matched controls (Figure 3.18). The inflammasome linked cytokines IL-1β and IL-18 were both increased but unlike in response to CS exposure, these increases did not seem to temporally correlate with an increase in caspase 1 activity or neutrophilia. The mRNA expression of IL-1β was increased at 2 and 6 hours following LPS exposure (Figure 3.19A). This finding was mirrored in the release of IL-1β and in the BALF, peaking at 2 hours following LPS exposure and gradually attenuating (Figure 3.19B). The mRNA expression of IL-18 was shown to be unaffected in response to LPS exposure (Figure 3.20A); however, IL-18 production was significantly increases at the 24 and 48 hour time points when compared to the time matched controls (Figure 3.20B).

In similar fashion to IL-1β, a significant increase in KC gene expression and release was demonstrated that peaked at 2 hours post LPS exposure and gradually decreased (Figure 3.21). Furthermore, attempts to examine the levels of ATP released into the BALF following LPS exposure proved to be unsuccessful as seen previously with samples from the CS model.

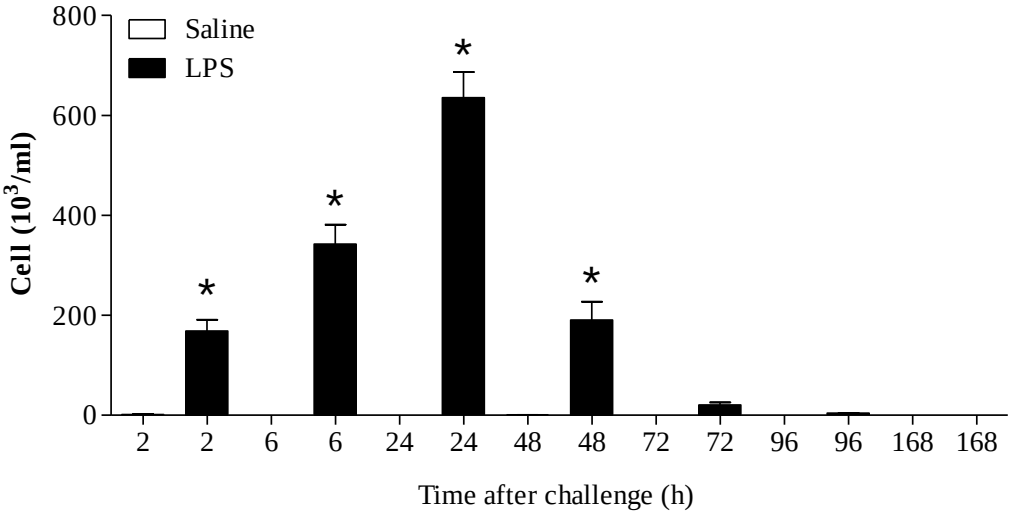

Figure 3.14 – Temporal characterisation of LPS exposure on airway neutrophilia in the BALF. *C57BL/6 mice were challenged with endotoxin free saline or 1 mg/ml LPS for 30 min. Samples were collected at 2, 6, 24, 48, 72, 96 and 168 hours after challenge and the BALF neutrophilia was determined by differential counting under light microscopy. Data represented as Mean ± SEM for n=6 observations. Statistical significance determined with a paired student's t-test for parametric data. * = P<0.05 and denotes a significant difference to the time-matched saline exposed control group.*

	Cells (10^3/ml)	Eosinophils	Lymphomononuclear
2 hrs	Saline	0.01±0.01	138.50±16.95
	LPS	31.06±2.61*	26.83±2.48*
6 hrs	Saline	0.01±0.01	86.25±10.85
	LPS	19.61±3.00*	52.70±7.71*
24 hrs	Saline	0.01±0.01	92.40±8.21
	LPS	12.55±1.60*	163.30±15.03*
48 hrs	Saline	0.19±0.12	84.18±3.37
	LPS	1.65±1.22	178.00±25.93*
72 hrs	Saline	0.01±0.01	58.69±4.81
	LPS	1.24±0.87	165.40±22.25*
96 hrs	Saline	0.11±0.11	70.95±3.87
	LPS	0.69±0.53	198.80±17.57*
168 hrs	Saline	0.08±0.08	60.81±5.18
	LPS	0.01±0.01	91.18±9.38*

Figure 3.15 – Temporal characterisation of LPS exposure on inflammatory cell recruitment in the BALF. *C57BL/6 mice were challenged with endotoxin free saline or 1 mg/ml LPS for 30 min. Samples were collected at 2, 6, 24, 48, 72, 96 and 168 hours after challenge and the numbers of neutrophils, eosinophils and, lymphomononuclear cells recovered from the BALF was determined by differential counting under light microscopy. Data represented as Mean ± SEM for n=6 observations. Statistical significance determined with a Mann-Whitney U-test for non-parametric data. * = P<0.05 and denotes a significant difference to the time-matched saline exposed control group.*

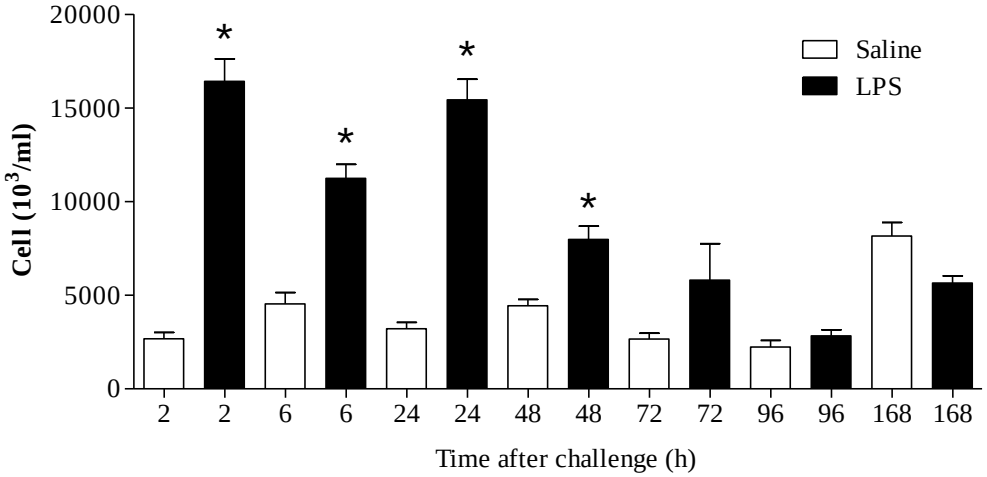

Figure 3.16 – Temporal characterisation of LPS exposure on neutrophilia in the lung tissue. *C57BL/6 mice were challenged with endotoxin free saline or 1 mg/ml LPS for 30 min. Samples were collected at 2, 6, 24, 48, 72, 96 and 168 hours after challenge and the numbers of neutrophils in the lung tissue was determined by differential counting under light microscopy. Data represented as Mean ± SEM for n=6 observations. Statistical significance determined with paired student's t-test for parametric data. * = P<0.05 and denotes a significant difference to the time-matched saline exposed control group.*

	Cells (10^3/ml)	Eosinophils	Lymphomononuclear
2 hrs	Saline	239.0±97.15	2734±609.8
	LPS	1161.0±165.3*	1802±190.7
6 hrs	Saline	384.3±73.28	2235±310.8
	LPS	865.3±164.7*	3070±373.7
24 hrs	Saline	380.0±43.05	2978±466.0
	LPS	678.2±66.72*	3747±425.5
48 hrs	Saline	455.4±97.04	4334±491.6
	LPS	455.8±87.36	8130±913.5*
72 hrs	Saline	248.8±45.92	2953±470.7
	LPS	668.5±303.2	5884±947.6*
96 hrs	Saline	242.8±52.27	2401±487.8
	LPS	348.0±32.92	5319±551.1*
168 hrs	Saline	544.2±127.7	6898±481.2
	LPS	633.5±79.22	7861±599.3

Figure 3.17 – Temporal characterisation of LPS exposure on inflammatory cell recruitment in the lung tissue. *C57BL/6 mice were challenged with endotoxin free saline or 1 mg/ml LPS for 30 min. Samples were collected at 2, 6, 24, 48, 72, 96 and 168 hours after challenge and the numbers of neutrophils, eosinophils and lymphomononuclear cells in the lung tissue was determined by differential counting under light microscopy. Data represented as Mean ± SEM for n=6 observations. Statistical significance determined with paired student's t-test for parametric data. * = P<0.05 and denotes a significant difference to the time-matched saline exposed control group.*

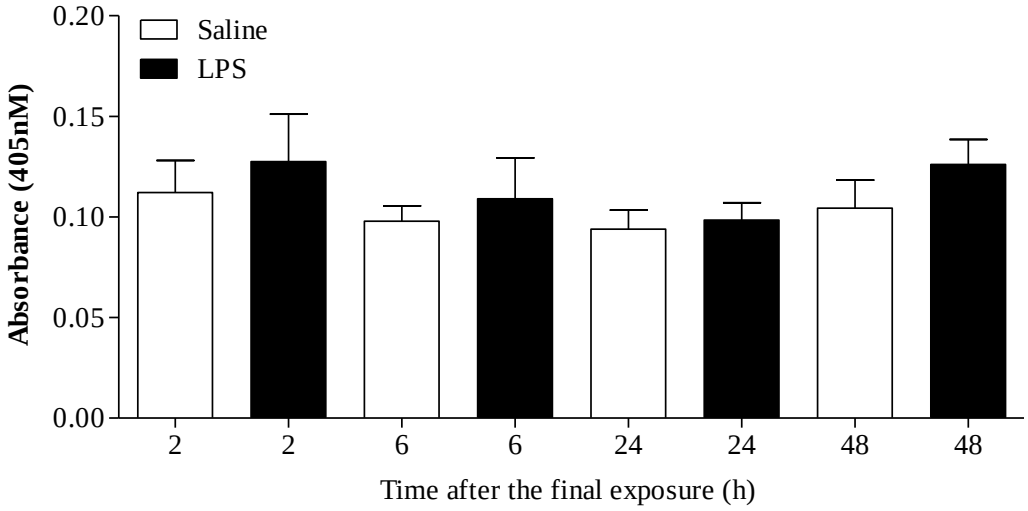

Figure 3.18 – Temporal characterisation of LPS exposure on Caspase 1 activity in the lung tissue. *C57BL/6 mice were challenged with endotoxin free saline or 1 mg/ml LPS for 30 min. Samples were collected at 2, 6, 24 and 48 hours after challenge and the Caspase 1 activity in the cytosolic fraction of the lung tissue was determined by a commercially available colourimetric assay. Data represented as Mean ± SEM for n=6 observations. Statistical significance determined with paired student's t-test for parametric data. * = P<0.05 and denotes a significant difference to the time-matched saline exposed control group.*

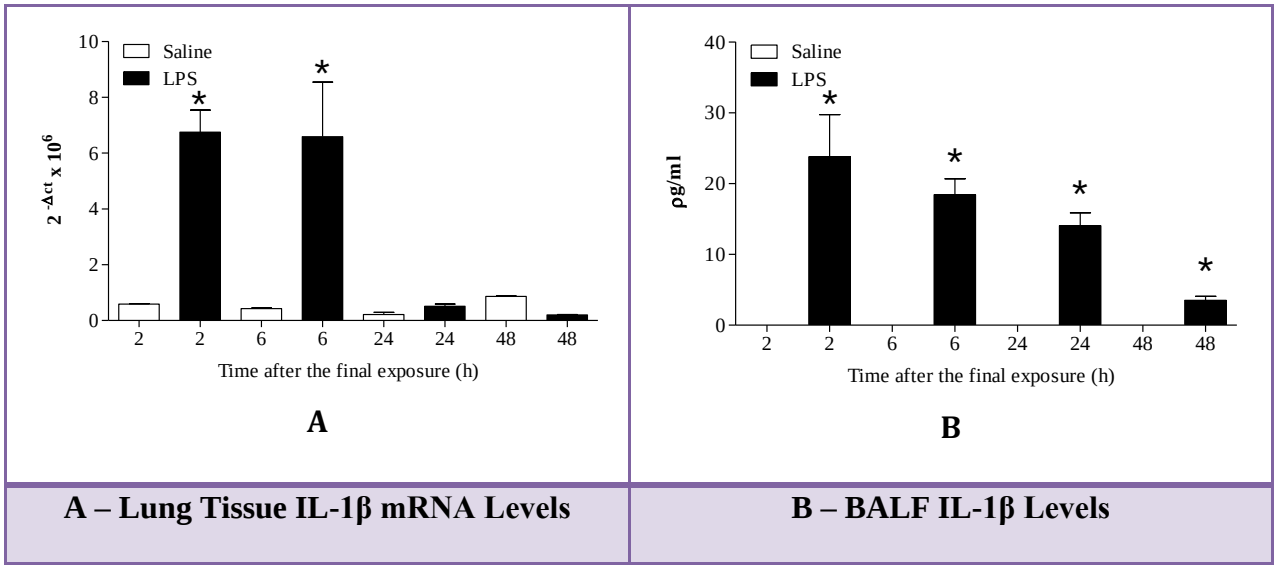

Figure 3.19 – Temporal characterisation of LPS exposure on IL-1β levels in the lung. *C57BL/6 mice were challenged with endotoxin free saline or 1 mg/ml LPS for 30 min. Samples were collected at 2, 6, 24 and 48 hours after challenge and the expression of IL-1β mRNA levels in lung tissue (A) and cytokine release in the BALF (B) were determined. Data represented as Mean ± SEM for n=6 observations. Statistical significance determined with a Mann-Whitney U-test for non-parametric data. * = P<0.05 and denotes a significant difference to the time-matched saline exposed control group.*

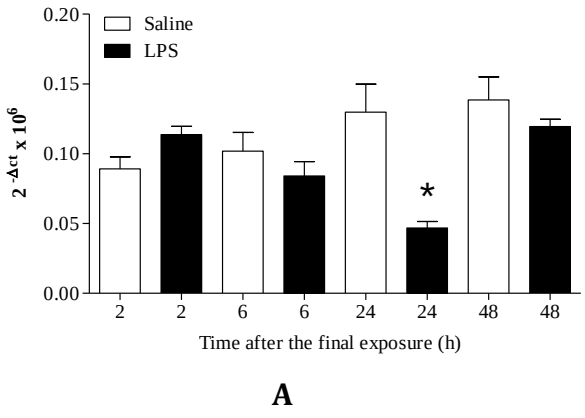

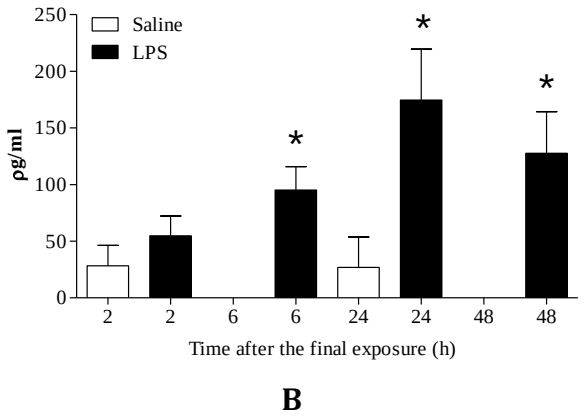

A – Lung Tissue IL-18 mRNA Levels | **B – BALF IL-18 Levels**

Figure 3.20 – Temporal characterisation of LPS exposure on IL-18 levels in the lung. *C57BL/6 mice were challenged with endotoxin free saline or 1 mg/ml LPS for 30 min. Samples were collected at 2, 6, 24 and 48 hours after challenge and the expression of IL-18 mRNA levels in lung tissue (A) and cytokine release in the BALF (B) were determined. Data represented as Mean ± SEM for n=6 observations. Statistical significance determined with a Mann-Whitney U-test for non-parametric data. * = P<0.05 and denotes a significant difference to the time-matched saline exposed control group.*

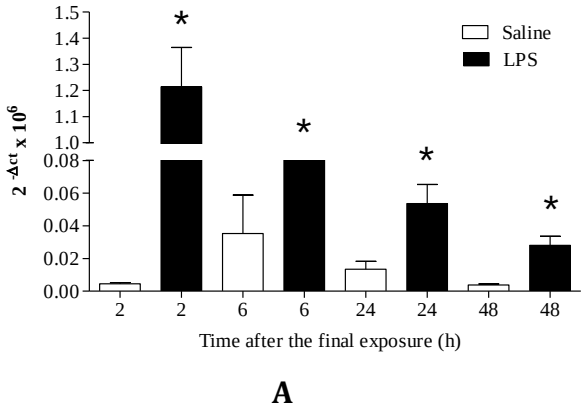

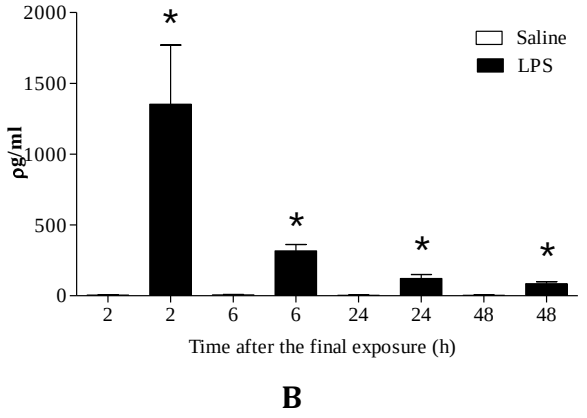

A – Lung Tissue KC mRNA Levels | **B – BALF KC Levels**

Figure 3.21 – Temporal characterisation of LPS exposure on KC levels in the lung. *C57BL/6 mice were challenged with endotoxin free saline or 1 mg/ml LPS for 30 min. Samples were collected at 2, 6, 24 and 48 hours after challenge and the expression of KC mRNA levels in lung tissue (A) and cytokine release in the BALF (B) were determined. Data represented as Mean ± SEM for n=6 observations. Statistical significance determined with a Mann-Whitney U-test for non-parametric data. * = P<0.05 and denotes a significant difference to the time-matched saline exposed control group.*

3.4 Discussion

Animal models of inflammation have long provided valuable insight in better understanding the underlying mechanisms driving disease pathophysiology and provided major contributions in drug discovery efforts. A wide range of *in vivo* models have been developed and utilised to tackle the growing problem that is COPD, including elastase, LPS and more recently cigarette smoke. Acute exposure to cigarette smoke elicits a neutrophil-driven inflammatory response; it remains the benchmark for *in vivo* models of COPD-like inflammation. In recent times, *in vivo* models of cigarette smoke induced lung inflammation have quickly become the preferred systems for investigating the underlying mechanisms driving the pathogenesis of COPD. With cigarette smoke being the primary etiological factor driving the pathogenesis of the disease combined with the fact that cigarette smoke contains over 4000 individual chemicals in every puff (Pryor and Church, 1993). More importantly, this model mimics disease pathogenesis more accurately and is in line with clinical findings. Furthermore, as seen in the clinic the inflammation seen in smoke exposure models is reported to be resistant to corticosteroid treatment (Marwick *et al*., 2004; Wan *et al*., 2010).

The aim of these studies was to develop and characterise two acute models of airway inflammation. This would enable the role of the inflammasome to be investigated in a disease-like setting utilising the primary etiological factor known to drive the pathogenesis of COPD, cigarette smoke. In addition, I wanted to parallel my investigation in the LPS driven model as it too is a predominantly neutrophilic model, but one that is known to activate the innate immune response rather than replicate the disease phenotype.

To characterise an acute model of airway inflammation driven by cigarette smoke, dose-response studies were performed to identify a robust sub-maximal exposure limit. These studies showed a significant dose-related increase in BALF neutrophilia in response to the twice daily exposures. This increase was not seen in the once daily exposure groups. Interestingly, although no changes were seen in the infiltration of eosinophils or lymphocytes in response to once or twice daily smoke exposure, the numbers of monocyte/macrophages in the lavage fluid demonstrated a significant decrease in the twice daily exposed animals.

An appropriate sub-maximal dose of cigarette smoke was selected (twice daily, 500 ml/min) in order to examine the temporal changes in response to acute (3 day) cigarette smoke exposure, and determine the profile of the inflammatory response and resolution of the inflammation. A significant increase in BALF neutrophilia was seen between the 24 and 72 hours time points that peaked at 48 hours following the final smoke exposure. As expected there were no differences in the eosinophil numbers when comparing the smoke exposed groups with their time-matched controls across all time-points. Monocyte/macrophage infiltration into the airway was shown to be significantly elevated at the 2, 24 and 72 hours time points when compared to their time-matched air exposed controls. Since the monocyte/macrophages demonstrated a variable response in the time course and showed decreased levels in the initial dose response study, the focus will be aimed at the neutrophil compartment of the cellular inflammation.

This discrepancy between the BALF monocyte/macrophages numbers in the dose response and time course studies is a peculiar finding, howeve, others have reported it previously (Stevenson et al., 2007). One possible explanation for this finding is that the observed decrease in BAL monocyte/macrophages numbers in the dose response is possibly due to the

variances in the activation of these cells in response to CS exposure. Additionally, oxidant modification to matrix proteins by CS extract has also been proposed to enhance the adhesion of macrophages to matrix (Kirkham et al., 2003). Furthermore, macrophages are damaged by oxidants and could become overloaded with particulate matter following repeated exposure to CS. These changes can result in reduced migration and enhanced activation of macrophages (Morrow et al., 1988, Nikula et al., 2001). The above described findings may explain the variability in the numbers of monocyte/macrophages recovered in the BALF in my model.

Lymphocytes showed a similar pattern of increased infiltration as that of the monocyte/macrophages however, these increases were less profound. Examining the cellular burden in the lung tissue showed no significant changes in any cell type at any time point when compared to their time matched controls. Closer examination of the numbers of cells in the BALF in comparison with the lung tissue demonstrates a ten-fold difference. This would make it difficult to identify any changes in the lung tissue since the increases in cellular burden in response to CS exposure are usually mild. Furthermore, upon activation these inflammatory cells might not be released into the tissue digest. Since no changes to cellular burden were seen in the lung tissue, from this point forward the inflammation in subsequent acute exposure experiment will be assessed in the BALF.

The pathophysiological changes seen in COPD are believed to be due to the progressive, persistent low-level inflammation in response to cigarette smoke. It has previously been reported that the inflammatory response to smoke exposure in animal models appears to have to two distinct phases. The acute phase, which is defined by neutrophilia in the first week following the initial exposure to cigarette smoke, followed by the progressive chronic phase that is made up of neutrophils, macrophages and lymphocytes infiltrating the lung after

approximately one month of consistent exposure (D'hulst *et al*., 2005; Stevenson *et al*., 2007). The protocol and dosing regimen developed here is similar to that of Morris *et al*., and produced results in line with those reported with 3 days of acute cigarette smoke exposure in C57BL/6 mice causing an increase in neutrophils peaking at 24 hours after challenge, followed later by macrophages (Doz *et al.*, 2008; Morris *et al*, 2008).

Examining markers of inflammasome activation in response to CS exposure revealed some interesting findings. A significant increase in caspase 1 activity in the lung tissue was seen 24 and 48 hours following the final smoke exposure when compared to their time matched controls. Furthermore, the increases at these specific time points were mirrored in the elevated levels of IL-1β and IL-18 detected in the BALF in response to CS exposure when compared to their time matched controls at 24 and 48 hours following the exposure. This finding suggests that there appears to be a temporal correlation between the increase in caspase 1 activity, IL-1β/IL-18 release and airway neutrophilia. The markers of inflammasome activation were only examined up to and including the 48 hour time point due to the expense involved with these specific assay kits.

Interestingly, increases in IL-1β were not reflected at the gene level upon examination of mRNA levels in the lung tissue. This finding may help explain why the inflammation observed in these models, and perhaps in COPD patients is resistant to glucocorticoid treatment, as their mechanism of action is believed to be via blockade of transcription/translation of inflammatory cytokines. Thus, if the inflammation in the disease is driven by a mechanism that is independent of transcription/translation this could explain why steroid treatment has limited impact on the inflammation. Alternatively, it could be proposed that the site of release of IL-1β in this model is different to the site at which the

gene expression was examined. If the IL-1β levels detected in the BALF are released from the epithelial and endothelial cells in the outer layers of the airways in response to the smoke, then this would mean that we would need to examine the mRNA expression of IL-1β in that specific cell type or cell layer.

A significant increase in KC expression was shown at all time points following the final smoke exposure at both the gene and protein levels. Interestingly, this increase in KC production did not seem to temporally correlate with the cellular inflammation. This may suggest that KC may not play an important role in driving the inflammation seen in this model.

Intriguingly, examination of ATP levels in the BALF in response to CS exposure proved to be unsuccessful. This was surprising as other groups have reported successfully detecting increased ATP levels in the lavage fluid in following CS exposure using the same assay kit (Mortaz *et al*., 2010; Lucattelli *et al*., 2010). It is unclear why ATP levels could not be detected following CS exposure, however, the literature suggests that ATP is rapidly broken down by ectonucleotidases (Robson *et al*., 1997). To address the notion that ATP was being broken down rapidly following sample collection or the sample preparation techniques were affecting the ATP presence in these samples breakdown experiments were performed. These highlighted that ATP levels were maintained under various sample preparation techniques/conditions. There are alternate techniques to examine ATP levels in biological samples, including many novel techniques that will provide data in real-time and in live animals. Some of these are currently being investigated in order to determine the role of ATP in this CS driven model.

The LPS-induced airway inflammation model has previously been shown to induce a large influx of neutrophils to the lung (Poynter *et al*., 2003; Birrell *et al*., 2006). As performed with the cigarette smoke model, the LPS model in mice was characterised initially with dose-response to LPS followed by a time-course to examine the temporal changes in the inflammation. The initial dose-response studies highlighted dose-related increases in neutrophils and eosinophils but not lymphomononuclear cells. Having selected the appropriate sub-maximal dose (1 mg/ml), the temporal changes following this LPS challenge were examined. Neutrophils peaked 24 hours after LPS exposure and were resolved by 48 hours post challenge. Eosinophils peaked at 2 hours post challenge and were back to baseline by 48 hours as well. Initially, lymphomononuclear cells were significantly reduced in response to the LPS exposure at 2 and 6 hours post challenge, however, they become significantly increased between 24 and 96 hours post challenge when compared to the time matched controls. Examination of the cellular burden in the lung tissue showed more profound changes when compared to the data from the cigarette smoke model. Increases in neutrophils, eosinophils and lymphomononuclear cells were seen that mirroring those seen in the BALF.

Examination of caspase 1 activity in the lung tissue highlighted that there was no increase in response to LPS exposure at any time point following LPS exposure when compared to their time matched controls. However, there was an increase in IL-1β and IL-18 levels. It is possible that the increase in caspase 1 activity responsible for the elevated levels of inflammasome linked cytokines may have taken place at an earlier time point than those examined following the LPS exposure. Alternatively, in this model the release of both IL-1β and IL-18 is not dependent on an increase in caspase 1 activity. Although caspase 1 may not be responsible in this LPS model, the literature suggests that neutrophil-derived serine

proteases such as cathepsin G, neutrophil elastase (NE) and proteinase 3 in addition to mast cell derived serine proteases granzyme A and chymase cleave the IL-1β precursor to produce a biologically active form (Black et al., 1991; Mizutani et al., 1991; Dinarello et al., 1986; Hazuda et al., 1990; Irmler et al., 1995). More recently, chromogranin A has also been demonstrated to process IL-1β into its mature active form (Terada et al., 2009).

The expression of IL-18 at the mRNA level was shown to be unaffected in response to LPS exposure, yet IL-18 levels were still significantly increased at the 24 and 48 hour time points when compared to the time matched controls. Once again, as in the CS exposure model, the release of IL-18 seems to be independent of increased mRNA expression. Another difference between the LPS and CS exposure model is the increase in IL-1β mRNA expression in response to LPS exposure. Combined with the lack of increase in caspase 1 activity, it could be suggested that IL-1β may be processed differently in this model. It is also possible that the increase in pro- IL-1β in response to LPS driven NFκB activation and basal levels of caspase 1 may be sufficient for IL-1β processing.

A role for IL-1β in T_H17 development has recently been proposed (Wilson et al., 2007). Furthermore, IL-1β is required for T_H17 production of IL-17 and the subsequent neutrophilia (Burgler et al., 2009). The levels of IL-17 have been shown to be increased in COPD and correlate with both neutrophila and the severity of lung function decline (Alcorn et al., 2010). Animal models have shown that IL-17 production and neutrophilia is enhanced in mice exposed to CS (Melgert et al., 2007; Van Der Deen et al., 2007) whilst IL-17RA$^{-/-}$ mice are protected against lung emphysema induced by CS. It is possible that IL-1β production may drive T_H17 development and influence the neutrophilic phenotype seen in these models and

explain some of the discrepancies with regards to the expression and production of IL-1β in both models.

Similarly to IL-1β a significant increase in KC gene expression and protein was demonstrated, peaking at 2 hours post LPS exposure. It is well documented that LPS-induced lung inflammation, characterised by a large influx of neutrophils to the lung is regulated by the release of chemokines, such as KC (Frevert *et al*., 1995). This correlates with the time course of this model, where neutrophilic chemokines such as KC are increased in the BALF at 2 hours, followed by an increase in lung tissue neutrophils (between 2 and 24 hours) and finally by an accumulation of neutrophils in the BALF.

		CS Exposure Model	LPS Challenge Model
BALF Inflammatory Cells	Neutrophils	Peak at 48 hours	Peak at 24 hours
	Eosinophils	No change	Peak at 2 hours
	Monocytes/ Macrophages	Variable increases	Variable
	Lymphocytes	Variable increases	
Tissue Inflammatory MCells	Neutrophils	No change	Peak at 2 hours
	Eosinophils	No change	Peak at 2 hours
	Monocytes/ Macrophages	No change	Peak at 48 hours
	Lymphocytes	No change	
Inflammasome Markers	Caspase 1 Activity	Increase at 24 & 48 hours	No change
	IL-1β (BALF)	Increase at 24 & 48 hours	Peak at 2 hours
	IL-1β mRNA (Lung Tissue)	No change	Increased at 2 & 6 hours
	IL-18 (BALF)	Increase at 24 & 48 hours	Peak at 24 hours
	IL-18 mRNA (Lung Tissue)	No change	No change
	KC (BALF)	Peak at 24 hours	Peak at 2 hours
	KC mRNA (Lung Tissue)	Peak at 24 hours	Peak at 2 hours

Figure 3.22 – Comparison table of time-course following CS and LPS driven models of inflammation.

Attempts to examine the levels of ATP released into the BALF following LPS exposure proved to be unsuccessful as seen previously with samples from the CS model.

The differences in the inflammatory responses and markers of inflammasome activation in the two models would suggest that the signalling axis in the two models is not the same (summarised in figure 3.22). With these two models characterised, it is now possible to examine the role of the $P2X_7$-inflammasome axis. In order to do this, the pathway will be manipulated using pharmacological and genetic tools.

Chapter 4

Genetic Manipulation of the Inflammasome Pathway

4.1 Rationale

Activation of the NLRP3 inflammasome can be achieved via different routes, however, the best characterised is through the actions of ATP on the $P2X_7$ purinergic receptor (Perregaux & Gabel, 1994; Sutterwala *et al*., 2006; Qu *et al*., 2007). Recent publications have reported elevated ATP levels in both *in vitro* and *in vivo* models of COPD and in clinical samples (Mohsenin *et al*., 2006; Polosa & Blackburn, 2009). It has been proposed that increased levels of ATP are involved in the chemotaxis and activation of inflammatory cells (e.g. neutrophils) via P2Y receptors (Mortaz *et al*., 2009; Cicko *et al*., 2010). Conversely, as the expression of the $P2X_7$ receptor has been shown to be increased in disease tissues and cells (Cicko *et al*., 2010; Lucattelli *et al*., 2010), an alternative hypothesis could be that the ATP is acting on the $P2X_7$ receptor leading to NLRP3 inflammasome and caspase 1 activation, sequentially processing IL-1β and IL-18 from their precursors into their mature active forms and facilitating their release. These cytokines then play a central role in the inflammation observed in COPD.

The findings of the previous chapter, specifically the increases in markers of inflammasome activation in response to CS exposure suggests a crucial role for the $P2X_7$ – inflammasome signalling axis in directing the inflammation associated with COPD pathogenesis in a disease relevant model. Therefore, modulation of this $P2X_7$ - inflammasome axis could attenuate CS-induced inflammation. In the clinic, patients suffering from COPD have been shown to have increased levels of ATP in the BALF which suggests that it may be driving this inflammation through activation of the $P2X_7$ receptor. Although levels of ATP could not be determined due to an absence of detection in the samples from the previous chapter, this does not rule out the possibility that it or an alternative activator of the $P2X_7$ receptor may still ultimately be driving this response.

The aim of this chapter is to manipulate activation of the $P2X_7$ – inflammasome signalling axis in response to cigarette smoke exposure by utilising genetically modified mice lacking the $P2X_7$ puringergic receptor from birth. Both wild-type (C57BL/6) and $P2X_7^{-/-}$ mice will be exposed to cigarette smoke. By comparing the differences in the inflammatory responses and markers of NLRP3 inflammasome activation (e.g. caspase 1 activity and IL-1β/IL-18 release) in both the wild-type and $P2X_7^{-/-}$ mice, it will be possible to elucidate the role of the $P2X_7$ – inflammasome signalling axis and more specifically the $P2X_7$ receptor in driving the inflammation in response to cigarette smoke exposure. These KO animals will also be paralleled in the LPS driven model to determine if these receptors play a role in the normal innate neutrophilic response.

4.2 Methods

4.2.1. The role of the $P2X_7$ receptor in cigarette smoke-induced airway inflammation.

In order to validate our previous finding that increases in markers of inflammasome activation temporally correlate with the inflammatory cell burden in response to CS exposure, the role of the $P2X_7$ – inflammasome pathway was further investigated by comparing the inflammatory responses to CS exposure in both wild-type and $P2X_7^{-/-}$ mice. Assessment of inflammatory end-points of interest including cellular infiltration and the markers of inflammasome activation, including pro-inflammatory mediator release and caspase 1 activity, will provide insight into the role of this receptor and its linked pathway in the inflammation associated with COPD using a disease relevant model.

To examine the role of the $P2X_7$ receptor, wild-type C57BL/6 mice and $P2X_7^{-/-}$ mice (bred on a C57BL/6 background) were exposed to either room air or a sub-maximal (500 ml/min) dose of cigarette smoke (as detailed in section *2.2.2*) for a total exposure period of 50 minutes (excluding 10 minute venting period), twice daily, for 3 consecutive days. Each group consisted of n=18 animals. Mice were euthanised with an overdose (200 mg/kg) of i.p sodium pentobarbitone 24 hours after the final challenge. BALF and lung tissue samples were collected for analysis as follows;

- BALF (processed as described in section *2.3.1*):
    - Total cell counts and 4-part differential cell counts (neutrophils, eosinophils, monocytes/macrophages and lymphocytes, as described in section 2.*3.3*), n=8.

- Cytokine analysis in BALF determined by standard ELISA, n=6 (as described in section *2.3.4.3*).
- NAD+ levels in the BALF examined by utilising a colorimetric assay, n=6 (as described in section *2.3.7*)

- Lung tissue (processed as described in section *2.3.1*):
  - Flash frozen in liquid nitrogen, n=6, for cytosolic and nuclear cell fraction extraction (as described in section *2.3.5.1*) for determination of caspase 1 activity (as described in section *2.3.5.2*).

4.2.2. The role of the $P2X_7$ receptor in LPS-induced airway inflammation.

Previous findings had suggested that the inflammatory response seen following an endotoxin challenge is independent of the $P2X_7$ – inflammasome pathway based on the absence of correlation in the markers of inflammasome activation i.e. caspase 1 activity and IL-1β/IL-18 processing and subsequent release. To further investigate this I compared the inflammatory responses to LPS exposure in both wild-type and $P2X_7^{-/-}$ mice.

To examine the role of the $P2X_7$ receptor in response to an endotoxin challenge, wild-type C57BL/6 mice and $P2X_7^{-/-}$ mice were challenged endotoxin free saline (Fresenius Kabi, Warrington, UK) or a sub-maximal dose of 1 mg/ml LPS (*Escherichia coli*, serotype 0111:B4, Sigma-Aldrich Ltd. Poole, UK) for 30 min (as detailed in section *2.2.1*). Mice were euthanised with an overdose (200 mg/kg) of i.p sodium pentobarbitone 6 hours after the final challenge. BALF and lung tissue samples were collected for analysis as detailed in section *4.2.1*.

4.2.3. Statistical analysis

Data is expressed as mean ± S.E.M of n observations. For multiple comparisons tests, statistical analysis was performed by applying a one-way ANOVA (analysis of variance) with a Dunnett's (comparing with a single control group) or Bonferroni's (multiple comparisons) post-test for parametric data or alternatively a Kruskal-Wallis incorporating Dunn's multiple comparison post-test for non-parametric data. A P value < 0.05 was taken as significant and all treatments were compared with the appropriate control group.

4.3. Results

4.3.1. The role of the $P2X_7$ receptor in cigarette smoke-induced airway inflammation.

In response to cigarette smoke exposure, markers of inflammasome activation were shown to be decreased in smoke exposed $P2X_7^{-/-}$ mice when compared to the smoke exposed wild-type. As expected, caspase 1 activity in the lung tissue was significantly increased in the smoke exposed wild-type when compared to the air exposed wild-type (Figure 4.1A). Additionally, smoke exposed $P2X_7^{-/-}$ showed decreased caspase 1 activity when compared to the smoke exposed wild-type (Figure 4.1A). The levels of IL-1β and IL-18 in the BALF following cigarette smoke exposure showed similar responses to the caspase 1 activity. The levels of both IL-1β (Figure 4.1B) and IL-18 (Figure 4.1C) were significantly increased in the smoke exposed wild-type when compared to the air exposed wild-type. Furthermore, smoke exposed $P2X_7^{-/-}$ showed decreased IL-1β and IL-18 levels in the BALF when compared to the smoke exposed wild-type. These findings further validate the temporal correlation in the activation of caspase 1 and the production/release of IL-1β and IL-18.

Interestingly, levels of KC production were significantly increased in both smoke exposed wild-type and $P2X_7^{-/-}$ animals when compared to the air exposed wild-type (Figure 4.1D). A significant increase in BALF neutrophils was seen in the smoke exposed wild-type when compared to the air exposed wild-type (Figure 4.2A). This increase in the smoke exposed wild-type was completely attenuated in smoke exposed $P2X_7^{-/-}$ animals (Figure 4.2A). Determination of the levels of NAD+ in the BALF was unsuccessful, although the assay conditions were validated (Figure 4.4).

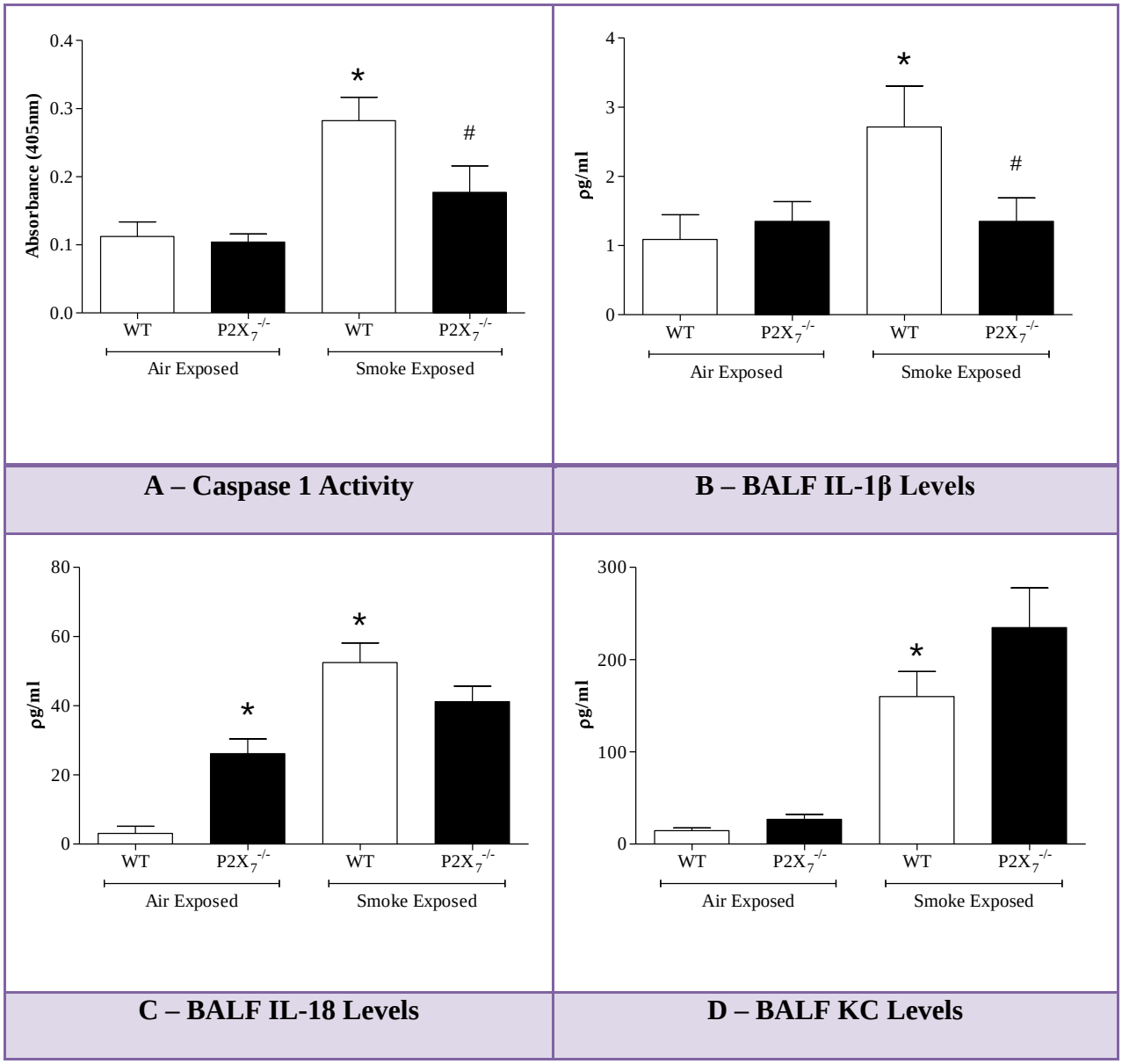

Figure 4.1 – The role of the P2X$_7$ receptor on markers of inflammasome activation in the lung following cigarette smoke exposure. *Wild-type C57BL/6 mice and P2X$_7^{-/-}$ mice were exposed to room air or 500 ml/min cigarette smoke, twice daily for 3 consecutive days. Samples were collected 24 hours after the final exposure and caspase 1 activity in the cytosolic fraction of the lung tissue (A) and the release of inflammatory cytokines IL-1β (B) IL-18 (C) and KC (D) in the BALF were measured using commercially available assays. Data represented as Mean ± SEM for n=6 observations. Statistical significance determined with a Kruskal-Wallis incorporating Dunn's post-test for non-parametric data. * = P<0.05 and denotes a significant difference to the air exposed wild-type group. # = P<0.05 and denotes a significant difference to the smoke exposed wild-type group.*

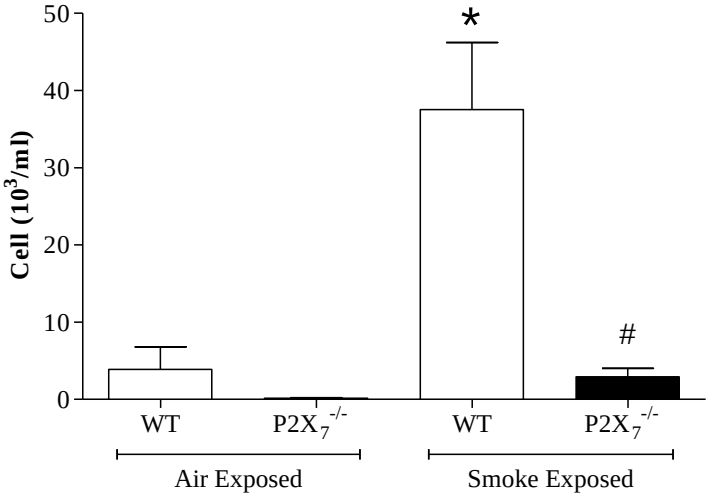

Figure 4.2 – The role of the P2X$_7$ receptor on airway neutrophilia in the BALF following cigarette smoke exposure. *Wild-type C57BL/6 mice and P2X$_7^{-/-}$ mice were exposed to room air or 500 ml/min cigarette smoke, twice daily for 3 consecutive days. Samples were collected 24 hours after the final exposure and the BALF neutrophilia was determined by differential counting under light microscopy. Data represented as Mean ± SEM for n=8 observations. Data represented as Mean ± SEM for n=8 observations. Statistical significance determined with a Kruskal-Wallis incorporating Dunn's post-test for non-parametric data. * = P<0.05 and denotes a significant difference to the air exposed wild-type group. # = P<0.05 and denotes a significant difference to the smoke exposed wild-type group.*

	BALF			
	Air Exposed		**Smoke Exposed**	
Cells (10^3/ml)	**WT**	**P2X$_7^{-/-}$**	**WT**	**P2X$_7^{-/-}$**
Eosinophils	0.23±0.16	0.06±0.06	0.35±0.24	0.0±0.0
Monocyte/ Macrophage	59.88±7.16	53.40±4.28	93.74±5.51*	89.89±5.46
Lymphocytes	8.53±1.63	6.40±1.30	3.39±1.38*	2.20±0.78

Figure 4.3 – The role of the P2X$_7$ receptor on inflammatory cell recruitment in the lung following cigarette smoke exposure. *Wild-type C57BL/6 mice and P2X$_7^{-/-}$ mice were exposed to room air or 500 ml/min cigarette smoke, twice daily for 3 consecutive days. Samples were collected 24 hours after the final exposure and the numbers of neutrophils, eosinophils, monocytes/macrophages and lymphocytes recovered from the BALF and lung tissue were determined by differential counting under light microscopy. Data represented as Mean ± SEM for n=8 observations. Data represented as Mean ± SEM for n=8 observations. Statistical significance determined with a Kruskal-Wallis incorporating Dunn's post-test for non-parametric data. * = P<0.05 and denotes a significant difference to the air exposed wild-type group. # = P<0.05 and denotes a significant difference to the smoke exposed wild-type group.*

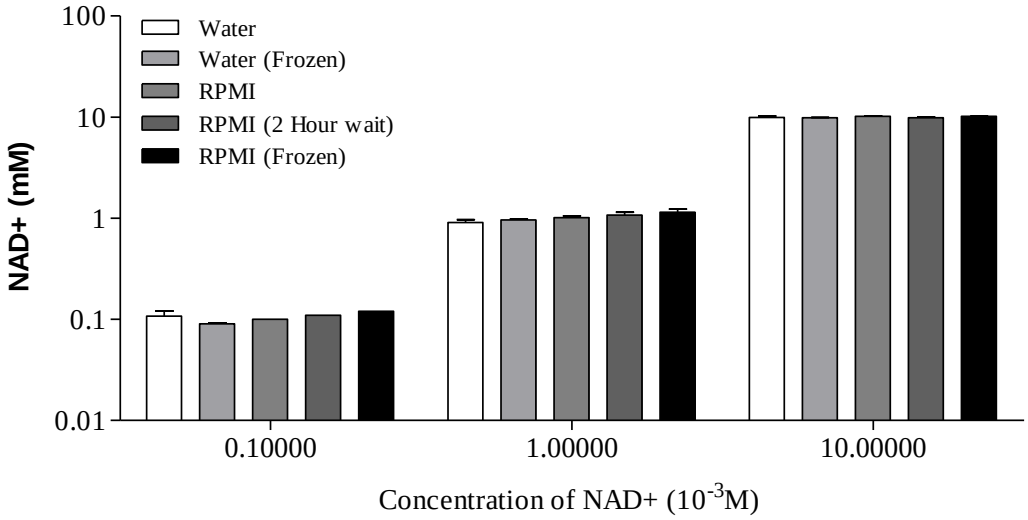

Figure 4.4 – Examination of various processing conditions on the detection of NAD+ using a commercially available assay. *Various mediums were prepared with increasing concentrations of NAD+. The levels of NAD+ in these solutions were then assessed in response to various processing conditions. Water, Water – Frozen and thawed, RPMI, RPMI – with NAD+ assessed 2 hours later, RPMI – Frozen and thawed. Data represented as Mean ± SEM for n=2 observations.*

4.3.2. The role of the $P2X_7$ receptor in LPS-induced airway inflammation.

As previously seen, the levels of IL-1β in the BALF following LPS challenge were significantly increased in the LPS challenged wild-type when compared to the saline challenged wild-type (Figure 4.4A). However, unlike in the CS model, this increase was maintained in the LPS exposed $P2X_7^{-/-}$ mice (Figure 4.4A). IL-18 levels in the BALF following LPS exposure were significantly increased; however, this was significantly reduced in the $P2X_7^{-/-}$ mice (Figure 4.4B). KC production was significantly increased in both LPS exposed wild-type and $P2X_7^{-/-}$ animals when compared to the air exposed wild-type (Figure 4.4C), but interestingly the LPS challenged $P2X_7^{-/-}$ animals showed a significant increase when compared to the LPS challenged wild-type animals (Figure 4.4C).

BALF neutrophilia was significantly increased in the LPS challenged wild-type when compared to the air exposed wild-type group (Figure 4.5A). Surprisingly, this increase was more profound in the LPS challenged $P2X_7^{-/-}$ mice that were significantly elevated when compared with the LPS challenged wild-type group (Figure 4.5A). The lymphomononuclear cells in the BALF were significantly decreased in both LPS challenged groups when compared to their saline exposed controls, however, this decrease was less significant in the LPS challenged $P2X_7^{-/-}$ animals (Figure 4.6).

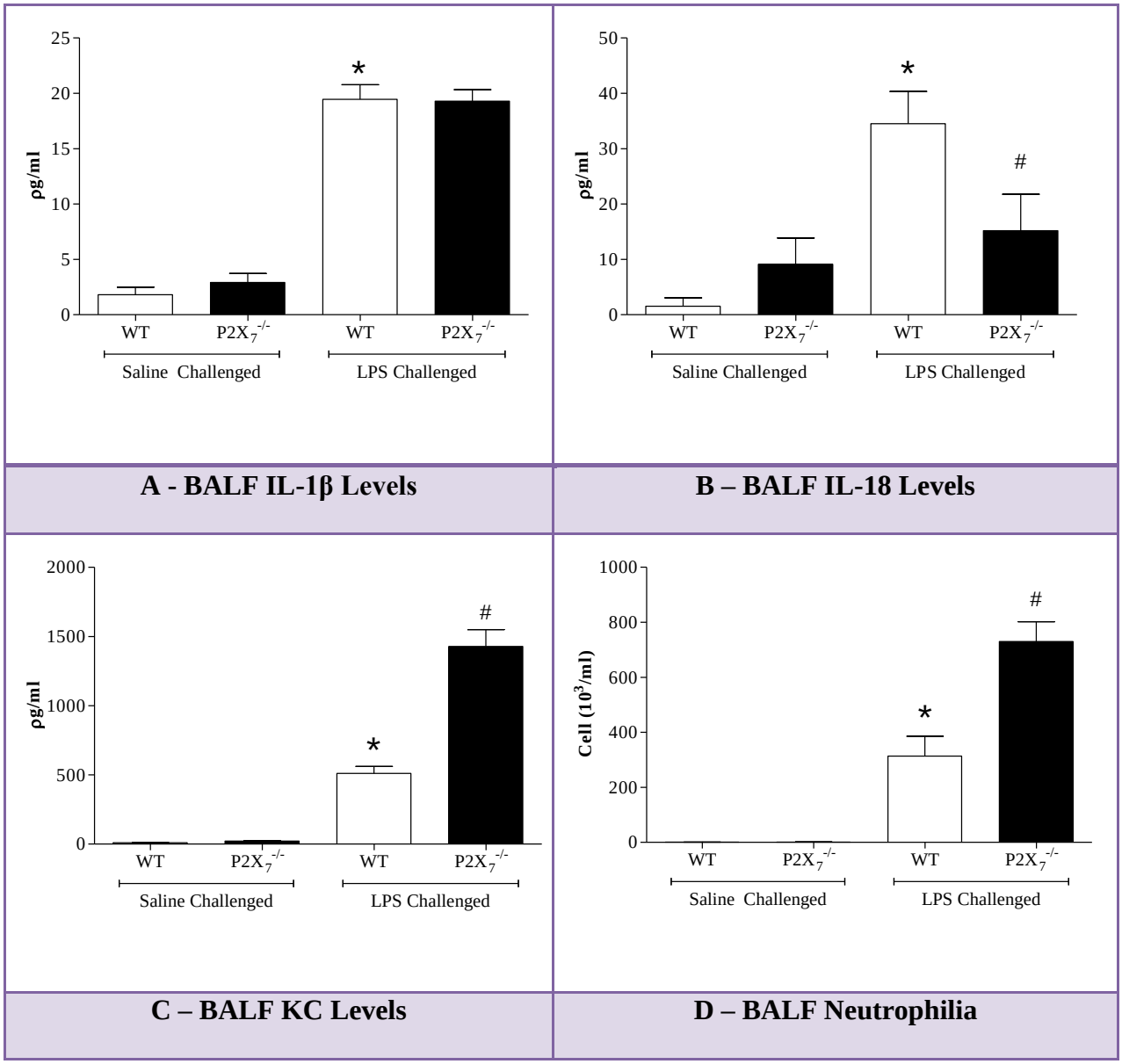

Figure 4.5 – The role of the $P2X_7$ receptor on markers of inflammasome activation and airway neutrophilia in the lung following an endotoxin (LPS) challenge. *Wild-type C57BL/6 mice and $P2X_7^{-/-}$ mice were challenged with endotoxin free saline or 1 mg/ml LPS for 30 min. Samples were collected 6 hours after the challenge and the release of inflammatory cytokines IL-1β (A), IL-18 (B) and KC (C) in the BALF were measured using commercially available assays. BALF neutrophilia (D) was determined by differential counting under light microscopy. Data represented as Mean ± SEM for n=6 (A-C) and n=8 (D) observations. Statistical significance determined with a Kruskal-Wallis incorporating Dunn's post-test for non-parametric data. * = P<0.05 and denotes a significant difference to the air exposed wild-type group. # = P<0.05 and denotes a significant difference to the smoke exposed wild-type group.*

	BALF			
	Saline Challenged		LPS Challenged	
Cells (10^3/ml)	**WT**	**$P2X_7^{-/-}$**	**WT**	**$P2X_7^{-/-}$**
Eosinophils	0.24±0.17	0.27±0.19	6.33±1.87*	3.23±1.34
Lymphomononuclear	76.02±4.32	91.44±9.72	38.98±4.14*	64.70±7.33#

Figure 4.6 – The role of the $P2X_7$ receptor on inflammatory cell recruitment in the lung following an endotoxin (LPS) challenge. *Wild-type C57BL/6 mice and $P2X_7^{-/-}$ mice were challenged with endotoxin free saline or 1 mg/ml LPS for 30 min. Samples were collected 6 hours after the challenge and the numbers of neutrophils, eosinophils and lymphomononuclear cells recovered from the BALF and lung tissue were determined by differential counting under light microscopy. Data represented as Mean ± SEM for n=8 observations. Data represented as Mean ± SEM for n=8 observations. Statistical significance determined with a Kruskal-Wallis incorporating Dunn's post-test for non-parametric data. * = P<0.05 and denotes a significant difference to the air exposed wild-type group. # = P<0.05 and denotes a significant difference to the smoke exposed wild-type group.*

4.4 Discussion

Having established temporal correlative data to suggest a role for the $P2X_7$-inflammasome pathway in CS-induced *in vivo* pre-clinical modelling system, I wanted to further my investigation. The aim of this chapter was to manipulate the activity of the $P2X_7$ – inflammasome signalling axis in response to CS exposure using genetically modified mice missing a functional $P2X_7$ receptor. Both wild-type (C57BL/6) and $P2X_7^{-/-}$ mice were exposed to CS in the *in vivo* pre-clinical modelling system developed in the Chapter 3. By comparing the differences in the inflammatory responses and markers of NLRP3 inflammasome activation (e.g. caspase 1 activity and IL-1β/IL-18 release) in both the wild-type and $P2X_7^{-/-}$ mice, it will be possible to elucidate the role of the $P2X_7$ – inflammasome signalling axis and more specifically the $P2X_7$ receptor in driving the inflammation in response to CS exposure. These $P2X_7^{-/-}$ mice were also examined in the LPS driven model to validate that this particular finding is specific to the disease, or less likely, as a result of a more general impact on airway neutrophilia.

Determining the effects of CS exposure on markers of inflammasome activation in the wild-type and $P2X_7^{-/-}$ mice produced some very interesting results. As expected, CS exposure significantly increased caspase 1 activity in wild-type mice; however, it failed to increase caspase 1 activity in $P2X_7^{-/-}$ animals. This effect was mirrored in the release of both IL-1β and IL-18, which were shown to be elevated in the smoke exposed wild-type, but not the $P2X_7^{-/-}$ animals. Surprisingly, it seems that basal levels of IL-18 in the $P2X_7^{-/-}$ mice were generally higher than in the wild-types, as seen in the air exposed animals; however this will require further investigation. This general increase in basal levels of $P2X_7^{-/-}$ mice might be

due to a biological compensatory mechanism that aims to protect these mice as they lack the functional $P2X_7$ receptors required for IL-18 processing and release.

Increases in KC production in response to CS exposure were seen in both wild-type and $P2X_7^{-/-}$ animals. This observation that KC levels remained unaffected by blockade of the $P2X_7$–inflammasome axis is intriguing. It would suggest that the CS-induced production/release of KC is via an alternative mechanism possibly being sourced from either recruited monocyte/macrophages or cells present in the lung, as opposed to the neutrophils being recruited as this observed neutrophilia in response to CS exposure was completely attenuated in the $P2X_7^{-/-}$ mice yet the increased KC levels in the BALF were maintained. Interestingly, $P2X_7^{-/-}$ animals show a non-significant increase in KC levels in response to CS exposure, possibly as a compensatory immunity mechanism as to compensate for the lack of inflammasome activity.

Examination of inflammatory cell burden in the lung demonstrated increased BALF neutrophilia following CS exposure in the wild-type mice. Remarkably, the BALF neutrophilia in response to CS exposure was completely attenuated in the $P2X_7^{-/-}$ mice. This finding highlights the importance of the $P2X_7$ receptor in driving the inflammation associated with CS exposure. A significant increase in BALF monocyte macrophages was seen in the smoke exposed wild-type and that was still maintained in the $P2X_7^{-/-}$ animals. Upon examination of eosinophils and lymphocytes, no differences in the numbers of cells could be identified when comparing the smoke exposed wild-type and $P2X_7^{-/-}$ animals.

Samples from both the clinic and animal models of COPD have been used to illustrate an increase in the levels of ATP in the disease, linked to activation of the $P2X_7$ – inflammasome

axis. I attempted to examine the release of ATP in this investigation and as we were unable to detect it previously (Chapter 3), I also examined the release of an alternative activator of the pathway, NAD+. Both ATP and NAD+ were not detected in any samples across all groups. As shown previously in chapter 3, the NAD+ assessment was conducted with all the correct controls to determine if our sampling techniques would affect the detection or sensitivity of the assay. I will continue to investigate the role of activators of the $P2X_7$ receptor using various techniques in order to identify what component of this pathway is responsible

In order to validate that the reduction in markers of inflammasome activation seen in the $P2X_7^{-/-}$ animals is specific to the disease, these animals were also challenged with LPS and the inflammatory responses were examined. $P2X_7^{-/-}$ animals failed to reduce the increased production of both IL-1β and KC in response to an endotoxin challenge. Interestingly, the release of KC in response to LPS was significantly increased in the $P2X_7^{-/-}$ when compared to the wild-type animals. Although unclear, this increase may be due to developmental changes in the $P2X_7^{-/-}$ mice from birth, though, this must be investigated further. By incorporating KC knockout mice into our models, we can then elucidate the role of this chemokine in driving the inflammatory responses seen in these *in vivo* models.

BALF neutrophilia in response to an endotoxin challenge was shown to be significantly increased in the $P2X_7^{-/-}$ when compared to the wild-type mice. Interestingly, the increases in both BALF neutrophilia and KC levels correlate, with similar proportional increases as KC is a known activator of neutrophils (Frevert *et al*., 1995). Interestingly, BALF eosinophils in LPS challenged groups were significantly reduced in the $P2X_7^{-/-}$ when compared to the wild-type mice. This is an interesting finding as much of the previous $P2X_7$ – inflammasome axis work has focused on neutrophils and monocyte/macrophages. This finding will require

further investigation, particularly examining the general immune response in these knockout mice, which may have adapted with developmental changes over time.

Having established there was temporal correlative data to suggest a role for the $P2X_7$-inflammasome pathway in CS driven inflammation, I further investigated its role by comparing wild-type and $P2X_7^{-/-}$ mice. CS exposure failed to increase caspase 1 activity, IL-1β and airway neutrophilia in $P2X_7^{-/-}$ mice. This is strong evidence for a role of the $P2X_7$-inflammasome axis in CS-induced airway neutrophilia. This data is consistent with data published recently by other groups, where $P2X_7^{-/-}$ mice were demonstrated to be protected against CS-induced inflammation (neutrophilia and macrophages) as well as the release of the inflammatory cytokine IL-1β (Lucattelli *et al.*, 2010). This pathway, however, was not involved in a similar inflammatory response (i.e. IL-1β release and neutrophilia) observed following LPS induced activation of the normal innate immune response suggesting that this pathway is only activated in disease settings. These significant findings must be supported using a pharmacological tool, to validate that they data seen in the $P2X_7^{-/-}$ mice is indeed due to blockade of the $P2X_7$-inflammasome axis and not developmental or physiological changes in the $P2X_7^{-/-}$ animals from birth. This will be the focus of the next chapter of this thesis.

Chapter 5

Pharmacological Modulation of the Inflammasome Pathway

5.1 Rationale

The data presented in this thesis thus far advocates a crucial role for the $P2X_7$-inflammasome signalling axis in driving the inflammation seen in response to CS exposure. With CS exposure being the primary etiological factor driving the pathogenesis of the disease, it is envisaged that blocking this inflammation provides a huge therapeutic benefit to combat the relentless progression of COPD.

In the previous chapter, it was demonstrated that deletion of the $P2X_7$ receptor significantly reduced the markers of inflammasome activation, and more importantly, the ensuing inflammation in response to CS exposure. To confirm the finding with the $P2X_7^{-/-}$ mice, the aim of this chapter was to parallel the study using a selective small molecular weight receptor inhibitor. To achieve this, an appropriate tool to use in the *in vivo* murine models must be identified and validated. Cell based assays were developed in appropriate human (to compare to published data) and mouse (as the *in vivo* model is developed in this species) cells to develop a $P2X_7$-inflammasome driven *in vitro* assay. The human THP-1 monocytic and mouse J774.2 monocytes/macrophages cell lines were selected to perform this work from a range of cell types based on positive expression of key inflammasome targets: the $P2X_7$ receptor (Humphreys & Dubyak, 1998; Coutinho-Silva *et al*., 1997) and caspase 1 (Miller *et al*., 1993; Karahashi & Amano, 2000). Furthermore, both cell lines have been extensively used to investigate inflammation in response to activation of the NLRP3 inflammasome through the activity of LPS and ATP (Martinon *et al*., 2004; Pelegrin & Surprenant 2007; Hu *et al*., 2010).

Selection of an appropriate pharmacological tool was made based on findings in the literature combined with the efficacy and selectivity of the compounds. Two specific $P2X_7$ receptor antagonists that are reported to block the activity of the receptor were selected. The first compound produced by AstraZeneca (AZ11645373) is a highly selective antagonist that is reported to function only at the human $P2X_7$ receptor (Stokes *et al*., 2006). The second inhibitor, produced by Abbott Laboratories (A438079) is also a highly selective $P2X_7$ receptor antagonist that is reported to function at both the human and murine variants of the receptor (Donnelly-Roberts *et al*., 2009). The *in vitro* cell based assays will investigate the effect of two different $P2X_7$ inhibitors on the enhanced release of inflammasome-linked cytokines (and inflammasome independent cytokines i.e. TNFα and IL-6) in response to LPS and ATPγS combination treatment.

Once an appropriate pharmacological tool to block murine $P2X_7$ receptors was identified, it was then be utilised to determine its effect on the inflammatory response to cigarette smoke exposure. By comparing the differences in the inflammatory responses and markers of NLRP3 inflammasome activation in both the vehicle and $P2X_7$ inhibitor treated groups, it was possible to validate the role of the $P2X_7$ – inflammasome signalling axis and more specifically the findings using the $P2X_7^{-/-}$ mice. The selected $P2X_7$ inhibitor was also tested in the LPS driven model to parallel the data generated with the genetically modified animals in chapter 4.

5.2 Methods

5.2.1 *In vitro* system development in human and mouse cell based assays.

In vitro cell based assays were developed using the human monocytic THP-1 and mouse J774.2 monocyte/macrophage cell lines. The cell lines were maintained (as described in section *2.4*) and conditions for this assay were optimised (Birrell et al., 2006). 400,000 cells were added to each well in a 24 well plate. The cells were treated and incubated for 24 hours at 37°C in a humidified atmosphere (95% air, 5% (v/v) CO_2). Where necessary the cells were pre-treated with relevant antagonist/vehicle and incubated for 1 hour. The following day (24 hours) the cell suspension was removed and cell viability was determined (as described in section *2.4.2*). The cell suspension was then centrifuged at 800 x g and the supernatant removed and stored at -80°C until required for cytokine analysis. All studies were repeated on three separate experimental days.

The release of the inflammatory cytokines in the cell culture supernatant was determined by using specific sandwich ELISA kits for both human and mouse cytokines. IL-1β and IL-18 release was measured as it is a reported product of inflammasome activation. Other known inflammatory cytokines such as TNF-α, IL-6 and IL-8 (human) or KC (mouse) were measured as negative controls since they are not believed to be released upon inflammasome activation. Results were obtained by reading the signal on the ELISA plate at 450nm.

5.2.1.1 Determining the optimum concentration of LPS for sub-maximal release of inflammatory cytokines from THP-1 cells.

LPS is a well characterised endotoxin that induces potent immune responses from immune cells via the activation of the TLR4 receptor and the subsequent NFκB activation. The aim of these preliminary cell based assays was to determine the optimum concentration of LPS for sub-maximal release of inflammatory cytokines from both human THP-1 and mouse J774.2 cells.

5.2.1.2 Determining the optimum concentration of ATPγS for sub-maximal release of inflammatory cytokines from THP-1 cells.

Recent evidence has highlighted the possible role of ATP as an activator of the inflammasome via the $P2X_7$ receptor. For the purpose of these studies, a stable ATP analogue, ATPγS (Sigma, Poole, UK) was used to target the $P2X_7$ receptor. The aim is to establish an appropriate sub-maximal concentration of ATPγS for sub-maximal release of inflammatory cytokines from both human THP-1 and mouse J774.2 cells.

5.2.1.2 Determining the optimum concentration of LPS and ATPγS for sub-maximal release of inflammatory cytokines from THP-1 cells.

Once appropriate sub-maximal concentrations of LPS and ATPγS had been established, the aim was to use both stimuli in combination to activate the inflammasome.

5.2.2 *In vitro* $P2X_7$ inhibitor testing in human and mouse cell based assays.

Having developed a cell based system that models $P2X_7$ receptor mediated activation of the NLRP3 inflammasome and the subsequent release of IL-1β and IL-18; I was ready to examine the activity of the two $P2X_7$ receptor antagonists.

5.2.3 Determining the effect of $P2X_7$ receptor antagonist on cigarette smoke-induced airway inflammation.

Previous data using genetic manipulation had highlighted an important role for the $P2X_7$ receptor in driving the inflammation associated with CS exposure (Chapter 4). In order to validate this finding, two specific $P2X_7$ receptor antagonists were tested in cell based assays to determine their activity at the receptor. The cell based assays identified A438079 as an appropriate tool to block murine $P2X_7$ receptors. The role of the $P2X_7$ – inflammasome pathway was investigated using this pharmacological tool and comparing the inflammatory responses to CS exposure in mice treated with either vehicle or increasing doses of the inhibitor A438079. Assessment of inflammatory end-points of interest including cellular infiltration and the markers of inflammasome activation, including pro-inflammatory mediator release and caspase 1 activity, would validate the previous findings utilising $P2X_7^{-/-}$ mice and determine whether the effects seen in the $P2X_7^{-/-}$ mice can be achieved using pharmacological tools. Therefore the aim of this section was to parallel the effect of A438079 in the CS driven model.

C57BL/6 mice were treated with vehicle (0.5% methyl cellulose and 0.2% tween80 in distilled H_2O, 10 ml/kg) or A438079, 1 hour prior to the first exposure and 1 hour after the

second exposure on each of the 3 exposure days. The animals were also given a final dose of the compound 1 hour prior to the cull on the fourth day. Animals were exposed to either room air or a sub-maximal (500 ml/min) dose of cigarette smoke (as detailed in section *2.2.2*) for a total exposure period of 50 minutes (excluding 10 minute venting period), twice daily, for 3 consecutive days. Mice were euthanised with an overdose (200 mg/kg) of i.p sodium pentobarbitone 24 hours after the final challenge. BALF and lung tissue samples were collected for analysis as follows;

- BALF (processed as described in section *2.3.1*):
  - Total cell counts and 4-part differential cell counts (neutrophils, eosinophils, monocytes/macrophages and lymphocytes, as described in section 2.*3.3*), n=8.
  - Cytokine analysis in BALF determined by standard ELISA, n=6 (as described in section *2.3.4.3*).

- Lung tissue (processed as described in section *2.3.1*):
  - Flash frozen in liquid nitrogen, n=6, for cytosolic and nuclear cell fraction extraction (as described in section *2.3.5.1*) for determination of caspase 1 activity (as described in section *2.3.5.2*).

5.2.4 Determining the effect of $P2X_7$ receptor antagonist on LPS-induced airway inflammation.

The results from the previous chapter identified that the inflammatory response seen following an endotoxin challenge is independent of the $P2X_7$ – inflammasome pathway based on the absence of correlation in the markers of inflammasome activation and sustained

inflammation in $P2X_7^{-/-}$ mice. Furthermore, LPS challenged $P2X_7^{-/-}$ mice showed an increased numbers of neutrophils in the BALF when compared to the LPS exposed wild-type mice. To validate these findings highlighted above I examined the effects of a $P2X_7$ receptor antagonist on the inflammatory response in mice seen following LPS exposure.

C57BL/6 mice were treated with vehicle (0.5% methyl cellulose and 0.2% tween80 in distilled H_2O, 10 ml/kg) or A438079, 1 hour prior to the first exposure and 1 hour after the LPS challenge. Animals were challenged with endotoxin free saline (Fresenius Kabi, Warrington, UK) or a sub-maximal dose of 1 mg/ml LPS (*Escherichia coli*, serotype 0111:B4, Sigma-Aldrich Ltd. Poole, UK) for 30 min (as detailed in section *2.2.1*). Mice were euthanised with an overdose (200 mg/kg) of i.p sodium pentobarbitone 24 hours after the final challenge. BALF and lung tissue samples were collected for analysis as detailed in section 5.*2.4*.

5.2.5 Statistical analysis

Data is expressed as mean ± S.E.M of n observations. For data where each independent group is compared to its time matched control, statistical significance was determined using a Student's t-test for parametric or a Mann-Whitney U-test (or Wilcoxon rank test) for non-parametric data. For multiple comparisons tests, statistical analysis was performed by applying a one-way ANOVA (analysis of variance) with a Dunnett's (comparing with a single control group) or Bonferroni's (multiple comparisons) post-test for parametric data or alternatively a Kruskal-Wallis incorporating Dunn's multiple comparison post-test for non-parametric data. A P value < 0.05 was taken as significant and all treatments were compared with the appropriate control group.

5.3 Results

5.3.1 *In vitro* system development in human and mouse cell based assays.

5.3.1.1 Determining the optimum concentration of LPS for sub-maximal release of inflammatory cytokines from THP-1 cells.

To establish an appropriate sub-maximal concentration of LPS that would elicit inflammatory cytokine release, both human THP-1 and mouse J774.2 cells were treated with either vehicle (RPMI) or increasing concentrations of LPS (0.00001 – 10 μg/ml).

LPS increased the release of inflammatory cytokines from both THP-1 (Figure 5.1A - D) and J774.2 (Figure 5.2A - D) cells in a concentration-dependent manner. A submaximal LPS concentration of 0.1μg/ml was chosen to perform subsequent studies involving a combination of stimuli. The Trypan Blue Exclusion test showed that both THP-1 (Figure 5.1E) and J774.2 (Figure 5.2E) cells were still viable even at the high concentration of LPS.

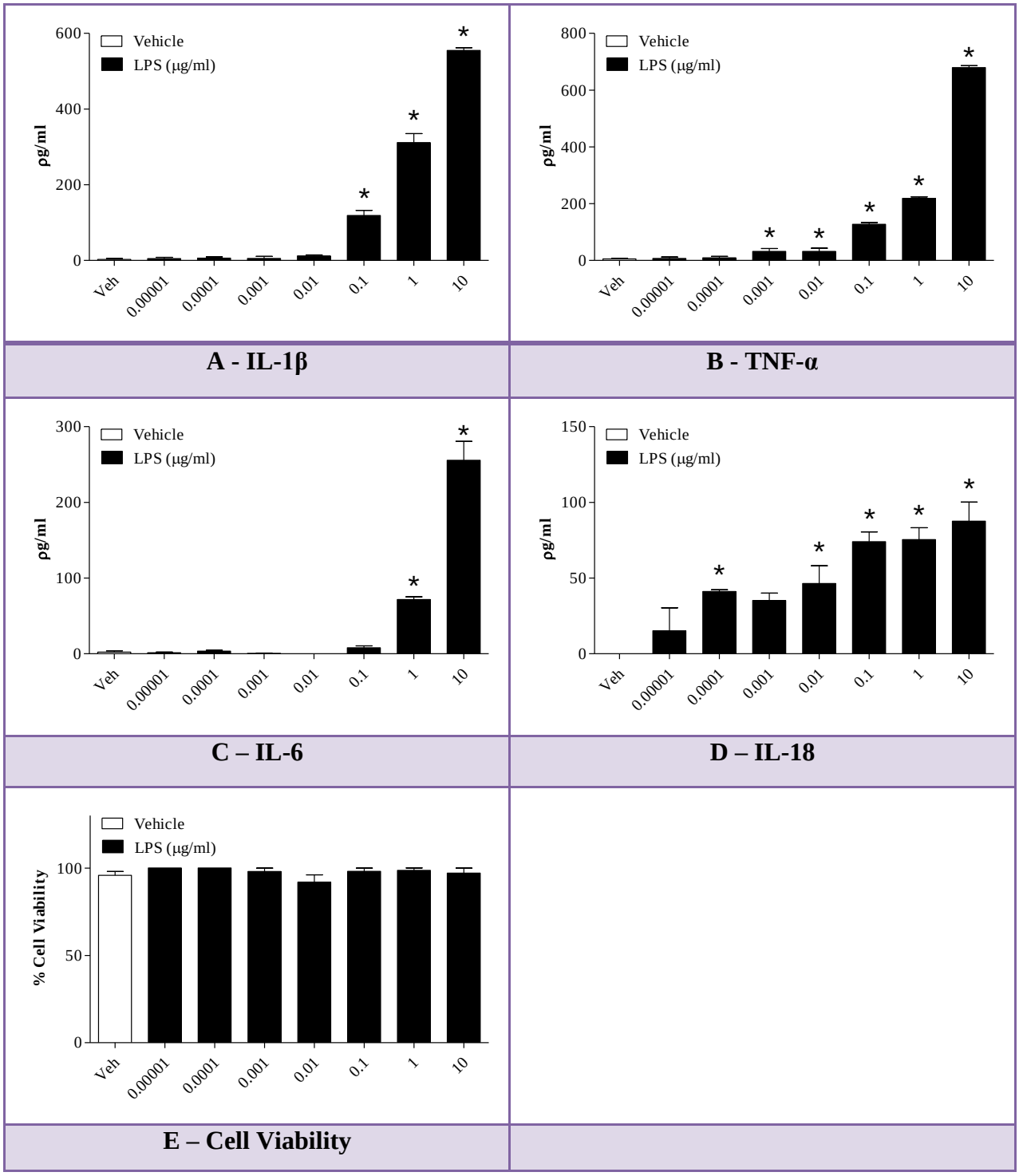

Figure 5.1 – Characterisation of LPS-mediated release of inflammatory cytokines from human THP-1 cells. *The release of inflammatory cytokines by THP-1 cells in response to increasing concentrations of LPS. Cytokine levels in the cell culture supernatant were measured by ELISA in ρg/ml. Cell viability was determined as a percentage of viable cells from the cell pellet sample. All studies were repeated on three separate experimental days, n=6, with data represented as mean ± SEM. Statistical significance determined with One-way ANOVA incorporating Dunnett's post-test for parametric data. * = P<0.05 and denotes a significant difference to the vehicle treated control group.*

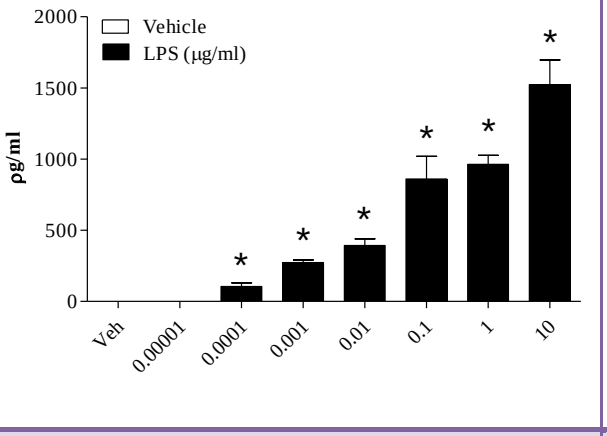

A - IL-1β

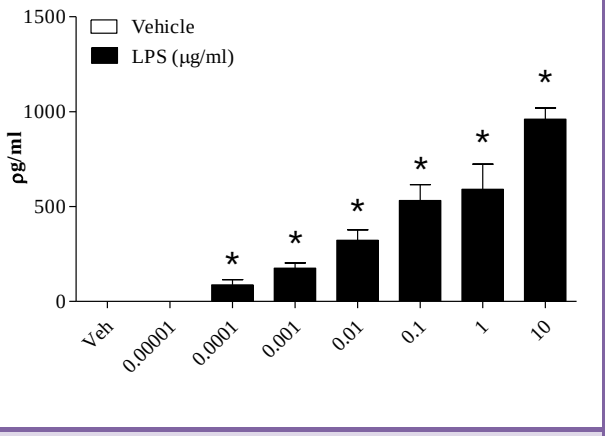

B - TNF-α

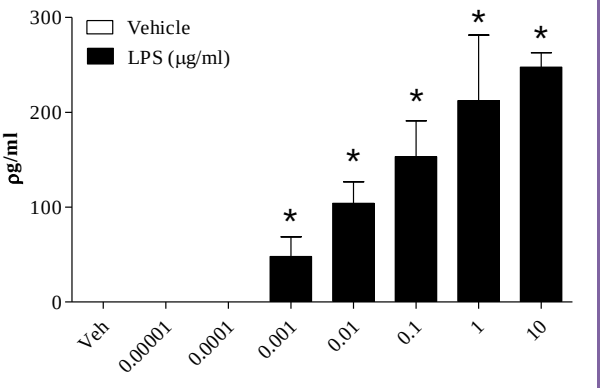

C – IL-6

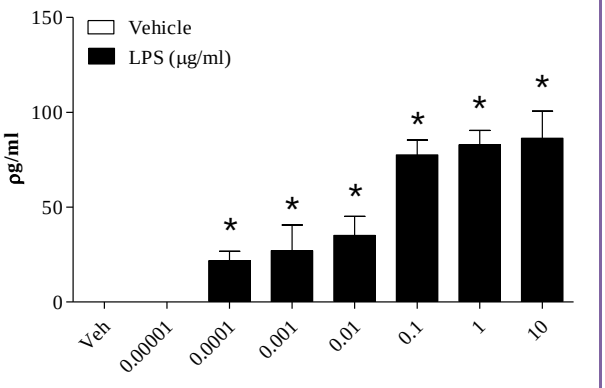

D – IL-18

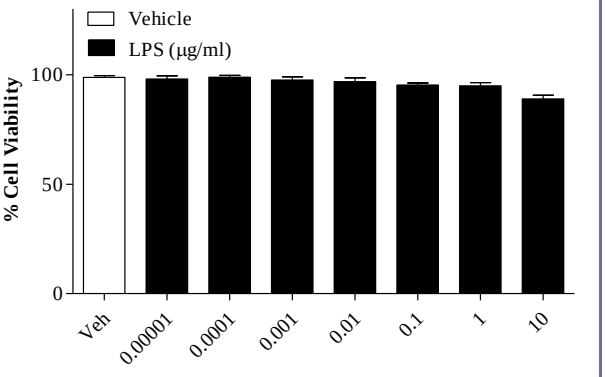

E – Cell Viability

Figure 5.2 – Characterisation of LPS-mediated release of inflammatory cytokines from mouse J774.2 cells. *The release of inflammatory cytokines by J774.2 cells in response to increasing concentrations of LPS. Cytokine levels in the cell culture supernatant were measured by ELISA in ρg/ml. Cell viability was determined as a percentage of viable cells from the cell pellet sample. All studies were repeated on three separate experimental days, n=6, with data represented as mean ± SEM. Statistical significance determined with One-way ANOVA incorporating Dunnett's post-test for parametric data. * = P<0.05 and denotes a significant difference to the vehicle treated control group.*

5.3.1.2 Determining the optimum concentration of ATPγS for sub-maximal release of inflammatory cytokines from THP-1 cells.

To establish an appropriate sub-maximal concentration of ATPγS that would elicit inflammatory cytokine release, both human THP-1 and mouse J774.2 cells were treated with either vehicle (RPMI) or increasing concentrations of ATPγS (10^{-5} – $10^{-2.5}$ M).

Increasing concentrations of ATPγS treatment were shown to proportionally increase the release of inflammatory cytokines IL-1β and IL-18 from THP-1 cells (Figure 5.3A & D) and J774.2 cells (Figure 5.4A & D) cells, whilst an ATPγS concentration of 10^{-3}M was demonstrated to provide a sub-maximal release of inflammatory cytokines. No changes in the release of TNF-α or IL-6 in THP-1 cells (Figure 5.3B & C) or J774.2 cells (Figure 5.4B & C) was seen in response to ATPγS treatment. The Trypan Blue Exclusion test confirmed no cell death up to the highest concentration of ATPγS tested ($10^{-2.5}$ M) in both THP-1 (Figure 5.3E) and J774.2 (Figure 5.4E) cells.

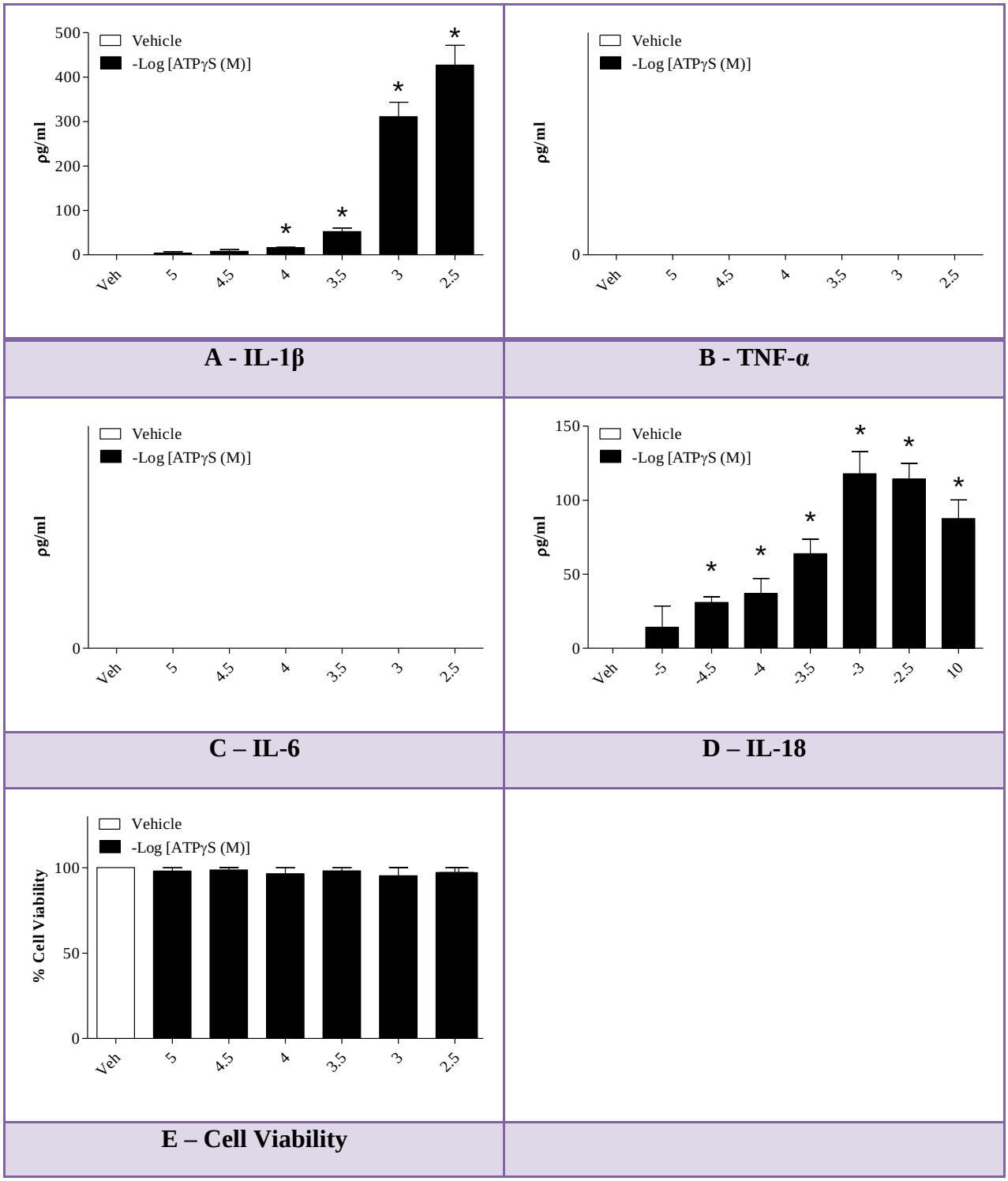

Figure 5.3 – Characterisation of ATPγS-mediated release of inflammatory cytokines from human THP-1 cells. *The release of inflammatory cytokines by THP-1 cells in response to increasing concentrations of ATPγS. Cytokine levels in the cell culture supernatant were measured by ELISA in ρg/ml. Cell viability was determined as a percentage of viable cells from the cell pellet sample. All studies were repeated on three separate experimental days, n=6, with data represented as mean ± SEM. Statistical significance determined with One-way ANOVA incorporating Dunnett's post-test for parametric data. * = P<0.05 and denotes a significant difference to the vehicle treated control group.*

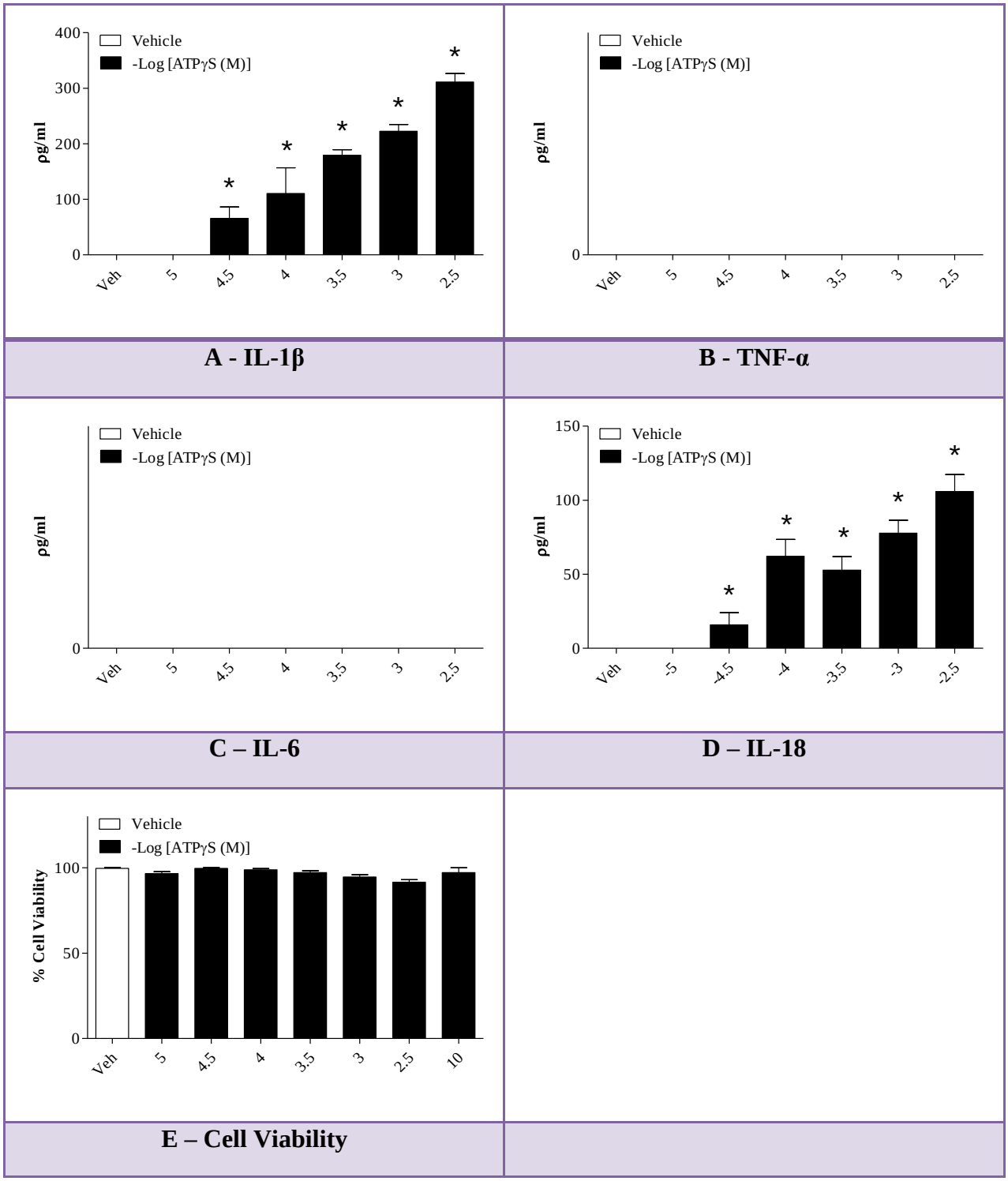

Figure 5.4 – Characterisation of ATPγS-mediated release of inflammatory cytokines from mouse J774.2 cells. *The release of inflammatory cytokines by J774.2 cells in response to increasing concentrations of ATPγS. Cytokine levels in the cell culture supernatant were measured by ELISA in ρg/ml. Cell viability was determined as a percentage of viable cells from the cell pellet sample. All studies were repeated on three separate experimental days, n=6, with data represented as mean ± SEM. Statistical significance determined with One-way ANOVA incorporating Dunnett's post-test for parametric data. * = P<0.05 and denotes a significant difference to the vehicle treated control group.*

5.2.1.2 Determining the optimum concentration of LPS and ATPγS for sub-maximal release of inflammatory cytokines from THP-1 cells.

Having identified appropriate sub-maximal concentrations to elicit the release of inflammatory cytokines in THP-1 and J774.2 cells, the stimuli were combined. Treatment of the cells with the sub-maximal concentration of ATPγS (10^{-3} M) and increasing concentrations of LPS appears to result in greater release of IL-1β compared to the sum of its two parts in both THP-1 (Figure 5.5A) and J774.2 (Figure 5.6A) cells whilst IL-18 showed only additive effects in both the THP-1 (Figure 5.5C) and J774.2 (Figure 5.6C) cell lines. This effect was not seen in the release of TNF-α in THP-1 (Figure 5.5B) or J774.2 (Figure 5.6B) cells. Trypan Blue exclusion following the combination treatment showed no effects on cell viability in both THP-1 (Figure 5.5D) and J774.2 (Figure 5.6D) cell lines.

In reverse, using the previously determined sub-maximal concentration of LPS (0.1 μg/ml) and treating the cells with increasing concentrations of ATPγS again demonstrated greater release of IL-1β compared to the sum of its two parts in both THP-1 (Figure 5.7A) and J774.2 (Figure 5.8A) cells whilst IL-18 showed only additive effects in both the THP-1 (Figure 5.7C) and J774.2 (Figure 5.8C) cell lines. This effect was not seen in the release of TNF-α in THP-1 (Figure 5.7B) or J774.2 (Figure 5.8B) cells. Trypan Blue exclusion following the combination treatment showed no effects on cell viability in both THP-1 (Figure 5.7D) and J774.2 (Figure 5.8D) cell lines.

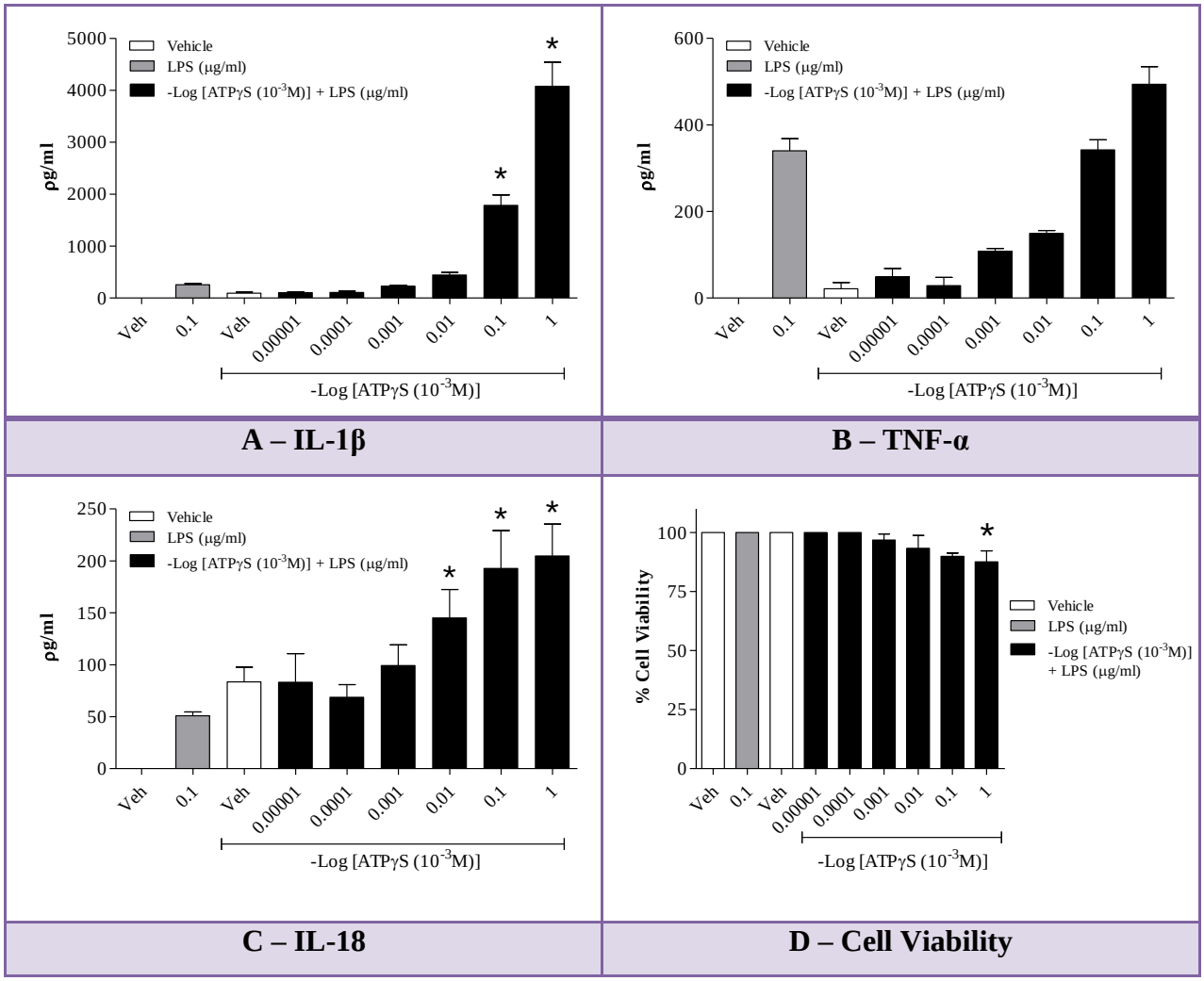

Figure 5.5 – The effects of a combination treatment of LPS and ATPγS on the release of inflammatory cytokines from human THP-1 cells. *Examining the possible synergistic effects of the combination treatment with increasing concentrations of LPS versus a sub-maximal concentration of ATPγS (10^{-3}M) on the release of inflammatory cytokines from THP-1 cells. Cytokine levels in the cell culture supernatant were measured by ELISA in ρg/ml. Cell viability was determined as a percentage of viable cells from the cell pellet sample. All studies were repeated on three separate experimental days, n=6, with data represented as mean ± SEM. Statistical significance determined with a Kruskal-Wallis incorporating Dunn's post-test for non-parametric data. * = P<0.05 and denotes a significant difference to the air exposed control group.*

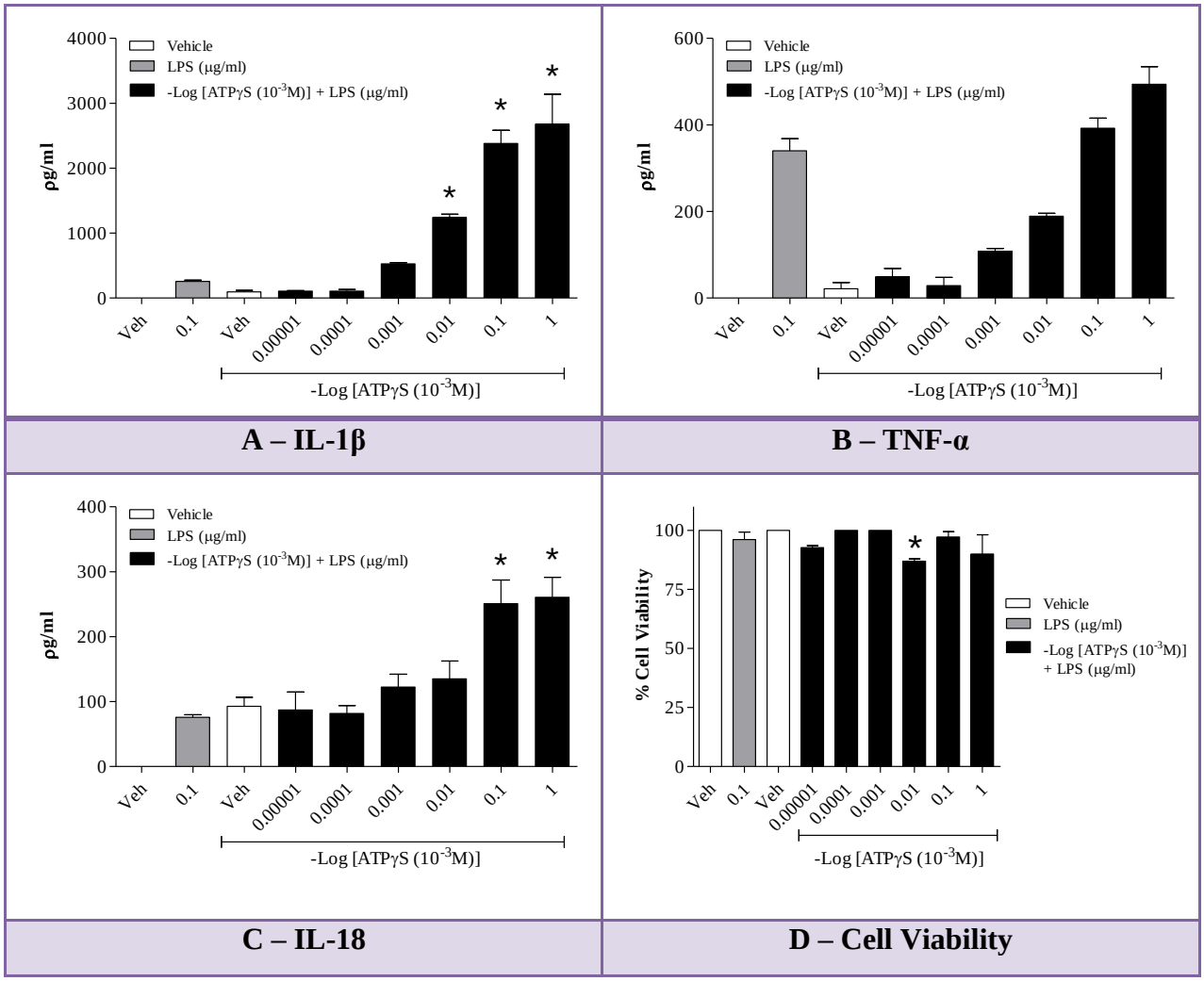

Figure 5.6 – The effects of a combination treatment of LPS and ATPγS on the release of inflammatory cytokines from mouse J774.2 cells. *Examining the possible synergistic effects of the combination treatment with increasing concentrations of LPS versus a sub-maximal concentration of ATPγS (10^{-3}M) on the release of inflammatory cytokines from J774.2 cells. Cytokine levels in the cell culture supernatant were measured by ELISA in ρg/ml. Cell viability was determined as a percentage of viable cells from the cell pellet sample. All studies were repeated on three separate experimental days, n=6, with data represented as mean ± SEM. Statistical significance determined with a Kruskal-Wallis incorporating Dunn's post-test for non-parametric data. * = P<0.05 and denotes a significant difference to the air exposed control group.*

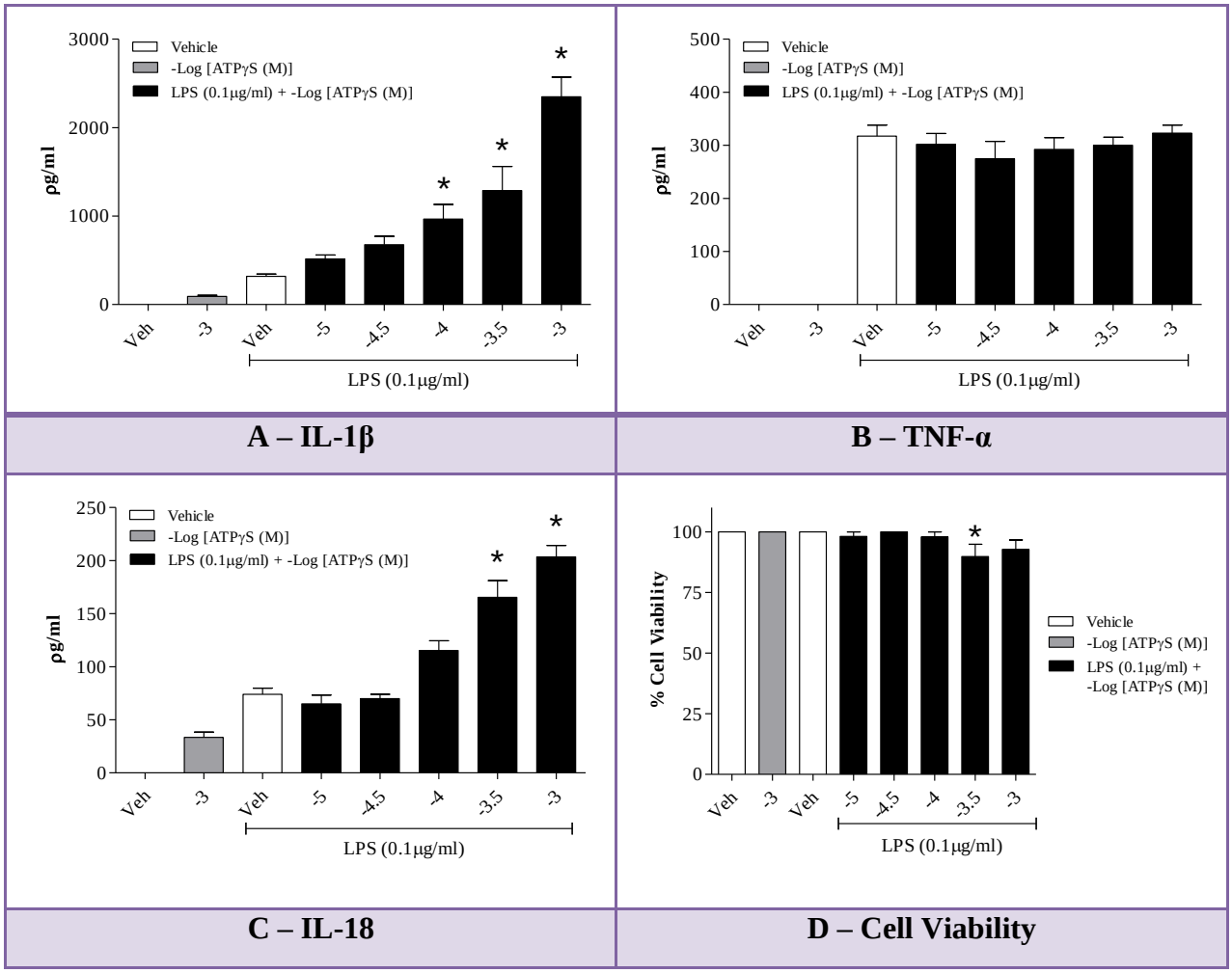

Figure 5.7 – The effects of a combination treatment of ATPγS and LPS on the release of inflammatory cytokines from human THP-1 cells. *Examining the possible synergistic effects of the combination treatment with increasing concentrations of ATPγS versus a sub-maximal concentration of LPS (0.1 μg/ml) on the release of inflammatory cytokines from THP-1 cells. Cytokine levels in the cell culture supernatant were measured by ELISA in ρg/ml. Cell viability was determined as a percentage of viable cells from the cell pellet sample. All studies were repeated on three separate experimental days, n=6, with data represented as mean ± SEM. Statistical significance determined with a Kruskal-Wallis incorporating Dunn's post-test for non-parametric data. * = P<0.05 and denotes a significant difference to the air exposed control group.*

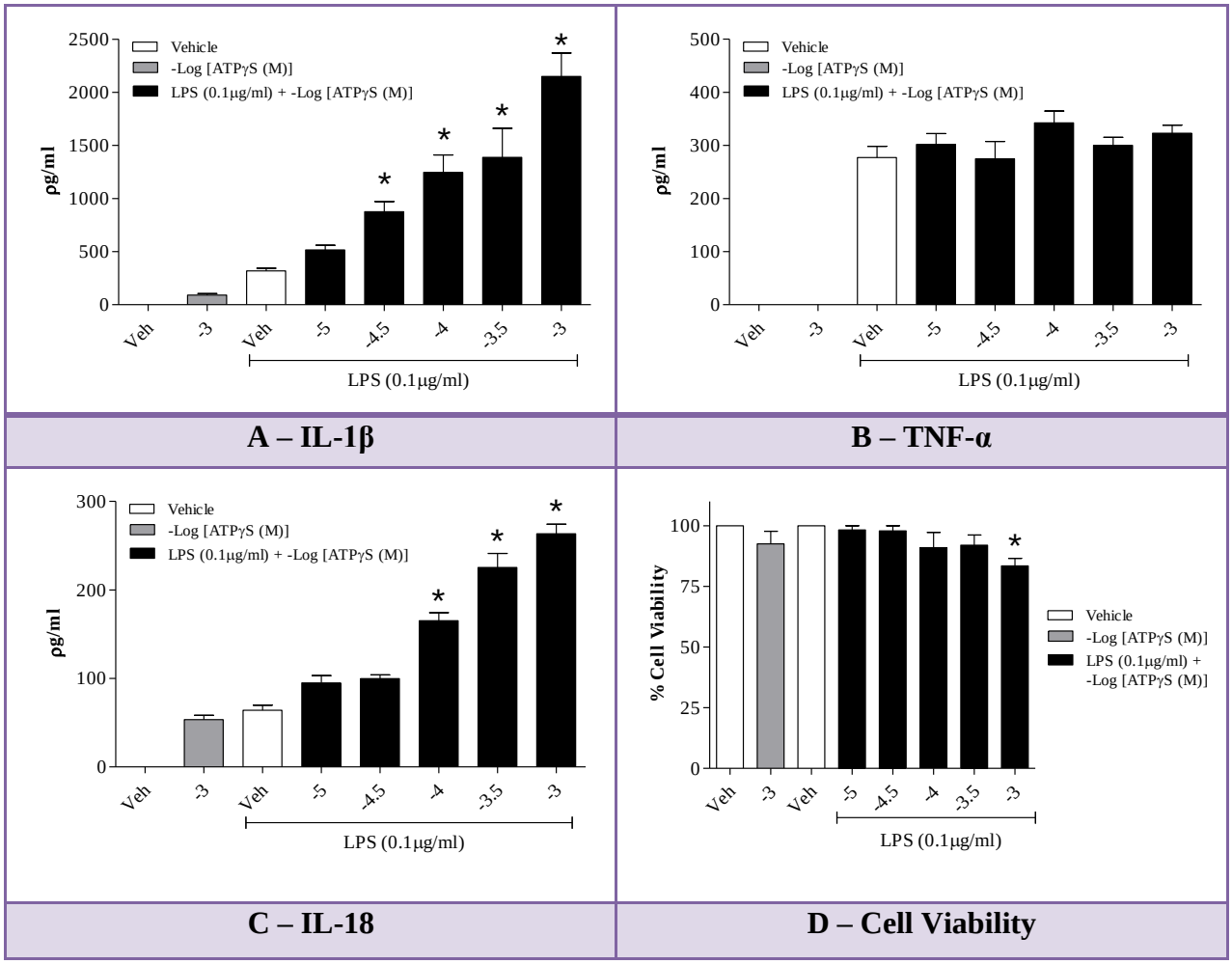

Figure 5.8 – The effects of a combination treatment of ATPγS and LPS on the release of inflammatory cytokines from mouse J774.2 cells. *Examining the possible synergistic effects of the combination treatment with increasing concentrations of ATPγS versus a sub-maximal concentration of LPS (0.1 μg/ml) on the release of inflammatory cytokines from J774.2 cells. Cytokine levels in the cell culture supernatant were measured by ELISA in ρg/ml. Cell viability was determined as a percentage of viable cells from the cell pellet sample. All studies were repeated on three separate experimental days, n=6, with data represented as mean ± SEM. Statistical significance determined with a Kruskal-Wallis incorporating Dunn's post-test for non-parametric data. * = P<0.05 and denotes a significant difference to the air exposed control group.*

5.3.2 Establishing optimum concentration of $P2X_7$ inhibitor in human and mouse cell based assays.

Having shown that a combination of endotoxin (LPS) and a $P2X_7$ receptor agonist (ATP) leads to enhanced release of inflammasome-linked cytokines, I then wanted to use this assay system to test two specific $P2X_7$ receptor antagonists. Cells were treated with a sub-maximal concentration of both LPS (0.1 μg/ml) and ATPγS (10^{-3} M) in the presence of the $P2X_7$ antagonist (1 hour pre-treat). Where necessary the appropriate vehicle was used to treat the cells as a replacement (LPS or ATPγS – RPMI, AZ11645373 or A438079 - DMSO).

In the THP-1 cell line, AZ11645373 significantly inhibited the enhanced release of both IL-1β and IL-18 (Figure 5.9A & D) but not the release of TNF-α (Figure 5.9B). Production of IL-1β in response to ATP-alone was attenuated (50% inhibition) by treatment with a $P2X_7$ antagonist, whereas LPS-induced IL-1β release was not affected by the inhibitor. The effects seen with AZ11645373 in the THP-1 cell line were not seen in the murine cell line. The compound failed to inhibit the enhanced release of both IL-1β and IL-18 (Figure 5.10A & C). Furthermore, it had no impact on the release of TNF-α (Figure 5.10B). The antagonist had a minor effect on cell viability in either cell line when treated alone or with the combination (LPS & ATPγS) (Figure 5.9D & 5.10D).

The alternative $P2X_7$ receptor antagonist, A438079, failed to inhibit the release of both IL-1β and IL-18 in response to the combination treatment in the THP-1 cell line (Figure 5.11A & C). Furthermore, it had no impact on the standard release of TNF-α (Figure 5.11B). In the J774.2 cell line, however, the increases in the production of IL-1β and IL-18 in response to the combination treatment were both significantly inhibited by 58 and 42% respectively

(Figure 5.12A & C) but not the standard release of TNF-α (Figure 5.12B). Production of IL-1β & IL-18 in response to ATP-alone was attenuated by treatment with a $P2X_7$ antagonist. Furthermore, A438079 showed minor toxic effects on cell viability in either cell line when treated alone or with the combination (LPS & ATPγS) (Figure 5.11D & 5.12D).

Based on the results obtained testing both antagonists in human and mouse cell lines, A438079 was selected as the appropriate pharmacological tool to use in our *in vivo* murine models of inflammation.

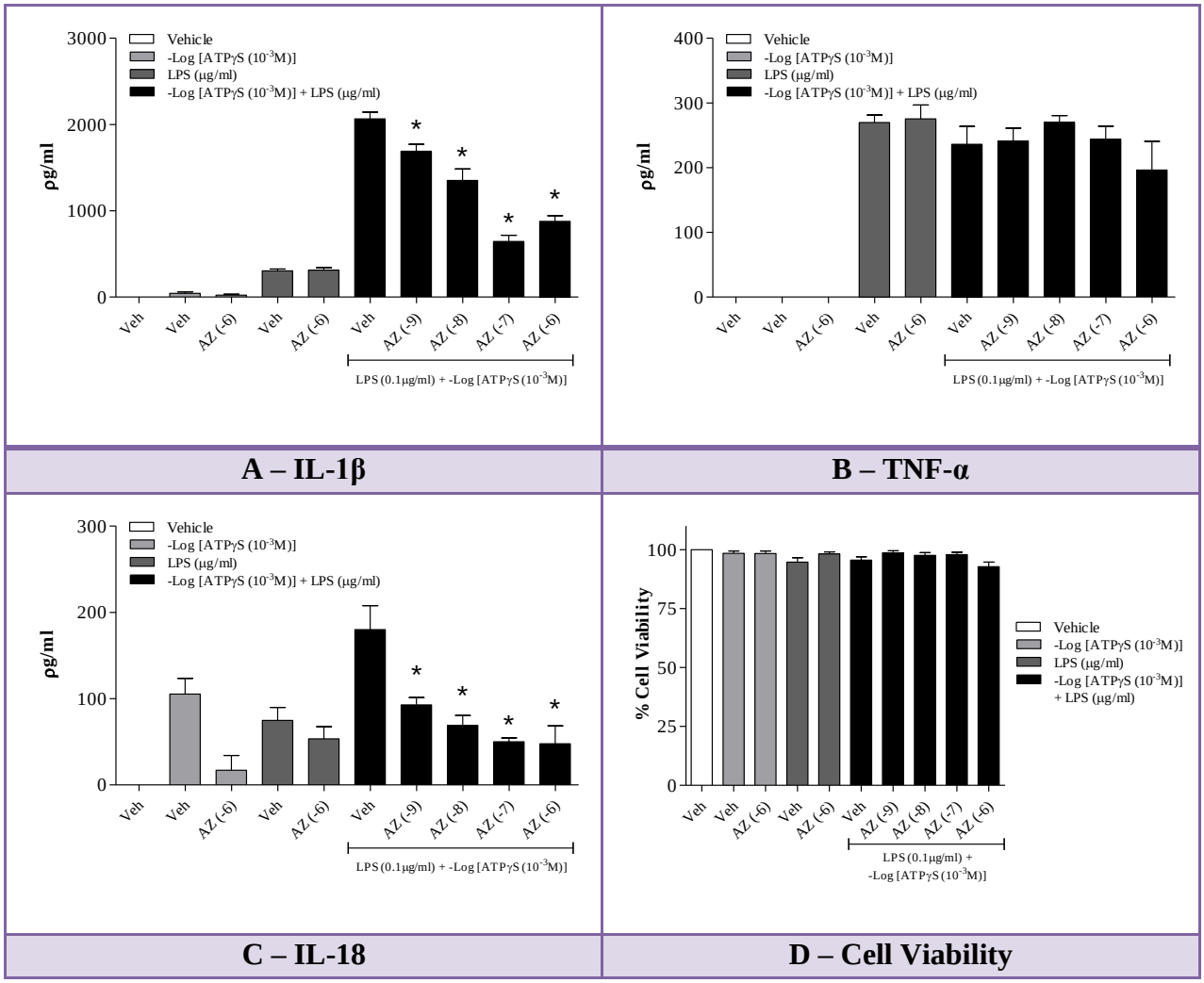

Figure 5.9 – The effect of the specific $P2X_7$ antagonist AZ11645373 on inflammatory cytokine release in response to a combination treatment of LPS and ATPγS in human THP-1 cells. *Examining the release of inflammatory cytokines from human THP-1 cells in response to a combination treatment of LPS (0.1 μg/ml) and ATPγS (10^{-3}M) in the presence of a $P2X_7$ antagonist. Cytokine levels in the cell culture supernatant were measured by ELISA in ρg/ml. Cell viability was determined as a percentage of viable cells from the cell pellet sample. All studies were repeated on three separate experimental days, n=6, with data represented as mean ± SEM. Statistical significance determined with a Kruskal-Wallis incorporating Dunn's post-test for non-parametric data. * = P<0.05 and denotes a significant difference to the air exposed control group.*

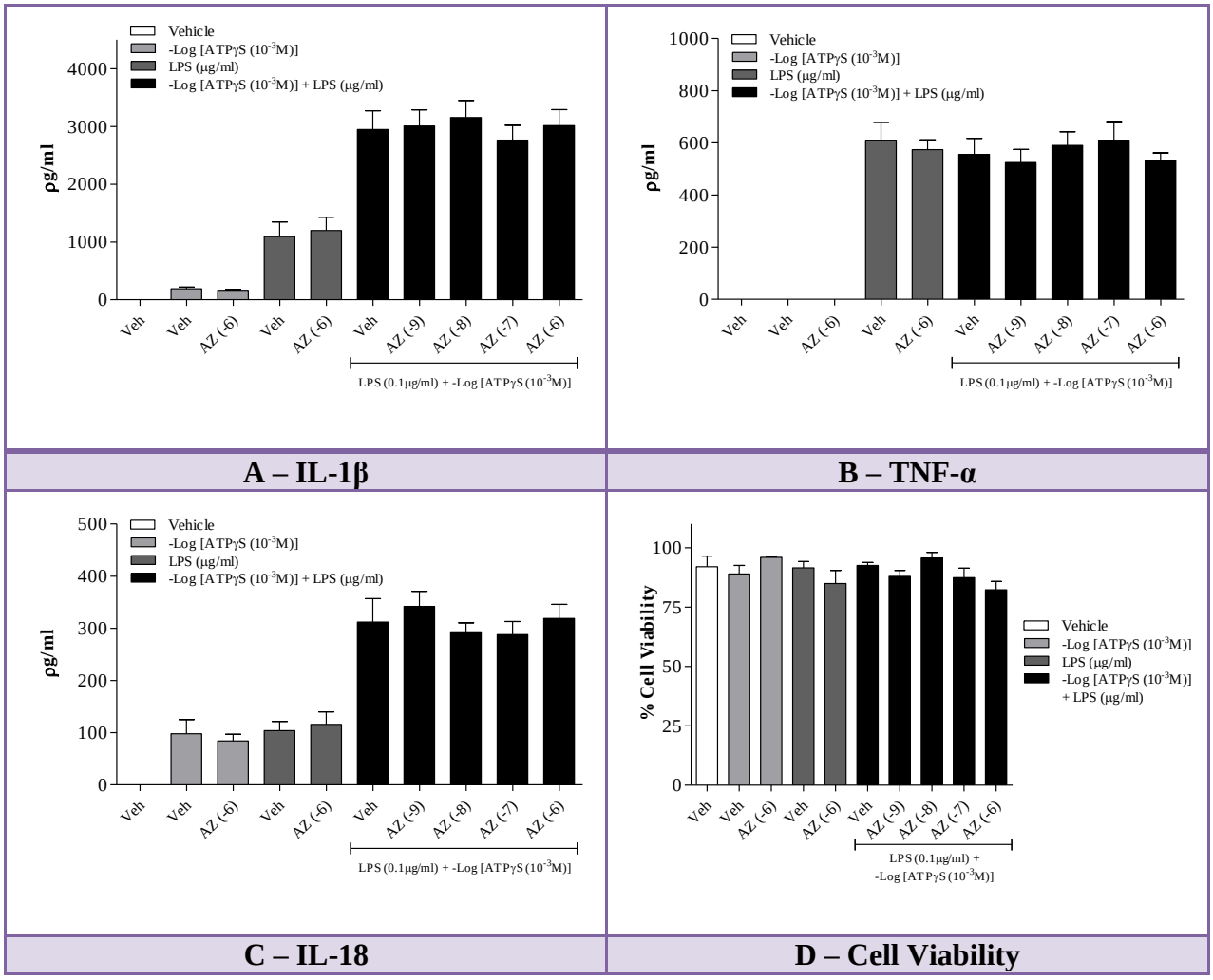

Figure 5.10 – The effect of the specific $P2X_7$ antagonist AZ11645373 on inflammatory cytokine release in response to a combination treatment of LPS and ATPγS in mouse J774.2 cells. *Examining the release of inflammatory cytokines from mouse J774.2 cells in response to a combination treatment of LPS (0.1 μg/ml) and ATPγS (10^{-3}M) in the presence of a $P2X_7$ antagonist. Cytokine levels in the cell culture supernatant were measured by ELISA in ρg/ml. Cell viability was determined as a percentage of viable cells from the cell pellet sample. All studies were repeated on three separate experimental days, n=6, with data represented as mean ± SEM. Statistical significance determined with a Kruskal-Wallis incorporating Dunn's post-test for non-parametric data. * = P<0.05 and denotes a significant difference to the air exposed control group.*

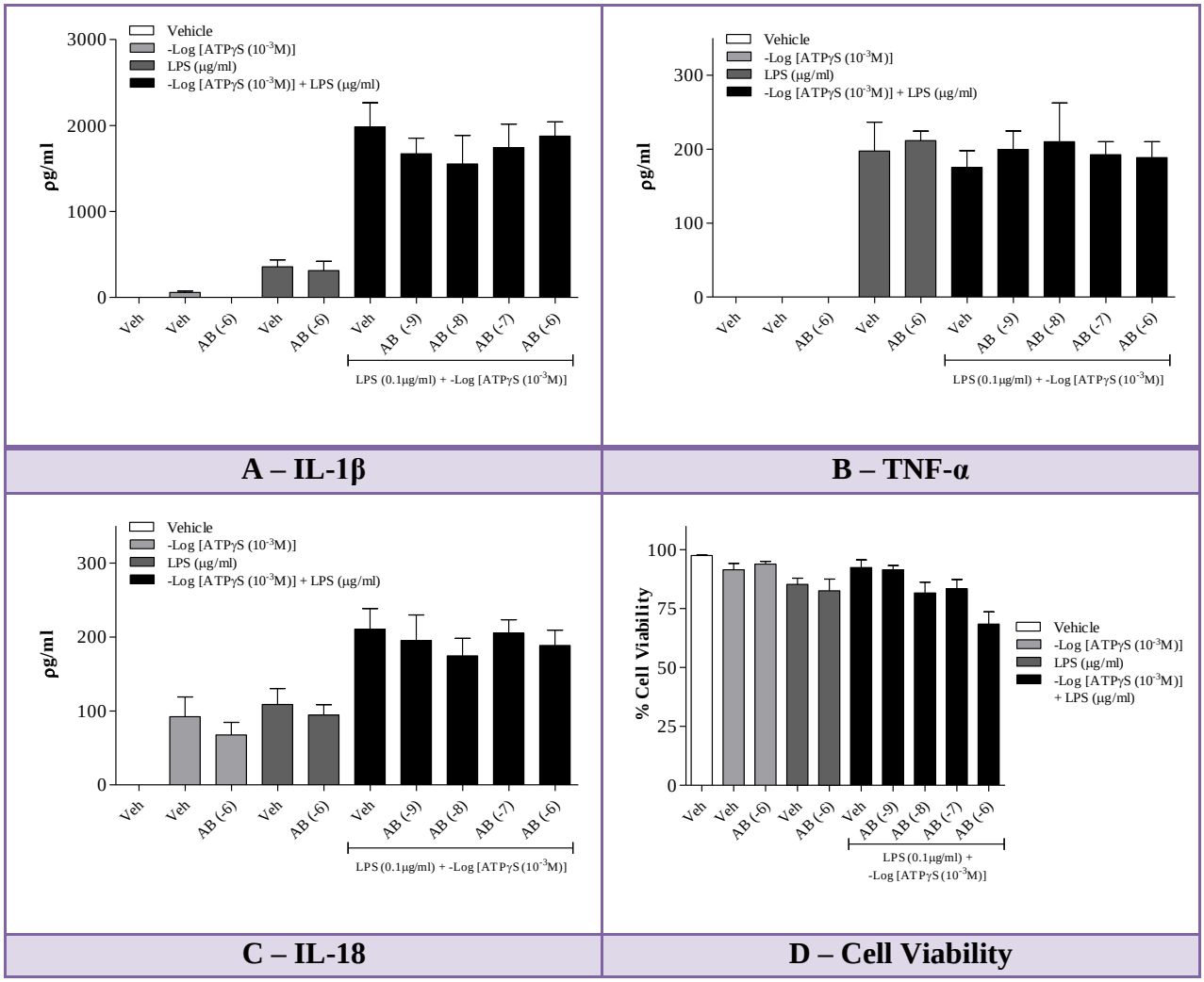

Figure 5.11 – The effect of the specific $P2X_7$ antagonist A438079 on inflammatory cytokine release in response to a combination treatment of LPS and ATPγS in human THP-1 cells. *Examining the release of inflammatory cytokines from human THP-1 cells in response to a combination treatment of LPS (0.1 μg/ml) and ATPγS (10^{-3}M) in the presence of a $P2X_7$ antagonist. Cytokine levels in the cell culture supernatant were measured by ELISA in ρg/ml. Cell viability was determined as a percentage of viable cells from the cell pellet sample. All studies were repeated on three separate experimental days, n=6, with data represented as mean ± SEM. Statistical significance determined with a Kruskal-Wallis incorporating Dunn's post-test for non-parametric data. * = P<0.05 and denotes a significant difference to the air exposed control group.*

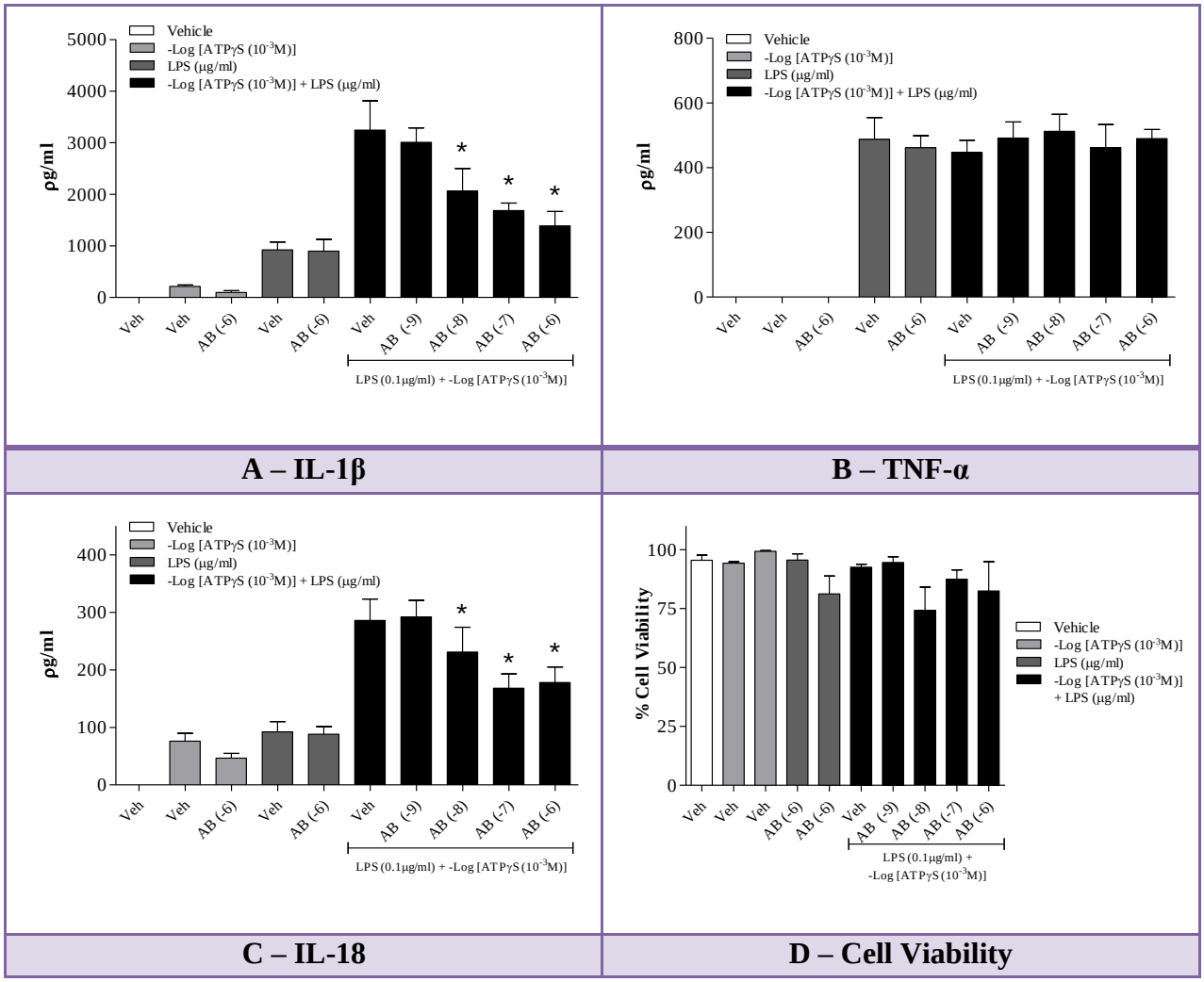

Figure 5.12 – The effect of the specific $P2X_7$ antagonist A438079 on inflammatory cytokine release in response to a combination treatment of LPS and ATPγS in mouse J774.2 cells. *Examining the release of inflammatory cytokines from mouse J774.2 cells in response to a combination treatment of LPS (0.1 μg/ml) and ATPγS (10^{-3}M) in the presence of a $P2X_7$ antagonist. Cytokine levels in the cell culture supernatant were measured by ELISA in ρg/ml. Cell viability was determined as a percentage of viable cells from the cell pellet sample. All studies were repeated on three separate experimental days, n=6, with data represented as mean ± SEM. Statistical significance determined with a Kruskal-Wallis incorporating Dunn's post-test for non-parametric data. * = P<0.05 and denotes a significant difference to the air exposed control group.*

5.3.3 Determining the effect of $P2X_7$ receptor antagonist on cigarette smoke-induced airway inflammation.

A significant increase in BALF neutrophils was seen in the smoke exposed vehicle-treated group when compared to the air exposed vehicle-treated animals (Figure 5.14). This increase in the BALF neutrophilia in response to CS exposure was significantly decreased in a dose dependent manner in smoke exposed inhibitor-treated animals (Figure 5.14). The monocyte/macrophages in the BALF were significantly elevated in smoke exposed groups when compared to their air exposed controls (Figure 5.15); however, the antagonist did not have any effect on this increase in response to smoke exposure. There were no significant changes in eosinophil or lymphocyte numbers in response to cigarette smoke exposure in the BALF (Figure 5.15).

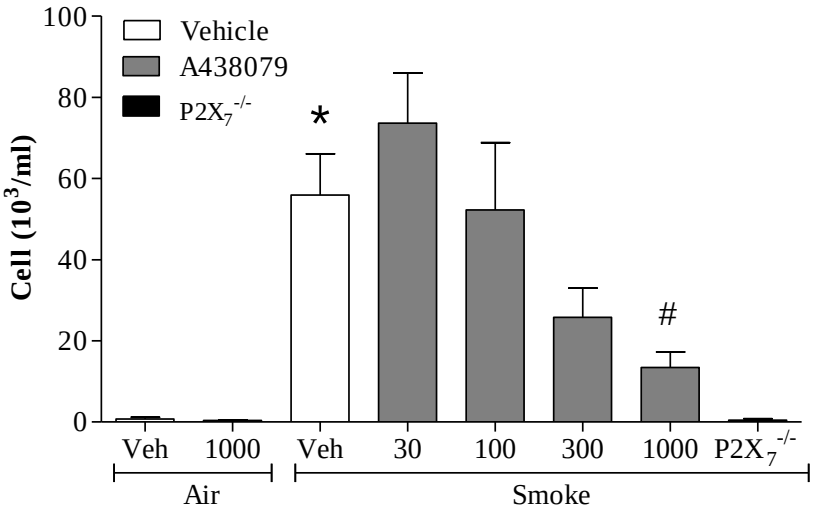

Figure 5.13 – The effect of a $P2X_7$ receptor antagonist on airway neutrophilia in the BALF following cigarette smoke exposure. *C57BL/6 mice were treated with vehicle or A438079 and exposed to either room air or 500 ml/min cigarette smoke, twice daily for 3 consecutive days. Samples were collected 24 hours after the final exposure and neutrophilia was determined by differential counting under light microscopy. Data represented as Mean ± SEM for n=8 observations. Data represented as Mean ± SEM for n=8 observations. Statistical significance determined with a Kruskal-Wallis incorporating Dunn's post-test for non-parametric data. * = P<0.05 and denotes a significant difference to the air exposed vehicle-treated group. # = P<0.05 and denotes a significant difference to the smoke exposed vehicle-treated group.*

Cells (10^3/ml)	Group	Eosinophils	Monocytes/ Macrophages	Lymphocytes
Air Exposed	Veh	0.35±0.26	77.98±5.93	2.19±0.53
	1000	0.00±0.00	68.74±3.46	2.15±0.93
Smoke Exposed	Veh	0.43±0.28	119.40±11.70*	1.73±0.59
	30	0.73±0.36	131.90±12.58	2.50±0.56
	100	0.69±0.35	107.90±8.87	1.61±0.32
	300	0.36±0.24	121.20±9.20	1.38±0.53
	1000	0.16±0.16	138.90±9.28	1.30±0.21
	$P2X_7^{-/-}$	0.00±0.00	120.90±10.94	2.40±0.54

Figure 5.14 – The effect of a $P2X_7$ receptor antagonist on airway neutrophilia in the BALF following cigarette smoke exposure. *C57BL/6 mice were treated with vehicle or A438079 and exposed to either room air or 500 ml/min cigarette smoke, twice daily for 3 consecutive days. Samples were collected 24 hours after the final exposure and the numbers of eosinophils, monocytes/macrophages and lymphocytes recovered from the BALF was determined by differential counting under light microscopy. Data represented as Mean ± SEM for n=8 observations. Statistical significance determined with a Kruskal-Wallis incorporating Dunn's post-test for non-parametric data. * = P<0.05 and denotes a significant difference to the air exposed vehicle-treated group. # = P<0.05 and denotes a significant difference to the smoke exposed vehicle-treated group.*

5.3.4 Determining the effect of $P2X_7$ receptor antagonist on LPS-induced airway inflammation.

The LPS challenge elicited a significant increase in BALF neutrophils (Figure 5.16). This increase in the neutrophilia in response to LPS exposure was unaffected in the groups treated with the $P2X_7$ inhibitor (Figure 5.15). Similarly, increases in BALF eosinophil numbers in response to the endotoxin challenge were also unaffected in the $P2X_7$ inhibitor treated animals (Figure 5.16). The monocyte/macrophages in the BALF were significantly increased in the $P2X_7$ inhibitor treated groups in an almost dose dependent manner (Figure 5.16). Conversely, the lymphocytes demonstrated no significant changes in the following LPS exposure (Figure 5.16).

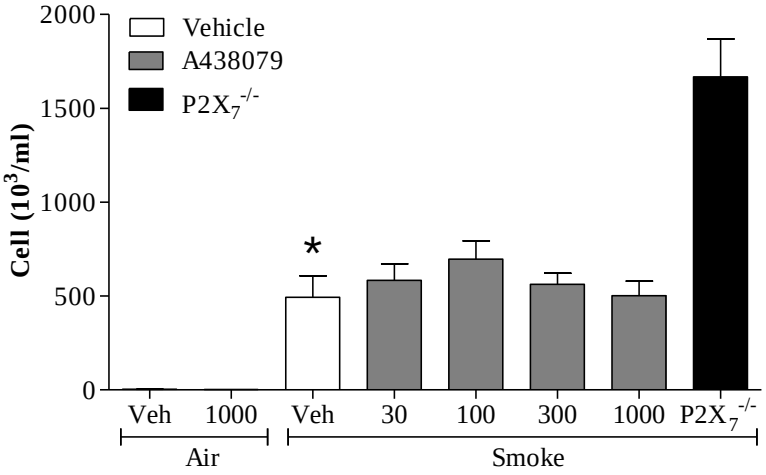

Figure 5.15 – The effect of a $P2X_7$ receptor antagonist on airway neutrophilia in the BALF following LPS challenge. *C57BL/6 mice were treated with vehicle or A438079 and challenged with endotoxin free saline or 1 mg/ml LPS for 30 min. Samples were collected 6 hours after the final exposure and neutrophilia was determined by differential counting under light microscopy. Data represented as Mean ± SEM for n=8 observations. Data represented as Mean ± SEM for n=8 observations. Statistical significance determined with a Kruskal-Wallis incorporating Dunn's post-test for non-parametric data. * = P<0.05 and denotes a significant difference to the air exposed vehicle-treated group. # = P<0.05 and denotes a significant difference to the smoke exposed vehicle-treated group.*

Cells (10^3/ml)	Group	Eosinophils	Monocytes/ Macrophages	Lymphocytes
Air Exposed	Veh	0.31±0.15	69.30±5.23	7.53±2.28
	1000	0.23±0.15	96.24±7.99	5.85±1.60
Smoke Exposed	Veh	18.16±3.61*	38.94±6.42	8.70±2.02
	30	18.25±5.67	44.86±5.54	19.79±4.96*
	100	14.75±4.97	56.68±7.28	4.96±2.34
	300	13.26±2.11	48.60±3.94	9.06±1.80
	1000	5.43±1.56	88.64±56.65	9.06±1.56
	$P2X_7^{-/-}$	23.77±5.69	54.10±7.29	7.77±3.84

Figure 5.16 – The effect of a $P2X_7$ receptor antagonist on airway neutrophilia in the BALF following LPS challenge. *C57BL/6 mice were treated with vehicle or A438079 and challenged with endotoxin free saline or 1 mg/ml LPS for 30 min. Samples were collected 6 hours after the final exposure and the numbers of neutrophils, eosinophils, monocytes/macrophages and lymphocytes recovered from the BALF was determined by differential counting under light microscopy. Data represented as Mean ± SEM for n=8 observations. Statistical significance determined with a Kruskal-Wallis incorporating Dunn's post-test for non-parametric data. * = P<0.05 and denotes a significant difference to the air exposed vehicle-treated group. # = P<0.05 and denotes a significant difference to the smoke exposed vehicle-treated group.*

5.4 Discussion

Previously I have shown that markers of inflammasome activation are increased in response to CS exposure, and the ensuing inflammation in response to CS exposure is significantly inhibited in mice lacking a functional $P2X_7$ receptor, thus advocating a crucial role for the $P2X_7$-inflammasome signalling axis in driving the inflammation seen in response to CS exposure. To confirm this I wanted to use a pharmacological tool that can block the $P2X_7$ receptor.

To establish an appropriate pharmacological $P2X_7$ tool to use in the murine models, human and murine cell based assays were developed using appropriate human and mouse cells lines (human THP-1 monocytic and mouse J774.2 monocytes/macrophages cell lines) based on positive expression of key inflammasome targets. Both cell lines were stimulated with combination treatments of LPS and ATPγS which elicited IL-1β release that was greater than the sum of the stimuli individually. This *in vitro* modelling system allowed me to demonstrate that the $P2X_7$ receptor was involved in this enhanced release of IL-1β that has been demonstrated previously by various groups (Grahames *et al*., 1999; Solle *et al*., 2001; Labasi *et al*., 2002; Ferrari *et al*., 2006; Qu *et al*., 2007). Upon testing the efficacy of both $P2X_7$ receptor antagonists, it was apparent that AZ11645373 failed to impact murine cells, whilst A438079 was only active murine cells and not the human receptor as reported by others (Donnelly-Roberts *et al*., 2009). Although A438079 was shown in my cell based assays to lack activity on the human $P2X_7$ receptor it was still the ideal tool to use in the *in vivo* models as it was demonstrated to have high efficacy *in vitro*.

In the CS driven model, A438079 managed to attenuate the significant increase BALF neutrophilia in response to CS exposure in a dose dependent manner providing further validation to the results seen in chapter 4 using the $P2X_7^{-/-}$ mice. No changes were seen in other inflammatory cell types, particularly the monocyte/macrophages that were significantly increased in response to CS exposure. These finding provide further validation to the results I have demonstrated in the previous chapter, where deletion of the function $P2X_7$ receptor, significantly attenuated the inflammatory response following CS exposure. These findings are in line with those reported by Lucattelli et al., where an alternative $P2X_7$ inhibitor (KN62) was demonstrated to significantly reduce the inflammation in mice following acute (3 day) CS exposure (Lucattelli *et al*., 2010).

Conversely, the compound had no apparent effect on the airway neutrophilia seen in response to the endotoxin challenge, different from the response seen in the $P2X_7^{-/-}$ animals where increased neutrophilia was seen in response to an endotoxin challenge. However, this difference in response comparing genetic knockouts and pharmacology may be one that has arisen due to developmental issue in the KO mice that is avoided by using pharmacological tools. Therefore, one could postulate that a $P2X_7$ receptor antagonist would have therapeutic benefit in combating inflammation in response to the disease progression, without affecting the general innate immune defence system.

Having determined that the $P2X_7$ – inflammasome axis may play a crucial role in the acute phase of disease pathogenesis (induction of inflammation), it would be interesting to examine whether the change in phenotype of the disease under more chronic conditions will alter the role or involvement of the pathway. This will require extended exposure protocol of the

current CS driven *in vivo* pre-clinical modelling system. However, this may provide crucial insight into the role of the inflammasome in the latter stages of disease pathogenesis.

Chapter 6

Inflammasome Activation in Sub-Chronic Models of Airway Inflammation

6.1 Rationale

The studies in this thesis so far have focused on acute neutrophilia; however, COPD is a slowly progressive inflammatory disease that manifests itself over a prolonged period of time with a cellular phenotype that features a large macrophage component. Thus, it is envisaged that the development of more chronic models of CS exposure (4 weeks or more) in mice may more closely resemble human disease. Whilst the data strongly suggests that the $P2X_7$-inflammasome axis may play an important role in the acute neutrophilia, it is important to study its role in a more chronic disease setting. Therefore I wanted to look for evidence of a role of the "axis" in longer-term smoke models and in human tissue from donors and patients with COPD.

6.2 Methods

6.2.1. Characterisation of a sub-chronic model of cigarette smoke induced-inflammation in C57BL/6 mice.

The data obtained thus far strongly advocates a central role for the $P2X_7$-inflammasome axis in driving the inflammation in response to cigarette smoke exposure. To validate whether this pathway is involved in sustaining the on-going inflammation seen clinically in COPD patients and not just restricted to the initial induction stage, we measured markers of the pathway in a more chronic 28 day exposure model. Assessment of inflammatory end-points of interest including cellular infiltration and the markers of inflammasome activation, including pro-inflammatory mediator release and caspase 1 activity, will identify it this receptor and its associated pathway are involved in sustaining the inflammation associated with COPD using a more chronic disease model.

To examine the role of the inflammasome in a more chronic inflammatory setting, mice were exposed to either room air or a sub-maximal (500 ml/min) dose of cigarette smoke (as detailed in section *2.2.2*) for a total exposure period of 50 minutes (excluding 10 minute venting period), twice daily, for 28 consecutive days. Each group consisted of n=12 animals at each time point. Mice were euthanised with an overdose (200 mg/kg) of i.p sodium pentobarbitone 24 hours after the final smoke exposure at 3 and 7 day intervals during the sub-chronic 28 day exposure (3, 7, 10, 14, 17, 21, 24 and 28 days). BALF and lung tissue samples were collected for analysis as follows;

- BALF (processed as described in section *2.3.1*):
    - Total cell counts and 4-part differential cell counts (neutrophils, eosinophils, monocytes/macrophages and lymphocytes, as described in section 2.*3.3*), n=6.
    - Cytokine analysis in BALF determined by standard ELISA, n=6 (as described in section *2.3.4.3*).

- Lung tissue (processed as described in section *2.3.1*):
    - Flash frozen in liquid nitrogen, n=6, for cytosolic and nuclear cell fraction extraction (as described in section *2.3.5.1*) for determination of caspase 1 activity (as described in section *2.3.5.2).*

6.2.2. Examination of inflammasome axis expression in human tissue.

Thus far, the data from the *in vivo* models suggests a major role for the $P2X_7$ – inflammasome pathway in driving the inflammation seen in a COPD-like setting. To determine if the observations seen in the pre-clinical models translated into the human disease, caspase 1 activity in lung tissue from non-smoking donors, smoking donors and emphysema patients was investigated.

Human tissue samples were obtained with support of the NIHR Biomedical Research Unit in Advanced Lung Disease at the Royal Brompton and Harefield NHS Foundation Trust and Imperial College London and partly funded by the NIHR Biomedical Research Unit funding scheme.

Parenchyma from human lung tissue samples was flash frozen in liquid nitrogen and stored at -80°c upon receipt. Samples were then selected for caspase 1 activity analysis based on patient data. Cytosolic and nuclear cell fraction extraction was performed (as described in section *2.3.5.1*) for determination of caspase 1 activity (as described in section *2.3.5.2).*

6.2.3. Statistical analysis

Data is expressed as mean ± S.E.M of n observations. The data was assessed for statistical significance by applying an unpaired t-test for parametric data or alternatively Mann-Whitney U-test for non-parametric data with independent groups compared with their specific time-matched controls. For multiple comparisons tests, statistical analysis was performed by applying a one-way ANOVA (analysis of variance) with a Dunnett's or Bonferroni's multiple comparisons post-test for parametric data or alternatively a Kruskal-Wallis incorporating Dunn's multiple comparison post-test for non-parametric data. A P value < 0.05 was taken as significant and all treatments were compared with the appropriate control group.

6.3. Results

6.3.1. Characterisation of a sub-chronic model of cigarette smoke induced-inflammation in C57BL/6 mice.

A significant increase in BALF neutrophils in response to CS exposure was seen at all the time points throughout the 28 day exposure period when compared to their time matched controls (Figure 6.1A). This increase peaked at 10 days and remained elevated at all later time points (Figure 6.1A). The monocyte/macrophages began to infiltrate the BALF at 10 days and remained elevated at all later time points (Figure 6.1B). They were significantly elevated at the 10, 14 and 21 day time points when compared to their time-matched air exposed controls (Figure 6.1B). Furthermore, lymphocytes demonstrated increases at similar time points to the monocyte/macrophages, shown to be significantly elevated from 10 days until the final 28 day time point when compared to their time matched controls (Figure 6.2). There were no significant changes in eosinophil numbers in response to CS exposure in the BALF at any time point throughout the 28 days exposure period (Figure 6.2).

Determining markers of inflammasome activation in this sub-chronic model demonstrated an increase in caspase 1 activity in the lung tissue at all time points (significant at 14, 21, 24 and 28 days) following the final smoke exposure when compared to their time matched controls (Figure 6.3A). Furthermore, this increase in caspase 1 activity throughout the 28 day CS exposure period was mirrored in the levels of IL-1β and IL-18 detected in the BALF in response to CS exposure (Figure 6.3B & Figure 6.3C). Additionally, the levels of IL-1β in the BALF were shown to be significantly increased at the 7 – 28 day time points, whilst IL-18

was significantly increased at the 10 – 28 day time points when compared to their appropriate time matched controls (Figure 6.3B & Figure 6.3C).

Efforts to determine the levels of the ATP released into the BALF following sub-chronic CS exposure proved to be unsuccessful.

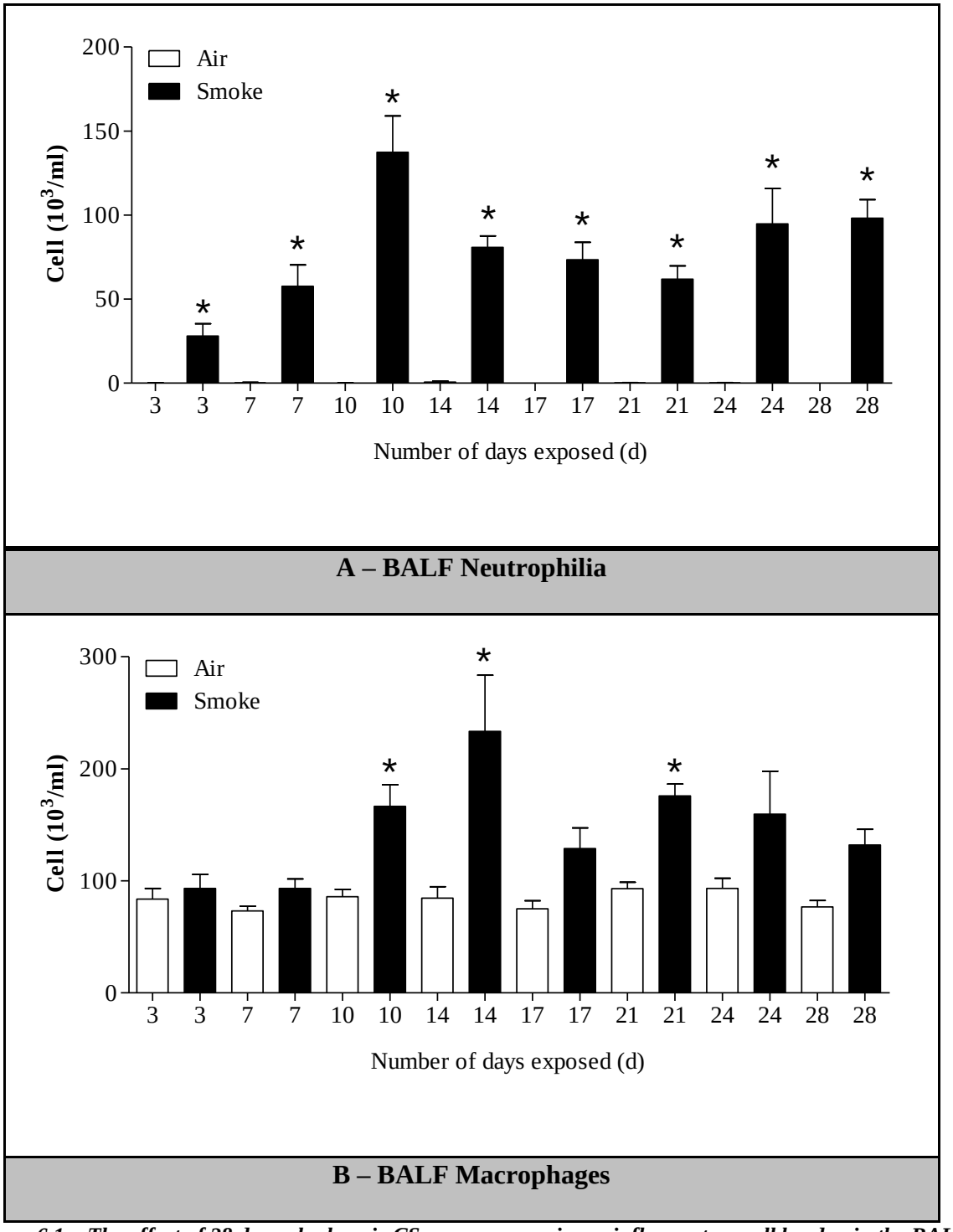

Figure 6.1 – The effect of 28 day sub-chronic CS exposure on airway inflammatory cell burden in the BALF. *C57BL/6 mice were challenged with room air or 500 ml/min cigarette smoke, twice daily for 28 consecutive days. Samples were collected 24 hours after the final smoke exposure at 3 and 7 day intervals and the BALF neutrophil (A) and monocyte/macrophage (B) numbers were determined by differential counting under light microscopy. Data represented as Mean ± SEM for n=8 observations. Statistical significance determined with a Mann-Whitney U-test for non-parametric data. * = P<0.05 and denotes a significant difference to the time-matched air exposed control group.*

	Cells (10^3/ml)	Eosinophils	Lymphocytes
3 days	Air	0.17±0.17	2.73±0.73
	Smoke	0.93±0.33	2.87±1.00
7 days	Air	0.25±0.16	6.33±1.58
	Smoke	2.27±1.04	11.78±3.83
10 days	Air	0.00±0.00	4.03±1.19
	Smoke	3.48±1.85	47.72±17.99*
14 days	Air	0.00±0.00	4.75±1.25
	Smoke	0.80±0.80	94.95±33.24*
17 days	Air	0.00±0.00	5.03±2.17
	Smoke	0.80±0.51	26.88±2.70*
21 days	Air	0.15±0.15	3.18±0.86
	Smoke	1.55±0.71	40.58±7.17*
24 days	Air	0.00±0.00	6.68±1.86
	Smoke	2.37±0.90	56.80±9.48*
28 days	Air	0.00±0.00	4.92±0.75
	Smoke	2.23±0.93	27.67±2.80*

Figure 6.2 – The effect of 28 day sub-chronic CS exposure on airway inflammatory cell burden in the BALF. *C57BL/6 mice were challenged with room air or 500 ml/min cigarette smoke, twice daily for 28 consecutive days. Samples were collected 24 hours after the final smoke exposure at 3 and 7 day intervals and the numbers of eosinophils and lymphocytes recovered from the BALF were determined by differential counting under light microscopy. Data represented as Mean ± SEM for n=8 observations. Data represented as Mean ± SEM for n=8 observations. Statistical significance determined with a Mann-Whitney U-test for non-parametric data. * = P<0.05 and denotes a significant difference to the time-matched air exposed control group.*

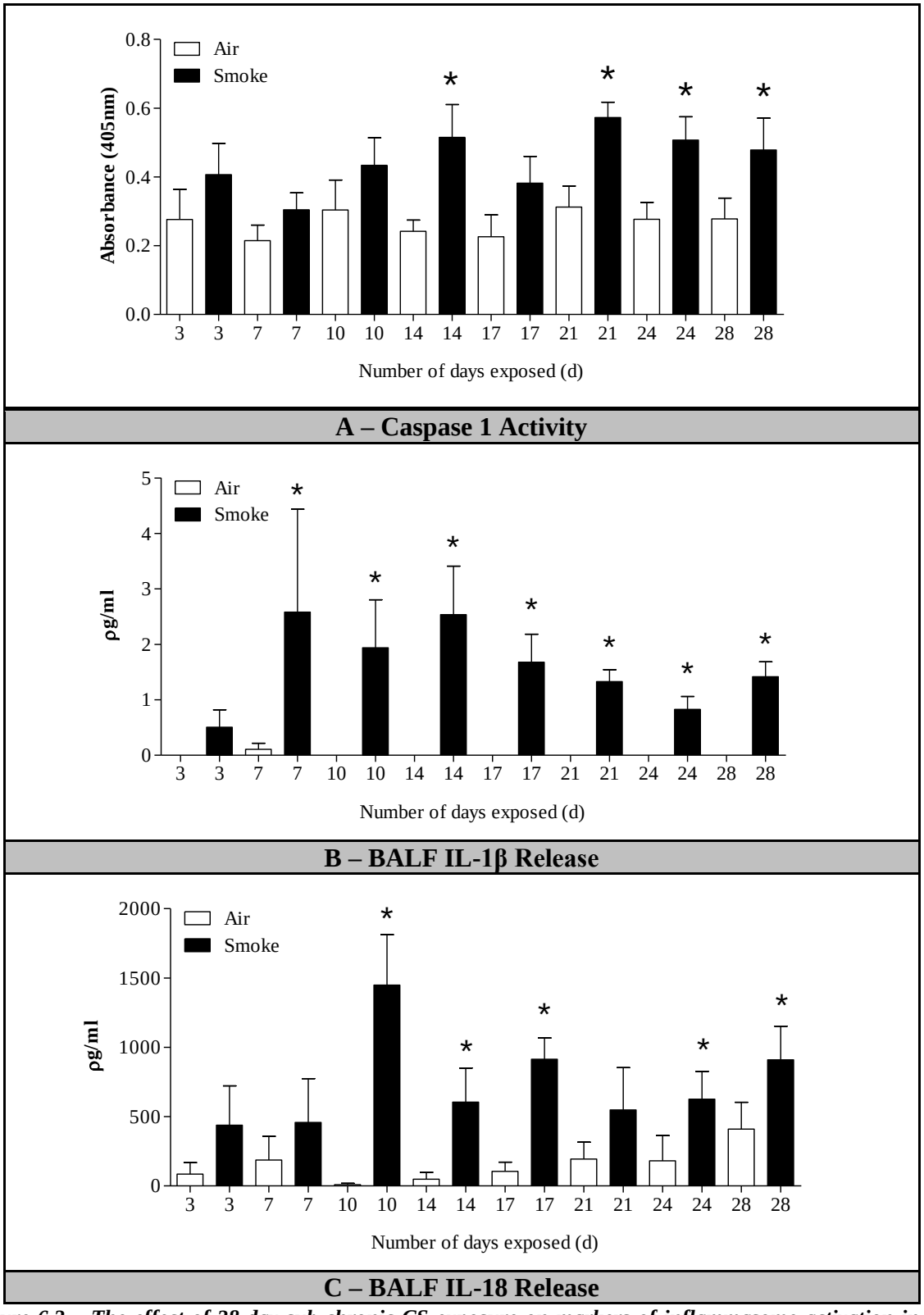

Figure 6.3 – The effect of 28 day sub-chronic CS exposure on markers of inflammasome activation in the lung. *C57BL/6 mice were challenged with room air or 500 ml/min cigarette smoke, twice daily for 28 consecutive days. Samples were collected 24 hours after the final smoke exposure at 3 and 7 day intervals and caspase 1 activity in the cytosolic fraction of the lung tissue (A) and the release of inflammatory cytokines IL-1β (B) and IL-18 (C) in the BALF were measured using commercially available assays. Data represented as Mean ± SEM for n=8 observations. Statistical significance determined with a Mann-Whitney U-test for non-parametric data. * = P<0.05 and denotes a significant difference to the time-matched air exposed control group.*

6.3.2. Examination of inflammasome axis expression in human tissue.

Although the numbers are limited, the data illustrates that caspase 1 activity is increased in both smoking donors and emphysema patients when compared to non-smoking donors (Figure 6.4). Furthermore, there seems to be minimal difference in caspase 1 activity when comparing the increased levels seen in the smoking donors and emphysema patients (Figure 6.4).

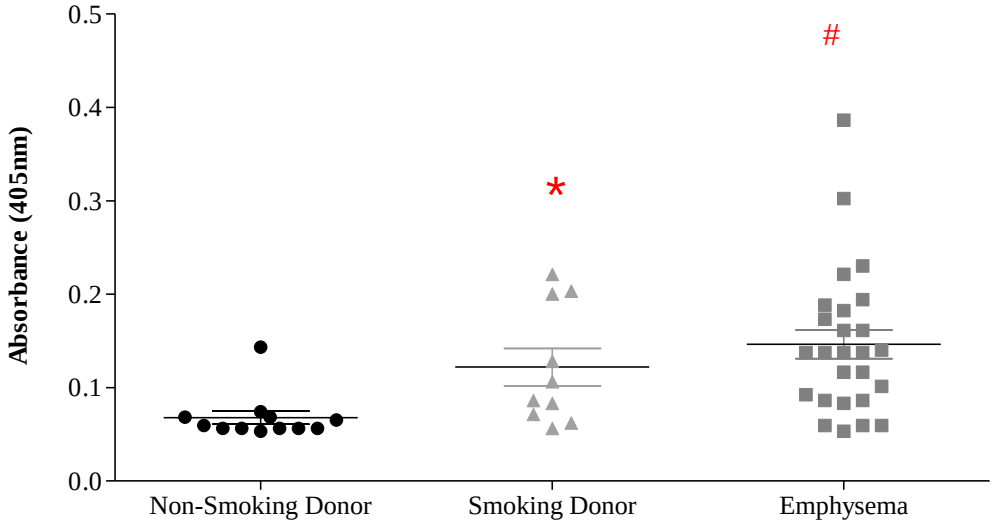

Figure 6.4 – Caspase 1 activity in human lung tissue samples. *Parenchyma from human lung tissue samples was flash frozen in liquid nitrogen and stored at -80°c upon receipt. Cytosolic and nuclear cell fraction extraction was performed and the cytosolic fraction was used to determine caspase 1 activity. Data represented as Mean ± SEM. Statistical significance determined with One-way ANOVA incorporating Bonferroni's post-test for parametric data. * = P<0.05 and denotes a significant difference to the non-smoking donor group.*

Disease Group	Age (years)	Sex (M/F)
Non-Smoking Donor	27 - 72	3/9
Smoking Donor	22 - 62	7/3
Emphysema	49 - 69	17/8

Figure 6.5 – Human lung tissue patient details list. *Details of patient sex, age and condition for samples used to assess caspase 1 activity in lung tissue from human patients with various disease conditions.*

6.4 Discussion

The positive data highlighting the important role of the $P2X_7$-inflammasome axis in driving acute CS induced inflammation raised further questions with regards to the function of this pathway in more chronic conditions associated with the development of COPD. The phenotype of the disease in the clinic has been shown to shift from being driven predominantly by neutrophils in the acute phase, to include the actions of macrophages in chronic phase (O'Donnell *et al*., 2006). Thus, it is envisaged that the development of more chronic models of CS exposure (4 weeks or more) in mice may more closely resemble human disease. Furthermore, the role of the inflammasome is unclear in the response to the shift in the phenotype of the disease in chronic conditions.

To validate the role of the inflammasome in the on-going inflammation in a more chronic model of CS exposure, markers of inflammasome activation were investigated in the sub-chronic (28 day) exposure model. Additionally, caspase 1 activity was examined in human lung tissue samples from non-smoking donors, smoking donors and emphysema patients to establish if the previous findings in the *in vivo* pre-clinical models translate into the human disease.

Both neutrophil and monocyte/macrophage numbers in the BALF were demonstrated to be elevated in response to sub-chronic CS exposure, with the later becoming involved at a later 10 day time point. Furthermore, lymphocyte numbers were also significantly increased in response to the CS exposure, following a similar profile to that of the monocyte/macrophage component of the airway inflammation. These findings support those reported by other groups utilising chronic models of CS exposure in mice (D'Hulst *et al*., 2005; Maes *et al*.,

2006). Temporally correlated with the increase in neutrophils and macrophages observed in the BALF, an increase in caspase 1 activity, IL-1β and IL-18 levels was also seen in response to the CS exposure throughout the 28 day exposure protocol. This suggests that the $P2X_7$-inflammasome axis is not only central to the induction of CS-induced inflammation but also in the on-going inflammation.

A similar increase in caspase 1 activity was observed in lung tissue from patients with COPD and smokers. Although the numbers are limited this data clearly demonstrates that as seen in the pre-clinical models, caspase 1 activity is increased in diseased tissue. Therefore, it can be assumed that the pre-clinical model reflects the clinical disease and that the role of caspase 1 is not restricted to the induction of the inflammation but is chronically elevated. This finding supports those reported by others investigating markers of inflammasome activation, demonstrating that IL-1β (Ekberg-Jansson *et al*., 2001; Zeidel *et al*., 2002; Singh *et al*., 2010) and IL-18 (Petersen *et al*., 2007; Imaoka *et al*., 2008; Rovina *et al*., 2009) are both increased in clinic samples taken from COPD patients. Based on these findings, it can be assumed that the increases in markers of inflammasome activation seen in these clinical samples from COPD patients advocate a central role for the $P2X_7$-inflammasome axis in driving the inflammation seen in COPD patients.

These results clearly promote the critical role of the $P2X_7$ - inflammasome axis in CS induced inflammation. Testing the $P2X_7$ KO mice in the 28 day sub-chronic model would provide further validation of the importance of this "axis" in CS-induced inflammation. Furthermore, the data suggests that the pathway has an on-going role in the pathogenesis of COPD with translational data in human tissue from both donors and patients to validate this hypothesis. Further investigation of the pathway in a more chronic (6 month) CS exposure model will

provide further justification for the role of the inflammasome in the chronic stages of the disease to validate the findings in the human patient samples.

Chapter 7

Summary & Future Directions

7.1 Summary

COPD remains a severe healthcare problem globally, with the incidence of the disease predicted to further increase. Although much research focus has been aimed at better understanding the disease, there still remains much that is unknown about the cellular components and molecular mechanisms that drive COPD pathogenesis. The aim of this thesis was to attempt to elucidate the mechanisms that promote the pathogenesis of the disease by examining how CS exposure leads to the inflammation linked with markers of inflammasome activation that have been reported to be increased in both the clinic and animal models of COPD.

I developed an acute CS driven model of inflammation in C57BL/6 mice and characterised the inflammatory response elicited. The data was consistent with those of other groups (Doz *et al*., 2008; Morris *et al*., 2008). Having validated the model, markers of inflammasome activation were then investigated. The data clearly suggests that acute exposure to CS causes an increase in caspase 1 activity as well as the release of the NLRP3 inflammasome linked cytokines IL-1β and IL-18. Surprisingly, no increases were seen in cytokine mRNA levels. However, as the glucocorticoids are believed to function by blocking the transcription/translation of inflammatory cytokines (Barnes *et al*., 2009) this lack of increase in cytokine mRNA levels may explain why the inflammation seen in COPD patients has been shown to be resistant to steroid treatment. Since, the release of inflammatory cytokines in this pathway may be independent of transcription/translation; the actions of steroids would have limited impact on the inflammation driving the disease.

The inflammatory chemokine KC was seen to be increased in response to cigarette smoke at both the gene and protein level. However, the increase in KC production did not temporally correlate with the cellular inflammation suggesting that KC may not play an important role in driving the inflammation in this model. Surprisingly, I was also unable to detect increased ATP levels in the samples, a finding that is reported by other groups using CS models of inflammation (Mortaz *et al*., 2009; Lucattelli *et al*., 2010). Furthermore, as I was unable to detect an increase in ATP production I attempted to investigate an increase in an alternative $P2X_7$ receptor activator NAD+ oxidase. Both $P2X_7$ receptor ligands were not detected in any samples across all groups.

I wanted to parallel my investigation in an alternative neutrophilic model of inflammation to validate that the increases seen in the markers of inflammasome activation are specific to inflammation associated with the disease and not through the normal innate immune response. I examined changes in markers of inflammasome activation in response to an LPS challenge. Although significant increases were seen in neutrophilia and inflammasome linked cytokines, these were not temporally correlated and more significantly, not linked to any increase in the central inflammasome processing protein caspase 1. This suggests that activation of the inflammasome is specific to the inflammation associated with the disease and not triggered by activation of the innate immune response.

Intriguingly, the release of the two inflammasome-linked cytokines IL-1β and IL-18 seems to differ in this model as the release of IL-18 seems to be independent of increased mRNA expression. The lack of caspase 1 activity would suggest that IL-1β may be processed differently in this model. In parallel, increases in the production of the neutrophilic

chemokine KC at both the gene and protein levels were seen that temporally correlated with the neutrophilia in this model.

In order to define the integral role played by the $P2X_7$ – NLRP3 inflammasome pathway in CS-induced inflammation, I incorporated mice lacking a functional $P2X_7$ receptor into both *in vivo* models of inflammation. These mice showed decreases in caspase 1 activity and the release of IL-1β and IL-18 in response to CS exposure. Furthermore, the airway neutrophilia in response to the CS exposure was completely attenuated in the $P2X_7^{-/-}$ mice. All these findings are consistent with those of other groups investigating $P2X_7^{-/-}$ mice in CS exposure (Lucattelli *et al*., 2010). The basal levels of IL-18 in these $P2X_7^{-/-}$ mice were higher than in the WT mice in air exposed groups. It is envisaged that this increase in the $P2X_7^{-/-}$ mice might be due to a biological compensatory mechanism that aims to protect these mice as they lack the functional $P2X_7$ receptor required for inflammatory cytokine processing. Interestingly, BALF KC production was unaffected by blockade of the $P2X_7$ – inflammasome axis whilst the neutrophilia was completely attenuated. Furthermore, these KO animals show an increase in KC levels when compared to the CS exposed WT animals. This finding will require further investigation particularly as the neutrophilia in these KO animals is completely attenuated in the presence of an increase in the chemokine KC.

I examined the role of the $P2X_7$ receptor in LPS-induced inflammation to find that the inflammation was similar in both wild-type and $P2X_7^{-/-}$ mice. In contrast to the CS model, $P2X_7^{-/-}$ mice failed to reduce the increased neutrophilia or production of IL-1β in response to LPS exposure. Furthermore, the release of KC in response to LPS was significantly increased in the $P2X_7^{-/-}$ mice when compared with the WT, which provides further evidence of a developmental change in the KO animals from birth.

I wanted to validate the findings seen using the $P2X_7^{-/-}$ mice in the CS model of inflammation using a small molecular weight inhibitor to block the $P2X_7$ receptor. In order to identify an appropriate pharmacological tool to use in my *in vivo* models, I tested the $P2X_7$ inhibitors in human and murine *in vitr*o cell based assays. The release of both IL-1β and IL-18 was examined in response to treatment with LPS and ATP and shown to be greater than the sum of both stimuli individually. This significant increase in the release of inflammasome linked cytokines in response to the combination treatment was significantly attenuated in the presence of a $P2X_7$ antagonist. However, AZ11645373 failed to impact on the murine cells, whereas A438079 only impacted on the murine system, even though it is reported to act on the human receptor. These studies allowed me to select A438079 as the appropriate tool to use in the murine models.

The integral role of the $P2X_7$ – NLRP3 inflammasome pathway in CS-induced inflammation was further validated by the fact that very similar data was obtained by blocking the $P2X_7$ receptor using a pharmacological tool as with the $P2X_7^{-/-}$ mice in the CS model of inflammation. Moreover, the $P2X_7$ inhibitor did not affect neutrophilia induced by endotoxin challenge. This finding combined with the lack of caspase 1 activity seen in this model suggests that the $P2X_7$ – NLRP3 inflammasome axis is not critical in the inflammatory response driven by the innate immune response. This is a highly significant finding as it suggests that utilising a $P2X_7$ antagonist in the clinic would attenuate the inflammation linked to the disease whilst not affecting any essential innate defence mechanisms.

In order to investigate the role of this pathway in a more chronic setting, I exposed mice to CS for a longer (sub-chronic) 28 day period. A significant increase in airway neutrophilia,

and more interestingly, macrophages was seen in this sub-chronic model. This is similar to what is seen in the clinic, where macrophages are present in the inflammatory milieu seen in COPD patient lungs. Increases in caspase 1 activity and release of inflammasome linked cytokines IL-1β and IL-18 were also seen. To support these findings I wanted to examine the role of the pathway in the human disease so I investigated caspase 1 activity in human lung tissue samples and demonstrated that it was elevated in samples from smokers and patients with COPD, which suggests that the pre-clinical model reflects the clinical disease and that the role of caspase 1 is not restricted to the induction of the inflammation but is chronically elevated. To my knowledge the role of caspase 1 has not been previously investigated in human disease, thus this finding provides valuable insight into the role of this pathway in chronic conditions.

When studied as a whole, the data presented in this thesis provides valuable insight into the underlying processes that drive the pathogenesis of COPD. Furthermore, the data in all the chapters provides *in vivo* insight into the role of this pathway in driving the inflammation associated with the disease. Furthermore, the results in Chapter 6 indicate that this pathway plays a role in chronic disease and the pathogenesis of COPD thus highlighting the potential of this pathway and its components as possible therapeutic targets in battling this fatal disease.

7.2 Future Directions

7.2.1 Investigate activation of the inflammasome

As of yet there is currently no conclusive evidence in the literature to validate what factor or mediators drive the activation of the inflammasome in response to $P2X_7$ ligand binding. Current dogma suggests that this process may be dependent upon pore formation or membrane disruption in response to receptor activation (Mariathasan & Monack, 2007). It is envisaged that identifying this missing step in the pathway will facilitate better understanding of the underlying mechanisms as well as provide further potential therapeutic targets.

Furthermore, I have attempted to validate the reported increased in ATP in response to CS exposure that may lead to inflammasome activation (Lucattelli *et al*., 2010). However, although the same methods and materials were used, the results reported by other groups could not be replicated in our *in vivo* model. I further investigated the possibility that an alternative activator of the inflammasome such as NADPH oxidase might responsible; however I was also unable to detect it in any of my samples. Therefore it will be important to identify if ATP is truly responsible for driving this inflammasome mediated inflammation or whether it is dependent on another activator of the pathway.

To elucidate the role of ATP in this modelling system, I suggest using alternative methods to detect its levels; such as *in vivo* bioluminescence imaging to detect the presence of ATP in a whole living animal. Bioluminescence is the process of light emission in living organisms, which uses native light emission from an organism that bioluminesce. I have attempted to use this technique to determine ATP levels in the BALF samples from CS exposed mice, however it was unsuccessful. This detection of ATP via luciferin-luciferase assay in

supernatants is both laborious and inaccurate due to the presence of endogenous ectonucleotidases that break down the ATP at a very fast rate. Recently, various groups have demonstrated the ability to engineer specific cell/membrane-targeted luciferase to allow *in vivo* real-time imaging of extracellular ATP by detecting a change based on an increase/decrease in activity that will be represented in the change of light emitted (Pellegatti *et al*., 2008). This technique would remain non-invasive and thus have limited impact on the physiology of the animals whilst they are exposed to the various challenges in these *in vivo* models.

Alternatively, if these ectonucleotidases are indeed breaking down the ATP at a rapid rate in the BALF samples this could be prevented by using an inhibitor of ectonucleotidases in the lavage fluid. Dipyridamole, a thromboxane synthase inhibitor is reported to inhibit the breakdown of ATP (Connolly *et al*., 2000). This may preserve the ATP produced as a result of CS exposure and facilitate it's detection in the BALF samples using the standard luciferase assay I used in this thesis.

7.2.2 The role of the inflammasome in chronic model of CS exposure

Having seen the increases in markers of inflammasome activation in the sub-chronic CS exposure model, it would be of great interest to examine whether the inflammasome is truly activated chronically in response to prolonged 6 – 9 months CS exposure. A more chronic model will also provide more disease like changes in the lungs of these animals, including emphysema, mucus production and lung function changes. Furthermore, it would be of great interest to compare the findings/observations of this chronic exposure to those of the disease in the clinic. This would provide further insight into how accurate this *in vivo* model is in

replicating the disease phenotype as well as provide a platform to investigate activation of the inflammasome. Other end-points of interest would also include investigating histopathology to measure mucus production and airway remodelling (emphysema) as well as investigating markers of inflammasome activation using IHC (immunohistochemistry). Moreover, it would also facilitate examining other markers of COPD currently investigated in the clinic, such as lung function changes (e.g. FEV_1, residual volume and exercise ability).

7.2.3 Genetic manipulation of the inflammasome

Due to time constraints I was only able to utilise the $P2X_7^{-/-}$ mice in our *in vivo* models of inflammation to investigate the role of the NLRP3 inflammasome. However, I have recently obtained animals lacking other components of the $P2X_7$ – NLRP3 inflammasome axis including NLRP3, ASC and caspase 1. These animals will provide valuable insight into the importance of each component in driving the inflammation seen in response to inflammasome activation. Furthermore, there are also animals lacking the adaptor molecules for other inflammasome complexes including AIM2, NLRC4 and NLRP1. To my knowledge none of these inflammasome complexes have been investigated in *in vivo* models of airway inflammation or investigated in this disease area. This would provide novel data and insight into the roles these other inflammasome complexes, which remain poorly understood, may play in inflammation.

Other available knockout mice that would provide valuable assets to this project include mice lacking receptors and proteins for the inflammasome linked cytokines that include IL-1β and IL-18. There are currently available IL-1 receptor KO and IL-18 receptor KO animals, as well as mice that do not produce both cytokines. By investigating the inflammation in

response to CS exposure in these animals it would be possible to identify if therapies targeted at these cytokines may be of clinical benefit.

7.2.4 Pharmacological manipulation of the inflammasome

Having seen the successful effects of a $P2X_7$ antagonist in reducing the inflammation in response to CS exposure, I wish to further examine the role of the inflammasome by using pharmacological tools to target various components of the inflammasome and its products. This will provide valuable insight in validating therapeutic targets and tools that can be used in the clinic to meet this urgent need for therapies to combat this relentless disease. These include inhibitors of NLRP3 (Glyburide), caspase 1 (VX-765, Parthenolide, Thimerasol and Auranofin) and anti-bodies to neutralise IL-1β and IL-18. Using these anti-bodies will circumvent the developmental issues of using KO mice and also provide a therapeutic benefit in the clinic. There are also antagonists available that can target the receptors of the inflammasome linked cytokines IL-1β (IL-1R e.g. ANAKINRA) and IL-18 (IL-18R).

7.2.5 The role of KC in cigarette smoke-induced inflammation

Whilst investigating the role of the inflammasome in these in vivo models, I saw intriguing results with regards to the role of the neutrophilic chemokine KC in these *in vivo* models. Whilst it was shown to be increased in response to CS at both the gene and protein level it did not temporally correlate with the cellular inflammation suggesting that KC may not play an important role in driving the inflammation in this model. In the LPS model increases in KC at both the gene and protein levels temporally correlated with the neutrophilia. Furthermore, BALF KC production in response to CS exposure was unaffected by $P2X_7$ receptor blockade

whilst the neutrophilia was completely attenuated. Surprisingly, these KO animals showed a significant increase in KC levels when compared to the CS exposed WT animals.

Thus it is important to elucidate the role of the chemokine KC that is believed to function as a neutrophil chemoattractant. This can be achieved by incorporating $KC^{-/-}$ mice into both in vivo models and investigating the effects on the different mechanisms of inflammation.

7.2.6 The role of other inflammasomes in COPD

As it stands the inflammasome family of intracellular receptors still remains a poorly understood field. Although various inflammasome complexes have been identified that all vary based on the main adaptor molecule that constitutes the complex, the differences in their function and activation is still poorly understood. Investigating the role of various inflammasome in our *in vivo* disease models may highlight differences in their roles, or alternatively identify any possible similarities in their functions. This still remains an unmet need, particularly with interest in this field gathering pace.

7.2.7 Investigating the pathway in samples from COPD patients

The data obtained from examining the activity of caspase 1 in donors, smokers and emphysema patients was promising. Obtaining a better range and wider selection of samples from patients across all stages of the disease (GOLD I – IV) would facilitate better investigating activity of various components of the pathway throughout different stages of disease development.

Reference List

Aaron, S. D., Angel, J. B., Lunau, M., Wright, K., Fex, C., Le Saux, N., & Dales, R. E. (2001). Granulocyte inflammatory markers and airway infection during acute exacerbation of chronic obstructive pulmonary disease. *Am. J. Respir. Crit. Care Med 163,* 349–355.

Adcock, I. M., Ito, K., & Barnes, P. J. (2005). Histone deacetylation: an important mechanism in inflammatory lung diseases. *COPD 2*, 445–455.

Adcock, I. M., Marwick, J., Casolari, P., Contoli, M., Chung, K. F., Kirkham, P., Papi, A., & Caramori, G. (2010). Mechanisms of corticosteroid resistance in severe asthma and chronic obstructive pulmonary disease (COPD). *Curr. Pharm. Des 16*, 3554–3573.

Adler, K. B., & Li, Y. (2001). Airway epithelium and mucus: intracellular signaling pathways for gene expression and secretion. *Am. J. Respir. Cell Mol. Biol 25*, 397–400.

Agostini, L., Martinon, F., Burns, K., McDermott, M. F., Hawkins, P. N., & Tschopp, J. (2004). NALP3 forms an IL-1beta-processing inflammasome with increased activity in Muckle-Wells autoinflammatory disorder. *Immunity 20*, 319–325.

Alcorn, J.F., Crowe, C.R., and Kolls, J.K. (2010). TH17 cells in asthma and COPD. *Annu. Rev. Physiol. 72*, 495–516.

Aldonyte, R., Jansson, L., Piitulainen, E., & Janciauskiene, S. (2003). Circulating monocytes from healthy individuals and COPD patients. *Respir. Res 4*, 11.

Alsaeedi, A., Sin, D. D., & McAlister, F. A. (2002). The effects of inhaled corticosteroids in chronic obstructive pulmonary disease: a systematic review of randomized placebo-controlled trials. *Am. J. Med 113*, 59–65.

American Lung Association, 2007 American Lung Association, COPD and Asthma Factsheet (2007).

Anthonisen, N. R., Connett, J. E., Kiley, J. P., Altose, M. D., Bailey, W. C., Buist, A. S., Conway, W. A., Jr, Enright, P. L., Kanner, R. E., & O'Hara, P. (1994). Effects of smoking intervention and the use of an inhaled anticholinergic bronchodilator on the rate of decline of FEV1. The Lung Health Study. *JAMA 272*, 1497–1505.

Anyanwu, A. C., McGuire, A., Rogers, C. A., & Murday, A. J. (2002). An economic evaluation of lung transplantation. *J. Thorac. Cardiovasc. Surg 123*, 411–418; discussion 418–420.

Aoshiba, K., Yokohori, N., & Nagai, A. (2003). Alveolar Wall Apoptosis Causes Lung Destruction and Emphysematous Changes. *Am. J. Respir. Cell Mol. Biol. 28*, 555–562.

Arulkumaran, N., Unwin, R.J., and Tam, F.W. (2011). A potential therapeutic role for P2X7 receptor (P2X7R) antagonists in the treatment of inflammatory diseases. *Expert Opin Investig Drugs 20*, 897–915.

Babior, B. M. (2000). Phagocytes and oxidative stress. *Am. J. Med 109*, 33–44.

Balbi, B., Bason, C., Balleari, E., Fiasella, F., Pesci, A., Ghio, R., & Fabiano, F. (1997). Increased bronchoalveolar granulocytes and granulocyte/macrophage colony-stimulating factor during exacerbations of chronic bronchitis. *Eur. Respir. J 10*, 846–850.

Barnes, P. J. (2000). Chronic obstructive pulmonary disease. *N. Engl. J. Med 343*, 269–280.

Barnes, P. J., Shapiro, S. D., & Pauwels, R. A. (2003). Chronic obstructive pulmonary disease: molecular and cellular mechanisms. *Eur. Respir. J 22*, 672–688.

Barnes, P. J. (2004a). Alveolar macrophages as orchestrators of COPD. *COPD 1*, 59–70.

Barnes, P. J. (2004b). Corticosteroid resistance in airway disease. *Proc Am Thorac Soc 1*, 264–268.

Barnes, P. J., Ito, K., & Adcock, I. M. (2004). Corticosteroid resistance in chronic obstructive pulmonary disease: inactivation of histone deacetylase. *Lancet 363*, 731–733.

Barnes, P. J. (2006). Reduced histone deacetylase in COPD: clinical implications. *Chest 129*, 151–155.

Barnes, P. J. (2009). Role of HDAC2 in the pathophysiology of COPD. *Annu. Rev. Physiol 71*, 451–464.

Bayne, E. K., Rupp, E. A., Limjuco, G., Chin, J., & Schmidt, J. A. (1986). Immunocytochemical detection of interleukin 1 within stimulated human monocytes. *J. Exp. Med 163*, 1267–1280.

Beeh, K. M., Kornmann, O., Buhl, R., Culpitt, S. V., Giembycz, M. A., & Barnes, P. J. (2003). Neutrophil chemotactic activity of sputum from patients with COPD: role of interleukin 8 and leukotriene B4. *Chest 123*, 1240–1247.

Bernhard, D., Huck, C. W., Jakschitz, T., Pfister, G., Henderson, B., Bonn, G. K., & Wick, G. (2004). Development and evaluation of an in vitro model for the analysis of cigarette smoke effects on cultured cells and tissues. *J Pharmacol Toxicol Methods 50*, 45–51.

Betsuyaku, T., Nishimura, M., Takeyabu, K., Tanino, M., Miyamoto, K., & Kawakami, Y. (2000). Decline in FEV(1) in community-based older volunteers with higher levels of neutrophil elastase in bronchoalveolar lavage fluid. *Respiration 67*, 261–267.

Bhowmik, A., Seemungal, T. A., Sapsford, R. J., & Wedzicha, J. A. (2000). Relation of sputum inflammatory markers to symptoms and lung function changes in COPD exacerbations. *Thorax 55*, 114–120.

Birrell, M. A., McCluskie, K., Wong, S., Donnelly, L. E., Barnes, P. J., & Belvisi, M. G. (2005). Resveratrol, an extract of red wine, inhibits lipopolysaccharide induced airway neutrophilia and inflammatory mediators through an NF-kappaB-independent mechanism. *FASEB J 19*, 840–841.

Birrell, M. A., Wong, S., Dekkak, A., De Alba, J., Haj-Yahia, S., & Belvisi, M. G. (2006). Role of matrix metalloproteinases in the inflammatory response in human airway cell-based assays and in rodent models of airway disease. *J. Pharmacol. Exp. Ther 318*, 741–750.

Black, R., Kronheim, S., Sleath, P., Greenstreet, T., Virca, G.D., March, C., and Kupper, T. (1991). The proteolytic activation of interleukin-1 beta. *Agents Actions Suppl. 35*, 85–89.

de Boer, W. I., Sont, J. K., van Schadewijk, A., Stolk, J., van Krieken, J. H., & Hiemstra, P. S. (2000). Monocyte chemoattractant protein 1, interleukin 8, and chronic airways inflammation in COPD. *J. Pathol 190*, 619–626.

Boueri, F. M., Bucher-Bartelson, B. L., Glenn, K. A., & Make, B. J. (2001). Quality of life measured with a generic instrument (Short Form-36) improves following pulmonary rehabilitation in patients with COPD. *Chest 119*, 77–84.

Boyden, E. D., and Dietrich, W. F. (2006). Nalp1b controls mouse macrophage susceptibility to anthrax lethal toxin. *Nat Genet 38*, 240–244.

Brough, D., Pelegrin, P., & Rothwell, N. J. (2009). Pannexin-1-dependent caspase-1 activation and secretion of IL-1β is regulated by zinc. *Eur J Immunol 39*, 352–358.

Bruey, J.-M., Bruey-Sedano, N., Luciano, F., Zhai, D., Balpai, R., Xu, C., Kress, C. L., Bailly-Maitre, B., Li, X., Osterman, A., et al. (2007). Bcl-2 and Bcl-XL Regulate Proinflammatory Caspase-1 Activation by Interaction with NALP1. *Cell 129*, 45–56.

Bucchioni, E., Kharitonov, S. A., Allegra, L., & Barnes, P. J. (2003). High levels of interleukin-6 in the exhaled breath condensate of patients with COPD. *Respir Med 97*, 1299–1302.

Burge, P. S., Calverley, P. M., Jones, P. W., Spencer, S., Anderson, J. A., & Maslen, T. K. (2000). Randomised, double blind, placebo controlled study of fluticasone propionate in patients with moderate to severe chronic obstructive pulmonary disease: the ISOLDE trial. *BMJ 320*, 1297–1303.

Burgler, S., Ouaked, N., Bassin, C., Basinski, T.M., Mantel, P.-Y., Siegmund, K., Meyer, N., Akdis, C.A., and Schmidt-Weber, C.B. (2009). Differentiation and functional analysis of human T(H)17 cells. *J. Allergy Clin. Immunol. 123*, 588–595, 595.e1–e7.

Calverley, P. M. (2001). Modern treatment of chronic obstructive pulmonary disease. *Eur Respir J Suppl 34*, 60s-66s.

Carswell, E. A., Old, L. J., Kassel, R. L., Green, S., Fiore, N., & Williamson, B. (1975). An endotoxin-induced serum factor that causes necrosis of tumors. *Proc. Natl. Acad. Sci. U.S.A 72*, 3666–3670.

Cassel, S. L., Eisenbarth, S. C., Iyer, S. S., Sadler, J. J., Colegio, O. R., Tephly, L. A., Carter, A. B., Rothman, P. B., Flavell, R. A., & Sutterwala, F. S. (2008). The Nalp3 inflammasome is essential for the development of silicosis. *Proceedings of the National Academy of Sciences 105*, 9035–9040.

Cazzola, M., & Donner, C. F. (2000). Long-acting beta2 agonists in the management of stable chronic obstructive pulmonary disease. *Drugs 60*, 307–320.

Ceylan, E., Kocyigit, A., Gencer, M., Aksoy, N., & Selek, S. (2006). Increased DNA damage in patients with chronic obstructive pulmonary disease who had once smoked or been exposed to biomass. *Respir Med 100*, 1270–1276.

Chan, A., & Murin, S. (2011). Up in Smoke. *Chest 139*, 737–738.

Chung, K. F. (2001). Cytokines in chronic obstructive pulmonary disease. *Eur Respir J Suppl 34*, 50s-59s.

Churg, A., & Wright, J. L. (2007). Animal models of cigarette smoke-induced chronic obstructive lung disease. *Contrib Microbiol 14*, 113–125.

Churg, A., Cosio, M., & Wright, J. L. (2008). Mechanisms of cigarette smoke-induced COPD: insights from animal models. *Am. J. Physiol. Lung Cell Mol. Physiol 294*, L612–L631.

Churg, A., Wang, R. D., Tai, H., Wang, X., Xie, C., & Wright, J. L. (2004). Tumor necrosis factor-alpha drives 70% of cigarette smoke-induced emphysema in the mouse. *Am. J. Respir. Crit. Care Med 170*, 492–498.

Churg, A., Zhou, S., Wang, X., Wang, R., & Wright, J. L. (2009). The role of interleukin-1beta in murine cigarette smoke-induced emphysema and small airway remodeling. *Am. J. Respir. Cell Mol. Biol 40*, 482–490.

Cicko, S., Lucattelli, M., Müller, T., Lommatzsch, M., De Cunto, G., Cardini, S., Sundas, W., Grimm, M., Zeiser, R., Dürk, T., et al. (2010). Purinergic receptor inhibition prevents the development of smoke-induced lung injury and emphysema. *J. Immunol 185*, 688–697.

Connolly, G. P., & Duley, J. A. (2000). Ecto-nucleotidase of cultured rat superior cervical ganglia: dipyridamole is a novel inhibitor. *Eur. J. Pharmacol 397*, 271–277.

Couillin, I., Vasseur, V., Charron, S., Gasse, P., Tavernier, M., Guillet, J., Lagente, V., Fick, L., Jacobs, M., Coelho, F. R., et al. (2009). IL-1R1/MyD88 Signaling Is Critical for Elastase-Induced Lung Inflammation and Emphysema. *The Journal of Immunology 183*, 8195–8202.

Coulter, K. R., Wewers, M. D., Lowe, M. P., & Knoell, D. L. (1999). Extracellular regulation of interleukin (IL)-1beta through lung epithelial cells and defective IL-1 type II receptor expression. *Am. J. Respir. Cell Mol. Biol 20*, 964–975.

Coutinho-Silva, R., & Persechini, P. M. (1997). P2Z purinoceptor-associated pores induced by extracellular ATP in macrophages and J774 cells. *Am. J. Physiol 273*, C1793–C1800.

Creagh, E.M., & O'Neill, L.A., (2006). TLRs, NLRs and RLRs: a trinity of pathogen sensors that co-operate in innate immunity. *Trends in Immunology*, 27(8), pp.352-357.

Crockett, A. J., Cranston, J. M., Moss, J. R., & Alpers, J. H. (2001). Survival on long-term oxygen therapy in chronic airflow limitation: from evidence to outcomes in the routine clinical setting. *Intern Med J 31*, 448–454.

Crooks, S. W., Bayley, D. L., Hill, S. L., & Stockley, R. A. (2000). Bronchial inflammation in acute bacterial exacerbations of chronic bronchitis: the role of leukotriene B4. *Eur. Respir. J 15*, 274–280.

Cruz, C. M., Rinna, A., Forman, H. J., Ventura, A. L. M., Persechini, P. M., & Ojcius, D. M. (2007). ATP activates a reactive oxygen species-dependent oxidative stress response and secretion of proinflammatory cytokines in macrophages. *J. Biol. Chem 282*, 2871–2879.

Culpitt, S. V., Maziak, W., Loukidis, S., Nightingale, J. A., Matthews, J. L., & Barnes, P. J. (1999). Effect of high dose inhaled steroid on cells, cytokines, and proteases in induced sputum in chronic obstructive pulmonary disease. *Am. J. Respir. Crit. Care Med 160*, 1635–1639.

Culpitt, S. V., Rogers, D. F., Shah, P., De Matos, C., Russell, R. E. K., Donnelly, L. E., & Barnes, P. J. (2003). Impaired inhibition by dexamethasone of cytokine release by alveolar macrophages from patients with chronic obstructive pulmonary disease. *Am. J. Respir. Crit. Care Med 167*, 24–31.

D'hulst, A. I., Vermaelen, K. Y., Brusselle, G. G., Joos, G. F., & Pauwels, R. A. (2005). Time course of cigarette smoke-induced pulmonary inflammation in mice. *Eur. Respir. J 26*, 204–213.

Debigaré, R., Marquis, K., Côté, C. H., Tremblay, R. R., Michaud, A., LeBlanc, P., & Maltais, F. (2003). Catabolic/anabolic balance and muscle wasting in patients with COPD. *Chest 124*, 83–89.

Dinarello, C.A., Cannon, J.G., Mier, J.W., Bernheim, H.A., LoPreste, G., Lynn, D.L., Love, R.N., Webb, A.C., Auron, P.E., and Reuben, R.C. (1986). Multiple biological activities of human recombinant interleukin 1. *J. Clin. Invest. 77*, 1734–1739.

Dodé, C., Le Dû, N., Cuisset, L., Letourneur, F., Berthelot, J.-M., Vaudour, G., Meyrier, A., Watts, R. A., David Scott, G. I., Nicholls, A., et al. (2002). New Mutations of CIAS1 That Are Responsible for Muckle-Wells Syndrome and Familial Cold Urticaria: A Novel Mutation Underlies Both Syndromes. *The American Journal of Human Genetics 70*, 1498–1506.

Donnelly-Roberts, D. L., Namovic, M. T., Han, P., & Jarvis, M. F. (2009). Mammalian P2X7 receptor pharmacology: comparison of recombinant mouse, rat and human P2X7 receptors. *Br. J. Pharmacol 157*, 1203–1214.

Dostert, C., Meylan, E., & Tschopp, J. (2008a). Intracellular pattern-recognition receptors. *Advanced Drug Delivery Reviews 60*, 830–840.

Dostert, C., Pétrilli, V., Van Bruggen, R., Steele, C., Mossman, B. T., & Tschopp, J. (2008b). Innate immune activation through Nalp3 inflammasome sensing of asbestos and silica. *Science 320*, 674–677.

Doz, E., Noulin, N., Boichot, E., Guénon, I., Fick, L., Le Bert, M., Lagente, V., Ryffel, B., Schnyder, B., Quesniaux, V. F. J., et al. (2008). Cigarette smoke-induced pulmonary inflammation is TLR4/MyD88 and IL-1R1/MyD88 signaling dependent. *J. Immunol 180*, 1169–1178.

Dunne, A., & O'Neill, L.A. (2003). The interleukin-1 receptor/Toll-like receptor superfamily: signal transduction during inflammation and host defense. *Sci. STKE* (171):re3.

Effect of inhaled triamcinolone on the decline in pulmonary function in chronic obstructive pulmonary disease (2000). *N. Engl. J. Med 343*, 1902–1909.

Eisenbarth, S. C., Colegio, O. R., O/'Connor, W., Sutterwala, F. S., & Flavell, R. A. (2008). Crucial role for the Nalp3 inflammasome in the immunostimulatory properties of aluminium adjuvants. *Nature 453*, 1122–1126.

Ekberg-Jansson, A., Andersson, B., Bake, B., Boijsen, M., Enanden, I., Rosengren, A., Skoogh, B. E., Tylén, U., Venge, P., & Löfdahl, C. G. (2001). Neutrophil-associated activation markers in healthy smokers relates to a fall in DL(CO) and to emphysematous changes on high resolution CT. *Respir Med 95*, 363–373.

Etter, J., & Bullen, C. (2010). Electronic cigarette: users profile, utilization, satisfaction and perceived efficacy. Addiction. Available at: http://onlinelibrary.wiley.com/doi/10.1111/j.1360-0443.2011.03505.x/abstract

Faustin, B., Lartigue, L., Bruey, J.-M., Luciano, F., Sergienko, E., Bailly-Maitre, B., Volkmann, N., Hanein, D., Rouiller, I., & Reed, J. C. (2007). Reconstituted NALP1 Inflammasome Reveals Two-Step Mechanism of Caspase-1 Activation. *Molecular Cell 25*, 713–724.

Ferrari, D., Pizzirani, C., Adinolfi, E., Lemoli, R. M., Curti, A., Idzko, M., Panther, E., & Di Virgilio, F. (2006). The P2X7 receptor: a key player in IL-1 processing and release. *J. Immunol 176*, 3877–3883.

Fields, W. R., Leonard, R. M., Odom, P. S., Nordskog, B. K., Ogden, M. W., & Doolittle, D. J. (2005). Gene expression in normal human bronchial epithelial (NHBE) cells following in vitro exposure to cigarette smoke condensate. *Toxicol. Sci 86*, 84–91.

Finkelstein, R., Fraser, R. S., Ghezzo, H., & Cosio, M. G. (1995). Alveolar inflammation and its relation to emphysema in smokers. *Am. J. Respir. Crit. Care Med 152*, 1666–1672.

Floreani, A. A., Wyatt, T. A., Stoner, J., Sanderson, S. D., Thompson, E. G., Allen-Gipson, D., & Heires, A. J. (2003). Smoke and C5a induce airway epithelial intercellular adhesion molecule-1 and cell adhesion. *Am. J. Respir. Cell Mol. Biol 29*, 472–482.

Flouris, A. D., & Oikonomou, D. N. (2010). Electronic cigarettes: miracle or menace? *BMJ 340*, c311.

Ford, P. A., Durham, A. L., Russell, R. E. K., Gordon, F., Adcock, I. M., & Barnes, P. J. (2010). Treatment effects of low-dose theophylline combined with an inhaled corticosteroid in COPD. *Chest 137*, 1338–1344.

Foster, W. M. (2002). Mucociliary transport and cough in humans. *Pulm Pharmacol Ther 15*, 277–282.

Franchi, L., Eigenbrod, T., Munoz-Planillo, R., & Nunez, G. (2009). The inflammasome: a caspase-1-activation platform that regulates immune responses and disease pathogenesis. *Nat Immunol 10*, 241–247.

Franchi, L., McDonald, C., Kanneganti, T.-D., Amer, A., & Núñez, G. (2006). Nucleotide-Binding Oligomerization Domain-Like Receptors: Intracellular Pattern Recognition Molecules for Pathogen Detection and Host Defense. *The Journal of Immunology 177*, 3507–3513.

Franchi, L., Muñoz-Planillo, R., Reimer, T., Eigenbrod, T., & Núñez, G. (2010). Inflammasomes as microbial sensors. *Eur. J. Immunol 40*, 611–615.

Franchi, L., Stoolman, J., Kanneganti, T.-D., Verma, A., Ramphal, R., & Núñez, G. (2007). Critical role for Ipaf inPseudomonas aeruginosa-induced caspase-1 activation. *Eur. J. Immunol. 37*, 3030–3039.

Frevert, C. W., Huang, S., Danaee, H., Paulauskis, J. D., & Kobzik, L. (1995). Functional characterization of the rat chemokine KC and its importance in neutrophil recruitment in a rat model of pulmonary inflammation. *J. Immunol 154*, 335–344.

Gaschler, G. J., Skrtic, M., Zavitz, C. C. J., Lindahl, M., Onnervik, P.-O., Murphy, T. F., Sethi, S., & Stämpfli, M. R. (2009). Bacteria challenge in smoke-exposed mice exacerbates inflammation and skews the inflammatory profile. *Am. J. Respir. Crit. Care Med 179*, 666–675.

Geraghty, P., Rogan, M. P., Greene, C. M., Boxio, R. M. M., Poiriert, T., O'Mahony, M., Belaaouaj, A., O'Neill, S. J., Taggart, C. C., & McElvaney, N. G. (2007). Neutrophil elastase up-regulates cathepsin B and matrix metalloprotease-2 expression. *J. Immunol 178*, 5871–5878.

Giri, J. G., Lomedico, P. T., & Mizel, S. B. (1985). Studies on the synthesis and secretion of interleukin 1. I. A 33,000 molecular weight precursor for interleukin 1. *J. Immunol 134*, 343–349.

Godoy, I., Campana, A. O., Geraldo, R. R. C., Padovani, C. R., & Paiva, S. A. R. (2003). Cytokines and dietary energy restriction in stable chronic obstructive pulmonary disease patients. *Eur. Respir. J 22*, 920–925.

Gomez, C., & Reynaud-Gaubert, M. (2010). [Long-term outcome of lung transplantation]. *Rev Pneumol Clin 67*, 64–73.

Gompertz, S., O'Brien, C., Bayley, D. L., Hill, S. L., & Stockley, R. A. (2001). Changes in bronchial inflammation during acute exacerbations of chronic bronchitis. *Eur. Respir. J 17*, 1112–1119.

Grahames, C. B., Michel, A. D., Chessell, I. P., & Humphrey, P. P. (1999). Pharmacological characterization of ATP- and LPS-induced IL-1beta release in human monocytes. *Br. J. Pharmacol 127*, 1915–1921.

Green, C., Ingebrethsen, B., & Heavner, D. (1985). Measurement of nicotine in building air as an indicator of tobacco smoke levels. *Environ. Health Perspect 63*, 249.

Groneberg, D. A., & Chung, K. F. (2004). Models of chronic obstructive pulmonary disease. *Respir. Res 5*, 18.

Grumelli, S., Corry, D. B., Song, L.-Z., Song, L., Green, L., Huh, J., Hacken, J., Espada, R., Bag, R., Lewis, D. E., et al. (2004). An immune basis for lung parenchymal destruction in chronic obstructive pulmonary disease and emphysema. *PLoS Med 1*, e8.

Gunnell, D., Irvine, D., Wise, L., Davies, C., & Martin, R. M. (2009). Varenicline and suicidal behaviour: a cohort study based on data from the General Practice Research Database. *BMJ 339*, b3805.

Gurcel, L., Abrami, L., Girardin, S., Tschopp, J., & van der Goot, F. G. (2006). Caspase-1 Activation of Lipid Metabolic Pathways in Response to Bacterial Pore-Forming Toxins Promotes Cell Survival. *Cell 126*, 1135–1145.

Hadwiger, M. E., Trehy, M. L., Ye, W., Moore, T., Allgire, J., & Westenberger, B. (2010). Identification of amino-tadalafil and rimonabant in electronic cigarette products using high pressure liquid chromatography with diode array and tandem mass spectrometric detection. *J Chromatogr A 1217*, 7547–7555.

Hakim, F., Hellou, E., Goldbart, A., Katz, R., Bentur, Y., & Bentur, L. (2011). The Acute Effects of Water-Pipe Smoking on the Cardiorespiratory System. *Chest 139*, 775–781.

Halle, A., Hornung, V., Petzold, G. C., Stewart, C. R., Monks, B. G., Reinheckel, T., Fitzgerald, K. A., Latz, E., Moore, K. J., & Golenbock, D. T. (2008). The NALP3 inflammasome is involved in the innate immune response to amyloid-[beta]. *Nat Immunol 9*, 857–865.

Harris, J. O., Swenson, E. W., & Johnson, J. E., 3rd (1970). Human alveolar macrophages: comparison of phagocytic ability, glucose utilization, and ultrastructure in smokers and nonsmokers. *J. Clin. Invest 49*, 2086–2096.

Hay, D. W. (2000). Chronic obstructive pulmonary disease: emerging therapies. *Curr Opin Chem Biol 4*, 412–419.

Hazuda, D.J., Strickler, J., Kueppers, F., Simon, P.L., and Young, P.R. (1990). Processing of precursor interleukin 1 beta and inflammatory disease. *J. Biol. Chem. 265*, 6318–6322.

Hellermann, G. R., Nagy, S. B., Kong, X., Lockey, R. F., & Mohapatra, S. S. (2002). Mechanism of cigarette smoke condensate-induced acute inflammatory response in human bronchial epithelial cells. *Respir. Res 3*, 22.

Highland, K. B., Strange, C., & Heffner, J. E. (2003). Long-term effects of inhaled corticosteroids on FEV1 in patients with chronic obstructive pulmonary disease. A meta-analysis. *Ann. Intern. Med 138*, 969–973.

Hill, A. T., Bayley, D., & Stockley, R. A. (1999). The interrelationship of sputum inflammatory markers in patients with chronic bronchitis. *Am. J. Respir. Crit. Care Med 160*, 893–898.

Hodge, S., Hodge, G., Scicchitano, R., Reynolds, P. N., & Holmes, M. (2003). Alveolar macrophages from subjects with chronic obstructive pulmonary disease are deficient in their ability to phagocytose apoptotic airway epithelial cells. *Immunol. Cell Biol 81*, 289–296.

Hoffman, H. M., Rosengren, S., Boyle, D. L., Cho, J. Y., Nayar, J., Mueller, J. L., Anderson, J. P., Wanderer, A. A., & Firestein, G. S. (2004). Prevention of cold-associated acute inflammation in familial cold autoinflammatory syndrome by interleukin-1 receptor antagonist. *The Lancet 364*, 1779–1785.

Hoffman, H. M., Mueller, J. L., Broide, D. H., Wanderer, A. A., & Kolodner, R. D. (2001). Mutation of a new gene encoding a putative pyrin-like protein causes familial cold autoinflammatory syndrome and Muckle-Wells syndrome. *Nat Genet 29*, 301–305.

Hogg, J. C. (2004). Pathophysiology of airflow limitation in chronic obstructive pulmonary disease. *Lancet 364*, 709–721.

Hornung, V., Bauernfeind, F., Halle, A., Samstad, E. O., Kono, H., Rock, K. L., Fitzgerald, K. A., & Latz, E. (2008). Silica crystals and aluminum salts activate the NALP3 inflammasome through phagosomal destabilization. *Nat Immunol 9*, 847–856.

Hornung, V., & Latz E. (2010). Intracellular DNA recognition. *Nat. Rev. Immunol*. 10(2):123-130.

Hoshino, T., Kato, S., Oka, N., Imaoka, H., Kinoshita, T., Takei, S., Kitasato, Y., Kawayama, T., Imaizumi, T., Yamada, K., et al. (2007a). Pulmonary inflammation and emphysema: role of the cytokines IL-18 and IL-13. *Am. J. Respir. Crit. Care Med 176*, 49–62.

Hoshino, Y., Nakamura, T., Sato, A., Mishima, M., Yodoi, J., & Nakamura, H. (2007b). Neurotropin demonstrates cytoprotective effects in lung cells through the induction of thioredoxin-1. *Am. J. Respir. Cell Mol. Biol 37*, 438–446.

Hu, Y., Mao, K., Zeng, Y., Chen, S., Tao, Z., Yang, C., Sun, S., Wu, X., Meng, G., & Sun, B. (2010). Tripartite-motif protein 30 negatively regulates NLRP3 inflammasome activation by modulating reactive oxygen species production. *J. Immunol 185*, 7699–7705.

Humphreys, B. D., & Dubyak, G. R. (1998). Modulation of P2X7 nucleotide receptor expression by pro- and anti-inflammatory stimuli in THP-1 monocytes. *J. Leukoc. Biol 64*, 265–273.

Hurst, J. R., Vestbo, J., Anzueto, A., Locantore, N., Müllerova, H., Tal-Singer, R., Miller, B., Lomas, D. A., Agusti, A., Macnee, W., et al. (2010). Susceptibility to exacerbation in chronic obstructive pulmonary disease. *N. Engl. J. Med 363*, 1128–1138.

Imaoka, H., Hoshino, T., Takei, S., Kinoshita, T., Okamoto, M., Kawayama, T., Kato, S., Iwasaki, H., Watanabe, K., & Aizawa, H. (2008). Interleukin-18 production and pulmonary function in COPD. *Eur. Respir. J 31*, 287–297.

Ingenito, E. P., Loring, S. H., Moy, M. L., Mentzer, S. J., Swanson, S. J., & Reilly, J. J. (2001). Interpreting improvement in expiratory flows after lung volume reduction surgery in terms of flow limitation theory. *Am. J. Respir. Crit. Care Med 163*, 1074–1080.

Irmler, M., Hertig, S., MacDonald, H.R., Sadoul, R., Becherer, J.D., Proudfoot, A., Solari, R., and Tschopp, J. (1995). Granzyme A is an interleukin 1 beta-converting enzyme. *J. Exp. Med. 181*, 1917–1922.

Ishii, K. J., Koyama, S., Nakagawa, A., Coban, C., & Akira, S. (2008). Host innate immune receptors and beyond: making sense of microbial infections. *Cell Host Microbe 3*, 352–363.

Janeway C.A., Travers P., Walport M., Shlomick M., (2001). *Immunobiology*. 5th Edition, Garland Publishing.

Jin, Y., Mailloux, C. M., Gowan, K., Riccardi, S. L., LaBerge, G., Bennett, D. C., Fain, P. R., & Spritz, R. A. (2007). NALP1 in vitiligo-associated multiple autoimmune disease. *N. Engl. J. Med 356*, 1216–1225.

Jones, P. W., & Bosh, T. K. (1997). Quality of life changes in COPD patients treated with salmeterol. *Am. J. Respir. Crit. Care Med 155*, 1283–1289.

Jorenby, D. E., Leischow, S. J., Nides, M. A., Rennard, S. I., Johnston, J. A., Hughes, A. R., Smith, S. S., Muramoto, M. L., Daughton, D. M., Doan, K., et al. (1999). A controlled trial of sustained-release bupropion, a nicotine patch, or both for smoking cessation. *N. Engl. J. Med 340*, 685–691.

Jorenby, D. E., Hays, J. T., Rigotti, N. A., Azoulay, S., Watsky, E. J., Williams, K. E., Billing, C. B., Gong, J., & Reeves, K. R. (2006). Efficacy of varenicline, an alpha4beta2 nicotinic acetylcholine receptor partial agonist, vs placebo or sustained-release bupropion for smoking cessation: a randomized controlled trial. *JAMA 296*, 56–63.

Kanazawa, H., & Yoshikawa, J. (2005). Elevated oxidative stress and reciprocal reduction of vascular endothelial growth factor levels with severity of COPD. *Chest 128*, 3191–3197.

Kang, M.-J., Homer, R. J., Gallo, A., Lee, C. G., Crothers, K. A., Cho, S. J., Rochester, C., Cain, H., Chupp, G., Yoon, H. J., et al. (2007). IL-18 is induced and IL-18 receptor alpha plays a critical role in the pathogenesis of cigarette smoke-induced pulmonary emphysema and inflammation. *J. Immunol 178*, 1948–1959.

Kang, M.-J., Lee, C. G., Lee, J.-Y., Dela Cruz, C. S., Chen, Z. J., Enelow, R., & Elias, J. A. (2008). Cigarette smoke selectively enhances viral PAMP- and virus-induced pulmonary innate immune and remodeling responses in mice. *J. Clin. Invest 118*, 2771–2784.

Kanneganti, T.-D., Body-Malapel, M., Amer, A., Park, J.-H., Whitfield, J., Franchi, L., Taraporewala, Z. F., Miller, D., Patton, J. T., Inohara, N., et al. (2006a). Critical Role for Cryopyrin/Nalp3 in Activation of Caspase-1 in Response to Viral Infection and Double-stranded RNA. *Journal of Biological Chemistry 281*, 36560–36568.

Kanneganti, T.-D., Ozoren, N., Body-Malapel, M., Amer, A., Park, J.-H., Franchi, L., Whitfield, J., Barchet, W., Colonna, M., Vandenabeele, P., et al. (2006b). Bacterial RNA and small antiviral compounds activate caspase-1 through cryopyrin/Nalp3. *Nature 440*, 233–236.

Kanner, R. E., Anthonisen, N. R., & Connett, J. E. (2001). Lower respiratory illnesses promote FEV(1) decline in current smokers but not ex-smokers with mild chronic obstructive pulmonary disease: results from the lung health study. *Am. J. Respir. Crit. Care Med 164*, 358–364.

Karahashi, H., & Amano, F. (2000). Changes of caspase activities involved in apoptosis of a macrophage-like cell line J774.1/JA-4 treated with lipopolysaccharide (LPS) and cycloheximide. *Biol. Pharm. Bull 23*, 140–144.

Keatings, V. M., & Barnes, P. J. (1997). Granulocyte activation markers in induced sputum: comparison between chronic obstructive pulmonary disease, asthma, and normal subjects. *Am. J. Respir. Crit. Care Med 155*, 449–453.

Keatings, V. M., Collins, P. D., Scott, D. M., & Barnes, P. J. (1996). Differences in interleukin-8 and tumor necrosis factor-alpha in induced sputum from patients with chronic obstructive pulmonary disease or asthma. *Am. J. Respir. Crit. Care Med 153*, 530–534.

Keatings, V. M., Jatakanon, A., Worsdell, Y. M., & Barnes, P. J. (1997). Effects of inhaled and oral glucocorticoids on inflammatory indices in asthma and COPD. *Am. J. Respir. Crit. Care Med 155*, 542–548.

Kerstjens, H., & Postma, D. (2003). Chronic obstructive pulmonary disease. *Clin Evid*, 1645–1663.

Kode, A., Yang, S.-R., & Rahman, I. (2006). Differential effects of cigarette smoke on oxidative stress and proinflammatory cytokine release in primary human airway epithelial cells and in a variety of transformed alveolar epithelial cells. *Respir. Res 7*, 132.

Kono, H., & Rock, K. L. (2008). How dying cells alert the immune system to danger. *Nat. Rev. Immunol 8*, 279–289.

Koo, I. C., Wang, C., Raghavan, S., Morisaki, J. H., Cox, J. S., & Brown, E. J. (2008). ESX-1-dependent cytolysis in lysosome secretion and inflammasome activation during mycobacterial infection. *Cellular Microbiology 10*, 1866–1878.

Kool, M., Pétrilli, V., De Smedt, T., Rolaz, A., Hammad, H., van Nimwegen, M., Bergen, I. M., Castillo, R., Lambrecht, B. N., & Tschopp, J. (2008). Cutting Edge: Alum Adjuvant Stimulates Inflammatory Dendritic Cells through Activation of the NALP3 Inflammasome. *The Journal of Immunology 181*, 3755–3759.

Kool, M., Willart, M.A.M., van Nimwegen, M., Bergen, I., Pouliot, P., Virchow, J.C., Rogers, N., Osorio, F., Reis E Sousa, C., Hammad, H., et al. (2011). An unexpected role for uric acid as an inducer of T helper 2 cell immunity to inhaled antigens and inflammatory mediator of allergic asthma. *Immunity 34,* 527–540.

Labasi, J. M., Petrushova, N., Donovan, C., McCurdy, S., Lira, P., Payette, M. M., Brissette, W., Wicks, J. R., Audoly, L., & Gabel, C. A. (2002). Absence of the P2X7 receptor alters leukocyte function and attenuates an inflammatory response. *J. Immunol 168,* 6436–6445.

Lacasse, Y., Wong, E., Guyatt, G. H., King, D., Cook, D. J., & Goldstein, R. S. (1996). Meta-analysis of respiratory rehabilitation in chronic obstructive pulmonary disease. *Lancet 348,* 1115–1119.

Lacoste, J. Y., Bousquet, J., Chanez, P., Van Vyve, T., Simony-Lafontaine, J., Lequeu, N., Vic, P., Enander, I., Godard, P., & Michel, F. B. (1993). Eosinophilic and neutrophilic inflammation in asthma, chronic bronchitis, and chronic obstructive pulmonary disease. *J. Allergy Clin. Immunol 92,* 537–548.

Lappalainen, U., Whitsett, J. A., Wert, S. E., Tichelaar, J. W., & Bry, K. (2005). Interleukin-1beta causes pulmonary inflammation, emphysema, and airway remodeling in the adult murine lung. *Am. J. Respir. Cell Mol. Biol 32,* 311–318.

Laws, T. R., Davey, M. S., Titball, R. W., & Lukaszewski, R. (2010). Neutrophils are important in early control of lung infection by Yersinia pestis. *Microbes Infect 12,* 331–335.

Lawther, P. J., Waller, R. E., and Henderson, M. (1970). Air pollution and exacerbations of bronchitis. *Thorax 25,* 525–539.

Lazarowski, E. R., Boucher, R. C., & Harden, T. K. (2003). Mechanisms of release of nucleotides and integration of their action as P2X- and P2Y-receptor activating molecules. *Mol. Pharmacol 64,* 785–795.

Leckie, M. J., Bryan, S. A., Hansel, T. T., & Barnes, P. J. (2000). Novel therapy for COPD. *Expert Opin Investig Drugs 9,* 3–23.

Levitsky M.G., (1999). *Pulmonary Physiology*. 5th Edition, McGraw Hill

Lommatzsch, M., Cicko, S., Müller, T., Lucattelli, M., Bratke, K., Stoll, P., Grimm, M., Dürk, T., Zissel, G., Ferrari, D., et al. (2010). Extracellular adenosine triphosphate and chronic obstructive pulmonary disease. *Am. J. Respir. Crit. Care Med 181*, 928–934.

Lopez, A. D., & Murray, C. C. (1998). The global burden of disease, 1990-2020. *Nat. Med 4*, 1241–1243.

Lucattelli, M., Cicko, S., Müller, T., Lommatzsch, M., de Cunto, G., Cardini, S., Sundas, W., Grimm, M., Zeiser, R., Dürk, T., et al. (2010). P2X7 Receptor Signalling in the Pathogenesis of Smoke-induced Lung Inflammation and Emphysema. *Am J Respir Cell Mol Biol. 44(3):*423-9.

Lucey, E. C., Keane, J., Kuang, P.-P., Snider, G. L., & Goldstein, R. H. (2002). Severity of elastase-induced emphysema is decreased in tumor necrosis factor-alpha and interleukin-1beta receptor-deficient mice. *Lab. Invest 82*, 79–85.

MacNee, W., & Donaldson, K. (2000). Exacerbations of COPD: environmental mechanisms. *Chest 117*, 390S-7S.

MacNee, W., Wiggs, B., Belzberg, A. S., & Hogg, J. C. (1989). The effect of cigarette smoking on neutrophil kinetics in human lungs. *N. Engl. J. Med 321*, 924–928.

MacNee, W. (2005). Pathogenesis of chronic obstructive pulmonary disease. *Proc Am Thorac Soc 2*, 258–266; discussion 290–291.

Maes, T., Bracke, K. R., Vermaelen, K. Y., Demedts, I. K., Joos, G. F., Pauwels, R. A., & Brusselle, G. G. (2006). Murine TLR4 is implicated in cigarette smoke-induced pulmonary inflammation. *Int. Arch. Allergy Immunol 141*, 354–368.

Maesen, F. P., Smeets, J. J., Sledsens, T. J., Wald, F. D., & Cornelissen, P. J. (1995). Tiotropium bromide, a new long-acting antimuscarinic bronchodilator: a pharmacodynamic study in patients with chronic obstructive pulmonary disease (COPD). *Dutch Study Group. Eur. Respir. J 8*, 1506–1513.

Mahadeva, R., & Shapiro, S. D. (2002). Chronic obstructive pulmonary disease * 3: Experimental animal models of pulmonary emphysema. *Thorax 57*, 908–914.

Mahvan, T., Namdar, R., Voorhees, K., Smith, P. C., & Flake, D. (2011). Clinical Inquiry: which smoking cessation interventions work best? *J Fam Pract 60*, 430–431.

Majo, J., Ghezzo, H., & Cosio, M. G. (2001). Lymphocyte population and apoptosis in the lungs of smokers and their relation to emphysema. *Eur. Respir. J 17*, 946–953.

Mallia, P., & Johnston, S. L. (2005). Mechanisms and experimental models of chronic obstructive pulmonary disease exacerbations. *Proc Am Thorac Soc 2*, 361–366; discussion 371–372.

Mariathasan, S., & Monack, D. M. (2007). Inflammasome adaptors and sensors: intracellular regulators of infection and inflammation. *Nat Rev Immunol 7*, 31–40.

Mariathasan, S., Newton, K., Monack, D. M., Vucic, D., French, D. M., Lee, W. P., Roose-Girma, M., Erickson, S., & Dixit, V. M. (2004). Differential activation of the inflammasome by caspase-1 adaptors ASC and Ipaf. *Nature 430*, 213–218.

Mariathasan, S., Weiss, D. S., Newton, K., McBride, J., O'Rourke, K., Roose-Girma, M., Lee, W. P., Weinrauch, Y., Monack, D. M., & Dixit, V. M. (2006). Cryopyrin activates the inflammasome in response to toxins and ATP. *Nature 440*, 228–232.

Martin, T. R., & Frevert, C. W. (2005). Innate immunity in the lungs. *Proc Am Thorac Soc 2*, 403–411.

Martinon, F., & Tschopp, J. (2006). Inflammatory caspases and inflammasomes: master switches of inflammation. *Cell Death Differ 14*, 10–22.

Martinon, F., Agostini, L., Meylan, E., & Tschopp, J. (2004). Identification of bacterial muramyl dipeptide as activator of the NALP3/cryopyrin inflammasome. *Curr. Biol 14*, 1929–1934.

Martinon, F., & Tschopp, J. (2004). Inflammatory Caspases: Linking an Intracellular Innate Immune System to Autoinflammatory Diseases. *Cell 117*, 561–574.

Martinon, F., Burns, K., & Tschopp, J. (2002). The Inflammasome: A Molecular Platform Triggering Activation of Inflammatory Caspases and Processing of proIL-[beta]. *Molecular Cell 10*, 417–426.

Martinon, F., Petrilli, V., Mayor, A., Tardivel, A., & Tschopp, J. (2006). Gout-associated uric acid crystals activate the NALP3 inflammasome. *Nature 440*, 237–241.

Marwick, J. A., Caramori, G., Stevenson, C. S., Casolari, P., Jazrawi, E., Barnes, P. J., Ito, K., Adcock, I. M., Kirkham, P. A., & Papi, A. (2009). Inhibition of PI3Kdelta restores glucocorticoid function in smoking-induced airway inflammation in mice. *Am. J. Respir. Crit. Care Med 179*, 542–548.

Marwick, J. A., Kirkham, P. A., Stevenson, C. S., Danahay, H., Giddings, J., Butler, K., Donaldson, K., Macnee, W., & Rahman, I. (2004). Cigarette smoke alters chromatin remodeling and induces proinflammatory genes in rat lungs. *Am. J. Respir. Cell Mol. Biol 31*, 633–642.

Master, S. S., Rampini, S. K., Davis, A. S., Keller, C., Ehlers, S., Springer, B., Timmins, G. S., Sander, P., & Deretic, V. (2008). Mycobacterium tuberculosis Prevents Inflammasome Activation. *Cell Host & Microbe 3*, 224–232.

Matzinger, P. (1994). Tolerance, Danger, and the Extended Family. *Annu. Rev. Immunol. 12*, 991–1045.

Medzhitov, R., & Janeway, C. A., Jr (1997). Innate immunity: impact on the adaptive immune response. *Curr. Opin. Immunol 9*, 4–9.

Meissner, F., Molawi, K., & Zychlinsky, A. (2008). Superoxide dismutase 1 regulates caspase-1 and endotoxic shock. *Nat Immunol 9*, 866–872.

Melgert, B.N., Timens, W., Kerstjens, H.A., Geerlings, M., Luinge, M.A., Schouten, J.P., Postma, D.S., and Hylkema, M.N. (2007). Effects of 4 months of smoking in mice with ovalbumin-induced airway inflammation. *Clin. Exp. Allergy 37*, 1798–1808.

Meylan, E., Tschopp, J., & Karin, M. (2006). Intracellular pattern recognition receptors in the host response. *Nature 442*, 39–44.

Miller, D. K., Ayala, J. M., Egger, L. A., Raju, S. M., Yamin, T. T., Ding, G. J., Gaffney, E. P., Howard, A. D., Palyha, O. C., & Rolando, A. M. (1993). Purification and characterization of active human interleukin-1 beta-converting enzyme from THP.1 monocytic cells. *J. Biol. Chem 268*, 18062–18069.

Mio, T., Romberger, D. J., Thompson, A. B., Robbins, R. A., Heires, A., & Rennard, S. I. (1997). Cigarette smoke induces interleukin-8 release from human bronchial epithelial cells. *Am. J. Respir. Crit. Care Med 155*, 1770–1776.

Miotto, D., Ruggieri, M. P., Boschetto, P., Cavallesco, G., Papi, A., Bononi, I., Piola, C., Murer, B., Fabbri, L. M., & Mapp, C. E. (2003). Interleukin-13 and -4 expression in the central airways of smokers with chronic bronchitis. *Eur. Respir. J 22*, 602–608.

Mizutani, H., Schechter, N., Lazarus, G., Black, R.A., and Kupper, T.S. (1991). Rapid and specific conversion of precursor interleukin 1 beta (IL-1 beta) to an active IL-1 species by human mast cell chymase. *J. Exp. Med. 174*, 821–825.

Mohsenin, A., & Blackburn, M. R. (2006). Adenosine signaling in asthma and chronic obstructive pulmonary disease. *Curr Opin Pulm Med 12*, 54–59.

Moore, T. J., & Furberg, C. D. (2009). Varenicline and suicide. Risk of psychiatric side effects with varenicline. *BMJ 339*, b4964.

Morris, A., Kinnear, G., Wan, W.-Y. H., Wyss, D., Bahra, P., & Stevenson, C. S. (2008). Comparison of cigarette smoke-induced acute inflammation in multiple strains of mice and the effect of a matrix metalloproteinase inhibitor on these responses. *J. Pharmacol. Exp. Ther 327*, 851–862.

Mortaz, E., Braber, S., Nazary, M., Givi, M. E., Nijkamp, F. P., & Folkerts, G. (2009). ATP in the pathogenesis of lung emphysema. *Eur. J. Pharmacol 619*, 92–96.

Mortaz, E., Folkerts, G., Nijkamp, F. P., & Henricks, P. A. J. (2010). ATP and the pathogenesis of COPD. *Eur. J. Pharmacol 638*, 1–4.

Mukaida, N. (2003). Pathophysiological roles of interleukin-8/CXCL8 in pulmonary diseases. *Am. J. Physiol. Lung Cell Mol. Physiol 284*, L566–L577.

Muneta, Y., Inumaru, S., Shimoji, Y., & Mori, Y. (2001). Efficient production of biologically active porcine interleukin-18 by coexpression with porcine caspase-1 using a baculovirus expression system. *J. Interferon Cytokine Res 21*, 125–130.

Muruve, D. A., Petrilli, V., Zaiss, A. K., White, L. R., Clark, S. A., Ross, P. J., Parks, R. J., & Tschopp, J. (2008). The inflammasome recognizes cytosolic microbial and host DNA and triggers an innate immune response. *Nature 452*, 103–107.

Dal Negro, R. W., Micheletto, C., Tognella, S., Visconti, M., Guerriero, M., & Sandri, M. F. (2005). A two-stage logistic model based on the measurement of pro-inflammatory cytokines in bronchial secretions for assessing bacterial, viral, and non-infectious origin of COPD exacerbations. *COPD 2*, 7–16.

Ng, G., Sharma, K., Ward, S. M., Desrosiers, M. D., Stephens, L. A., Schoel, W. M., Li, T., Lowell, C. A., Ling, C.-C., Amrein, M. W., et al. (2008). Receptor-independent, direct membrane binding leads to cell-surface lipid sorting and Syk kinase activation in dendritic cells. *Immunity 29*, 807–818.

Nicholson, D. W. (1999). Caspase structure, proteolytic substrates, and function during apoptotic cell death. *Cell Death Differ 6*, 1028–1042.

Nocker, R. E., Schoonbrood, D. F., van de Graaf, E. A., Hack, C. E., Lutter, R., Jansen, H. M., & Out, T. A. (1996). Interleukin-8 in airway inflammation in patients with asthma and chronic obstructive pulmonary disease. *Int. Arch. Allergy Immunol 109*, 183–191.

O'Donnell, R., Breen, D., Wilson, S., & Djukanovic, R. (2006). Inflammatory cells in the airways in COPD. *Thorax 61*, 448–454.

O'Donohue, W. J., Jr, & Plummer, A. L. (1995). Magnitude of usage and cost of home oxygen therapy in the United States. *Chest 107*, 301–302.

Ogura, Y., Sutterwala, F. S., & Flavell, R. A. (2006). The Inflammasome: First Line of the Immune Response to Cell Stress. *Cell 126*, 659–662.

Pålsson-McDermott, E.M., & O'Neill, L.A. (2007). Building an immune system from nine domains. *Biochem. Soc. Trans* 35:1437-1444.

Papi, A., Luppi, F., Franco, F., & Fabbri, L. M. (2006). Pathophysiology of exacerbations of chronic obstructive pulmonary disease. *Proc Am Thorac Soc 3*, 245–251.

Patel, N., DeCamp, M., & Criner, G. J. (2008). Lung transplantation and lung volume reduction surgery versus transplantation in chronic obstructive pulmonary disease. *Proc Am Thorac Soc 5*, 447–453.

Pawels, N. S., Bracke, K. R., Dupont, L. L., Van Pottelberge, G. R., Provoost, S., Berghe, T. T. V., Vandenabeele, P., Lambrecht, B. N., Joos, G. F., & Brusselle G. G. (2011). Role of IL-1α and the Nlrp3/caspase-1/IL-1β axis in cigarette smoke-induced pulmonary inflammation and COPD. *Eur. Respir. J 38*, 1019-28.

Pauwels, R. A. (2001). Global initiative for chronic obstructive lung diseases (GOLD): time to act. *Eur. Respir. J 18*, 901–902.

Pauwels, R. A., Buist, A. S., Calverley, P. M., Jenkins, C. R., & Hurd, S. S. (2001). Global strategy for the diagnosis, management, and prevention of chronic obstructive pulmonary disease. NHLBI/WHO Global Initiative for Chronic Obstructive Lung Disease (GOLD) Workshop summary. *Am. J. Respir. Crit. Care Med 163*, 1256–1276.

Pauwels, R. A., Löfdahl, C. G., Laitinen, L. A., Schouten, J. P., Postma, D. S., Pride, N. B., & Ohlsson, S. V. (1999). Long-term treatment with inhaled budesonide in persons with mild chronic obstructive pulmonary disease who continue smoking. European Respiratory Society Study on Chronic Obstructive Pulmonary Disease. *N. Engl. J. Med 340*, 1948–1953.

Pelegrin, P., & Surprenant, A. (2007). Pannexin-1 couples to maitotoxin- and nigericin-induced interleukin-1beta release through a dye uptake-independent pathway. *J. Biol. Chem 282*, 2386–2394.

Pelegrin, P., & Surprenant, A. (2006). Pannexin-1 mediates large pore formation and interleukin-1[beta] release by the ATP-gated P2X7 receptor. *EMBO J 25*, 5071–5082.

Peleman, R. A., Rytilä, P. H., Kips, J. C., Joos, G. F., & Pauwels, R. A. (1999). The cellular composition of induced sputum in chronic obstructive pulmonary disease. *Eur. Respir. J 13*, 839–843.

Pellegatti, P., Raffaghello, L., Bianchi, G., Piccardi, F., Pistoia, V., & Di Virgilio, F. (2008). Increased level of extracellular ATP at tumor sites: in vivo imaging with plasma membrane luciferase. *PLoS ONE 3*, e2599.

Perregaux, D., & Gabel, C. A. (1994). Interleukin-1 beta maturation and release in response to ATP and nigericin. Evidence that potassium depletion mediated by these agents is a necessary and common feature of their activity. *J. Biol. Chem 269*, 15195–15203.

Petersen, A. M. W., Penkowa, M., Iversen, M., Frydelund-Larsen, L., Andersen, J. L., Mortensen, J., Lange, P., & Pedersen, B. K. (2007). Elevated levels of IL-18 in plasma and skeletal muscle in chronic obstructive pulmonary disease. *Lung 185*, 161–171.

Petrilli, V., Papin, S., Dostert, C., Mayor, A., Martinon, F., & Tschopp, J. (2007). Activation of the NALP3 inflammasome is triggered by low intracellular potassium concentration. *Cell Death Differ 14*, 1583–1589.

Polosa, R., & Blackburn, M. R. (2009). Adenosine receptors as targets for therapeutic intervention in asthma and chronic obstructive pulmonary disease. *Trends Pharmacol. Sci 30*, 528–535.

Poynter, M. E., Irvin, C. G., & Janssen-Heininger, Y. M. W. (2003). A prominent role for airway epithelial NF-kappa B activation in lipopolysaccharide-induced airway inflammation. *J. Immunol 170*, 6257–6265.

Prescott, E., Bjerg, A. M., Andersen, P. K., Lange, P., & Vestbo, J. (1997). Gender difference in smoking effects on lung function and risk of hospitalization for COPD: results from a Danish longitudinal population study. *Eur. Respir. J 10*, 822–827.

Pryor, W. A., & Stone, K. (1993). Oxidants in cigarette smoke. Radicals, hydrogen peroxide, peroxynitrate, and peroxynitrite. *Ann. N. Y. Acad. Sci 686*, 12–27; discussion 27–28.

Punturieri, A., Filippov, S., Allen, E., Caras, I., Murray, R., Reddy, V., & Weiss, S. J. (2000). Regulation of elastinolytic cysteine proteinase activity in normal and cathepsin K-deficient human macrophages. *J. Exp. Med 192*, 789–799.

Qu, Y., Franchi, L., Nunez, G., & Dubyak, G. R. (2007). Nonclassical IL-1 beta secretion stimulated by P2X7 receptors is dependent on inflammasome activation and correlated with exosome release in murine macrophages. *J. Immunol 179*, 1913–1925.

Raad, D., Gaddam, S., Schunemann, H. J., Irani, J., Abou Jaoude, P., Honeine, R., & Akl, E. A. (2011). Effects of water-pipe smoking on lung function: a systematic review and meta-analysis. *Chest 139*, 764–774.

Rabe, K. F., Hurd, S., Anzueto, A., Barnes, P. J., Buist, S. A., Calverley, P., Fukuchi, Y., Jenkins, C., Rodriguez-Roisin, R., van Weel, C., et al. (2007). Global strategy for the diagnosis, management, and prevention of chronic obstructive pulmonary disease: GOLD executive summary. *Am. J. Respir. Crit. Care Med 176*, 532–555.

Ramsey, S. D., Patrick, D. L., Albert, R. K., Larson, E. B., Wood, D. E., & Raghu, G. (1995a). The cost-effectiveness of lung transplantation. A pilot study. University of Washington Medical Center Lung Transplant Study Group. *Chest 108*, 1594–1601.

Ramsey, S. D., Patrick, D. L., Lewis, S., Albert, R. K., & Raghu, G. (1995b). Improvement in quality of life after lung transplantation: a preliminary study. The University of Washington Medical Center Lung Transplant Study Group. *J. Heart Lung Transplant 14*, 870–877.

Rang H.P., Dale M.M., Ritter J.M., (1999). *Pharmacology*. 4th Edition, Churchill Livingstone.

Reddy, P. (2004). Interleukin-18: recent advances. *Curr. Opin. Hematol 11*, 405–410.

Rennard, S. I., Anderson, W., ZuWallack, R., Broughton, J., Bailey, W., Friedman, M., Wisniewski, M., & Rickard, K. (2001). Use of a long-acting inhaled beta2-adrenergic agonist, salmeterol xinafoate, in patients with chronic obstructive pulmonary disease. *Am. J. Respir. Crit. Care Med 163*, 1087–1092.

Rennard, S. I., Fogarty, C., Kelsen, S., Long, W., Ramsdell, J., Allison, J., Mahler, D., Saadeh, C., Siler, T., Snell, P., et al. (2007). The safety and efficacy of infliximab in moderate to severe chronic obstructive pulmonary disease. *Am. J. Respir. Crit. Care Med 175*, 926–934.

Retamales, I., Elliott, W. M., Meshi, B., Coxson, H. O., Pare, P. D., Sciurba, F. C., Rogers, R. M., Hayashi, S., & Hogg, J. C. (2001). Amplification of inflammation in emphysema and its association with latent adenoviral infection. *Am. J. Respir. Crit. Care Med 164*, 469–473.

Robson, S. C., Kaczmarek, E., Siegel, J. B., Candinas, D., Koziak, K., Millan, M., Hancock, W. W., & Bach, F. H. (1997). Loss of ATP diphosphohydrolase activity with endothelial cell activation. *J. Exp. Med 185*, 153–163.

Rodriguez-Roisin, R. (2000). Toward a consensus definition for COPD exacerbations. *Chest 117*, 398S-401S.

Rovina, N., Dima, E., Gerassimou, C., Kollintza, A., Gratziou, C., & Roussos, C. (2009). Interleukin-18 in induced sputum: Association with lung function in chronic obstructive pulmonary disease. *Respiratory Medicine 103*, 1056–1062.

Russell, R. E. K., Thorley, A., Culpitt, S. V., Dodd, S., Donnelly, L. E., Demattos, C., Fitzgerald, M., & Barnes, P. J. (2002). Alveolar macrophage-mediated elastolysis: roles of matrix metalloproteinases, cysteine, and serine proteases. *Am. J. Physiol. Lung Cell Mol. Physiol 283*, L867–L873.

Saetta, M., Baraldo, S., Corbino, L., Turato, G., Braccioni, F., Rea, F., Cavallesco, G., Tropeano, G., Mapp, C. E., Maestrelli, P., et al. (1999). CD8+ve cells in the lungs of smokers with chronic obstructive pulmonary disease. *Am. J. Respir. Crit. Care Med 160*, 711–717.

Saetta, M., Di Stefano, A., Turato, G., Facchini, F. M., Corbino, L., Mapp, C. E., Maestrelli, P., Ciaccia, A., & Fabbri, L. M. (1998). CD8+ T-lymphocytes in peripheral airways of smokers with chronic obstructive pulmonary disease. *Am. J. Respir. Crit. Care Med 157*, 822–826.

Saetta, M., Turato, G., Facchini, F. M., Corbino, L., Lucchini, R. E., Casoni, G., Maestrelli, P., Mapp, C. E., Ciaccia, A., & Fabbri, L. M. (1997). Inflammatory cells in the bronchial glands of smokers with chronic bronchitis. *Am. J. Respir. Crit. Care Med 156*, 1633–1639.

Sandford, A. J., Weir, T. D., Spinelli, J. J., & Paré, P. D. (1999). Z and S mutations of the alpha1-antitrypsin gene and the risk of chronic obstructive pulmonary disease. *Am. J. Respir. Cell Mol. Biol 20*, 287–291.

Schulz, C., Krätzel, K., Wolf, K., Schroll, S., Köhler, M., & Pfeifer, M. (2004). Activation of bronchial epithelial cells in smokers without airway obstruction and patients with COPD. *Chest 125*, 1706–1713.

Senior, R. M., Tegner, H., Kuhn, C., Ohlsson, K., Starcher, B. C., & Pierce, J. A. (1977). The induction of pulmonary emphysema with human leukocyte elastase. *Am. Rev. Respir. Dis 116*, 469–475.

Shapiro, S. D. (2000). Animal models for COPD. *Chest 117*, 223S-7S.

Shapiro, S. D., Goldstein, N. M., Houghton, A. M., Kobayashi, D. K., Kelley, D., & Belaaouaj, A. (2003). Neutrophil elastase contributes to cigarette smoke-induced emphysema in mice. *Am. J. Pathol 163*, 2329–2335.

Shi, Y., Evans, J. E., Rock, K. L. Molecular identification of a danger signal that alerts the immune system to dying cells (2003). Nature *425*, 516–521.

Singh, D., Edwards, L., Tal-Singer, R., & Rennard, S. (2010). Sputum neutrophils as a biomarker in COPD: findings from the ECLIPSE study. *Respir. Res 11*, 77.

Skoberne, M., Beignon, A.-S., & Bhardwaj, N. (2004). Danger signals: a time and space continuum. *Trends in Molecular Medicine 10*, 251–257.

Soler-Cataluña, J. J., Martínez-García, M. A., Román Sánchez, P., Salcedo, E., Navarro, M., & Ochando, R. (2005). Severe acute exacerbations and mortality in patients with chronic obstructive pulmonary disease. *Thorax 60*, 925–931.

Solle, M., Labasi, J., Perregaux, D. G., Stam, E., Petrushova, N., Koller, B. H., Griffiths, R. J., & Gabel, C. A. (2001). Altered cytokine production in mice lacking P2X(7) receptors. *J. Biol. Chem 276*, 125–132.

Song, W., Zhao, J., & Li, Z. (2001). Interleukin-6 in bronchoalveolar lavage fluid from patients with COPD. *Chin. Med. J 114*, 1140–1142.

Di Stefano, A., Caramori, G., Capelli, A., Gnemmi, I., Ricciardolo, F. L., Oates, T., Donner, C. F., Chung, K. F., Barnes, P. J., & Adcock, I. M. (2004). STAT4 activation in smokers and patients with chronic obstructive pulmonary disease. *Eur. Respir. J 24*, 78–85.

Di Stefano, A., Turato, G., Maestrelli, P., Mapp, C. E., Ruggieri, M. P., Roggeri, A., Boschetto, P., Fabbri, L. M., & Saetta, M. (1996). Airflow limitation in chronic bronchitis is associated with T-lymphocyte and macrophage infiltration of the bronchial mucosa. *Am. J. Respir. Crit. Care Med 153*, 629–632.

Stevenson, C. S., & Birrell, M. A. (2011). Moving towards a new generation of animal models for asthma and COPD with improved clinical relevance. *Pharmacol. Ther 130*, 93–105.

Stevenson, C. S., Coote, K., Webster, R., Johnston, H., Atherton, H. C., Nicholls, A., Giddings, J., Sugar, R., Jackson, A., Press, N. J., et al. (2005). Characterization of cigarette smoke-induced inflammatory and mucus hypersecretory changes in rat lung and the role of CXCR2 ligands in mediating this effect. *Am. J. Physiol. Lung Cell Mol. Physiol 288*, L514–L522.

Stokes, L., Jiang, L.-H., Alcaraz, L., Bent, J., Bowers, K., Fagura, M., Furber, M., Mortimore, M., Lawson, M., Theaker, J., et al. (2006). Characterization of a selective and potent antagonist of human P2X(7) receptors, AZ11645373. *Br. J. Pharmacol 149*, 880–887.

van der Strate, B. W. A., Postma, D. S., Brandsma, C.-A., Melgert, B. N., Luinge, M. A., Geerlings, M., Hylkema, M. N., van den Berg, A., Timens, W., & Kerstjens, H. A. M. (2006). Cigarette smoke-induced emphysema: A role for the B cell? *Am. J. Respir. Crit. Care Med 173*, 751–758.

Strieter, R.M. (2008). What differentiates normal lung repair and fibrosis? Inflammation, resolution of repair, and fibrosis. *Proc Am Thorac Soc 5*, 305–310.

Sutterwala, F. S., Ogura, Y., Szczepanik, M., Lara-Tejero, M., Lichtenberger, G. S., Grant, E. P., Bertin, J., Coyle, A. J., Galán, J. E., Askenase, P. W., et al. (2006). Critical role for NALP3/CIAS1/Cryopyrin in innate and adaptive immunity through its regulation of caspase-1. *Immunity 24*, 317–327.

Sutterwala, F. S., Mijares, L. A., Li, L., Ogura, Y., Kazmierczak, B. I., & Flavell, R. A. (2007). Immune recognition of Pseudomonas aeruginosa mediated by the IPAF/NLRC4 inflammasome. *The Journal of Experimental Medicine 204*, 3235–3245.

Suzuki, T., Franchi, L., Toma, C., Ashida, H., Ogawa, M., Yoshikawa, Y., Mimuro, H., Inohara, N., Sasakawa, C., & Nuñez, G. (2007). Differential Regulation of Caspase-1 Activation, Pyroptosis, and Autophagy via Ipaf and ASC in Shigella-Infected Macrophages. *PLoS Pathog 3*, e111.

Tate, M. D., Deng, Y.-M., Jones, J. E., Anderson, G. P., Brooks, A. G., & Reading, P. C. (2009). Neutrophils ameliorate lung injury and the development of severe disease during influenza infection. *J. Immunol 183*, 7441–7450.

Terada, K., Yamada, J., Hayashi, Y., Wu, Z., Uchiyama, Y., Peters, C., and Nakanishi, H. (2010). Involvement of cathepsin B in the processing and secretion of interleukin-1beta in chromogranin A-stimulated microglia. *Glia 58*, 114–124.

Tetley, T. D. (2002). Macrophages and the pathogenesis of COPD. *Chest 121*, 156S-159S.

Thornberry, N. A., Bull, H. G., Calaycay, J. R., Chapman, K. T., Howard, A. D., Kostura, M. J., Miller, D. K., Molineaux, S. M., Weidner, J. R., & Aunins, J. (1992). A novel heterodimeric cysteine protease is required for interleukin-1 beta processing in monocytes. *Nature 356*, 768–774.

Ting, J. P.-Y., Kastner, D. L., & Hoffman, H. M. (2006). CATERPILLERs, pyrin and hereditary immunological disorders. *Nat Rev Immunol 6*, 183–195.

Ting, J. P.-Y., Lovering, R. C., Alnemri, E. S., Bertin, J., Boss, J. M., Davis, B. K., Flavell, R. A., Girardin, S. E., Godzik, A., Harton, J. A., et al. (2008). The NLR Gene Family: A Standard Nomenclature. *Immunity 28*, 285–287.

Torigoe, K., Ushio, S., Okura, T., Kobayashi, S., Taniai, M., Kunikata, T., Murakami, T., Sanou, O., Kojima, H., Fujii, M., et al. (1997). Purification and characterization of the human interleukin-18 receptor. *J. Biol. Chem 272*, 25737–25742.

Traves, S. L., Culpitt, S. V., Russell, R. E. K., Barnes, P. J., & Donnelly, L. E. (2002). Increased levels of the chemokines GROalpha and MCP-1 in sputum samples from patients with COPD. *Thorax 57*, 590–595.

Trinchieri, G., & Sher, A. (2007). Cooperation of Toll-like receptor signals in innate immune defence. *Nat Rev Immunol 7*, 179–190.

Trulock, E. P., Christie, J. D., Edwards, L. B., Boucek, M. M., Aurora, P., Taylor, D. O., Dobbels, F., Rahmel, A. O., Keck, B. M., & Hertz, M. I. (2007). Registry of the International Society for Heart and Lung Transplantation: twenty-fourth official adult lung and heart-lung transplantation report-2007. *J. Heart Lung Transplant 26*, 782–795.

Tschoeke, S. K., Oberholzer, A., & Moldawer, L. L. (2006). Interleukin-18: a novel prognostic cytokine in bacteria-induced sepsis. *Crit. Care Med 34*, 1225–1233.

Turino, G. M. (2002). The origins of a concept: the protease-antiprotease imbalance hypothesis. *Chest 122*, 1058–1060.

Tzortzaki, E. G., & Siafakas, N. M. (2009). A hypothesis for the initiation of COPD. *Eur. Respir. J 34*, 310–315.

van der Deen, M., Timens, W., Timmer-Bosscha, H., van der Strate, B.W., Scheper, R.J., Postma, D.S., de Vries, E.G., and Kerstjens, H.A. (2007). Reduced inflammatory response in cigarette smoke exposed Mrp1/Mdr1a/1b deficient mice. *Respir. Res. 8*, 49.

van der Vaart, H., Koëter, G. H., Postma, D. S., Kauffman, H. F., & ten Hacken, N. H. T. (2005). First study of infliximab treatment in patients with chronic obstructive pulmonary disease. *Am. J. Respir. Crit. Care Med 172*, 465–469.

Vestbo, J., Sørensen, T., Lange, P., Brix, A., Torre, P., & Viskum, K. (1999). Long-term effect of inhaled budesonide in mild and moderate chronic obstructive pulmonary disease: a randomised controlled trial. *Lancet 353*, 1819–1823.

Vlahos, R., Bozinovski, S., Hamilton, J. A., & Anderson, G. P. (2006a). Therapeutic potential of treating chronic obstructive pulmonary disease (COPD) by neutralising granulocyte macrophage-colony stimulating factor (GM-CSF). *Pharmacol. Ther 112*, 106–115.

Vlahos, R., Bozinovski, S., Jones, J. E., Powell, J., Gras, J., Lilja, A., Hansen, M. J., Gualano, R. C., Irving, L., & Anderson, G. P. (2006b). Differential protease, innate immunity, and NF-kappaB induction profiles during lung inflammation induced by subchronic cigarette smoke exposure in mice. *Am. J. Physiol. Lung Cell Mol. Physiol 290*, L931–L945.

Vlahos, R., Bozinovski, S., Chan, S. P. J., Ivanov, S., Lindén, A., Hamilton, J. A., & Anderson, G. P. (2010). Neutralizing granulocyte/macrophage colony-stimulating factor inhibits cigarette smoke-induced lung inflammation. *Am. J. Respir. Crit. Care Med 182*, 34–40.

Wan, W.-Y. H., Morris, A., Kinnear, G., Pearce, W., Mok, J., Wyss, D., & Stevenson, C. S. (2010). Pharmacological characterisation of anti-inflammatory compounds in acute and chronic mouse models of cigarette smoke-induced inflammation. *Respir. Res 11*, 126.

Wang, Z., Zheng, T., Zhu, Z., Homer, R. J., Riese, R. J., Chapman, H. A., Jr, Shapiro, S. D., & Elias, J. A. (2000). Interferon gamma induction of pulmonary emphysema in the adult murine lung. *J. Exp. Med 192*, 1587–1600.

Wedzicha, J. A. (2001). Airway infection accelerates decline of lung function in chronic obstructive pulmonary disease. *Am. J. Respir. Crit. Care Med 164*, 1757–1758.

WHO WHO | Chronic obstructive pulmonary disease (COPD). Available at: http://www.who.int/respiratory/copd/en/ [Accessed August 25, 2011].

Wilson, N.J., Boniface, K., Chan, J.R., McKenzie, B.S., Blumenschein, W.M., Mattson, J.D., Basham, B., Smith, K., Chen, T., Morel, F., et al. (2007). Development, cytokine profile and function of human interleukin 17-producing helper T cells. *Nat. Immunol. 8*, 950–957.

Witherden, I. R., Vanden Bon, E. J., Goldstraw, P., Ratcliffe, C., Pastorino, U., & Tetley, T. D. (2004). Primary human alveolar type II epithelial cell chemokine release: effects of cigarette smoke and neutrophil elastase. *Am. J. Respir. Cell Mol. Biol 30*, 500–509.

Woolhouse, I. S., Bayley, D. L., & Stockley, R. A. (2002). Sputum chemotactic activity in chronic obstructive pulmonary disease: effect of alpha(1)-antitrypsin deficiency and the role of leukotriene B(4) and interleukin 8. *Thorax 57*, 709–714.

Wright, J. L., & Churg, A. (1990). Cigarette smoke causes physiologic and morphologic changes of emphysema in the guinea pig. *Am. Rev. Respir. Dis 142*, 1422–1428.

Wright, J. L., Postma, D. S., Kerstjens, H. A. M., Timens, W., Whittaker, P., & Churg, A. (2007). Airway remodeling in the smoke exposed guinea pig model. *Inhal Toxicol 19*, 915–923.

Wright, J. L., Cosio, M., & Churg, A. (2008). Animal models of chronic obstructive pulmonary disease. *Am. J. Physiol. Lung Cell Mol. Physiol 295*, L1–L15.

Yamamoto, C., Yoneda, T., Yoshikawa, M., Fu, A., Tokuyama, T., Tsukaguchi, K., & Narita, N. (1997). Airway inflammation in COPD assessed by sputum levels of interleukin-8. *Chest 112*, 505–510.

Yang, X. D., Corvalan, J. R., Wang, P., Roy, C. M., & Davis, C. G. (1999). Fully human anti-interleukin-8 monoclonal antibodies: potential therapeutics for the treatment of inflammatory disease states. *J. Leukoc. Biol 66*, 401–410.

Zamboni, D. S., Kobayashi, K. S., Kohlsdorf, T., Ogura, Y., Long, E. M., Vance, R. E., Kuida, K., Mariathasan, S., Dixit, V. M., Flavell, R. A., et al. (2006). The Birc1e cytosolic pattern-recognition receptor contributes to the detection and control of Legionella pneumophila infection. *Nat Immunol 7*, 318–325.

Zeidel, A., Beilin, B., Yardeni, I., Mayburd, E., Smirnov, G., & Bessler, H. (2002). Immune response in asymptomatic smokers. *Acta Anaesthesiol Scand 46*, 959–964.

Zheng, H., Liu, Y., Huang, T., Fang, Z., Li, G., & He, S. (2009). Development and characterization of a rat model of chronic obstructive pulmonary disease (COPD) induced by sidestream cigarette smoke. *Toxicol. Lett 189*, 225–234.

Zheng, T., Zhu, Z., Wang, Z., Homer, R. J., Ma, B., Riese, R. J., Jr, Chapman, H. A., Jr, Shapiro, S. D., & Elias, J. A. (2000). Inducible targeting of IL-13 to the adult lung causes matrix metalloproteinase- and cathepsin-dependent emphysema. *J. Clin. Invest 106*, 1081–1093.

Zhou, R., Yazdi, A. S., Menu, P., & Tschopp, J. (2011). A role for mitochondria in NLRP3 inflammasome activation. *Nature 469*, 221–225.